An investigation of the stem steady state heat energy balance technique in determining water use by trees

by

M.J. SAVAGE, A.N.D. GRAHAM and K.E. LIGHTBODY

School of Applied Environmental Sciences, University of Natal
Pietermaritzburg, South Africa
E-mail: savage@agron.unp.ac.za

Final report to the Water Research Commission on the project:

"Water use and root development of a commercial forest species"

WRC Report No : 348/1/00
ISBN No : 1 86845 617 X

Table of Contents

Executive summary

1. Motivation

Do trees use vast amounts of water? Can we accurately measure the water use by trees as the water is transpired? What techniques can be used to measure the water use of trees? The answers to some of these questions are addressed in this report.

The United Nations Food and Agriculture Organisation (FAO, 1985 Forestry Technical Papers: 59, 60, 62 and 64) has indicated that the rate of deforestation in many developing countries today is greater than afforestation to the extent that as little as 1 ha is planted for every 10 ha that are cut. The Republic of South Africa (R.S.A.) conforms essentially to a developing third world scenario where associated to a current population increase are increasing demands on the country's natural resources, not the least of which include timber products and water.

The R.S.A. is poorly endowed with natural forests and consequently relies heavily on man-made forests for timber products. In an attempt to meet the increasing demands for these, fast growing exotic tree species have often been selected due to their high adaptability, fast growth rate and wide range of end uses.

Very early on in the history of afforestation of the R.S.A., forestry was seen to yield a profitable return on capital invested. The first exotic timber plantations established in the R.S.A were by the Government of the Cape Colony towards the end of the nineteenth century. Commercial afforestation accelerated as the diamond and gold mining industries expanded, and again during the 1914-1918 World War (mainly *Eucalyptus grandis and Eucalyptus saligna),* in response to increasing local demands and using costs of imported timber (Department of Forestry, 1968: South Africa Department of Forestry 1966 Interdepartmental Committee of Investigation into Afforestation and Water supplies in South Africa, 115 pp.). In 1989 the R.S.A., with a land area of approximately 112 000 000 ha, comprised 1 197 850 ha of commercial plantations (that is, *1.1* % of the total land area). Half this area was situated in the then Transvaal province, 40 % in Natal, and the remaining 10 % in the former Cape province (Department of Environment Affairs, 1989: South Africa Department of Environmental Affairs 1989, Strategic Forestry Plan for South Africa, 215 pp.).

In 1975, however, a State Interdepartmental Committee concluded that a land area of approximately 834 600 ha was suitable for afforestation in the R.S.A. Prognostic studies conducted in 1981 and 1982, which excluded fuel-wood requirements, indicated that an annual establishment rate of 39 000 ha $year^{-1}$ was required until the year 2000 in order to meet R.S.A. wood requirements. This implies that an area of 2 million ha will be covered by forests in the R.S.A. by the turn of the century. It is likely, therefore, that a vast area of marginal or submarginal land, possibly previously occupied by less profitable crops such as pasture, maize or sugarcane, will have been planted to trees.

Water deficits develop readily in forest trees, even in trees growing in wet soil, because of excess transpiration over absorption of water. Water deficits adversely affect seed germination and cause tissue shrinkage (leaves, stems, roots, fruits and cones). On coastal sands, pine seedlings have been known to perish during midsummer droughts. The importance of water deficits in trees is sometimes underemphasised when growth reduction or death of trees is attributed to such factors as plant

competition, disease or insects. Root diseases and insect injury to roots reduce water absorption, thereby inducing shoot water deficits. The desiccation of tree crowns following occlusion of vessels after infection by fungi causing vascular wilt disease leads sequentially to growth reduction and death of trees. Water deficits may also predispose trees to onslaughts of fungus pathogens and insects.

Marginal land may be defined as that which, due to poor growing conditions, will require careful selection of species and special establishment techniques in order to produce a crop of positive nett value. A positive nett value need not necessarily be a pure economic return. It may also include benefits to the community and should also take into consideration exploitation costs Hence, marginality of a site may be attributed to a number of limitations such as:

(1) climatic factors: mainly determined by temperature extremes, total evaporation (transpiration plus soil evaporation) potential, and the nature and distribution of rainfall;

(2) soils: where depth and water retention may be critical to profitable growth or plant survival;

(3) site suitability: where after assessing: (a) impacts of afforestation on archaeological, faunisitic and floristic heritage, (b) potential risks associated with, fire, predators, plant invader species, water run-off and soil erosion - more suitable alternatives are found to exist;

(4) economic factors: such as establishment costs and the potential volume of quality timber per unit area possible, that are likely to affect break-even dimensions and profit margins.

Eucalyptus spp. make up 40 % of the R.S.A. commercial plantations (ie. 476 770 ha). These are generally grown in the areas of: 1. The KwaZulu-Natal Midlands and Zululand coastal hinterland; 2. Eastern Mpumalanga and South-Eastern Gauteng below the Drakensberg escarpment, both of which are situated mostly in a narrow belt along the east coast and eastern interior which receive summer rainfall is in excess of 750 mm per annum.

Eucalyptus spp., however have the reputation of being voracious water consumers and their establishment is currently a source of concern, world-wide, amongst organisations wishing to assert their socioeconomic responsibilities - which is resulting in increasing duress for environmental impact studies on their afforestation.

In R.S.A. concern about the reduction of water supplies, ascribed to afforestation, has increased with the increase in commercial forestry. Over the last 60 years numerous letters and reports expressing this concern have been addressed to the State Forestry Department and have appeared in the press. Most concern has been directed at *E grandis, E saligna and Pinus spp.*

Areas that have specifically been referred to in KwaZulu-Natal are: Harding and Ixopo where tributaries of the Umzimkulu and Umkomaas rivers are fed; the Richmond district, including the upper catchment of the Illovo river; the Rietvlei and Midlands districts, where catchments of the Umvoti, Mnyamvuba, Yarrrow, Umgeni, and Umzunkulwana rivers are fed; and the sandy coastal plain of northern Zululand near lake St. Lucia. Areas in and around Barberton and White River in Mpumalanga and also further north in the Northern Province, where tributaries of the Crocodile,

Klaserie, Levubu, Olifants, and Crocodile rivers are fed, have also been implicated.

In 1932 the R.S.A. State Department of Forestry decided to leave the banks of streams unplanted for 20 m on either side. Campaigns against forestry became so serious at the time of the British Empire Forestry Conference held in South Africa in 1935 that a committee was appointed to report on the effects of forests on climate, water conservation and erosion in South Africa. This committee recommended that a comprehensive scientific investigation be conducted on the effects of tree planting upon local water supplies. The State Forestry Department responded promptly and the Jonkershoek Research Station was established in the seine year. In 1936 and 1955 the Cathedral Peak and Mokobulaan Research Stations respectively were established.

To investigate whether the fears of voracious water use by *Eucalypts* are justified it is necessary to consider the processes which determine evaporation loss from vegetation, and to understand how these are affected by different climates, plant species, soil types and availability of soil water. In this report, we concentrate on the use of techniques to measure transpiration in trees and review some aspects, covered by available literature, on *Eucalyptus* plant-water interactions, in an endeavor to assess the potential of afforestation of marginal areas.

2. Objectives

2.1 Project aims

2.1.1 Original aims

(a) Establishment of a root research facility at the University of Natal and an investigation into the establishment of a rhizotron facility to be used for the measurement of the water use of selected tree species.

b) Investigation of the root development of the selected tree species under conditions of marginal soil water availability and growth under these conditions.

(c) Determination of water usage by the selected tree species. In conjunction with these measurements, some field measurements of transpiration will be obtained (using the so-called cut-tree and sap flow techniques) in order to better understand the field situation and specifically the water usage by mature trees.

(d) Determination of the lower limit of plant available water and the amount of soil water required for adequate root growth for selected tree species.

2.1.2 Rationale for proposed deviation from original aims

Initial field measurements illustrated that the confines of the proposed laboratory facility, within the time period of 4 years considered, would not provide rooting patterns and rooting depths similar to those found in the field situation.

Furthermore, the stem steady state heat energy balance technique required a full investigation and lysimetric calibration before it could be used in the field. Successful use of stem state heat energy

balance technique would result in a sap flow measurement technique much more useful than the use of the lysimeter columns originally proposed.

2.1.3 Proposed revised aims

Our revised aim was to concentrate on the field application and development of 50 and 100 mm diameter stem steady heat balance (SSS) technique gauges for *in situ* sap flow monitoring, in stems and roots, as a more precise alternative to lysimeter gravimetric determination of tree water utilisation as proposed in the original aim. We also reviewed the heat pulse velocity and stem steady state techniques and undertook a review on plant water interactions in trees.

2.2 Background

This project was primarily concerned with the measurement of transpiration using the stem steady state heat energy balance technique (SSS). Rooting strategies by plantation trees on the deep Zululand sands have previously been researched by excavation, tracers in water and complemented by plant water stress measurements. We therefore did not duplicate these findings. Our procedures using the SSS technique involved checking procedures for the correct use of the technique and its validation. After these methods had been developed, the aim was to use these measurement systems for the routine field measurement of transpiration at three sites: Zululand coast, Bloemendal and Shafton near Howick in KwaZulu-Natal.

2.3 Investigation of the stem steady state heat energy balance technique

2.3.1 Summary of the technique

The stem steady state heat energy balance technique may be applied to woody and herbaceous stems from 2 to 125 mm in diameter. The advantage of the technique is that the methods are reasonably non-destructive, reasonable to automate and allow a continuous record of mass of water per unit time to be monitored for individual trees. The technique has numerous advantages in scaling from tree to stand over others that require conversions to convert individual leaf or branch measurements to that of the whole tree to stand measurements. The method has a better time resolution than soil water balance techniques and is less complex than the eddy correlation and Bowen ratio techniques. The technique only requires the measurement of four voltages and a continuous supply of heat to the plant stem.

2.3.2 Theoretical considerations

The theory of the technique was fully investigated and expressions for error calculations derived.

2.3.3 Power supply and datalogger considerations

The technique is critically dependent on power supply and datalogger function. We developed a switched mode power supply.

2.3.4 Baseline comparisons

Prior to our study, the technique had not been used on *E grandis*. It was our intention to validate the technique, using a lysimeter, and to use two stem gauges on the same tree to investigate the quality of transpiration measurements and identify possible errors. Further validation was investigated using an artificial laboratory system supplying a known flow rate.

2.3.5 Tree response by shading

A *E grandis* part of a tree was shaded to investigate the response of the stem gauge transpiration measurements to the shading.

2.3.6 Comparison with Class-A pan evaporation

An experiment at a marginal site allowed both stem gauge transpiration measurements and class-A pan evaporation measurements for purposes of comparison.

2.3.7 Storage correction and the influence of naturally occurring vertical temperature gradients on transpiration

At the initial stages of the project, the influence of naturally occurring temperature gradients of transpiration measurements had not been documented in the literature. We developed theory for the correction of this and investigated the magnitude of the effect in the field (root and sap flow measurements). Fortuitously, the storage and naturally occurring temperature gradients oppose each other with the measurement error in sap flux M_{sap} being about 15 % during peak flow times. The measured, adjusted and natural stem temperature differences allow the energy balance components to be redetermined, including the sap energy flux E_{sap} value corrected for storage and the storage term $E_{storage}$.

2.3.8 Stem thermal conductivity

Most workers used a fixed stem thermal conductivity value for their measurements of transpiration. We developed procedures for the direct and indirect measurement of stem thermal conductivity of E *grandis*.

2.3.9 Field measurements of transpiration

2.3.9.1 Vineyard experiment

We wished to use the SSS technique, in an integrated fashion, together with Bowen ratio and eddy correlation techniques for determining the soil water evaporation in a partially covered row crop in a vineyard. In the process of testing our techniques, we wished to obtain some measurements of transpiration. An energy balance approach was used in which terms for both the canopy and the soil were developed.

2.3.9.2 Bloemendal experiment on sapflow in roots and stems in a marginal site

Our aim was to evaluate the technique in terms of its capability of providing information on lateral root and stem water flow rates. We used root severing to stop soil water utilization from different depths, as may be represented by soil water depletion in different rooting zones.

2.3.9.3 Zululand experiment to test the functionality of the 120 mm diameter stem gauges

The field use of the largest sized (120-mm diameter) stem steady state heat energy balance technique is discussed. Measurements were performed at mainly Kwa-Mbonambi, Zululand and at Bloemendal near Pietermaritzburg. The technique was validated using a cut-stem technique. Measurements were performed at Kwa-Mbonambi on fertilised and unfertilised trees. Aspects addressed in this study include: diurnal stem and gauge temperature gradients; stem heating; a mathematical determination of the influence of stem gauge conductance and stem thermal conductivity on gauge accuracy, using the cut-stem technique for verification of sap flow.

2.3.10 Heat pulse velocity technique for estimation of sap flux
We reviewed the use of the intrusive heat pulse velocity technique.

3. Results and Conclusions

3.1 Investigation of the stem steady state heat energy balance technique

3.1.1 Theoretical considerations
The theory of the technique was fully investigated and expressions for error calculations derived.

3.1.2 Comparison between two gauges on the same stem
Two gauges on the same *E grandis* tree yielded very similar data although there was some evidence that the upper gauge measurements were being affected by heating from the lower gauge.

3.1.3 Comparison between lysimeter and stem gauge flow rates
Good comparisons between SSS flow rates and lysimetric evaporation rates for 30-min data were obtained. Standard deviations of all component energy terms increase dramatically at sunrise and sunset.

3.1.4 Tree response to shading
When a portion of the tree was shaded from the incident solar irradiance, there was an immediate decrease in sap flow rate implying a rapid response to physiological events. The surprising aspect of this experiment is the speed at which the sap flow decreased after shading given that the shaded branches were above the upper thermocouple of the gauge! When the shading was removed, the sap flow almost immediately increased. In conclusion therefore, tree water capacitance did not affect our measurements of M_{sap} at high flow rates.

3.1.5 Artificial verification of stem gauges
Experimentation with an artificial system to test the functionality and precision of gauges on *E. grandis* stems was conducted. Different magnitudes in power supplied to the gauge require the use of different gauge conductance K_{gauge} values for the determination of radial energy flux E_{radial}. These results provide a basis for modifying K_{gauge} for changes in source voltage. Changes in battery voltage are a frequent occurrence as batteries become progressively discharged. Also, there could be changes in gauge heater resistance due to the application of voltage to the heater or due to changes in the environmental temperature.

3.1.6 The effect of heater voltage on sap flow measurements
The SSS technique is critically dependent on the value of the continuous power supplied to the heater and the resultant stem temperature differential dT_{stem} measured. The expression used for calculating the sap flux M_{sap} *has* dT_{stem} in the denominator. If heater power is too low and/or transpiration rates are high, then dT_{stem} tends to zero with the M_{sap} value calculated becoming unstable when compared with lysimeter values.

3.1.7 Storage correction and the influence and measurement of naturally occurring vertical temperature gradients on SSS flow rates
Naturally occurring vertical temperature gradients in the stem of E *grandis* may affect the

measurement accuracy of the calculated sap flux (M_{sap}) values. Corrections may be performed based on actual stem temperature gradients in the absence of heat applied to the heater. It is advisable to measure these stem gradients, in the absence of any heating, for a range of environmental conditions. The error is much larger for the larger diameter gauges (diameters greater than 35 mm) but this has yet to be fully determined. Before 11h30 when the sap flow is increasing, the errors in M_{sap} are large negative (corresponding to an overestimation in M_{sap} by the gauge). After this time, the errors become increasingly positive. At night, the large errors are often of no consequence since M_{sap} is small. If the data were integrated for a complete day, the overestimation in M_{sap} before noon would not cancel with the underestimation after noon.

The assumption of energy balance assumes that there is no storage. We have developed methodology for identifying the storage heat flux. Fortuitously, the storage and naturally occurring temperature gradients oppose each other with the measurement error in M_{sap} being about 15 % during peak flow times.

3.1.8 Stem thermal conductivity K_{stem} and gauge conductance K_{gauge}

Laboratory measurements of the thermal conductivity of 25-mm diameter *E. grandis* stems averaged 0.3435 W m^{-1} K^{-1}. This value is lower than the value of 0.54 W m^{-1} K^{-1} used by many workers for herbaceous plants. Dowel rod thermal conductivity averaged 0.1081 W m^{-1} K^{-1} (with a standard deviation of 0.0122 W m^{-1} K^{-1}). Stem gauge conductance was determined by measuring the component energy fluxes with gauges applied to dowel rods (with known thermal conductivity values). These data allowed the sap flux to be calculated as a function of gauge conductance varying between 1.0 and 2.5 W mV^{-1} . The gauge conductance corresponding to a zero sap flux was 1.32, 1.18 and 1.91 W mV^{-1} for gauges 1, 3 and 4 respectively. We conclude then that it is necessary to determine the gauge conductance, in the manner described, for each gauge used.

3.2 Use of sap flow and aerodynamic evaporation techniques for the separation of total evaporation into canopy evaporation and soil water evaporation

In this integrative study, sap flow was measured using 25-mm diameter stem gauges using the SSS technique and total evaporation was measured using Bowen ratio (BR) and eddy correlation (EC) techniques. Soil water evaporation was estimated by subtracting transpiration from total evaporation. The integrity of the data was checked by comparing the calculated soil latent heat density as the difference between latent heat density (averaged from BR and EC data) and the actual soil water evaporation obtained from the sunrise to sunset mass differences from 19 soil microlysimeters. The spatial variation in the soil microlysimeter evaporation was between 0.77 to 1.75 mm. If the soil microlysimetric measurements are not in error, then either the total evaporation (Bowen ratio and eddy correlation) measurements are too high or the canopy evaporation (sap flow) measurements are too low. The study further confirmed the use of the 25-mm diameter gauges for the measurement of sap flow in plant stems. Soil evaporation exceeded transpiration during the experiment. The management of the soil may therefore be as important as managing the crop under water-limiting conditions.

3.3 Sap flow in roots and stems in a marginal site

We evaluated the use of the technique for measurement of lateral root and stem sap flow rates in E *grandis*. Gauges were attached to three *E grandis* stems, approximately 100 mm in diameter, and

to a lateral root of each tree, approximately 28 mm in diameter. The roots exhibited a similar sap flow pattern to the stems, but with reduced magnitude during the day, Following the diurnal comparison, the lateral roots on one tree were severed, while the tap root of another was also severed. Following severing, the lateral and tap root flow rates increased to meet continued stem sap flow.

3.4 The functionality of the Dynamax sgb100-ws stem steady state heat energy balance (SSS) technique gauges on E *grandis trees*

The field use of the largest sized (120-mm diameter) stem steady state heat energy balance technique is discussed. Measurements were performed at Kwa-Mbonambi, Zululand and at Bloemendal near Pietermaritzburg. The technique was validated using a cut-stem technique. Measurements were performed at Kwa-Mbonambi on fertilised and unfertilised trees. Aspects addressed in this study include: diurnal stem and gauge temperature gradients; stem heating; a mathematical determination of the influence of stem gauge conductance and stem thermal conductivity on gauge accuracy, using the cut-stem technique for verification of sap flow. Our data suggested that a storage term in the heat energy balance be included for the 120-mm diameter gauges. In the cut-stem experiment, a gauge conductance of between 1.6 and 1.8 W mV^{-1} resulted in an adequate comparison with the day-time cumulative sap flow, measured using a portable lysimeter. The maximum daily sap flow was more than 35 kg (for an unfertilised tree) compared to a 24 kg maximum for a fertilised tree.

3.5 Heat pulse velocity technique for estimation of sap flux

The heat pulse velocity technique is reviewed with emphasis on the physiological consequences of technique use. The technique involves the application of a pulse of heat in the sap stream. The rate at which the heat moves is assumed to be a function of transpiration rate. Various sensor configurations have been used. The main advantage to using heat as a tracer is that it allows temporal variations in transpiration to be monitored. Furthermore, the data are produced in the form of an electrical signal, suitable for further processing and storage. If properly calibrated as a system for long term measurements of temporal changes in total transpiration, the measurements can serve as a tool for studying plant physiology as well as an input to a control system of irrigation, $C0_2$ enrichment etc. Lysimetric techniques are expensive and impracticable on a large scale. The stem steady state heat energy balance technique, which forms the bulk of this report, should be regarded as complementary rather than competitive or as an alternative technique for the determination of transpiration.

The disadvantages of the technique includes: the invasiveness of the technique causing possible damage to the plant and disturbance of the natural sap flow; the theoretical assumptions are unrealistic; the evaluation of total transpiration based on locally measured sap flow values is a complicated task; the relation between the local sap flow and the total evaporation needs to be established with the probes implanted into the plant exactly in the same position as in actual leaf measurement; thermal inhomogeneities in the volume undergoing measurement, resulting in part from the wound caused to the plant by the insertion of the heater and from thermal trauma due to the heat pulse perturbation; the temperature elevation at the heater may be significantly greater than at the sensor; technical problems in manufacturing both the temperature sensing microprobes and the heat transmitters should also be considered. Moreover, in practice it is difficult to determine the exact times of maximum or zero temperature differences between the upstream and downstream

thermocouples. The wound area can only be accurately determined by severing the tree stem and then assuming that the wound area is the same for all trees used for measurements. These drawbacks are counterbalanced by the almost unique feature of providing continuous measurements of the flow velocity.

3.6 Plant water interactions pertaining to *Eucalyptus* afforestation of marginal land in southern Africa

We review literature on the plant water interactions pertaining to the afforestation by *Eucalyptus* of marginal land. The Republic of South Africa (R.S.A.) conforms essentially to a developing third world scenario where associated with a current population increase there are increasing demands on the country's natural resources, not the least of which include timber products and water. While water is vital to any economy, wood products are also very necessary. Water uptake from *Eucalyptus spp. per se* is likely to vary according the particular species under consideration and the environmental conditions in which they are growing, viz. climate, including nature and duration of rainfall, evaporative demand, including windspeed and effects of the aerodynamic resistance of the canopy of the particular species under consideration; water availability, either through access to a water table or from soil storage. The effects of afforestation are likely to be greater if the replacing species is taller, aerodynamically more resistant to wind, and presents a greater rooting volume to the soil than the replaced vegetation. There is considerable scope for research into assessment of the growth and water utilisation characteristics of different *Eucalyptus* or similar spp. in the R.S.A. in response to differential water availability and soil type.

3.7 Switched mode power supply

One of the major problems in the continuous use of stem gauges is the requirement for the continuous application of power. We developed, with the cooperation of the Electronics Unit of the University of Natal, an energy efficient power supply. Previous power supplies we have used were unsatisfactory and operated at very high temperatures and were therefore energy inefficient. In these cases, batteries had to be replaced frequently. In order to conserve battery power and to reduce the build up of heat in the stem section under the gauge at night, when one might expect sap flow rates to be low, a switched mode power supply was developed. The power supply applied a voltage source either between On and Off or between independent adjustable High and Low voltage states. Usually a number of batteries in parallel were connected to the gauge heater.

3.8 Use of a palmtop computer for data transfer between datalogger or data storage module

We developed the use of a Palmtop computer as a means for transferring data from datalogger to a desktop computer.

3.9 Heat pulse velocity techniques using thermocouple probes

The theory and practical use of thermocouple heat pulse velocity probes is described.

4. Extent to which Contract Objectives have been Met

Good initial progress with the use of the stem steady state heat energy balance technique for small

diameter stems and a poor simulation of field conditions in the root laboratory facility necessitated a change in the aims of the project with greater emphasis on the use of the 120 mm and 25 mm diameter gauges. The influence of naturally occurring stem temperature gradients, an aspect that was unknown at the commencement of the study, resulted in more investigations on the use of the technique before initiating the field program. We also did not anticipate having to develop methodology to account for heat storage since other workers had not done so for tree diameters approaching 120 mm. These investigations also necessitated the development of a switched mode power supply for use with multiple gauges. Some additional aspects were investigated that had not been originally planned, and this necessitated more detailed research.

5. Useful Contributions of the Research

- Thorough investigation of the stem steady state heat energy balance technique for 25 and 120 mm diameter stems: (a) laboratory and field validation; (b) technique limitations; effect of heater voltage;
- separation of total evaporation into canopy evaporation and soil water evaporation;
- measurement of lateral and stem sap flow rates at a marginal site;
- root severing studies using the SSS technique;
- field use of the largest sized 120-mm diameter stem gauge;
- review of plant water interactions in relation to the afforestation of marginal land in southern Africa is presented;
- review of the heat pulse velocity technique and the presentation of the theory and practical use of heat pulse velocity sensors;
- review of literature on the dynamic sap flow in trees and applicability to water use efficiency research using the SSS technique;
- construction of a switched mode power supply;
- two papers published in the Journal of the South African Society for Horticultural Sciences on the use of the SSS technique;
- best paper award at the South African Agrometeorology and Remote Sensing Conference for the research on the use of sap flow and aerodynamic evaporation techniques for the separation of total evaporation into canopy evaporation and soil water evaporation
- one Masters thesis successfully completed and a PhD in progress
- numerous (national and one international) conferences were attended and the results of our investigations were presented.

6. Project Publications and Conference Presentations

1. Graham, A.D.N, 1992. Do eucalypts suck? Natal University Focus on Water 3, 18.

2. Graham, A.D.N., M.J. Savage and K.E. Lightbody, 1993. Use of a stem steady state heat energy balance technique for the *in situ* measurement of transpiration. 2. Field application to *Eucalyptus grandis*. Supplement to Journal of the South African Society for Horticultural Science 3, 19.
3. Graham, A.D.N., M.J. Savage and B.W. Olbrecht, 1994. Application of a stem steady state heat energy balance technique for sap flow determination in a hollow stemmed plant. Southern

African Society for Crop Production, Cedara, Natal.

4. Hellman, J.L., K.J. McInnes, M.J. Savage, R.W. Gesch and R.J. Lascano, 1994. Soil and canopy energy balances in a west Texas vineyard. *Agricultural and Forest Meteorology* 71:99-114.
5. Heilman, J.L., K.J. McInnes, R.W. Gesch, R.J. Lascano, and M.J. Savage, 1996. Effects of trellising on the energy balance of a vineyard. *Agricultural and Forest Meteorology* 81: 79-93.
6. Lightbody, K.E., M.J. Savage and A.D.N. Graham, 1993. The use of a stem steady state heat energy balance technique for the in situ measurement of water flow in Eucalyptus grandis roots. Supplement to *Journal of the South African Society for Horticultural Sciences* 3, 40.
7. Lightbody, K.L., 1994. Use of a stem steady state heat energy balance technique for the measurement of sap flux in *Eucalyptus grandis.* M.Sc.Agric. thesis, Department of Agronomy, University of Natal, Pietermaritzburg. Pp 111.
8. Lightbody, K.E., M.J. SAVAGE and A.D.N. Graham, 1994. *In situ* measurement of sap flow rate in lateral roots and stems of *Eucalyptus grandis* using a steady state heat energy balance technique. *Journal of the South African Society for Horticultural Sciences* 4, 1-7.
9. Salisbury, F.B. and M.J. Savage, 1996. Energy transfer. In Units, Symbols and Terminology for Plant Physiology: A Reference for Presentation of Research Results in the Plant Sciences (Ed. F.B. Salisbury). Chapter 7, 65-7 1. Oxford University Press, Oxford. Oxford University Press.
10. Savage, M.J., 1991. Energy and water relations techniques in the soil-plant-atmosphere continuum. Dohne Research Station, Dohne, Cape. Invited seminar.
11. Savage, M.J., 1992a. Evaporation measurement using aerodynamic and sap flow techniques. Department of Agronomy and Soil Science, Washington State University, Pullman, Washington, USA.
12. Savage, M.J., 1992b. Water flux and water potential measurement techniques. Invited seminar delivered to the Department of Horticultural Sciences (cosponsored with Plant Physiology), Texas A and M University, College Station, Texas, USA.
13. Savage, M.J., 1992c. Measurement of sap flow using a stem steady state heat energy balance technique. Invited Visiting Scientist Seminar delivered to the Departments of Crop and Soil Sciences and the Department of Horticulture, Michigan State University, Lansing, Michigan, USA.
14. Savage, M.J., 1992d. Thermodynamics and the soil-plant-atmosphere system: examples from sap flow and water potential measurement techniques. Invited Crop Science Seminar delivered to the Department of Soil and Crop Sciences, Texas A and M University, College Station, Texas, USA.
15. Savage, M,J., 1996. Basic thermodynamic quantities. In Units, Symbols and Terminology for Plant Physiology: A Reference for Presentation of Research Results in the Plant Sciences (Ed. F.B. Salisbury). Oxford University Press. Chapter 4, 45-54. Oxford University Press, Oxford.
16. Savage, M.J. and A.D.N. Graham, 1994. Aspects of sap flow determination using a steady state heat energy balance technique. Southern African Society for Crop Production, Cedara, Natal.
17. Savage, M.J., A.D.N. Graham and K.E. Lightbody, 1993. Use of a stem steady state heat energy balance technique for the in situ measurement of transpiration in *Eucalyptus grandis:* Theory and errors. *Journal of the South African Society for Horticultural Sciences* 3 (2), 46-

51.
18. Savage, M.J., A.D.N. Graham and K.E. Lightbody, 1993. Use of a stem steady state heat energy balance technique for the in situ measurement of transpiration. 1. Theory and errors. Supplement to *Journal of the South African Society for Horticultural Sciences* 3, 19.
19. Savage, M.J. and K.E. Lightbody, 1992. Sap flow of Eucalyptus grandis using a stem steady state heat energy balance technique. Abstracts of the First International Crop Science Congress Meeting, Ames, Iowa. Pp. 71
20. Savage, M.J. and K. A. Monnik 1993. Sensible heat transfer in a vineyard. South African Agrometeorology and Remote Sensing Conference, Department of Agriculture and Water Supply, Stellenbosch, Westem Cape Region.
21. Savage, M.J. 1996. Micrometeorological techniques in the environmental sciences. Workshop on Biological Simulation, Potchefstroom.
22. Savage, M.J. 1997. Sap flow measurement. Presenter of a Two-day Workshop at the invitation of the University of Stellenbosch.
23. Savage, M.J. 1998. Measurement techniques and Instrumentation. Workshop on Crop Modelling and Irrigation Scheduling: Theory Meets the Real World. Pietersburg, University of the North, Northern Province.
24. Savage, M.J. 1998. Datalogging and environmental instrumentation for students and researchers at the Univ of the North and Univ of Venda. Workshop on Crop Modelling and Irrigation Scheduling: Theory Meets the Real World. Pietersburg, University of the North, Northern Province.

7. Future Research

7.1 General comments

One of the major limitations to real economic growth of South Africa is water resources. Research in the field of evaporation measurement needs to be continued and for the benefit of all in South Africa. Lack of research interest and funding in this crucial area will impact on, for example, land management controversies such as the use of sugar cane as opposed to afforestation.

7.2 Stem steady state heat energy balance methodology

Our research has concentrated on transpiration measurement using the SSS technique exclusively and therefore has ignored the important aspect of plant productivity in terms of the amount of water used. The use of the heat pulse velocity technique should be regarded as complementary to the SSS technique. We recommend that both techniques be used on the large diameter stems (120 mm) but that for the SSS technique, the storage term can be accounted for.

8. Technology Transfer

A two-day Workshop on the use of the stem steady state heat energy balance technique was held in 1997 at the University of Stellenbosch. Eighteen scientists for many parts of southern Africa attended. The Workshop was partly sponsored by the Water Research Commission. This forum encouraged young scientists. 'The results of our research have also been presented to eighteen

postgraduate students of the University of the North in 1998 also partly sponsored by the Water Research Commission.

Much of the research described here has already benefitted students, researchers and technical staff at the University of Natal, University of Pretoria, University of Stellenbosch, University of the North, Texas A and M University and Environmentek (CSIR). Most of the material has already been presented at local and international conferences.

9. Acknowledgements

The research in this report emanated from a project funded by the Water Research Commission entitled: "Water use and root development of a commercial forest species"

The Steering Committee responsible for this project consisted of the following persons:
Dr G.C. Green (Water Research Commission, Chairman;)
Dr C.W. Smith (Institute for Commercial Forestry Research ICFR);
Mr H. Maaren (Water Research Commission);
Professor R.E. Schulze (Department of Agricultural Engineering, University of Natal, Pietermaritzburg, UNP);
Dr C.S. Everson (FORESTEK/CSIR);
Mr D.B. Versfeld (FORESTEK/CSIR).,
Mr D.J. Huyser (Water Research Commission), Secretary.

The financing of the project by the Water Research Commission and the contribution of the members of the Steering Committee is gratefully acknowledged. The project was only possible with the cooperation of the following:

Staff of the Electronic Centre of the University of Natal for their support in the repair and checking of equipment;

Ms Jothi (Jody) Moodley (Agrometeorology) of the School of Applied Environmental Sciences,

University of Natal for the endless list of tasks, including the Plotit graphics editing, that required attention;

Mr Peter N. Dovey (Agrometcorology) of the School of Applied Environmental Sciences, University of Natal for part of the technical support required for this project;

The University of Natal, the South African Foundation for Research Development, Texas A & M University and the United States Council for the International Exchange of Scholars (for a Fulbright grant to the project leader);

Professor N. Pammenter (University of Natal, Durban) for cooperation in the experimentation with an artificial system to test gauge functionality and precision;

Drs J.L. Hellman and K.J. McInnes (Department of Soil and Crop Sciences, Texas, A & M University, College Station, Texas, USA) for cooperation in the work described in Chapter;

Reviewers of the manuscript papers that have already been published from this research;

Mr Mike Howard (Mondi Forests), Dr Andrew Noble and Mr Clive McInnes (ICFR) and Mr Bruce Metelerkamp (formerly of UNP);

Mondi Forests who provided equipment, accommodation, and a 24 h guard to for the Zululand experiments;

The ICFR who provided equipment, accommodation and transport while the authors were being introduced to the Zululand coastal forestry industry; and

Meryl A. Savage for her support and encouragement.

"In the beginning God created the heavens and the earth" (Genesis 11, The Bible)

10. Information about this report

The report was generated using the desktop publishing program Ventura Publisher version 4.1 and WordPerfect 6. All of the computer graphics was generated using Plotit 3.1 (Scientific Programming Enterprises, Haslett, Michigan). The Plotit graphics were copied to the Windows 3.1 clipboard and pasted individually directly into Ventura frames and saved in the Windows metafile format (wmf). The report was printed using a Hewlett Packard LaserJet 4 Plus printer at the 300 dpi by 300 dpl resolution. Most of the calculations for this report were performed using Quattro Pro (Windows and DOS versions) and Plotit 3. 1. The data required to generate the graphics was copied from Quattro Pro to Plotit using the Windows 3.1 clipboard and saved in Plotit as pm files.

List of Figures

Table of Contents

List of Tables and Plates

Table of Contents

Chapter 1

Introduction

1.1 Abstract

The aims and objectives of this report are presented together with some background. While the stem steady state heat energy balance technique is based on fundamental theory, often researchers wish to apply the technique in as short a time as possible. We discuss the technique very briefly and without resorting to theoretical derivations. Practical precautions in the use of the technique, which may be applied to woody and herbaceous stems from 2 to 125 mm in diameter, are also discussed. It should be possible to use the technique from this information and without reference to the other chapters. The advantage of the technique is that the methods are reasonably non-destructive, reasonable to automate and allow a continuous record of mass of water per unit time to be monitored for individual trees. The technique has numerous advantages in scaling from tree to stand over others that require conversions to convert individual leaf or branch measurements to that of the whole tree to stand measurements. The method has a better time resolution than soil water balance techniques and is much less complex than the eddy correlation and Bowen ratio techniques. The technique only requires the measurement of four voltages and a continuous supply of heat to the stem.

1.2 Background

This project was primarily concerned with the measurement of transpiration using the stem steady state heat energy balance technique (SSS). One of our original aims was to investigate the rooting strategies by plantation trees on the deep Zululand sands. This was however researched by Scott (1993) by excavation, tracers in water and complemented by plant water stress measurements. We therefore did not duplicate these findings. Our procedures therefore concentrated on the field use of the SSS technique. This involved checking procedures for the correct use of the technique and its validation. After these methods had been developed, the aim was to use these measurement systems for the routine field measurement of transpiration at three sites: Zululand coast, Bloemendal and Shafton near Howick in KwaZulu-Natal.

Marginal land may be defined as that which, due to poor growing conditions, will require careful selection of species and special establishment techniques in order to produce a crop of positive nett value (Wessels, 1984). A positive nett value need not necessarily be a pure economic return. It may also include benefits to the community and should also take into consideration exploitation costs (Wessels, 1984; Von Dem Bussche, 1984; Alidi, 1984; Gwaitta-Magumba, 1984; Britz, 1984; Teixeira and Sarmento, 1991). Hence, marginality of a site may be attributed to a number of limitations such as:

(1) *climatic factors:* mainly determined by temperature extremes, total evaporation potential, and the nature and distribution of rainfall (Poynton, 1971);

(2) *soils:* where depth and water retention may be critical to profitable growth or plant survival (Macvicar, 1977);

(3) *site suitability:* where after assessing: (a) impacts of afforestation on archaeological, faunisitic and floristic heritage, (b) potential risks associated with, fire, predators, plant invader species, water

run-off and soil erosion - more suitable alternatives are found to exist;

(4) *economic factors:* such as establishment costs and the potential volume of quality timber per unit area possible, that are likely to affect break-even dimensions and profit margins.

Eucalyptus spp. make up 40% of the R.S.A. commercial plantations (ie. 476 770 ha). These are generally grown in the areas of: 1. The KwaZulu-Natal Midlands and Zululand coastal hinterland; 2. South-Eastern Gauteng and Mphumalanga areas below the Drakensberg escarpment; both of which are situated mostly in a narrow belt along the east coast and eastern interior which receives summer rainfall is in excess of 750 mm per annum (Rusk, Pennefather, Dobson and Ferguson, 1991).

Eucalyptus spp., however have the reputation of being voracious water consumers and their establishment is currently a source of concern, world-wide, amongst organisations wishing to assert their socio-economic responsibilities - which is resulting in increasing duress for environmental impact studies on their afforestation (Teixeira and Sarmento, 1991).

In R.S.A. concern about the reduction of water supplies, ascribed to afforestation, has increased with the increase in commercial forestry. Over the last 60 years numerous letters and reports expressing this concern have been addressed to the State Forestry Department and have appeared in the press. Most concern has been directed at *E. grandis*, *E. saligna* and *Pinus* spp.

Areas that have specifically been referred to in KwaZulu-Natal are: Harding and Ixopo where tributaries of the Umzimkulu and Umkomaas rivers are fed; the Richmond district, including the upper catchment of the Illovo river; the Rietvlei and Midlands districts, where catchments of the Umvoti, Mnyamvuba, Yarrrow, Umgeni, and Umzunkulwana rivers are fed; and the sandy coastal plain of northern Zululand near lake St. Lucia. Areas in and around Barbeton and White River, where tributaries of the Crocodile, Klaserie, Levubu, Olifants, and Crocodile rivers are fed, have also been implicated.

To investigate whether the fears of voracious water use by *Eucalyptus* are justified it is necessary to consider the processes which determine evaporative loss from vegetation, and to understand how these are effected by different climates, plant species, soil types and availability of soil water. In this report, we concentrate on the use of techniques to measure transpiration in trees and review some aspects, covered by available literature, on *Eucalyptus* plant-water interactions, in an endeavour to assess the potential of afforestation of marginal areas.

1.3 Motivation for this study

Eucalyptus spp. have the reputation of being voracious water consumers and their establishment is currently a source of concern. In R.S.A. concern about the reduction of water supplies, ascribed to afforestation, has increased with the increase in commercial forestry.

1.4 General aim

Our revised aim was to concentrate on the field application and development of 50 and 100 mm diameter stem steady stem heat balance (SSS) technique gauges for *in situ* sap flow monitoring, in stems and roots, as a more precise alternative to lysimeter gravimetric determination of tree water utilisation as proposed in the original aim.

1.5 Specific objectives

- Thorough investigation of the (SSS) technique for 25 and 120 mm diameter stems: (a) laboratory and field validation; (b) technique limitations; effect of heater voltage;
- thoroughly investigate the power requirements of the technique;
- separation of total evaporation into canopy evaporation and soil water evaporation;
- measurement of lateral and stem sap flow rates at a marginal site;
- root severing studies using the SSS technique;
- field use of the largest sized 120-mm diameter stem gauge;
- plant water interactions in relation to the afforestation of marginal land in southern Africa is presented;
- review of the heat pulse velocity technique and the presentation of the theory and practical use of thermocouple heat pulse velocity sensors;
- review of literature on the dynamic sap flow in trees and applicability to water use efficiency research using the SSS technique.

1.6 Brief description and practical precautions of the SSS technique

1.6.1 Introduction

While the SSS balance technique is based on fundamental theory, often researchers wish to apply the technique in as short a time as possible. This section describes the technique very briefly and without resorting to theoretical considerations. Practical precautions in the use of the technique are also discussed.

1.6.2 Brief description

By supplying a continuous constant heat energy flux (J s^{-1}) to a plant limb (using a surrounding heater) and accounting for its assumed component energy losses by: (i) conduction both vertically upwards and downwards (axially) through and radially from the stem, and (ii) heat stored in the plant limb, the heat component convected in sap can be determined (**Fig. 1.1**).

The conduction of heat vertically upwards and downwards is calculated by measuring voltages (V_{vertup} and $V_{vertdown}$) corresponding to the temperature difference between two points above and below the heater that completely surrounds the stem. Similarly, the radial heat is calculated by measuring the voltage ($V_{thermopile}$) corresponding to a temperature difference across a layer of cork that surrounds the heater. The fourth voltage that is measured, corresponds to the voltage applied to the heater V_{heater}. The heater voltage is measured between the points $V_{heater+}$ and $V_{heater-}$. The heater voltage is supplied by a power supply but because of the voltage drop due to the wires between the supply and the heater, the power supply voltage needs to be measured separately (voltages V_+ and V_-.)

The four voltages (V_{vertup}, $V_{vertdown}$, $V_{thermopile}$, and V_{heater}) allow the energy flux (J s^{-1}) terms $E_{conduction}$ (upper and lower), E_{radial}, and E_{heater} to be calculated. In addition, the increase in stem temperature corresponding to the convected heat in the sap stream (dT_{stem}), is calculated from the voltages V_{vertup} and $V_{vertdown}$.

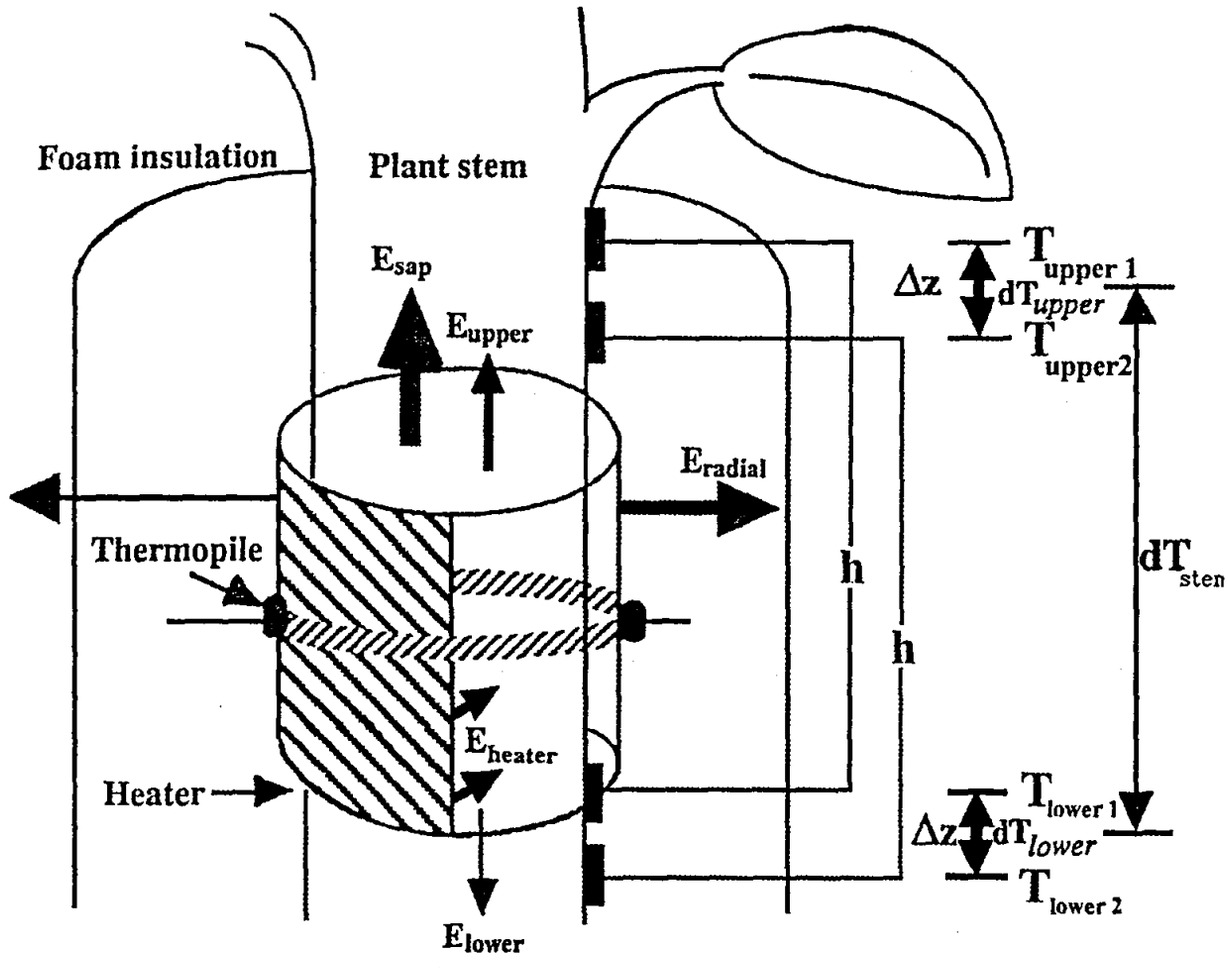

Fig. 1.1 Diagrammatic representation of the steady state stem heat energy balance technique. The heat energy flux terms E_{radial}, E_{upper}, E_{lower}, E_{heater} and E_{sap} are defined in the text. The thermopile surrounding the stem is shown as are the temperature sensors for the measurement of:
$(dT_{upper}/dz) + (dT_{lower}/dz) = [(T_{upper\,1} - T_{upper\,2})/dz] + [(T_{lower\,2} - T_{lower\,1})/dz]$
$= [(T_{upper\,1} - T_{lower\,1})/dz] - [(T_{upper\,2} - T_{lower\,2})/dz]$
and $dT_{stem} = [(T_{upper\,2} - T_{lower\,2}) + (T_{upper\,1} - T_{lower\,1})]/2$

In the precautions that follow, these five voltages, V_{vertup}, $V_{vertdown}$, $V_{thermopile}$, V_{heater}, and V_+ and V_- and the stem temperature difference dT_{stem} are central to the use of the technique.

1.6.3 Practical precautions and procedures

The practical precautions and procedures entail electrical checks, preparing the stem prior to sensor attachment, gauge attachment, the reduction of noise in the collected data, following certain procedures after gauge attachment and error checking.

1.6.3.1 Electrical check of the gauges before attachment to stems

The gauge wiring configuration is typically as follows (**Fig. 1.2**):

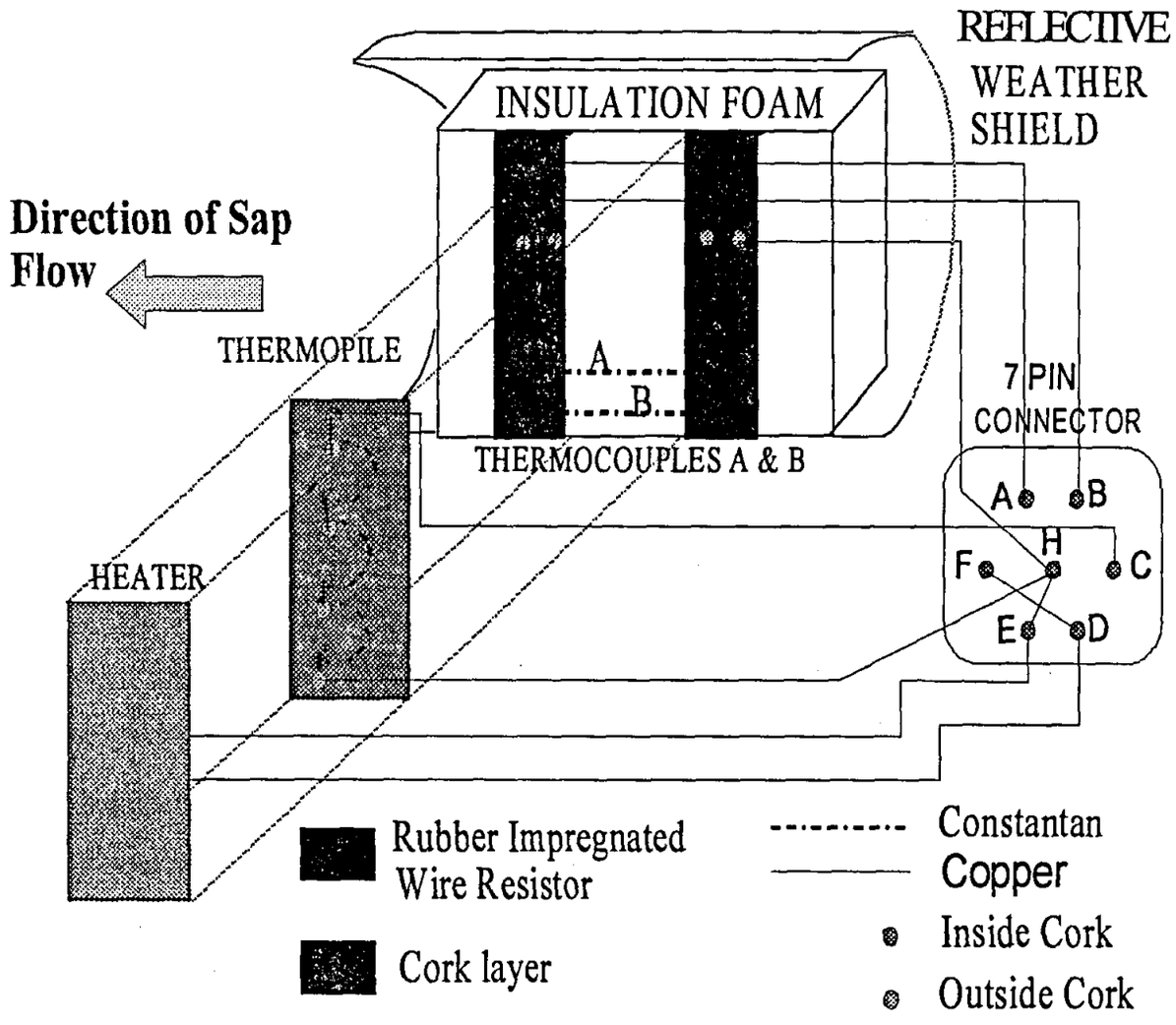

Fig. 1.2 Schematic of the construction and wiring of a typical 4-channel Dynamax SSHB sap flux technique gauge positioned horizontally. The four finely dotted lines show where the thermopile and heater fit sequentially between the two junctions of a thermocouple pair, A and B respectively. Letters A, B, C, D, E, F, and H on the 7 pin connector represent the pins connected to wires coded by colour (green, brown, blue, red, black, orange and white respectively) for connection to a data logger. An 8 th pin may also be used when using cables 25 m or longer to connect a sense lead (yellow) to the heater for more accurate determination of actual potential difference across the heater

Blue wire: $V_{thermopile}$ relative to a common datalogger low connection; connect to 1H (pin C on six connector)

Green wire: V_{vertup} relative to a common datalogger low connection; connect to 2H (pin A)

Brown wire: $V_{vertdown}$ relative to a common datalogger low connection; connect to 3H (pin B)

Make common 1L, 2L, 3L and connect white wire to 3L (pin H)

Orange wire: $V_{heater+}$; connect to 4H

Yellow wire: $V_{heater-}$; connect to 4L

Red wire: connect to V_+ of power supply (pin D)

Black wire: connect to V_- of power supply (pin E)

It is therefore possible to check the wiring within the sensor using simple continuity checks using a voltmeter. There are a total of seven continuity checks:

Check 1. The electrical resistance between the blue wire (pin C of the 6 connector, or logger channel 1 H) and the white wire (pin H or logger channel 3L) should correspond to the resistance of the thermopile;

Check 2. The electrical resistance between the green wire (pin A of the 6 connector, or logger channel 2 H) and the white wire (pin H or logger channel 3L) should correspond to the resistance of the upper thermocouple;

Check 3. The electrical resistance between the green wire (pin B of the 6 connector, or logger channel 3 H) and the white wire (pin H or logger channel 3L) should correspond to the resistance of the lower thermocouple;

Checks 4 and 5. The electrical resistance between 1L and 2L and 2L and 3L should be very low since 1L, 2L and 3L are all common where 3L is pin H;

Check 6. The electrical resistance between the orange and yellow wires (4H and 4L) is a measure of the heater resistance.

Check 7. The electrical resistance between the red and black wires (pins D and E) is a measure of the heater resistance.

1.6.3.2 Preparation of plant stem prior to sensor attachment

1. Measure the stem diameter in the late afternoon at the centre point of the gauge position to ensure that the stem diameter is the diameter range for the gauge. The best way is to attach adhesive tape to the perimeter of the stem, make a vertical mark in the overlapping region of the tape, remove tape and measure the distance between the marks. Divide this distance by π and square root the result to calculate the radius of the stem;

2. Perform stem diameter measurements in the late afternoon when the diameters are a minimum. An increase in stem diameter above the minimum will improve the contact between the stem and the gauge;

3. Carefully remove dirt, loose bark, and leaves and any small branches that sprout from the chosen stem area. Clean the stem with a clean cloth. The few small branches or leaves may be removed by cutting the petioles flush with the stem. The gauge should not be attached until healing of the wound has occurred so as to prevent oozing into the sensor areas. Irregularities from leaf scars or dead bark may be removed using fine sand paper. In trees such as birch, cherry and apples the bark should be sanded smooth. Thin bark (less than 1 mm) may not require sanding. For species with thicker bark, the sanding should not penetrate through the live green cambium layer. The living bark should not be visible, cut or damaged. Crops and herbaceous plants seldom require sanding and should be avoided.

4. Apply small amounts of electrically insulating compound. This should remove any air pockets and prevent fungus or pests from infecting the plant. The compound also ensures good thermal contact between stem and the gauge. It also allows slippage of the gauge during installation and prevents sensor corrosion and entry of water (including condensation). The compound also allows for movement of stem and gauge during windy periods and for diurnal expansion and contraction of the stem. The user should however be aware that the compound could restrict radial growth and gas exchange particularly if the gauge is attached to the stem for long periods of time. During initial measurements using the technique, the user should examine the condition of the stem twice a week to ensure that the covered area condition is not poor and possibly affecting stem flow;

5. Wrap plastic wrap securely around the stem, removing air pockets. This will prevent intrusion of water to the heater and thermocouples;

6. Ensure that the heater strip completely encircles the stem at least once;

7. Coat the stem O rings with electrically insulating compound. Attach the O rings above and below the gauge and tighten securely;

8. Wrap the aluminized shield around the upper and lower rings securely and apply clear package tape so that it holds a cylindrical shape;

9. To prevent water entry from the top of the gauge, apply white plastic to the gauge and stem;

10. To equalize stem and ambient temperatures, wrap three layers of aluminium foil from ground level to the gauge. If necessary, attach more foil to the gauge and above it. Punch holes in the aluminum foil to ensure air movement around the stem. In very hot climates, place a reflective umbrella around the gauge. The user must ensure the stem energy balance is not significantly altered by temperature gradients caused by rapid ambient changes (as may occur in a glasshouse), solar radiation incident on stem and the soil temperature-ambient temperature differences. Aluminium foil above and below the gauge will quickly equalize temperature than would using insulation material;

11. Attach the cable connector. Use insulation tape around connection to prevent water-entry;

12. Secure the cable with a nylon cable tie attached to the stem or attach the cable to a ground stake so that sudden tension on the cable does not dislodge or affect the sensor.

1.6.3.3 Gauge installation

Choose a length of stem about 200 to 700 mm from the soil surface that has the following characteristics:

(a) not below a graft since there may be too much scar tissue. Scar tissue may prevent good contact of the sensor with the stem;

(b) stem should not taper appreciably. A taper may prevent good contact and result in an error in the estimate of the stem cross-sectional area;

(c) the stem should be free from petioles, large scars or other irregularities. These irregularities may prevent good contact of the sensor;

(d) measure the stem diameter at the midpoint for the gauge position. Calculate the stem areas for the datalogger settings;

(e) attach the gauge in the mid-afternoon when the stem diameter is a minimum;

(f) check that the gauge cannot slide or twist when tugged gently. If not, open each strap in turn and use a strong and even pull over the entire insulation jacket. Adjust the size of the insulation by adding insulation strips to the gap if necessary. Proper closing of the insulation jacket is essential since there are four thermocouples that must be in direct contact with the stem.

1.6.3.4 Procedures for the reduction of noise in collected data

Thermal and electrical noise affect measurements. Many of the procedures previously described reduce the thermal noise. Avoiding areas of the stem near the base of the plant that may have large temperature gradients, reducing solar radiation effects and providing good temperature contact between the stem and the four thermocouples reduces thermal noise.

Electrical noise may be reduced by:

1. using short wires - longer wires result in increased electrical noise;

2. always using differential voltage measurements - single-ended voltage measurements result in increased noise since the potential of ground can vary whereas differential measurements are made independent of the ground potential;

3. connecting the battery negative terminal to chassis ground to remove ground loop noise and then connect this common point to earth. This procedure will also present lightening with a path to ground. The procedure can be tested by measuring the electrical resistance between chassis and ground to earth ground. A resistance of less than about 4 ohms indicates adequate grounding;

4. connecting a ground lead to the plant stem. In environmental chambers, the plant can act as an antenna that picks up induced electron magnetic interference from the high voltage sources. The electrical noise may be conducted to the sensor leads; checking all connections to check that there is good physical contact. Poor contacts may be evident by inspection of all voltages at the same time.

1.6.3.5 Procedures following gauge installation

1. Check that there are no exposed wires and that there are no signs of water into the gauge.

2. Check battery voltage. Ensure that the voltage to the gauge is being used to calculate E_{heater} and note the battery voltage.

3. Disconnect the heater power and monitor dT_{stem} for a day. This is referred to as the passive or the unheated mode. If the dT_{stem} value is less than 0.25 °C, then there may be no need to make any corrections. If the dT_{stem} value in the passive mode is greater than this:

(a) the gauge position could be elevated;

(b) the user may apply a correction: *e.g.* Savage (1992, unpublished) suggested that dT_{stem} in the heated mode should have the dT_{stem} value in the unheated mode subtracted;

(c) ensure that there is insulation around the stem from below the gauge to the soil surface. Holes in the aluminium ensure temperature equilibrium between ambient and the gauge.

4. Reconnect the power. After the first day, monitor the dT_{stem} values to ensure that these are greater than between 0.75 and 1 °C under high flow conditions. If the dT_{stem} value is less than 0.75 °C, the voltage applied to the heater should be increased provided it does not exceed the range recommended for that diameter gauge. However, the voltage applied should not result in excessive stem heating during conditions of low flow.

1.6.3.6 Error checking

Apart from the numerous checks already mentioned, one of the most important checks that a user can perform is the dT_{stem} check. Ideally, this should be greater than 0.75 °C for a heated gauge and less than 0.25 °C for an unheated gauge, the user needs to perform the procedures mentioned previously. If the dT_{stem} value for a heated gauge is less than 0.75 °C, then:

(a) the user may consider increasing the voltage applied to the heater (-provided that this does not increase above the gauge specifications). The user would need to ensure that there is no consequential dT_{stem} values that are too high at night;

(b) very high flow rates are being measured that are outside the gauge range;

(c) there may be inadequate contact between the four gauge thermocouples and the stem.

If all these procedures have been adhered to and the dT_{stem} values are still less than 0.75 °C, then the user need to improve thermocouple contact using destructive measures. Notch the stem into the xylem to a depth of 1 to 2 mm and fill with conductive paste. Attach the gauge with the TC installed in contact with the xylem.

Chapter 2

Plant water interactions

2.1 Abstract

We review literature on the plant water interactions, focusing on the afforestation by *Eucalyptus* of marginal lands. Aspects such as drought tolerance, plant water deficit, biomass production, catchment water balance, and plant evaporative processes enable an understanding and modelling of the water movement through trees. Ultimately, such modelling efforts require measurement of tree water use for validation.

2.2 Introduction

Water supply (*i.e.* total amount, variability and seasonal distribution) is the most important environmental factor determining distribution, species composition, and growth of plant communities (Daubenmire, 1978). Plants sometimes fail to survive due to drought which is frequently exacerbated by their own activity.

The United Nations Food and Agriculture Organisation (FAO)[1] has indicated that the rate of deforestation in many developing countries today is greater than afforestation to the extent that as little as one hectare is planted for every 10 ha that are cut. The Republic of South Africa (RSA) conforms essentially to a developing third world scenario where associated with the current population increase are increasing demands on the country's natural resources, not the least of which include timber products and water.

The RSA is poorly endowed with natural forests and consequently relies heavily on man-made forests for timber products. In an attempt to meet the increasing demands for these, fast growing exotic tree species have often been selected due to their high adaptability, fast growth rate and wide range of end uses.

Very early on in the history of afforestation of the RSA, forestry was seen to yield a profitable return on capital invested. The first exotic timber plantations established in the RSA were by the Government of the Cape Colony towards the end of the nineteenth century. Commercial afforestation accelerated as the diamond and gold mining industries expanded, and again during the 1914 to 1918 World War (mainly *E. grandis* and *E. saligna*), in response to increasing local demands and rising costs of imported timber (Department of Forestry, 1968).[2] In 1989 the R.S.A., with a land area of approximately 112 000 000 ha, comprised 1 197 850 ha of commercial plantations (*i.e.* 1.1 % of its total land area). At the time half this area was situated in the then province of Transvaal, 40 % in Natal, and the remaining 10 % in the Cape province (Department of Environment Affairs, 1989).[3]

1 FAO 1985 Forestry Technical Papers: 59,60,62 and 64.

2 South Africa Department of Forestry 1966 Interdepartmental Committee of Investigation into Afforestation and Water supplies in South Africa, 115 pp.

3 South Africa Department of Environmental Affairs 1989 Strategic Forestry Plan for South Africa, 215 pp.

In 1975, a State Interdepartmental Committee concluded that a land area of approximately 834 600 ha was suitable for afforestation in the RSA. Prognostic studies conducted in 1981 and 1982, which excluded fuel-wood requirements, indicated that an annual establishment rate of 39 000 ha $year^{-1}$ was required until the year 2000 in order to meet RSA wood requirements (Wessels, 1984). This implies that an area of approximately 2 million ha will be covered by forests in the RSA by the turn of the century. It is likely therefore that a vast area of marginal or submarginal land, possibly previously occupied by less profitable crops such as pasture, maize or sugarcane, will have been planted to trees.

Marginal land may be defined as that which, due to poor growing conditions, will require careful selection of species and special establishment techniques in order to produce a crop of positive nett value (Wessels, 1984). A positive nett value need not necessarily be a pure economic return. It may also include benefits to the community and should also take into consideration exploitation costs (Wessels, 1984; Von Dem Bussche, 1984; Alidi, 1984; Gwaitta-Magumba, 1984; Britz, 1984; Teixeira and Sarmento, 1991). Hence, marginality of a site may be attributed to a number of limitations such as:

(1) *climatic factors:* mainly determined by temperature extremes, total evaporation (transpiration plus soil evaporation) potential, and the nature and distribution of rainfall (Poynton, 1971);

(2) *soils:* where depth and soil water retention may be critical to profitable growth or plant survival (Macvicar *et al.*, 1977);

(3) *site suitability:* where after assessing: (a) impacts of afforestation on archaeological, faunistic and floristic heritage; (b) potential risks associated with, fire, predators, plant invader species, water run-off and soil erosion - more suitable alternatives are found to exist;

(4) *economic factors:* such as establishment costs and the potential volume of quality timber per unit area possible, that are likely to affect break-even dimensions and profit margins.

Eucalyptus spp. make up 40 % of the R.S.A. commercial plantations (*i.e.* 476 770 ha). In 1989 these were generally grown in the areas of: (i) the Natal Midlands and Zululand coastal hinterland; (ii) the Eastern and South-Eastern Transvaal below the Drakensberg escarpment; both of which are situated mostly in a narrow belt along the east coast and eastern interior which receives summer rainfall in excess of 750 mm per annum (Rusk, Pennefather, Dobson and Ferguson, 1991).

Eucalyptus spp. however have the reputation of being voracious water consumers and their establishment is currently a source of concern, world-wide, amongst organisations wishing to assert their socio-economic responsibilities - which is resulting in increasing duress for environmental impact studies on their afforestation (Teixeira and Sarmento, 1991).

In RSA concern about the reduction of water supplies, ascribed to afforestation, has increased with the increase in commercial forestry. Over the last 60 years numerous letters and reports expressing this concern have been addressed to the State Forestry Department and have appeared in the press. Most concern has been directed at *E. grandis*, *E. saligna* and *Pinus* spp.

Areas that have specifically been referred to in KwaZulu-Natal are: Harding and Ixopo where tributaries of the Umzimkulu and Umkomaas rivers are fed; the Richmond district, including the upper catchment of the Illovo river; the Rietvlei and Midlands districts, where catchments of the Umvoti, Mnyamvuba, Yarrrow, Umgeni, and Umzunkulwana rivers are fed; and the sandy coastal plain of northern Zululand near lake St. Lucia. In the Gauteng areas in and around Barbeton and White River,

where tributaries of the Crocodile, Klaserie, Levubu, Olifants, and Crocodile rivers are fed, have also been implicated.

In 1932 the R.S.A. State Department of Forestry decided to leave the banks of streams unplanted for 20 m on either side. Campaigns against forestry became so serious at the time of the British Empire Forestry Conference held in South Africa in 1935 that a committee was appointed to report on the effects of forests on climate, water conservation and erosion in South Africa. This committee recommended that a comprehensive scientific investigation be conducted on the effects of tree planting upon local water supplies. The State Forestry Department responded promptly and the Jonkershoek Research Station was established in the same year. In 1936 and 1955 the Cathedral Peak and Mokobulaan Research Stations respectively were established (Department of Forestry, 1968 - see footnote 2 on page 10).

To investigate whether the fears of voracious water use by *Eucalypts* are justified it is necessary to consider the processes which determine evaporative loss from vegetation, and to understand how these are effected by different climates, plant species, soil types and availability of soil water. This chapter reviews some aspects, covered by available literature, on *Eucalyptus* and *Pinus* plant-water interactions.

2.3 Drought tolerance

Growth in terrestrial plants is precarious, since an essential substrate for growth, carbon, is acquired only at the expense of losing water. Therefore reserves of the principal solvent in which growth processes take place is depleted, while replenishment of such reserves by rainfall is irregular and unpredictable. Drought generally reduces the growth rate of plants (Hsiao, Acevedo, Fereres and Henderson, 1976) and reduces the stomatal conductance to gas exchange. Plants sometimes fail to survive due to drought, exacerbated by their own activity. Until recently, the most commonly held view was that stomatal closure occurs in order to avoid damage by water stress to the biochemical machinery of plants. It is now becoming clear that xylem dysfunction induced by drought is a serious problem to plants. Resistance to xylem cavitation events is an important (perhaps the most important) parameter that may determine drought resistance.

In fact, water supply is the most important environmental factor determining distribution, species composition, and growth of forests (Kozlowski, 1968). Net annual primary production of forests varies from as much as 3000 g m^{-2} in wet regions to negligible amounts in dry regions (Fischer and Turner, 1978). Species composition of forests depends not only on the total amount of rainfall but also on its annual variability and seasonal distribution. The importance of seasonal distribution of rainfall is emphasised by failure of a phenomenally high rainfall (11610 mm) at Cherrapungi (India) to support mesophytic forest. Almost all of the rain falls in eight consecutive months, with the other four months receiving a total of less than 100 mm. When more evenly distributed throughout the year much less rain than falls at Cherrapungi can support rain forest (Daubenmire, 1978).

Although "drought resistance" has often been used to describe the capacity of trees to survive drought, "drought tolerance" is preferable because it more accurately describes plant reactions to drought (Kramer and Kozlowski, 1979). Overall desiccation avoidance of trees represents an integrated response to one or more morphological and physiological adaptions which may be present in leaves, stems and roots.

Among these are production of small or few leaves; small, few and sunken stomata; rapid stomatal

closure during drought; heavy wax deposition on leaf surfaces and in antestomatal chambers; and strong development of palisade mesophyll (Kozlowski, 1976). The most important desiccation avoiding adaption of roots is capacity for deep and extensive root development (*e.g.* high root to shoot ratio). Stem adaptions include capacity for twig and stem photosynthesis, presence of living wood fibres, and development of a wide cortex that prevents desiccation of vascular tissues (Fahn, 1964). Modification for low flow resistance (e.g. vessels of angiosperms versus tracheids of gymnosperms) reduces the water potential Ψ difference between soil and leaf (Carlquist, 1975). Viewed broadly, however, adaptions in leaves and roots are much more important than those in stems. Adaptions for desiccation avoidance often vary for different species growing side by side (Grieve and Hellmuth, 1970).

Stomatal movements appear to be the most rapid, and reversible, means that plants have to adjust to environmental changes. These might tend to open with changes in the environment which promote carbon fixation and close with changes which promote water loss (disregarding possible transpirational evaporative cooling mechanisms). Consequently their operation might have the effect of reducing the average rate of water loss relative to that of carbon fixation, and represent all possible compromises that could be made between linking CO_2 uptake and water loss. It is such a set of assumptions and empirical observations that has given rise to the theory of optimal variation, as proposed by Cowan (1977), and Cowan and Farquhar (1977).

Optimisation theory has been used, for example, to investigate the optimal partition of carbohydrates between root and shoot. Schulze, Schilling, and Nagarajah (1983) showed that when water was not limiting, maximum biomass is achieved by a plant that partitions the minimum amount of carbohydrates to new roots required to maintain leaf water status. Unfortunately, this model does not consider the situation where soil water becomes limiting, in which case a more pessimistic behaviour would be better, with the degree of pessimism depending on the probability of future rainfall (Jones, 1981). Other models have been used to investigate optimal root system form (Landsberg and Fowkes, 1978) and especially stomatal behaviour (Jones, 1976; 1981; Cowan and Farquhar, 1977; Cowan, 1982). It is, however only in relation to stomatal behaviour that attempts have been made to extend the models to more realistic variable climates (Jones, 1981; Cowan, 1982).

Cowan (1977), and Cowan and Farquhar (1977) envisaged a relationship: $E = E(A)$[see footnote [4]] in which stomatal aperture was an implicit parameter, and where A and E represent the instantaneous rates of assimilation of CO_2 and of transpiration respectively, per unit area of a particular leaf at a particular instant of time. This concept was then extended to a whole plant during a finite period of time.

Cowan and Farquhar (1977) defined optimality as that circumstance where, with variation in A and E with space, s, and time, t: $\bar{A}$ could not conceivably be increased or decreased without increasing or decreasing E. Using standard variational calculus this criterion requires that:

$$\int_0^t \int_0^s [E(A, s, t) - \lambda A]\, ds\, dt \text{ is a minimum value.} \qquad 2.1$$

where λ, a Lagrange multiplier, is a constant. This condition reduces to:

4 For convenience, a list of symbols appears at the end of this chapter.

$$(\frac{\partial E}{\partial A})_{s,t} = \lambda. \qquad 2.2$$

One might interpret λ as a physiological parameter that depends on the amount of plant available water, the magnitude of which possibly depends on the interaction of the plant under question and its environment at a specific time (Cowan, 1982). Alternatively, in circumstances where water is abundant, it might also represent the plant's ability for photosynthesis.

The concepts of Cowan and Farquhar (1977) are illustrated in **Fig. 2.1**.When λ is large, that is to say unit marginal cost is large, the optimal variations in gas exchange do not deviate greatly from those which would occur if leaf conductance were constant. With decreasing λ, the deviations become relatively greater and gas exchange is increasingly confined to those periods early in the morning and late in the afternoon, when irradiance and temperature are appropriate for rapid photosynthesis but, because the ambient vapour pressure deficit is relatively small, the potential rate of transpiration is relatively small.

The *dotted lines* are optimal relationships between rate of transpiration, E, and the rate of assimilation, A, corresponding to two constant magnitudes, $\lambda = 400$ and $\lambda = 600$, of $\delta E/\delta A$. The *broken lines* represent constant magnitudes of leaf epidermis conductance to vapour transfer, g_l (as distinct from that relating to the leaf boundary layer). The dotted trajectories traverse the surface in such a way that the slope, $\delta E/\delta A$ is constant. As the surface is curved in the sense $\delta^2 E/\delta A^2 > 0$, they are optimal trajectories, two of an infinite number of optimal trajectories each of which corresponds to a particular optimal variation in *stomatal aperture* and a particular magnitude of λ (Cowan, 1982).

Much interest has been shown by tree breeders in the role of stomata in desiccation avoidance

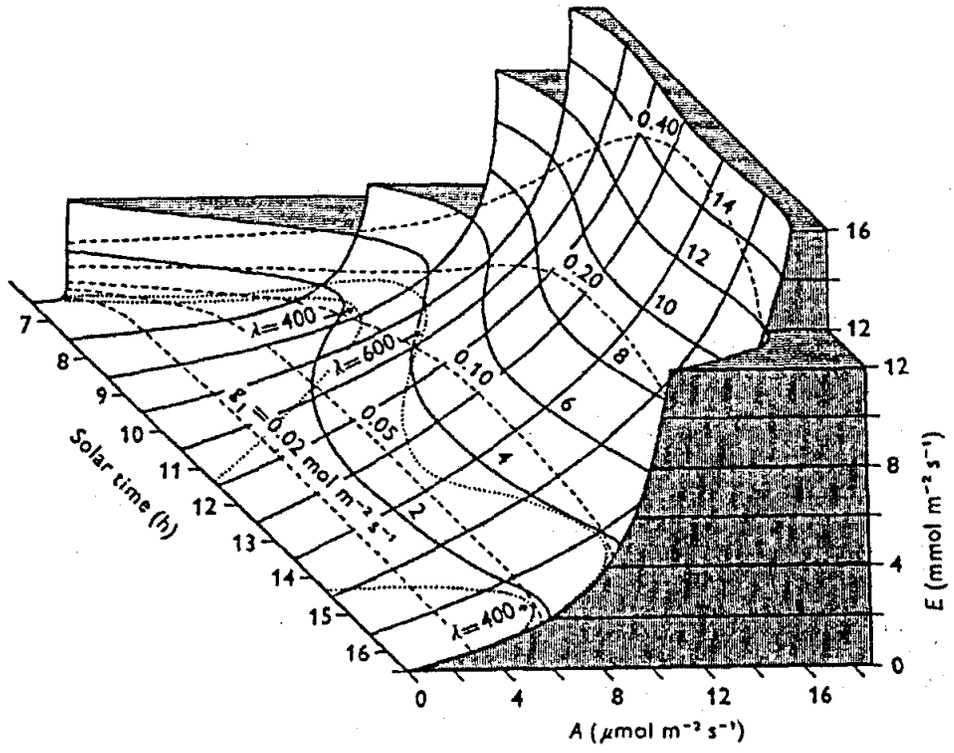

Fig. 2.1 A simulated transpiration function for a single leaf during the course of the day. It is a hypothetical example derived for a horizontally exposed leaf having assumed characteristics subject to an assumed diurnal variation in environment typical of a hot, dry, clear day in an arid subtropical environment (Cowan and Farquhar, 1977)

because genetic variations occur in stomatal size, stomatal frequency, and control of stomatal aperture under stress conditions. However variations in capacity for early stomatal closure are often more important in desiccation avoidance than are differences in stomatal size or frequency. Because of rapid stomatal movements it has been shown that *Eucalyptus sideroxylon* avoided or postponed desiccation better than *E. polyanthemos*, or *E. rostrata* (Quraishi and Kramer, 1970).

After stomata close cuticular control of water loss becomes critical. Mesophytic plants with closed stomata may lose up to 50 % as much water as they do with open stomata, but xerophytic plants lose only 2 to 20 % as much, emphasizing the importance of leaf waxes in water retention (Levitt, 1980). In some species adaptive changes in leaf waxes occur in response to selection by some environmental variable. In Tasmania clinal analysis of glaucousness in several species of *Eucalyptus* indicated a strong genetic control of wax deposition (Barber, 1955; Barber and Jackson, 1957).

Maintenance of partial or full turgor of leaf and root cells while Ψ is decreasing, thereby maintaining metabolism and growth, has been demonstrated for some herbaceous and woody plants. Maintenance of turgor can be achieved by low osmotic potential, capacity to accumulate solutes, and by changes in elasticity of cell walls (Turner and Jones, 1980). Because osmotic adjustment permits maintenance of turgor and turgor mediated processes at lower Ψ, it is sometimes considered as a desiccation tolerance mechanism.

Trees with deeply penetrating and branching roots avoid desiccation by providing an efficient water absorbing system (Kozlowski, 1972). On dry sites *E. socialis* grew better than *E. incrassata* partly because of a higher root to shoot ratio of the former. An important factor in greater desiccation avoidance of *E. camaldulensis* over *E. globulus* was the capacity of the former to produce a deep ramifying root system that absorbed water from deep soil layers after the surface dried (Pereira and Kozlowski, 1976). Deep rooting is also important in desiccation avoidance by several species of Western Australian sclerophylls (Grieve and Hellmuth, 1970).

It is fairly well documented that tree characteristics that confer drought tolerance generally conflict with crop production. The main considerations relating to optimal water use (whether controlled by stomatal movements or by leaf area changes) are illustrated in **Fig. 2.2**. The curves in Fig. 2.2 indicate that the rate of water use ideally declines with time during a rainless period, with the curve shape depending on the probability of rainfall and on processes that compete for water, *e.g.* soil evaporation. The upper curves represent ("optimistic") plants that are adapted to conditions where the average time between rainfall is short, and the lower curves represent the more conservative behaviour necessary by those adapted to situations where the period between rainfalls is long (Cowan, 1982). This information can help in the definition of ideal patterns of stomatal behaviour or leaf area development for specific environments.

There would tend, therefore, to be an inverse relationship between growth rate and probability of survival. One may presume that through selective adaption, plants have acquired some characteristics that enable them to grow more quickly without diminishing the probability of survival, and to increase the probability of survival without diminishing their growth rate, for a particular set of environmental variables.

2.4 Plant water deficit

A decrease in water content may be termed a water deficit. When the decrease in water content, or increase in water deficit, reaches a level such that it negatively affects a physiological process (*e.g.*

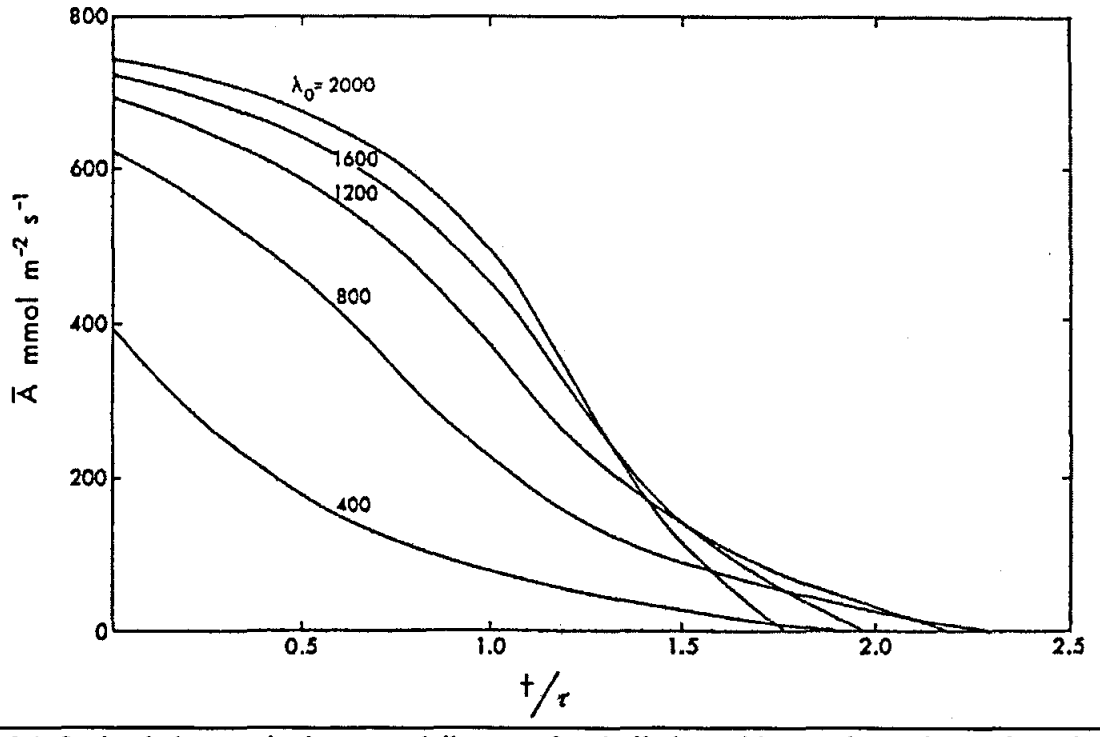

Fig. 2.2 Optimal changes in the mean daily rate of assimilation with t/τ where t is the time since it last rained, and τ is the average interval between rainfalls. The different curves represent the optimal sequences for different initial rates of water use (and hence assimilation), and depend among other things, on τ, with low initial rates being necessary if the expected wait until the next rainfall is long (Cowan, 1982)

photosynthesis), the tree may said to be experiencing water stress. How to characterize the degree of water deficit experienced by plants is a pertinent question and has been a source of controversy. The water balance of trees is most frequently characterised by wilting, tissue water content, relative water content (RWC, also called relative turgidity), saturation deficit (SD), and water potential (Ψ) (Kramer, 1988; Passioura, 1988; Schulze, Steudle, Gollan and Schurr, 1988; Boyer, 1989).

Water deficits develop readily in forest trees, even in trees growing in wet soil, because of excess transpiration over absorption of water. Water deficits adversely affect seed germination and cause tissue shrinkage (leaves, stems, roots, fruits and cones). In Australia, germination of *Eucalyptus* seeds exceeded 80 % but seedling survival was less than 1 % because of dessication (Jacobs, 1955). The importance of water deficits in trees is sometimes under-emphasised when growth reduction or death of trees is attributed to such factors as competition, disease or insects. Water deficits may predispose trees to onslaughts of fungus pathogens and insects. Root diseases and insect injury to roots further reduce water absorption, thereby inducing enhanced shoot water deficits. The desiccation of tree crowns following occlusion of vessels after infection by fungi causing vascular wilt disease may lead sequentially to growth reduction and death of trees (Ayers, 1978).

2.4.1 Wilting

Wilting is sometimes used to determine when internal water deficits develop in plants. Wilting varies as to degree and may be incipient, temporary or permanent. Incipient wilting, characterised by slight loss of turgor, usually does not cause drooping of leaves. Incipient wilting grades into temporary

wilting, characterised by visible drooping of dehydrated leaves during the day, followed by rehydration and recovery from wilting during the night when stomata are closed and evaporative demand declines. While some species like *Prunus serotina*, and *Cornus* spp. wilt early during a drought, others that are permeated with abundant sclerenchyma tissue, like *Pinus* and *Ilex*, do not wilt even after their parenchyma cells have lost turgor. Unfortunately visible wilting of some plants reflects a very advanced and severe water stress condition. For these reasons observations of wilting do not allow for quantitative studies of water deficits in trees.

During sustained periods of soil drying, temporary wilting grades into a state of permanent wilting in which plants do not recover turgidity at night. According to Slatyer (1967), permanent wilting occurs when leaf, root, and root soil Ψ values are equal and turgor pressure is zero. This is because water movement into roots occurs only when Ψ of roots is lower than Ψ of soil. Permanently wilted plants can recover turgidity only when water is added to the soil. Prolonged permanent wilting usually kills most plants (Kramer, 1969).

2.4.2 Comparative water content

Both saturation deficit (SD) and relative water content (RWC) compare the water content of fresh tissue with the saturated water content for the same tissue, usually obtained by allowing the tissues to rehydrate while floating on water. The limitation of these measurements is that leaves of one species may be fully turgid at a water content found in wilted leaves of another species, or in leaves of different ages on the same tree.

The description of water status in energy terminology has become greatly accepted. Water potential quantifies the capacity of water to do work (per unit volume) in comparison to that of an equal volume of pure free water (Savage, 1978; 1996). This terminology provides the means for defining water status either within a tree or within the soil-plant-atmosphere continuum and allows for quantitative comparisons.

Several components contribute to measured plant tissue water potential (Ψ_p) including: (i) pressure potential (Ψ_w) which describes the pressure against a cell wall and is determined by turgor in plant cells or tension in xylem elements; (ii) solute or osmotic potential (Ψ_π) arising from osmotically active solutes dissolved in water; (iii) matric potential (Ψ_τ) arising from capillary or colloidal forces by soil colloids or cell walls; (iv) gravitation potential (Ψ_g). Water potential is partitioned using the following equation (Slatyer, 1967):

$$\Psi = \Psi_p + \Psi_\pi + \Psi_\tau + \Psi_g. \qquad 2.3$$

Both Ψ_π and Ψ_τ have negative values but Ψ_p is positive except rarely when wall pressure is negative. In xylem elements Ψ_p, is negative, 0, or under the influence of root pressure, positive. In plant cells Ψ, the sum of Ψ_π, Ψ_τ, Ψ_p, and Ψ_g is negative except in fully turgid cells when it is zero (Kramer and Kozlowski, 1979). Water potential is measured in energy per unit volume and is commonly reported in bars or megapascals (MPa). Frequently Ψ_τ and Ψ_g terms are omitted from measurement since they are assumed to be small, although Ψ_g can be important in tall trees (Scholander, Hammel, Bradstreet and Hemmingsen, 1965; Tobiessen, Rundel and Stecker, 1971).

Knowledge in any two plant parts or in the soil and plant enables an investigator to determine which way water will move (i.e., from a region of high Ψ to one of low Ψ), or if it will move at all. Water potential can be determined by vapour equilibration, thermocouple psychrometry, or using the

Scholander pressure chamber (Savage, Wiebe and Cass, 1983; Savage and Cass, 1984).

2.5 Biomass production

2.5.1 Canopy growth

It has been demonstrated for a wide range of crops, including forest trees, that dry matter increment is linearly related to leaf area and the amount of radiation intercepted over the same period, and also that manipulation of the environment is likely to change the slope of this relationship (Jarvis and Leverenz, 1983; Jarvis, 1986; Linder, 1985). Biomass production, therefore, by different *Eucalyptus* spp. is likely to depend on their leaf canopy dynamics and how these are influenced by environmental factors such as water availability and temperature.

Leaf primordia of angiosperm leaves generally form on apices of shoots and grow initially by cell division, producing layers of differentiated cells and the framework for leaf shape. The growth of a plant cell involves extension of the cell wall in response to the hydrostatic or turgor pressure exerted by the cell contents. Wall extension is combined with an influx of water and solutes which act to maintain cell turgor. A steady rate of growth is achieved when the rate of water uptake equals the rate of wall extension.

Biophysical analysis indicates that many environmental factors influence leaf growth by changing cell wall properties, and that reduced water availability with soil drying may have a particularly marked effect (Tomos, 1985; Cosgrove, 1986). Some of the variation in mature leaf size may be attributed to variation in the duration of meristematic activity and partly due to variation in final cell size. Rewatering after a short period of time may cause small unexpanded cells to swell such that a burst of outgrowth is seen after rewatering.

It has been suggested that as the soil dries, roots may generate a chemical signal which can limit leaf growth. Fine roots have been implicated as particularly important sensors of water status and there seem to be appreciable differences between species in their capacity to sustain root turgor in drying soil. Some also show enhanced root growth and/or deeper rooting as deficits develop (Van Volkenburgh and Davies, 1983; Davies, Metcalfe, Schurr, Taylor and Zhang, 1987; Zhang, Schurr and Davies, 1987).

The leaf growth (cm^2) of seedling *E. globulus* trees, grown in small pots over a period of 20 days in response to different watering regimes was recorded by Davies, Rhizopoulou, Sanderson, Taylor, Metcalfe and Zhang (1989). Leaf area in this circumstance was greatest in the highest watering regime and appeared to respond rapidly to watering after a period of relative deficiency.

In an experiment to determine the comparative water requirement and biomass (dry mass) production of a *Eucalyptus* hybrid (*E. tereticornis*) and some other selected tree species in their first year of establishment, Chaturvedi, Sharma, and Srivastava (1984; 1988) concluded that water consumption was strongly related to growth. Of interest is that while the *Eucalyptus* hybrid consumed the most water, it was also the most efficient user of water in terms of water consumption per gram of above ground biomass (**Table 2.1**).

In an experiment to quantify this further for such *Eucalyptus* trees, Dabral and Raturi (1985) grew a selection of six month old hybrid seedlings in 3 m × 3 m × 3 m lysimeters for a period of 27 months. They estimated that, for above ground biomass, 167 mm of water was required to produce 1 kg dry

Table 2.1 Water consumption and biomass produced by selected tree species after one year of establishment (Chaturvedi *et al.*, 1984)

Species	Water consumed (*l*)	Biomass produced (g)	Average water uptake per gram of Biomass (*l*)
Pongomia pinnata	697	520	1.30
Albizzia lebbek	1371	2335	0.58
Syzigium cuminii	1460	2386	0.61
Acacia auriculiformia	1475	1713	0.86
Dalbergia sissoo	1794	2005	0.89
Eucalyptus hybrid	2662	5209	0.51
Blank area	502	-	-

mass (0.501 *l* per gram of dry mass).

Similarly, using a lysimetric technique, Rawat, Negi, Rawat, and Gurumurti (1985) quantified the water loss of *E. tereticornis* under differential soil water conditions. They also determined the numbers of open and closed stomata under these conditions using polystyrene film impressions. In their conclusions they noted that the hybrids transpired "copiously", but that when soil water was restricted, partial stomatal closure occurred reducing the transpiration rate. Optimum water use (0.27 *l* of water per gram of dry mass), without a serious reduction in total dry matter, occurred at a soil water content of 15 %.

Like many other trees, *Eucalyptus* spp. show a dramatic difference in leaf morphology between juvenile and adult foliage, particularly specific leaf area (SLA) *i.e.*, leaf area per unit dry mass (Linder, 1985), and as a consequence probably also water consumption. Langford (1976), Bosch (1979) and Van Lille, Kruger, and Van Vyk (1980) have shown that the apparent water loss through *Eucalyptus* trees is not necessarily related to stand age in a linear function. This is possibly due to a number of factors including curvilinear relationships between forest stand variables and age. One example cited is that leaf area of even-aged stands increased with age only to a certain limit, whereupon it remained fairly constant. Further, Van Lill *et al.* (1980) noted that *E. grandis* trees exerted an observable influence on catchment streamflow from about the third year after afforestation, reached a maximum at about the fifth year, and then remained roughly constant for a further four years.

2.5.2 Stem Increment (Wood Production)

Up to 90 % of the annual variation in xylem increment of forest trees has been attributed to water deficits in arid regions and up to 80 % in humid regions (Zahner, 1968). This is substantiated by significant correlations found between xylem increment and rainfall or available soil water (Fritts, 1976), and from thinning and irrigation studies (Zahner and Whitmore, 1960; Zahner, 1968; Moehring, Grano and Bassett, 1975; Kramer and Kozlowski, 1979).

Such variations in wood production are the result of differences in both the rate and duration of cambial activity. These in turn determine the number of xylem cells produced, and the time of initiation and duration of latewood. Kozlowski (1979) has indicated that water deficits in trees are often most critical when radiation and temperature are optimal for growth. When several droughts occur during the same growing season multiple growth rings often form.Variation in growth ring patterns with climate (particularly rainfall) is the basis for dendrochronology (Fritts, 1976; Creber,

1977).

Cambial activity is inhibited directly by water deficits when cell turgor is low enough to reduce synthesis, downward transport and action in the stem of hormonal growth regulators (Whitmore and Zahner, 1976). In addition to restricting cambial activity during drought, water deficits may also have an indirect inhibitory effect on cambial growth in a subsequent year because cambial activity is regulated not only by hormonal plant growth regulators but also the basipetal flow of carbohydrates. Since this may be influenced by foliage amount which in turn may be influenced by xylem activity in previous years, the resultant feed forward effect is explained.

This is illustrated by evidence that water deficits often prevent any xylem forming in the lower stems is suppressed or old trees (Larson, 1963; Zahner, 1968). The lower rate of cambial activity and its cessation earlier in the season in suppressed rather than in dominant trees is also, to a large degree, a response to water deficit (Kozlowski and Peterson, 1962). In Wisconsin (Canada) xylem increment was greater and continued longer into the summer for *P. resinosa* trees growing on the lower part of a slope than for trees on the upper part. These differences were attributed to greater water deficits in the upper-slope trees (Braekke and Kozlowski, 1975).

Of interest is that cambial tissues of *Ecalyptus* trees may come under considerable water stress almost daily during the growing season because of the great tensile forces which develop in the adjacent mature xylem (Stewart, Tham and Rolfe, 1973).

2.5.3 Root Growth

Detailed discussions of water uptake in soil-plant systems have been presented by Taylor and Klepper (1978), Landsberg and Fowkes (1978), Atkinson (1980), Feddes (1981) and Passioura (1981). The main considerations in soil resource utilization by trees are the: (i) transfer characteristics of the soil; (ii) "abundance" of absorbing surfaces *e.g.* roots; (iii) absorbing surface characteristics.

Typically, upon demand, plants withdraw water from the soil immediately adjacent to their roots, with this zone being replenished from the bulk soil. If the rate of withdrawal exceeds the rate of water movement through the soil to the root *i.e.*, the rate of uptake exceeds the soil hydraulic conductivity, then the soil adjacent to the root becomes drier than the bulk soil and the rate of water flow into the roots will decrease, possibly causing stress (typically -1 MPa). Consequently water availability to trees is likely to depend on the nature of the soils in which they grow (*e.g.* water holding capacity, hydraulic conductivity) and to how the trees respond to such a soil environment.

For example, Fabião, Persson and Steen (1985) studied the growth of fine roots in the 0 to 400 mm top soil layer of 11 to 16 year old stands of *E. globulus* over the period of one year. They noted that approximately double the mass of fine roots were produced in clay soils than in sandy soils and that fine-root turn-over due to decomposition in the former was approximately one third higher than in the latter.

This is interesting since it has been observed that where soil resources (particularly water) are not limiting, maximum above-ground biomass is achieved by plants that partition a minimum of resources to the root structure, particularly fine root turnover (Cannell, 1985). Evidently in circumstances where resources do become limiting a more pessimistic behaviour is better - *i.e.*, the development of a more extensive root system.

Root systems can typically be divided into three main components: (i) major permanent *structural roots* usually much larger than the fine roots that they produce, analogous to the carbon skeleton of above ground parts; (ii) a system of temporary *fine roots* 1 to 2 mm in diameter, consisting of longer exploratory roots bearing lateral shorter roots; (iii) *Mycorrhizas* formed by infection of fine roots (Bowen, 1985).

A root study of *E. globulis* trees at 1, 3, 10 and 20 years of age has been presented by Mathur, Raj, and Rajagopal (1986). The characteristics of the four different aged plants is presented in **Table 2.2.** Mathur *et al.* (1986) noted that most of the lateral roots arose from the top portion of the tap roots and that the root volume in all the trees sampled was mostly confined to the upper one metre of soil. Root depth increased with age (one to ten years), with the exception of the trees at 20 years of age which they suggested had been restricted by some physical or edaphic factor (such as a stone, hard pan or soil availability) which had resulted in the tap root turning laterally.

Root abundance is often expressed as L_v (m root m^{-3} soil), L_a (m root m^{-2} soil surface) or L_m (kg dry mass m^{-2}). Interpretation of such numbers is complicated since contact with the soil and root activity with respect to water uptake, of the different root types is often uncertain. Atkinson (1980) has indicated that these can be as little as 40 %, and may decrease considerably due to root shrinkage during drying cycles (both diurnally and over longer drying periods).

Using a profile wall technique down to 1 m, Baldwin and Stewart (1987 noted that 77 % of roots 1 mm in diameter were in the top 300 mm of soil for *E. grandis* trees growing at a spacing of 1.5 m × 3 m at Mildura (Australia). Using a core sampling technique in this region they noted that roots 1 mm in diameter comprised 73 % of all roots counted and contributed to 85 % of the total length in this region. They also excavated the roots from a 2.80 m × 2.80 m × 1.20 m block of soil around an irrigated six-year-old *E. grandis* tree. The length and mass of these roots, is presented in **Table 2.3.** Measurements were not made below 300 mm for roots 2 mm in diameter. The tap root of the excavated root system was also noted to have been only 200 mm long and had appeared to be dead for some time. Intra-tree grafts with incomplete xylem fusion were also observed.

The L_a value for roots 1 mm in diameter from the six-year-old *E. grandis* tree (Table 2.3) excavated by Baldwin and Stewart (1987) is about three times the value of 374 m m^{-2} reported for roots of the same size in 29-year-old *E. regnans* forest (Incoll, 1979), while the L_m value of 3.13 kg m^{-2} compares reasonably with that of 4.54 kg m^{-2} for forest trees of *E. obliqua* and *E. dives* (Feller, 1980) and 6.19 kg m^{-2} for forest dominated by *E. signata* (Westman and Rogers, 1977).

The poor tap root development of the irrigated *E. grandis* tree (Table 2.3) contrasts with that of natural stands of *E. regnans* where young trees may produce a substantial tap root (Ashton, 1975; Incoll, 1979), although in 26-year-old stands the tap-root may be completely dead or missing (Ashton, 1975). For mature forest dominated by *E. signata*, tap roots contributed 19.6 % of the root mass

Table 2.2 Root characteristics of *E. globulus* trees at four different ages (Mathur *et al.*, 1986)

Parameters	Age of trees (years)			
	1	3	10	20
Lateral root extension (m)	3.12	5.12	6.40	9.52
Length of tap root	1.49	2.31	3.94	5.52
Area of concentration (m^2)	3.13	9.18	19.52	20.26

Table 2.3 Length and mass of roots in the 0 to1 m soil horizon for irrigated six-year-old *E. grandis* trees grown at Mildura, Australia. Data are from an excavated area of 7.84 m^2 (Baldwin and Stewart, 1987)

Root diameter (mm)	Root length (m m^{-2})	%	Root mass (kg m^{-2})	%
0 - 1	1029.8	86.3	0.11	3.5
> 1 - 2	114.2	9.6	0.07	2.3
> 2 - 5	28.7	2.4	0.21	6.7
> 5 - 10	12.9	1.1	0.34	11.0
> 10 - 20	5.4	0.4	0.48	15.4
> 20	2.2	0.2	1.92	61.1
Total	1193.2	100	3.13	100

(Westman and Rodgers, 1977).

Where a plant root system is non-uniformly distributed through the soil, as is usual, and has more than an adequate capacity to supply water to the tree, then the initial pattern of water depletion will reflect root density, assuming no great variations in soil hydraulic conductivity or root resistance. However, as the soil dries, the rate of water depletion will proportionally increase from those areas of soil with relatively low root densities (which remained relatively moist) and decrease from the drier areas of high root density. The rate of water depletion from the former areas (per unit root length) then will necessarily be higher than that found initially and possibly higher than that from the now drier areas of high root density, because of the higher flow rates needed to maintain transpiration from the now comparatively restricted root system (Atkinson, 1978).

Stuart-Crombie, Tippett and Gorddard (1987), in an attempt to simulate effects of *Phythophthora cinnamomi* infection of *E. marginata* saplings growing in Darling (Australia), noted that normal water relations were maintained with as little as 50 % or the root system remaining, when the surface soils were moist. However high variabilities in stomatal conductance and leaf water potential occurred when the soils were dry, suggesting no excess in root capacity under such conditions. Stomatal conductance was more sensitive to root loss due to severe pruning than was leaf water potential, where predawn leaf water potentials were relatively unaffected by removal of up to 80 % of roots irrespective of whether the surface soils were dry or moist. They concluded by suggesting that the vertically descending "sinker" roots, characteristic of *Eucalyptus* spp. in unimpeding deep soils, were essential to tap water held deep down in the soil profile so as to ensure plant survival during drought periods. Destruction of such roots by *P. cinnamomi* had greater effects on the water relations of *E. marginata* in summer than shallow roots.

Greenwood and Beresford (1979) inferred from their studies that since the average transpiration of a number of species of two-year-old trees growing at Popanyinning (Australia) increased threefold between early and late summer, that the roots of these trees had grown to reach the water table which was at a depth of between 3 and 5 m by the end of the summer season.

Similarly, Carbon, Bartle and Murray (1981) reported studies of water stress and transpiration rates from natural *E. marginata* and *E. calophylla* forest growing in five different catchments. Two of three catchments were in a 1200 mm annual rainfall region and three in a 700 mm region, all being in the Darling Range (Australia). The soil consisted of 1 m of surface sand overlying 3 m of sandy loam above 21 m of fine kaolinite clay. A permanent water table existed at a depth of 15 m at 15 out of 25 sites. They found little difference between *E. marginata* and *E. calophylla* in their transpiration

responses, subsequently confirmed by Colquhoun, Ridge, Bell, Loneragan and Kuo (1984), and little difference between sites, except in late summer when transpiration rates were generally found to be higher from sites with permanent water tables.

More recently Greenwood, Klein, Beresford and Watson (1985) reported studies on seven-year-old trees growing at Bannister in the Hothan valley (Australia). Their studies were conducted on two plantations, one up-slope and the other immediately above a saline seep. Annual evaporation from pasture in that area was 390 mm regardless of the position on the slope. Annual evaporation (interception + transpiration) from trees at the up-slope site was 2300 mm for *E. maculata* and 2700 mm for both *E. globulus* and *E. cladocalyx*, while at the mid-slope site values were 1600 mm for *E. wandoo*, 1800 mm for *E. leucoxylon* and 2200 mm for *E. globulus*. They concluded that to support these high rates, which exceeded the annual rainfall of 680 mm by a factor of approximately four, the trees must have been extracting water directly from groundwater. Soil coring studies which revealed roots at 6 m, 1 m below the water table at the time, supported this hypothesis.

Calder (1986) commented on this by noting that evaporation rates of this magnitude exceeded the rate that could be supported by the input of solar radiation alone and implied considerable advection of heat from the air mass moving over the forest. He suggested this was indeed possible and had been verified for wet forests (Calder, 1985).

2.6 Catchment water balance

A number of catchment studies on water use by *Eucalyptus* spp. have been reported, mostly from Australia, India and South Africa. However the results of these are usually site specific. Extrapolation to other areas is difficult since the mechanisms responsible for water loss are complex, and in the absence of an applicable generic model as a guide (Reynolds, Acock, Dogherty and Tenhunen, 1989) sufficient information is seldom published for meaningful comparisons to be made. A general pattern shown by these studies is similar to that found in the majority of catchment studies, which have compared runoff from forested and unforested catchments. Typically the runoff is usually less from forested catchments (Hibbert, 1967; Bosch and Hewlett, 1982; Calder, 1986).

Other catchment studies in Australia involving *Eucalyptus* spp. have been reviewed by Lima (1984).

Mathur, Ram Babu and Singh (1976) found, from catchment studies carried out near Dehra Dun (India) that a mixed plantation of *E. grandis* and *E. camaldulensis* reduced runoff by *ca* 28 % compared to the original brush vegetation *i.e.*, 14 mm of an annual runoff of 50 mm.

Similarly at Mokobulaan (South Africa), Van Lill *et al.* (1980) noted an apparent mean reduction in catchment streamflow of approximately 300 mm per year due to afforestation with *E. grandis* trees (*ca.* 25 % of mean annual rainfall). They also gave special mention of the fact that the soils in the area of study were extremely shallow - "only a few tens of millimetres deep", as discussed by Nänni (1971).

Interestingly from studies carried out at Lidsdale (New South Wales, Australia), Smith, Watson and Pilgrim (1974) concluded that conversion of *Eucalyptus* forest to *Pinus* forest resulted in a 50 % reduction in runoff (annual rainfall = 900 mm). More recent work (Dunin and Mackay, 1982; Sharma, 1984) indicated that transpiration losses from the two communities are similar, the differences in total loss being due to differences in interception. Similar results have been presented by Pook and Moore (1991a; b) where the storage capacities of the trees studied in southeastern New South Wales

(Australia) were 54 *l* and 11.3 *l* for *P. radiata* and *E. viminalis* respectively. These accounted for 26.5 % and 8.3 % interception loss of incident rainfall respectively. They also cited literature where hydrological resources modelling indicated substantial reductions in water yield resulting from increased total evaporation losses, mainly due to interception, following conversion of the land under study from *Eucalyptus* forest to *Pinus* forest.

Successful forest catchment hydrological modelling is likely to be most justified in: (a) the research field, where some sort of model is essential as a framework for formal and organised hypothesis formulation; (b) forest management and risk assessment, where forest managers may use them to estimate sustained productivity or predict the effects of management actions; (c) ecological impact assessment on both local and global scale.

Water balance models are, superficially, structured the same way whether the objective is to (i) calculate soil water content (or potential) as an input into a tree growth model or for determination of water availability to a forested stand; or (ii) calculate stream flow and water yield of a catchment.

If it is assumed that the water removed from a root zone is extracted uniformly and the rainfall reaching the soil is distributed uniformly, the forest water balance (rate) may be written as (Whitehead and Kelliher, 1991a; b):

$$R + F = (P - E_t - E_i - E_u - E_s) - (W_j - W_{j-1})/\Delta t \qquad 2.4$$

where R is the average rate of runoff, F is the average rate of drainage from the root zone, P is the average rate of rainfall, E_t is the average rate of transpiration from the dry tree canopy, E_i is the average rate of evaporation from the tree canopy and stems wetted by rainfall, and E_u and E_s are the average rates of evaporation from the understorey vegetation and forest floor respectively, over the time period Δt. The quantity $W_j - W_{j-1}$ is the change in root zone water storage (ΔW) during the j_{th} period.

2.7 Plant evaporative processes

Evaporative loss from vegetation can be differentiated into two essentially different components, namely: (i) interception, and (ii) transpiration. Interception is merely a physical process which involves the evaporation of water from the wet outer plant surfaces during and after rainfall. Transpiration is a physiological process involving the uptake of water by plant roots and transfer to and through the leaves, which is subject to more complex mechanisms.

2.7.1 Rainfall interception

Evaporative losses of intercepted water are determined by: (i) the rainfall duration and intensity, (ii) wet time evaporation rates, and (iii) the amount of water that is stored on the tree canopy (Calder, 1986). Consequently it is likely to vary according to tree canopy structure and the nature of the weather and climate in a particular area.

The amount of water stored on a tree (C_j) in any time period (j) following rainfall (P) can be determined from (Rutter, Kershaw, Robins, and Morton 1971; Rutter, Morton and Robins, 1975; Rutter and Morton, 1977):

$$C_j = C_{j-1} + [(1-p)P - E_{ic} - H_c]\,\Delta t \qquad 2.5$$

where p is the proportion of free throughfall (rain falling on to the ground without being intercepted by

the tree) and the terms E_{ic} and H_c are the average rates of evaporation and drainage of intercepted rainfall from the tree during the period Δt, respectively.

If S is the tree surface water storage capacity, then the fraction of the tree that is completely wet in the j_{th} period is C_j/S (Shuttleworth, 1976). Drainage of intercepted rainfall is expected to be zero when $C_j \leq S$. When rainfall directed to tree surface water storage is greater that S, over a period of time, drainage is taken as the amount of water on the canopy after evaporation has taken place ($[(1-p)P - E_{ic}]\,\Delta t$) which exceeds the remaining water storage capacity ($S > C_{j-1}$) (Kelliher, Black and Price, 1986; Whitehead and Kelliher, 1991a; b).

Interception storage capacity for a tree canopy is typically determined by the product of the total leaf surface area of the tree per unit ground area (leaf area index) and the water holding capacity per unit leaf area. Storage capacities of 2.2 to 8.3 mm m^{-2} have been reported on tropical rain forest trees (Herwitz, 1985). However, while *Eucalyptus* spp. may have storage capacities per unit leaf area similar to those of other tree species (Aston, 1979), they are likely to exhibit lower total interception storage capacities due to lower leaf area indices. In some cases this may be less than a half those of other tree species (Anderson, 1981). Compared to leaves, storage by woody parts such as trunk and branches, mostly remain undetermined.

Intercepted water lost through evaporation during rainfall is likely to become decreasingly significant, compared to that from storage in the canopy after rainfall cessation, with decreasing storm duration and increasing storm intensity and canopy sparseness. Some percentage rainfall loss data due to interception by some *Eucalyptus* spp. in relation to different parts of the world is presented in **Table 2.4**.

Evaporation rates from wet trees tend to be much higher than those of shorter vegetation as they present a relatively rougher surface to wind, increasing forced eddy convection which is the dominant mechanism responsible for the vertical transport of water from leaves to the atmosphere (Eq. 2.6 and **Fig. 2.3**).

The evaporation rate of intercepted water may be expressed as the sum of an equilibrium evaporation rate term and a transport term (Monteith, 1965):

$$E_I = [s/\gamma\,(R_n - H)]/[\,(s/\gamma + 1)\,\lambda] + g_{as}\,\rho\,c_p\,D_l \qquad 2.6$$

where E_l is the evaporation rate of intercepted water (mol m^{-2} s^{-1}), s the slope of the relationship: saturation vapour pressure *vs* air temperature, $\gamma = c_p P/\lambda$ *i.e.* psychometric constant (kPa K^{-1}), R_n the net irradiance (J m^{-2} s^{-1}), H the flux density of heat into storage (J m^{-2} s^{-1}), λ the molar latent heat of

Table 2.4 Comparative interception ratios of different *Eucalyptus* spp. from different parts of the world (Calder, 1986)

Species	Location	Mean annual rainfall (mm)	Interception (% rainfall)
E. hybrid	India	1670	12
E. globulus	India	1150	22
E. camaldulensis	Israel	700	15
E. regnans	Australia	810	11
E. regnans	Australia	1660	19
E. obliqua	Australia	1200	15

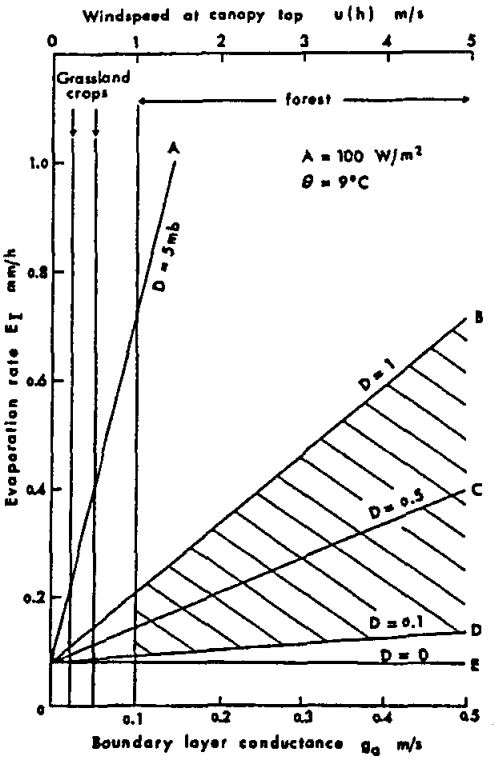

Fig. 2.3 The relation between the rate of evaporation of intercepted water (E_i), and boundary conductance (g_{as}) at a range of water vapour saturation deficits (D_i). The ranges of likely boundary conductances for grass, heath, shrub and forest canopies are shown. The shaded area includes the likely rates of evaporation from wet canopies of tree crops (Jarvis and Stewart, 1979)

vaporization of water (J mol^{-1}), g_{as} = surface conductance from the canopy to an independent mixed air layer above the canopy (mol m^{-2} s^{-1}), ρ the air density (kg m^{-3}), c_p the molar heat capacity of air at constant pressure (J mol^{-1} K^{-1}), D_i the water vapour saturation deficit of the planetary boundary air layer or at a reference height in the mixed layer well above the surface of the forest canopy (kPa). The constants λ, C_p and ρ are all weakly dependent on air temperature.

2.7.2 Transpiration

Transpiration losses from *Eucalyptus* spp., as for most other vegetation types, are likely to be determined principally by: (i) the climatic evaporative demand (which is related to prevailing solar irradiance); ii) atmospheric humidity deficit; (iii) air temperature; (iv) windspeed; (v) physiological response mechanisms which control stomatal apertures in response to environmental conditions (particularly soil water stress and atmospheric humidity deficits); (vi) soil water availability to roots, and (vii) the canopy structure (notably leaf area index).

One would expect the transpiration of tree crops, in terms of evaporation *per se*, to follow the water vapour saturation deficit of the ambient air-stream more closely than shorter agricultural vegetation which would be more significantly influenced by net irradiance (Fig. 2.3). Jarvis (1985) has presented a concept of using empirical coupling constants (Ω) in mathematical models on transpiration to take these phenomena into consideration.

2.7.2.1 Canopy conductance

Rates of transpiration (E_t) and evaporation (E_{ic}) from the tree canopy (excluding stems), may be

calculated using the Penman-Monteith equation (Monteith, 1965), assuming similarity between tree canopy aerodynamic conductances for sensible heat and water vapour (Hancock, Sellers and Crowther, 1983). This is based on one-dimensional aerodynamic and energy balance theory. When applied to forest stands, the canopy is often treated as a single layer in the Penman-Monteith model. The assumptions necessary in taking such a "big leaf" approach have been discussed by Jarvis *et al.* (1981). Total evaporation from a partially wet canopy may be expressed as:

$$E = [(s A + \rho c_p D_m g_A)/\lambda)] \cdot [\frac{1 - C/S}{s + \gamma (1 + g_A/g_c)} + \frac{C/S}{s + \gamma}] \qquad 2.7$$

where $E = E_\tau + E_{ic}$. A is the available energy flux density to the tree. The parameter g_A is the bulk aerodynamic conductance for the canopy from the surface to the reference height above it. Canopy conductance (g_c) may be given by ($L \times g_s$) where L is the leaf area (all surfaces) and g_s is the median stomatal conductance for the leaves in the canopy. When $C = 0$ this equation reduces to the Penman-Monteith equation where $E = E_t$ (Rutter *et al.*, 1975).

The importance of coupling between the leaves in a canopy and the surrounding air in determining the proportional effects of stomatal regulation and energy input on the rate of transpiration has been pointed out by McNaughton and Jarvis (1983) and Jarvis and McNaughton (1986). By adopting the approach of Jarvis (1985), the Penman-Monteith equation for a completely dry canopy may be written in the form:

$$E_t = \Omega E_{eq} + (1 - \Omega) E_{imp} \qquad 2.8$$

where the coupling coefficient, Ω, sets the relative importance of the two terms: (i) equilibrium rate of transpiration (E_{eq}), and (ii) imposed rate of transpiration (E_{imp}). Using the notation: A for the energy flux density available for transpiration, ε as the change of latent heat content relative to the change of sensible heat content of saturated air (s/γ) and P as the atmospheric pressure, the equilibrium rate of transpiration equation is:

$$E_{eq} = \gamma \varepsilon A/[(\varepsilon + 1) \lambda] \qquad 2.9$$

and that for the imposed rate of transpiration is:

$$E_{imp} = g_c D_m|/P \qquad 2.10$$

The air water vapour saturation deficit measured above tree height but within the canopy boundary layer (D) is related to D_m by:

$$D = \Omega D_{eq} + (1 - \Omega) D_m \qquad 2.11$$

where

$$D_{eq} = \gamma \varepsilon A/[(\varepsilon + 1) c_p g_c] \qquad 2.12$$

and coupling factor (Ω) is:

$$\Omega = (\varepsilon + 1)/(\varepsilon + 1 + g_A/g_c). \qquad 2.13$$

Aerodynamic conductance for transfer of water vapour (g_A) is frequently calculated for a canopy from the well-known momentum transfer equation (Monteith, 1965):

$$1/g_A = [ln\,(z-d)/z_o]^2/(k^2\,u) \qquad 2.14$$

The reference height above the canopy (z), windspeed (u), roughness length of the forest surface (z_o) and the zero plane displacement height (d) are measured values, while k is von Karman's constant. The canopy is considered to be a single layer sink for momentum and a source or sink of water vapour and sensible heat situated at one height (Monteith, 1965).

Because of the tall, aerodynamically rough nature of forest canopies: (i) g_A is much larger than g_c, and (ii) values of Ω are often low (*ca.* 0.1) and it follows that transpiration can be closely approximated by E_{imp} (Jarvis and Stewart, 1979). Consequently transpiration is largely driven by D_m and there is significant stomatal control of transpiration. In contrast values of Ω for short crops such as pasture are comparatively higher (*ca.* 0.9) and g_A is much less than g_c. The canopy is poorly coupled and transpiration is driven mainly by available energy and air temperature.

Values of Ω calculated for a number of crops has been presented by Jarvis and McNaughton (1986). The significance of the structure of vegetation on the degree of coupling is well illustrated in an Amazonian forest (Roberts, Cabral, and Aguiar, 1990). The value of Ω increased from 0.3 at the top of the canopy (36 m) to 0.8 in the understorey layer (1.5 m above ground level). This is consistent with less mixing of the air at lower levels in deep, multi-storied canopies (Jarvis and McNaughton, 1986).

The rate of evaporation from partially wet canopies is very sensitive to g_A (Raupach and Finnigan, 1988). These are high and occur largely during and immediately after rainfall (Gash, Wright, and Lloyd, 1980; Pearce and Rowe, 1981). The dominant driving force for evaporation is convective energy (Pearce, Rowe and Stewart, 1981) and rates are influenced more by the value of D_m during and immediately after rainfall than by the water storage capacity of the canopy (McNaughton and Jarvis, 1983). On an annual basis, loss of rainfall by evaporation from wet canopies is frequently a significant component of the water balance for forest canopies (Whitehead and Kelliher, 1991).

2.7.2.2 Stomatal conductance

Stomata begin to close when the turgor of guard cells decreases. Turgor changes that control stomatal aperture appear to be caused by gain or loss of ions, primarily potassium. During stomatal opening a net influx of potassium ions from an external solution in adjacent cells has been shown for many species (Allaway and Milthorpe, 1976). Both histochemical and microprobe studies show a linear dependency of stomatal opening on potassium content of guard cells (Humble and Raschke, 1971).

Evidence indicates that potassium uptake by guard cells may involve a passive or active uptake mechanism, or both. Production of organic acids in cells and export of hydrogen ions could increase electrochemical potential in cells to cause passive uptake of potassium ions. Alternatively potassium uptake against an electro-chemical potential gradient might be mediated by an active potassium pump (Allaway and Milthorpe, 1976).

Typically, three daily patterns of stomatal aperture have been reported: (i) stomata open in the morning, closed for a period during the middle of the day, reopen in the afternoon, and finally closed late in the day as the solar irradiance decreases; (ii) stomata open early in the morning, closed rather early in the day and remain closed until the following morning, or (iii) on days of low water vapour pressure deficit, abundant soil water and light overcast conditions, stomata remain open until evening when photosynthetically active radiation declines.

From the literature, it would appear that *Eucalyptus* spp. show very different stomatal responses between species and between sites, possibly reflecting physiological adaptive differences to the environmental conditions from which they originated.

Greenwood and Beresford (1979) found considerable variation in transpiration rates between various *Eucalyptus* spp. at sites of different annual rainfall in western Australia, and that the species with the highest transpiration rate was different at each site. *E. globulus* was highest at an 850 mm annual rainfall site, *E. cladocalyx* at a 500 mm site, and *E. wandoo* at a 420 mm site.

In the past *Eucalyptus* spp. have been classified into those that: (i) show "stomatal control" with significant diurnal and seasonal regulation, where stomatal resistances are typically low in the morning but increase later in the day and overall with seasonal progression broadly in line with increased vapour pressure deficit, *e.g. E. maculata, E. resinifera, E. saligna, E. wandoo* (Colquhoun *et al.*, 1984), *E. globulus* (Pereira, Tenhunen and Lange, 1987) and *E. grandis* (Dye and Olbricht, 1991), and (ii) show little stomatal control of water loss with low leaf resistance throughout the day, with no evidence of a correlation between stomatal resistance and atmospheric water vapour pressure deficit, *e.g. E. marginata, E. calophylla* (Colquhoun *et al.*, 1984), *E. microcarpa* (Attiwill and Clayton-Greene, 1984) and *E. terminalis* (Hoffmann, Barett and Fox, 1987).

Evidently species differ in the role played by stomatal functioning in assuring success under water deficiency. Levitt (1980) has classified species into those that: (i) are able to respond to early signs of drought in the air and soil and postpone dessication by maintaining high Ψ for extended periods of drought through use of a high degree of stomatal control. These he termed "drought avoiders of the saving type"; (ii) can keep their stomata open, but are able to extract water from the soil rapidly enough to compensate for water loss, typically achieved by genotypes with deep and large root systems or where rapid changes in water potential can take place, either by changes in turgor pressure or osmotic potential. These he termed "drought avoiders of the spending type".

Stomatal closure during the middle of the day has been reported for many species of forest and orchard trees (Kramer and Kozlowski, 1979). Although midday stomatal closure has been attributed to several causes, an important factor is the lag of water absorption behind transpiration. This induces leaf dehydration and a reduction in leaf Ψ to a critical level associated with stomatal closure. When leaf water deficits are not severe, midday stomatal closure may also be observed under high temperature conditions (Kozlowski, 1976).

The time of stomatal closure during leaf water deficits may vary with leaf age, stomatal size and location. Typically the stomata of shade leaves are more sensitive than those of sun leaves, and stomata of young leaves often close sooner than those of old leaves in response to water deficits. Young leaves of *E.* marginata transpired about 20 % less (per unit leaf area) than mature leaves on sunny days because of more effective stomatal closure in the young leaves (Doley, 1967). Similar responses were found in young and old leaves of *E. stuartiana* (Henrici, 1946).

In both herbaceous and woody amphistomatous plants stomata of the upper (adaxial) and lower (abaxial) leaf surfaces often close at different critical values of Ψ. Abaxial stomata of *E. camaldulensis* seedlings closed gradually at Ψ values between -0.8 to -1.2 MPa. Those of the adaxial surface closed rapidly at Ψ values near -0.9 MPa (Pereira and Kozlowski, 1976). Environmental and biological control of stomatal aperture is discussed by Pospisilova and Solarova (1980).

The critical leaf Ψ value at stomatal closure for different species varies for different clones and cultivars (Pallardy and Kozlowski, 1979) and is modified significantly by factors such as solar irradiance, CO_2 content of intercellular spaces, air humidity, windspeed, leaf age and, osmotic adjustment. Absolute causal relationships for such responses have not yet been established which has led some authors to conclude that the patterns in stomatal regulation observed may be due to factors besides water pressure deficit.

Pereira *et al.* (1987) reported that the stomata of *E. globulus* trees, growing in a winter rainfall area near Lisbon (Portugal), became more closed as the season became warmer and drier from winter to summer and were generally more closed in the afternoon than the morning at these times, at the same rates of net photosynthesis, temperature or leaf to air water vapour partial pressure difference (**Fig. 2.4**). They concluded that the observed asymmetry in diurnal patterns of stomatal conductance (g) and photosynthesis (P_n) could not be explained by the occurrence of a higher ambient air water vapour saturation deficit in the afternoon alone.

Alternatively the change in the relationship between P_n and g during the course of the day may also be explained by a mid-day high in solar irradiance or air temperature and by different phytohormonal regulation in the morning compared to the afternoon (Pereira *et al.*, 1987). These could possibly be related to photosynthesis and assimilate demand (Chaves, 1991). It also seems plausible that when plants are subjected to stress, abscisic acid (ABA) accumulated in the chloroplast is released into the apoplast, even at stress levels too mild to promote ABA synthesis (Schulze, 1986), presumably as a result of a pH-dependent process (Hartung, Slovik, and Baier, 1990). Some evidence has been presented relating stomatal closure during midday with an increase in leaf ABA content (Burschka, Tenhunen, and Hartung, 1983; Pereira, Chaves, Rodrigues, and Davies, 1989; Quarrie, 1990).

In the absence of water stress stomata generally opened when the summed PAR incident on both leaf surfaces was 100 mol m^{-2} s^{-1}. Maximum leaf conductance reached levels of 245 mmol m^{-2} total leaf area s^{-1} (Pereira *et al.*, 1987). This is similar to those reported for adult leaves of other *Eucalyptus* spp. under field conditions and in the absence of water stress in S. and S.E. Australia *e.g.*, *E. pauciflora* (Slatyer and Morrow, 1977; Körner and Cochrane, 1985), *E. Fasciculosa* and *E. Obliqua* (Sinclair, 1980), but higher than more xeromorphic species *e.g.*, *E. microcarpa* (Attiwill and Clayton-Greene, 1984).

2.7.2.3 Soil water availability

Bates and Hall (1981), Blackman and Davies (1985) and Gollan, Passioura and Munns (1986), have demonstrated that stomata were less open in plants with partially droughted root systems, despite leaf turgors at levels similar to those experienced during times of adequate water availability, than plants in a thoroughly wetted soil. They suggested that a reduction in the cytokinin/ABA balance due to the partial droughting of the roots was responsible for the observed diminished stomatal apertures.

In their work, Gollan, Turner and Schulze (1985) concluded that soil water availability rather than instantaneous values of leaf water potential (Ψ) were responsible for many of the observed fluctuations in leaf gas exchange. This might well explain the phenomenon of decreasing conductances as the season became warmer and drier in the work of Pereira *et al.* (1987).

Recent research increasingly supports earlier suggestions (Hsiao, 1973) that plant responses to water deficit are often not just by the chemical potential of the water *per se*, but rather due to other

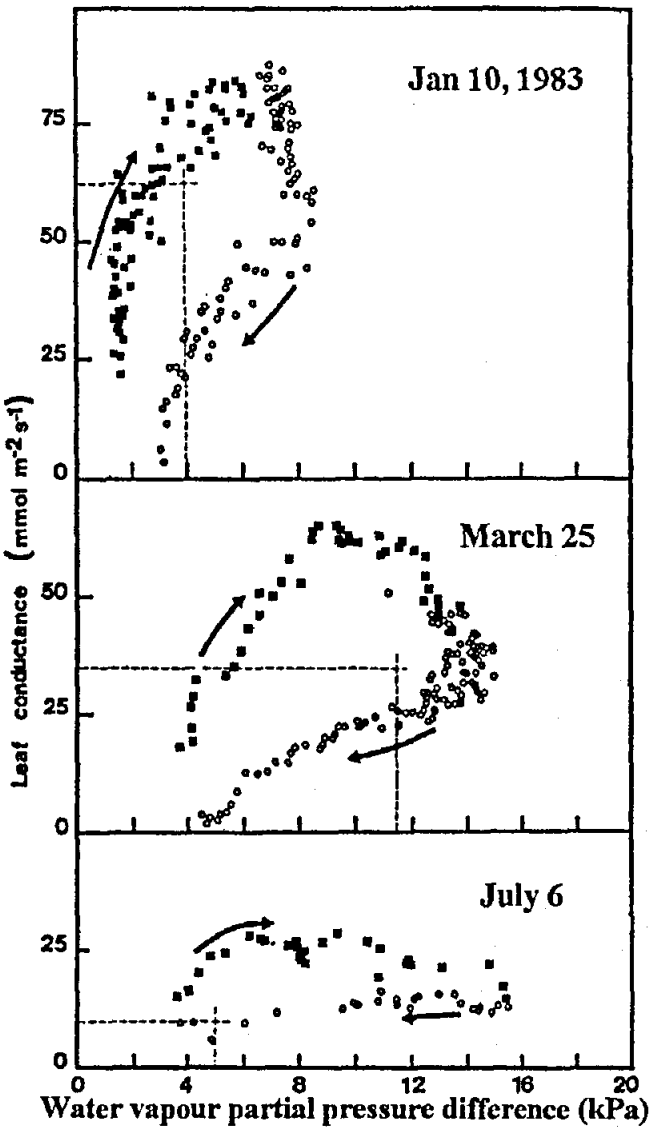

Fig. 2.4 A. Hysteresis was observed during the course of the day in the relationship between leaf conductance to water vapour on a single leaf surface area basis (g) and leaf-to-air water vapour partial pressure difference (D'). B. Relationship between net photosynthetic rate P_n and leaf conductance to water vapour pressure on a projected leaf area basis (g). Dashed lines delimit the period during which light limitation of stomatal conductance occurred (PAR < 100 mol m^{-2} s^{-1}).
Open circles refer to the afternoon and filled squares to the morning. Data shown was obtained on (i) a winter day (January 10, 1983); (ii) a spring day (March 25, 1983) and (iii) a day in early summer (July 6, 1983)] (Pereira *et al.*, 1987)

factors varying in concert with leaf or root water potential such as turgor (Bradford and Hsiao, 1982), increased concentrations of solutes (Kaiser, 1987) or chemical compounds coming from the roots (Zhang and Davies, 1989).

Theoretically predawn (base) leaf water potential (Ψ_b) may be considered an approximate measure of rhizosphere equilibrium water potential, under conditions of zero or low transpiration at night and where root pressurization effects are ignored. Consequently it is often used as an indicator of overall water stress in the field (typically Ψ_b decreases from about -1 MPa with increasing water stress). This is well illustrated in the work of Pereira *et al.* (1987), (Fig. 2.5) where maximum leaf conductance (g) decreased with decreased Ψ_b, (when Ψ_b was less than -1.0 MPa, values of maximum g were

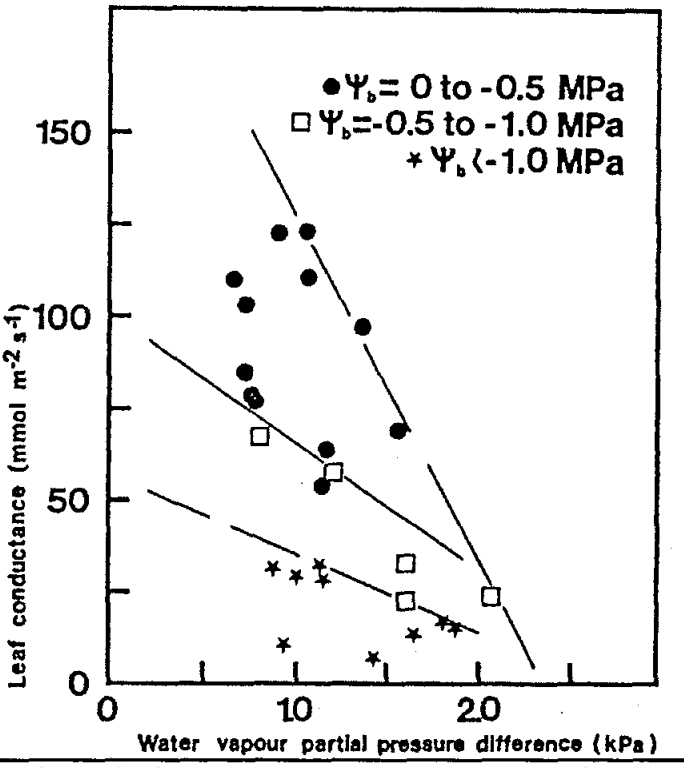

Fig. 2.5 A. Changes in maximum leaf conductance to water vapour on a single surface leaf area basis (g) in response to predawn leaf water potential (ψ_b). B. Changes in daily maximum leaf conductance to water vapour on a single surface leaf area basis (g) in response to the leaf to air water vapour partial pressure difference (D') at different predawn leaf water potentials (ψ_b), C. Relationship between maximum photosynthetic rates (P_n) and leaf conductance to water vapour on a projected leaf area basis (G) at the time of observation of maximal net photosynthetic rates, at different times over a year (Pereira *et al.*, 1987)

consistently low). Similar results have been presented by Schulze, Lange, Kappen, Evenari, and Buschbom (1975); Schulze and Küppers (1979), Lösch, Pereira, and Lange (1982), Pezeshki and Hinckley (1982), Körner and Cochrane (1985) and Turner, Schulze and Gollan (1985).

In the work of Pereira *et al.* (1987) discussed above, maximum g decreased with increasingly severe plant water stress as the season progressed, as did the slope of the decline in g with increasing water leaf to air water vapour partial pressure difference. Interestingly, at similar plant water stress, decreasing maximum values of g were also associated with decreasing leaf to air water vapour partial pressure differences (D') in Fig. 2.5B, the influence of which were greatest when Ψ_b was high.

Note also that in summer low rates of leaf conductance appeared to limit net photosynthetic rate (Figs 2.4 and 2.5). This is of particular importance because it emphasises a dependence of growth on water availability, where tree biomass production is ultimately dependant on net photosynthesis. Hence, ignoring relative photosynthetic efficiencies, one can speculate that stomatal behaviourial differences between species are likely to indicate yield differences and also reflect relative adaptions to drought tolerance.

Individual leaf water potential measurements are, however, likely to be subject to the nature of the leaf under consideration (*e.g.* metabolic activity and storage capacity) and to the path of water between roots and the foliage itself. Zimmermann (1983) has hypothesised that a priority system for water is

likely to be established in foliage depending on the development of conducting elements and differences in resistance to water movement at different junctions (*i.e.* root to stem, stem to branch, branch to branch and branch to leaf). Consequently it is likely that leaf water potential will vary considerably in the canopy, increasing the importance of replication of measurements within a canopy which practically is often a limiting factor in determinations of this nature.

2.8 Water movement through trees

Long distance water flow in trees occurs through the lumens of non-living tracheary elements (vessels and tracheids) of the xylem and through the lateral pits that interconnect the tracheary elements (Esau, 1965). Pits are thin and porous depressions in the wall where secondary wall material is absent. A vessel is composed of a series of vessel elements (vessel members) stacked end-to-end and interconnected by perforations at the end walls. Since vessels, like tracheids, are of finite length, water must eventually move from vessel to vessel or from tracheid to tracheid through lateral pit pairs.

Vessels can range from less than 1 mm to many meters in length in different species (Zimmermann and Jeje, 1981; Ewers, Fisher and Chiu, 1990). Coniferous trees lack vessels, and therefore are entirely dependent upon tracheids for their water transport. Tracheids are individual elongated conducting cells ranging in length from a mean of 2 to 6 mm (Panshin and de Zeeuw, 1980). In young stems tracheids are often 1 mm or less in length.

In addition to the tracheary elements, wood (secondary xylem) contains other cell types, including fibres and living parenchyma cells. Fibres are thick-walled cells specialised for mechanical support. Xylem parenchyma cells are involved with water and carbohydrate storage, and may be crucial in defence against disease. Non-living cells cannot respond to wounding or parasite entry, but living cells can and do by excreting substances (*e.g.*, gums and lignin precursors) or by growing into the vessel lumens to form tyloses (Panshin and de Zeeuw, 1980; Zimmermann, 1983; Bonsen and Kucera, 1990). These and other responses by living cells help to limit the spread of pathogens in the xylem. Some of these protective responses are also a normal part of heartwood formation, the non-conducting portion of the xylem, which is internal to the actively conducting sapwood and is incapable of water conduction (Esau, 1965; Panshin and de Zeeuw, 1980).

In heartwood, the parenchyma cells are non-living vessels filled with gums or tyloses, and pit membranes are often encrusted with "extractives" (Wheeler, 1983). The number of growth layers of sapwood varies considerably among species as well as within individual trees. The wood of trees is often designated as: (i) nonporous (*i.e.* without vessels as in conifers *e.g., P. ponderosa*, Ponderosa pine) or (ii) porous (**Fig. 2.6**). Porous woods can be classified as: (a) ring-porous, with extremely large early wood vessels and much smaller latewood vessels (*e.g. Castanes dentata*, American Chestnut), and (b) diffuse porous (*e.g. E. grandis*, Blue gum), where the vessels are rather uniform in diameter. Intermediate situations are classified as: (c) semi-ring-porous or semi-diffuse-porous. It should be noted that the number of growth rings tends to decrease with height above the ground (Ewers and Cruiziat, 1991).

2.8.1 Poisuille-Hagen equation

Many studies have applied Poiseuille's law to model xylem transport. In the nineteenth century Hagen and Poiseuille independently arrived at an equation (modified here) for fluid flow through a bundle of perfectly cylindrical pipes:

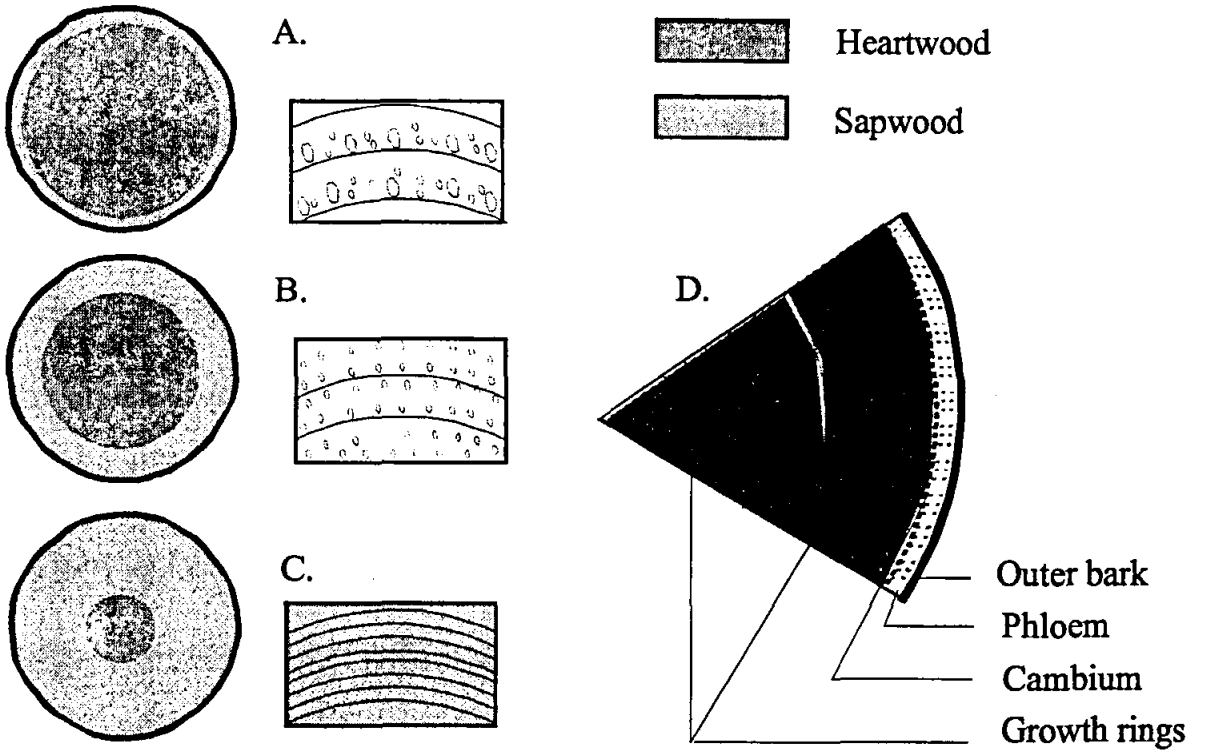

Fig. 2.6 Arrangement of heartwood, sapwood, vascular cambium, phloem, and outer bark in stems of trees. The number of layers of sapwood fewest in ring-porous species (A), intermediate in diffuse porous species (B), and greatest in nonporous wood (C). Transverse section details are also shown (D) (Ewers and Cruiziat, 1991)

$$k_h = (\pi\rho/128\eta)\sum_{i=1}^{n} D_i^4 \qquad 2.15$$

where k_h is the hydraulic conductivity (conductance per unit pressure gradient) of a bundle of pipes of different diameters and is the proportionality constant between flux (F, kg s^{-1}) and pressure gradient (dP/dx, MPa m^{-1}) causing the flux, ρ is the density of the fluid (kg m^{-3}), η is the dynamic viscosity of the fluid (MPa s^{-1}), D_i is the diameter of the i th pipe (m), and n represents the number of pipes in the bundle.

From the Poisuille-Hagen equation it is evident that the hydraulic contribution of one large vessel four times the median size will contribute the same conductivity as $4^4 = 256$ median diameter vessels. This demonstrates the marked effect of a few large vessels on the hydraulic conductivity of stems. It is not unusual for the median vessel diameter to be one half to one quarter the diameter of the largest vessels in wood (Tyree and Zimmermann, 1971; Zimmermann and Brown, 1971; Panshin and de Zeeuw, 1980; Gibson, Calkin and Nobel, 1985; Calkin, Gibson and Noble, 1986; Sperry and Tyree, 1988; Sperry and Tyree, 1990; Sperry, Tyree and Donnelly, 1988; Ewers and Cruiziat, 1991; Tyree and Ewers, 1991).

2.8.2 Pipe model

Leonardo da Vinci may have been the first person to suggest that the relative size of tree components follows a pattern. He wrote " ... the branches of a tree at every stage of its height when put together are equal in thickness to the trunk" (Richter, 1970). More than 400 years later Japanese researchers expanded upon this relationship, developing what they termed "...the pipe model theory of tree form" (Shinozaki, Yoda, Hozumi and Kira, 1964a; b). The plant was viewed as an assemblage of "unit

pipes" each of which supports a unit of leaves *i.e.*, a given unit area of water-conducting tissue at any point in the tree stem is necessary to supply water to a given unit mass of transpiring foliage above that point. This suggests a functional relationship between the water conducting stem xylem and transpiring foliage (Huber, 1928; Kline, Reed, Waring and Stewart, 1976).

However, stem cross-section allocated per unit leaf area and the vessel diameter in the stems vary widely within the crowns of many trees. Detailed studies of large trees, sectioned and delineated by conducting area at intervals below the crown (Huber, 1928; Morikawa, 1974) show that while the proportion of wood conducting water decreases towards the base, the area continues to increase. In trees where an extensive part of their bole length is free of branches it has been shown that sapwood tapers linearly between breast height (1.37 m) and the base of the crown. Trees tend to minimise a massive build up of "unit pipes" as they age. Those with secondary growth normally produce wider and longer vessels and tracheids at their lower parts as they age. This helps to compensate for the increased transport distances and invalidates the "unit pipe" hypothesis (Booker and Kininmonth, 1978; Aloni and Zimmermann, 1983; Raven and Handley, 1987; Aloni, 1987; 1991).

Different approaches to the pipe model have been of some value in understanding tree growth resource allocation and biomechanics (Ewers and Zimmermann, 1984a; b).

2.8.3 Sapwood area to leaf area ratio

The sapwood area to leaf area ratio in any one species changes with the environmental circumstances of the site on which the trees are growing, with stocking density, and with the dominance class of individual trees. This has been attributed to changes in the ability of the sapwood to conduct water (its permeability) under these different circumstances. Physiological mechanisms to explain these changes have not been elucidated fully (Grier and Waring, 1974;Waring, Gholz, Grier and Plummer, 1977; Whitehead, 1978; Snell and Brown, 1978; Rogers and Hinckley, 1979; Kaufmann and Troendle, 1981; Long, Smith and Scot, 1981;Waring, Newman and Bell, 1981; Waring; Schroeder, and Oren, 1982; Brix and Mitchell, 1983; Albrektson, 1984; Binkley, 1984; Marchand, 1984; Whitehead, Edwards and Jarvis, 1984; Whitehead *et al.*, 1984; Blanche, Hodges and Nebeker, 1985; Dean and Long, 1986; Espinosa Banclari, Perry and Marshall, 1987; Hungerford, 1987; Keane and Weetman, 1987; Long and Smith, 1988; 1989; Thompson 1989; Pothier *et al.* 1989a; b).

Edwards and Jarvis (1982) found a positive correlation between sapwood permeability and Lodgepole pine growth rate. Pothier, Margolis, Poliquin and Waring (1989) contributed towards modifying the pipe model by relating anatomical characteristics of sapwood to stem permeability. Since most water moves through earlywood rather than latewood cells (Zahner, Lotan and Baughman, 1964; Booker and Kininmonth, 1978; Kramer and Kozlowski, 1979), the proportion of early-wood in the sapwood may be decisive in the leaf area to sapwood relationship. Fast growth is often associated with a relatively high proportion of earlywood (Panshin and de Zeeuw, 1980).

In mathematical terms, these findings have led to reformulation of the pipe model as:

$$L_x = a\, s_x p_x \qquad 2.16$$

where L_x is the total leaf dry mass (kg) or area (m^2) supported by a tree above some height x (m) above ground level, s_x is the stem sapwood area (m^2) at x, p_x is the permeability of the sapwood (m^2) at x, and a is a parameter (kg m^{-4}). Whitehead *et al.* (1984d) are some of the few researchers who have collected data to test formally the applicability of Eq. 2.16. A synthesis selected from various literature sources

is provided by Waring, Schroeder and Oren (1982).

Work with this theory has dealt principally with conifers. Initially most analyses were expressed in foliage mass per unit of conducting area (Grier and Waring, 1974). However, leaves of more shade-tolerant species are known to vary in mass as a function of PAR (Larcher, 1980) so area is mostly substituted for mass. In general, larger leaf area to sapwood area coefficients are associated with taxa that grow in mild climates or that represent shade tolerant advanced successionary species such as *Abies grandis* or *Abies amabalis*. Species adapted to full exposure or desiccating environments show progressively smaller coefficients (Waring, Schroeder and Oren, 1982).

West and Wells (1990) developed a practical method along the lines of the pipe model to estimate leaf mass of standing *E. regnans* (F. Muell.) trees across a range of site and stand conditions. Their work was conducted on even aged, monoculture stands aged 8 to 20 years (Victoria, Tasmania). Since it was not considered practical to measure stem permeability (p_x) in the field nor was there any detailed understanding of how stand conditions affect permeability, their model involved the replacement of the expression $a \times p_x$ with an empirical function involving variables that could readily be measured. Their model requires an estimate of sapwood area from a single core taken at some measured height x above breast height and below the first live branch on the stem, the total height h of the tree, its diameter at breast height over bark, and its age.

2.8.4 Sapwood to composite root cross-sectional area

Carlson and Harrington (1987) found the taproot circumference and cross sectional area of loblolly pine (*P. taeda* L.) and short-leaf pine (*P. echinata* Mill.) at groundline to be significantly correlated to the sum of those of the first order lateral roots and the taproot below (composite cross sectional area). The slopes of the linear geometric mean regression lines were slightly less than but close to 1. Age correlations with the area and circumference variables were all positive and statistically significant, implying an overall developmental relationship. Tree age ranged from 3 to 9 years for shortleaf pine and from 4 to 9 years for loblolly pine.

A report by Benecke and Nordmeyer (1982) mentions a similar cross sectional area relationship in *P. contorta* (Dougl. ex Loud) ssp. *contorta* to that of Carlson and Harrington (1987). However, while Carlson and Harrington (1987) did not directly measure annual increment, the fact that the relationship between stem area and composite root area remained constant over age implies that stem increment and composite root increment are approximately equal. These results indicate that xylem differentiation and development from initials in the vascular cambium at various locations is tightly controlled *via* an interactive system, and that root system development is directly related to that of basal stem.

In contrast other workers (Fayle, 1983; Fayle and Axelsson, 1985) have reported that the ratio of root increment (measured at various distances from the centre of the stem) to stem increment (measured at 100 mm above groundline) may increase over time and is altered by silvicultural treatment. Such differences may be attributed to differences in method of measurement, the age and range of trees sampled, taprooted *vs* non-taprooted systems, and species.

Diameter development of split root systems of Sitka spruce (*Picea sitchensis* (Bong.) Carr.) has been shown to be regulated by the nutrient levels in the medium bathing a particular root (Coutts and Philipson, 1976; Philipson and Coutts, 1977). Wilson (1975) hypothesised that the close correlation between the cross-sectional area of a root above a branch point and the sum of the branch roots could be simply a function of the progressive removal of photosynthate from the phloem in proportion to

relative transport capacity. These proposals may be complementary where nutrient content in the xylem sap is related to sink strength.

2.8.5 Leaf senescence

Leaf metabolism is affected by xylem delivery rates. Changes in rates of delivery of xylem solutes to leaf tissues have rapid regulatory effects (within hours) on: (i) levels of nitrate reductase, (Shaner and Boyer, 1976), soluble protein and chlorophyll (Martin and Thimann, 1972); (ii) photosynthetic gas exchange, and (iii) stomatal resistance values (Harris, Cheeseborough and Walker, 1983).

In many species basal leaves begin senescence during early development while the apical leaves still show vigorous growth. Neumann and Stein (1984) have shown that progressive changes in both hydraulic resistances to flow into competing leaves and stomatal resistance to vapour loss leaves occur during ontogeny. The mechanisms underlying this sequential ordering of events have not been clearly defined. However, supplies of both ions and cytokinins which are delivered from roots to leaves *via* the xylem network (Torrey, 1976) do interact in the regulation of leaf senescence (Neumann and Stein, 1983; Neumann and Noodén, 1983).

A plausible explanation is that on-going declines in relative xylem delivery rates of solute to basal leaves, accompanied by changes in phloem transport from import to export, as leaves mature (Pate and Atkins, 1983; Thorpe and Lang, 1983) result in a progressive diversion of root produced regulatory solutes (cytokinins, mineral elements) from basal leaves towards more apical leaves. The resulting gradients of distribution would discriminate against basal leaves and be specifically involved in their senescence. Of interest is that localised applications of cytokinins may prevent senescence symptoms and accelerate the senescence of neighbouring untreated leaves (Leopold and Kawase, 1964).

Environmental factors such as water and nutrient stress or shading of the lower leaves could accentuate this diversion by selectively increasing still further the stomatal resistances in the basal leaves (Jordan, Brown and Thomas, 1975; Davis, Van Bavel and McCree, 1977). Further, progressive changes in the pathways of distribution and rates of delivery of growth regulatory xylem solutes to competing organs during shoot ontogeny, could also participate in regulating long-term developmental changes at the whole plant level. However, Davis, Van Bavel and McCree (1977) have concluded that relatively high stomatal resistances in basal leaves and the tendency for stomatal resistances to increase with leaf age may also be caused by internal rather than environmental factors.

Ion exchange between solutes carrying positive charges and negatively charged sites in the xylem walls may modify the distribution of calcium ions, amino acids and amides. Active uptake of solutes by xylem parenchyma and transfer cells, as well as xylem to xylem transfer and xylem to phloem transfers, also occur (Pate and Gunning, 1972; Layzell, Pate, Atkins and Canvin, 1981; Ficus, Klute and Kaufmann, 1983; Neumann and Noodén, 1984).

Xylem transport is particularly important where distribution of solutes to shoot tissues *via* the phloem transport pathway is restricted e.g., (i) Ca^{2+}, BO_3-3, NO_3- and cytokinins have relatively low phloem mobility (Epstein, 1972; Hall and Baker, 1972; Van Staden and Davey, 1979), (ii) young apical leaves of some species also obtain most of their requirements for N and K^+ *via* the xylem (Pate and Atkins, 1983), and (iii) mature leaf tissues tend to export solutes and not import them *via* the phloem (Pate and Atkins, 1983; Thorpe and Lang, 1983).

2.9 Ohm's Law analogy and modelled SPAC water flux

The fundamentals of water movement in plants have been understood for some time (Dixon 1914; Dixon and Joly, 1986; Huber, 1928; 1956; Van den Honert, 1948; Scholander, 1972) and have been reviewed by Zimmerman (1983) and Boyer (1985).

2.9.1 Description

Huber (1928) and Van den Honert (1948) made significant contributions to our comprehension of long distance water flow in plants through application of the Ohm's law analogy to plants where water flux through the various parts of the soil-plant-atmosphere-continuum (SPAC) are treated as a catena process, analogous to an electric circuit which is composed of a series of resistors (**Fig. 2.7**). Valuable discussion concerning some of the misunderstanding and misuse of the principle is provided in the literature of Richter (1973), Fiscus (1983), and Passoiura and Munns (1984).

In the Ohm's law analogy the flux of water through a discrete region from A to B in the liquid phase of the soil-plant-atmosphere continuum (SPAC) is proportional to the product of the hydraulic conductance (k_h, kg s^{-1} MPa^{-1}) of that region, and the water potential drop across the structure ($\Psi_A - \Psi_B$). Resistance (R) is the reciprocal of hydraulic conductance.

The classical Ohm's law analogy assumes that the resistance offered by the system is a constant and that water flux between points A and B does not reflect water movement through a single point within the system, rather k_h and R are averaged values between points A and B. If a system under study obeys Ohm's Law, it shows a linear relationship between the flux passing through and the driving force. This implies that *steady state conditions* must be achieved for both water flux and water potentials and that

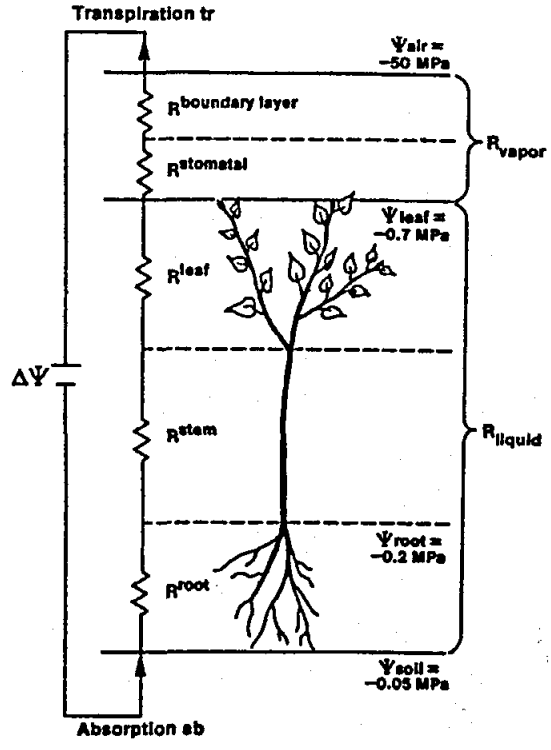

Fig. 2.7 Simple application of the Ohm's law analogy in an unbranched catena of a small number of resistance elements. The total conductance is seen as resultant conductance (k) of the root, stem, leaf, stomates and boundary layer in series. The conductances in the vapour pressure phase are much less than in the liquid phase. Water flow is driven by the differences in water potential between the soil (ψ_{soil}) and the atmosphere (ψ_{air}) (Ewers and Cruiziat, 1991)

the flux passing by points A and B must be the same.

In trees particularly the above analogy breaks down. Water potential is a function not only of transpiration but also of the amount of water moving in and out of storage. The Ohm's law analogy may be adjusted to allow for such hydraulic capacitances, C (kg MPa^{-1}). The following equation describes this situation:

$$flux_v = dV/dt = dV/d\Psi \cdot d\Psi/dt$$

where $flux_v$ indicates a flux due to a net release or gain of water into the system, dV/dt is the derivative of the water volume of the system with respect to time, and $d\Psi/dt$ is the derivative of Ψ with time. Capacitance is the relationship between water potential and water content ($dV/d\Psi$) which could be determined from "pressure volume curves" (Tyree and Jarvis, 1982; Pallardy, Pereira and Parker, 1991). Since the magnitude of C is most likely to be proportional to the size of the storage tissue, it has also frequently been defined per unit tissue volume or per unit dry mass, or for leaves per unit area. The effect of capacitance is to cause the water flux into a region (F_A) to be unequal to the water flux going out (F_B) whenever Ψ is changing in the region. The magnitude of the differences in fluxes in and out depends upon the product of C_{AB} and the rate of change of Ψ ($d\Psi/dt$, MPa s^{-1}).

The tissues of a plant may be considered as a number of alternative sources of water linked in parallel with each other and the soil (Jarvis, 1975). Thus the total flux from the plant as transpiration (E) may be made up of a number of partial flows in the plant. From a particular store this flow may be represented by:

$$q_i = (\Psi_i - \Psi_{xylem})/R_i \qquad 2.18$$

where R_i is the resistance of the tissue to water movement, and Ψ_i is a function of the tissue relative water content (RWC). Waring and Running (1978) have used the following formula to calculate relative water content (%):

$$RWC = [(W_f - W_d)/(V_f - V_s)] \times 100 \qquad 2.19$$

where W_f is the fresh mass of wood, W_d is the oven dry (70 °C) mass of wood, V_f is the volume of the wood, and V_s is the volume of the solid (cell wall) material in the wood.

The relative sizes and phasing of flows out of storage depend upon: (i) the resistances between the stores and xylem (ii) the capacity of the stores, and (iii) the relationships between the tissue characteristics, Ψ_i and RWC_i. Thus the volume of water that can come from storage, may be represented by:

$$\Delta V_i = V_i \cdot \Delta RWC_i = \int_{t_1}^{t_2} q_i \, dt. \qquad 2.20$$

Theoretically the water storage capacity of a plant (WSC) is the quantity of water that can be lost without irreversible wilting:

$$WSC = V(1 - \theta). \qquad 2.21$$

where V is the quantity (volume or mass) of water in the tissue at full turgidity and θ is the critical relative water content leading to irreversible wilting (unitless fraction).

2.9.2 Stored water

There is considerable evidence that trees undergo seasonal and diurnal fluctuations in water content. This fluctuation in water content may be viewed as water going into and out of storage.

Gibbs (1958) made seasonal measurements of the fresh mass and oven dry mass of stems of over 300 young trees. Following leaf fall in autumn, the wood increased in water content between 15 to 20 % of wood volume. The water content did not decrease until the leaves started to transpire in spring. Much less seasonal fluctuation occurred in ring-porous than diffuse-porous wood. This may be because the volume of sapwood is comparatively less in most ring-porous species.

Based on measurements of stem circumference, xylem pressure potential, and leaf surface resistance, Hinckley and Bruckerhoff (1975) concluded that significant amounts of water storage occurred in an 18.9 m high, ring porous, white oak (*Quercus alba*). Both daily and weekly stem shrinkage occurred with corresponding fluctuations in leaf water potential. A delayed response in stem hydration exhibited typical hysteresis loops in diurnal plots of stem circumference with potential.

In apple (*Malus pumila*), Landsberg *et al.* (1976) observed leaf capacitances twice as great as that of stems or roots. They calculated that a small fully hydrated apple tree, with a leaf area of 4 m^2 and a total mass (including roots) of 15 kg, had about 0.7 kg of stored water which could be released by a decrease in water potential of 2.0 MPa. This could present two hours of transpiration at a rate of 20 mg m^{-2} s^{-1}.

Interesting work is presented by Schulze, Cermák, Matyssek, Penka, Zimmermann, Vasícek, Gries, and Kucera (1985), who studied the canopy transpiration and xylem water fluxes in 72 year-old spruce (*Picea abies*) and 33-year-old larch (*Larix decidua*, *L. leptolepis*, and *L. leptolepis* × *decidua*) trees. The former, located at Ràjec (CSSR), possess a relatively complex canopy structure due to leaf age stratification and considerable self shading, while the latter, at Bayreuth (FRG), are deciduous and require relatively high levels of PAR and have a very open canopy structure.

Compared to a value of 3.7×10^{-8} kg^{-1} Pa^{-1} published by Landsberg *et al.* (1976) for young apple trees, significant water capacitance was located in the crowns of the two species *viz*, 5.5×10^{-8} kg^{-1} Pa^{-1} and 6.3×10^{-8} kg^{-1} Pa^{-1} respectively. These caused a time lag between the start of leaf transpiration and xylem flow at the crown bases. In both cases transpiration started at 04h00, two to three hours earlier than the stem flow. Transpiration decreased appreciably by late morning (10h00) despite increased xylem flow in the trunk. Similarly leaf water potentials decreased to minimum levels of -1.6 MPa and -1.7 MPa respectively. Over this period 4.1 kg in *Larix* and 8.7 kg in *Picea* was from stored water, contributing only 14 to 24 % of the daily transpiration compared to between 30 and 40 % in Douglas-fir (Waring *et al.*, 1979).

Schulze *et al.* (1985) noted that the difference between water efflux from the trunk to the crown and influx from the root, in *Larix*, was no more than 1.5 kg when the water potential had decreased to -1.2 MPa. They commented that this trunk specific capacitance appeared to be surprisingly low.

Waring, Whitehead and Jarvis (1979) worked on 40-year-old Scots pine (*P. sylvestris*) trees at Roseisle (Scotland), where over 90 % of plant water was located in sapwood. Considering annual and diurnal data, on average 64 % of this water in stem sapwood was made available for transpiration. In phloem, cambium and foliage it was less than 5 %.

Waring *et al.* (1979) noted that the largest change in sapwood relative water content occurred over a

2-week period. This was a reduction by 27 % which corresponded to extractions from sapwood of 2.5 and 5.1 mm of water in plots with population densities of : (i) 3281 trees ha^{-1} (*WSC* of 212 m^3 ha^{-1} = 21.2 mm) and (ii) 608 trees ha^{-1} (*WSC* of 124 m^3 ha^{-1} = 12.4 mm), respectively. Comparatively this was less than RWC seasonal changes of over 40 % reported by: Chalk and Bigg (1956) in *Picea sitchensis*; Gibbs (1958) in many species including *Tsuga canadensis*, *P. strobus* and *Larix europea*; Rothwell (1974) in *P. contorta*, and by Waring and Running (1978) in *Pseudotsuga menziesii*. Waring *et al.* (1979) attributed some differences between trees in RWC to differences in wood density.

Sapwood water content was generally lower at times of high transpiration. Resaturation took several months during winter. This trend was also observed in the RWC field studies of Chalk and Bigg (1956), in Great Britain, and Clark and Gibbs (1957), in Canada, on a variety of conifers including Douglas-fir.

In soft leaves and in herbaceous stems and roots the mechanism of water storage is primarily elastic *i.e.*, as the tissue Ψ increases or decreases, the volume of the tissue increases or decreases respectively. In woody stems and roots the bark changes considerably in volume with changes in Ψ, but the volume of the wood changes very little.

Two water storage areas can be distinguished within roots, branches, and trunks (Ewers and Cruiziat, 1991): (i) bark and (ii) xylem. The inner bark (*i.e.*, vascular cambium and phloem tissue) consists mostly of living tissue which has a small total *WSC* but a short response time constant (short-term *WSC*). Most of the total *WSC* of the plant is in the sapwood. However, this volume of water may only be slowly exchangeable over a period of several days or weeks (long term *WSC*).

Water storage and retrieval in woody stems involves two mechanisms in addition to elastic storage (Zimmermann, 1983): (i) capillary storage, and (ii) cavitation release. These mechanisms have been demonstrated by Tyree and Yang (1990).

Capillary storage is highest at Ψ_p values -0.5 MPa and occurs only in wood cell lumina (vessels, tracheids, or wood fibres) containing air bubbles because the lumina had cavitated previously. As the xylem pressure potential (Ψ_p) changes, the size and shape of the bubbles change so that the surface tension at the air / water interfaces exactly balances the Ψ_p When Ψ_p is -0.5 MPa a substantial volume of water is left in the cell lumen, but the volume decreases with decreasing Ψ_p. Consequently capillary water becomes vanishingly small at $\Psi_p < -0.5$. At much more negative Ψ_p values previously water-filled xylem lumina may cavitate, releasing their water to the transpiration stream. The Ψ_p at which cavitation starts releasing water to the stem varies between species. In some it can start at -0.5 MPa, whereas in others it may not start until -4 or -5 MPa.

An important phenomenon connected with inequality between transpiration and absorption is plant organ growth which may influence water storage. Another is that under conditions of low transpiration, root resistance estimates must consider the uptake of solutes as well as the pressure potential gradient as the driving force for water flow (Ficus, Klute and Kaufman, 1983).

2.9.3 Water movement patterns

Initially one would expect water to move out of storage from tissues closest to the evaporation sites, the leaves. With depletion of this source, Ψ would decrease and the main sources of supply would come from progressively lower down the plant. If storage within the plant is adequate and the resistances between storage tissue and xylem are lower than between xylem and soil sufficient water

might be drawn from the tissues to meet transpiration requirements for considerable periods.

One might think of water transport in terms of either balanced or non-balanced flux conditions - termed: (i) conservative and (ii) non conservative, respectively by Ewers and Cruiziat (1991).

Balanced flux means that throughout the considered interval of time, the quantity of water transpiring from the plant is equal to the quantity absorbed by roots (Situation 1 and 2 in **Fig. 2.8**). Under non-balanced flux conditions absorption and transpiration differ (Situation 3 and 4 in Fig.2.8). When absorption is greater than transpiration the plant experiences rehydration. When absorbtion is less than transpiration, the plant dehydrates. "Steady State" conditions mean, literally, a constant rate of transpiration and absorption (Situation 1 and 3 in Fig. 2.8). During the growing season, plants normally have neither a steady state nor a balanced flux situation for very long. Instead, Situation 4 in Fig. 2.8 prevails, where transpiration and absorption are closely coupled, but each is changing independently with time.

In *Larix* trees, Schulze *et al.* (1985) observed linear relationships between leaf water potential and transpiration as well as xylem flow in the trunk, both exhibiting hysteresis (**Fig. 2.9**A). The latter indicated a constant hydraulic conductance (k_h) throughout the day and a constant water supply from roots. However, the leaf water potential was lower at the end of the day than at the commencement of measurement. Similar trends were not observed in *Picea* trees (Fig. 2.9B), possibly reflecting differences in crown water storage capacity, hydraulic architecture and plant soil interactions between the two species.

Water was initially available to the needles at a very low conductance and at rapidly decreasing

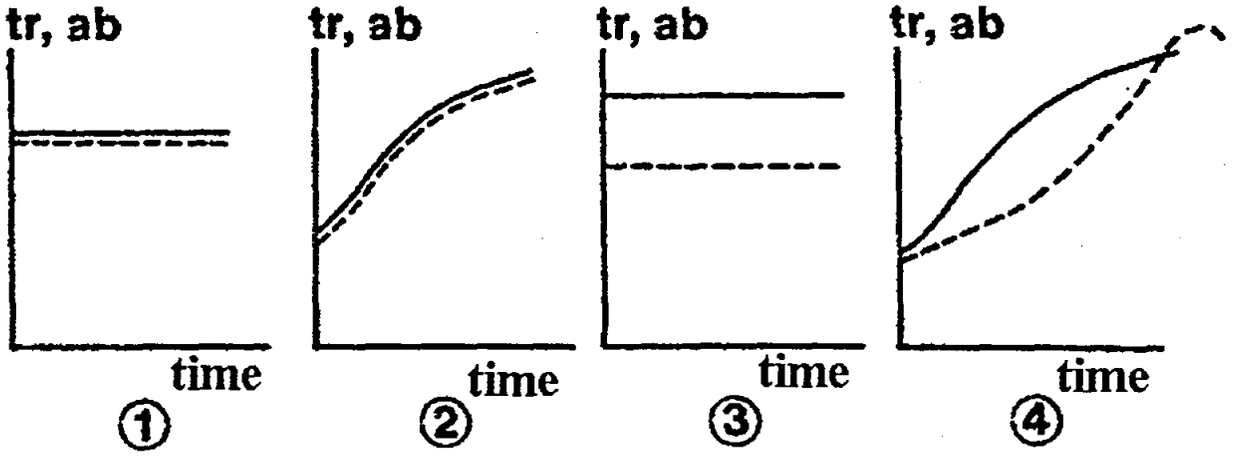

Fig. 2.8 Diagram of flux conditions showing absorption (dotted line), and transpiration (solid line), over time (t). Graphs (Situation) 1 and 2 represent balanced, conservative flux, conditions, while 3 and 4 represent nonbalanced, nonconservative, conditions. Only situations 1 and 3 indicate steady state conditions (Ewers and Cruiziat, 1991)

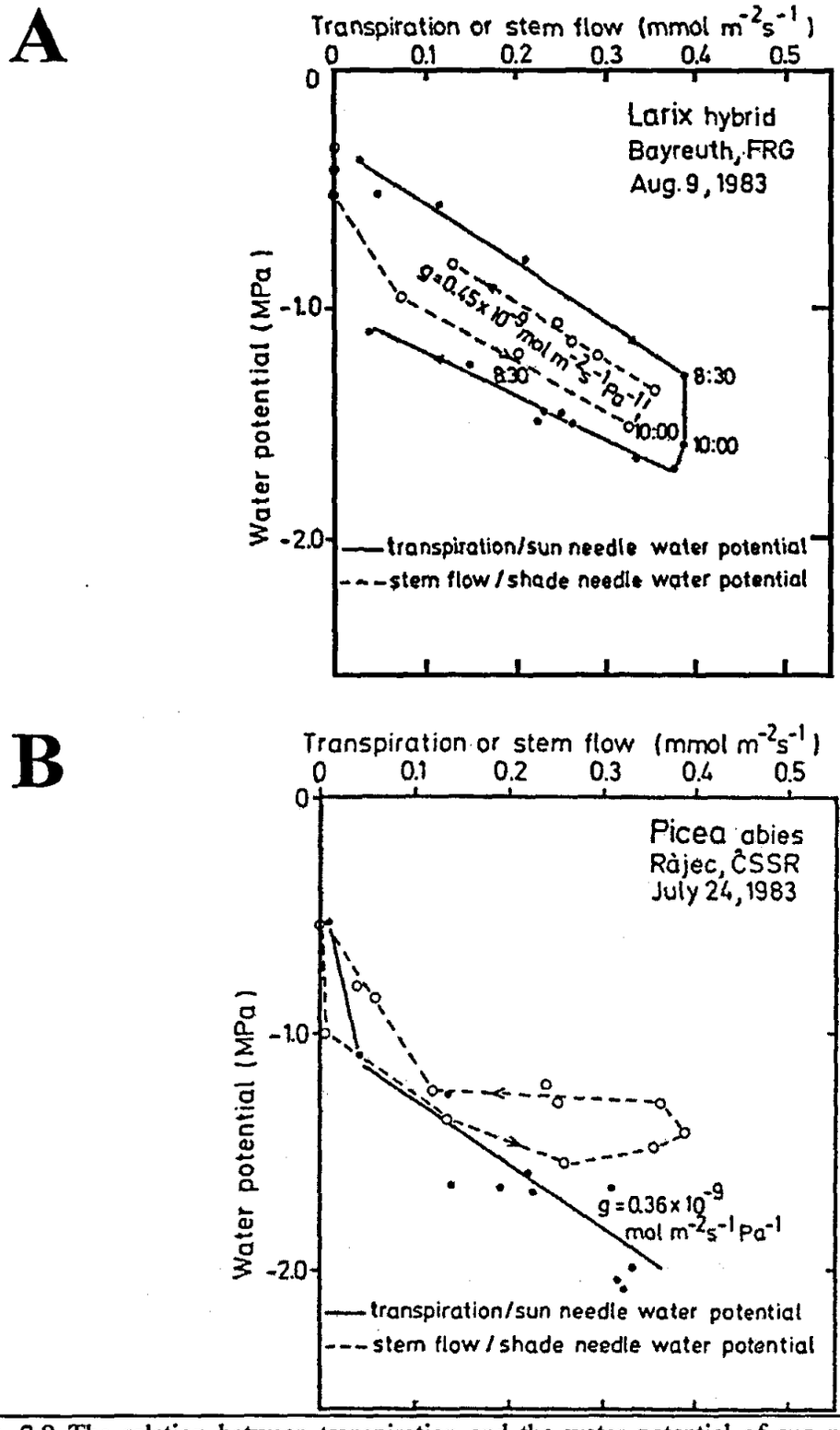

Fig. 2.9 The relation between transpiration and the water potential of sun needles, and the relation between xylem flow and the water potential of shade needles of: A. *Larix* and B. *Picea*. The arrows indicate the time course of measurement, the small numbers indicate equivalent times in the morning. The slope represents the liquid flow conductance

water potentials. This phase probably represented the use of stored water in very small twigs. The initial phase was followed by a higher water flux throughout the rest of the day, representing conductance drawn from the main stem in the crown and trunk. The availability of water to the leaves did not appear to change during the day, but the availability of water to the trunk changed considerably. Interestingly, at a water potential of -1.4 to -1.6 MPa, flux through the stem appeared to increase without any further decrease in water potential. The liquid flow conductance in the trunk decreased again when the water potential in the shaded needles increased above -1.2 MPa, possibly reflecting rapid rehydration from roots and an approach to full recharge of crown storage.

2.9.4 Stem hydraulic conductivity

Two relationships that are important in modelling water transport through the soil-plant-atmosphere continuum (Jarvis *et al.*, 1981) are: (i) changes in sapwood water content consequent to changes in xylem water potential, and (ii) the effect of reductions in water content on permeability of sapwood to water transport. One would expect to observe relationships between water potential, water content and permeability in sapwood to be similar to those found in soils, if pore size distribution is considered.The relative conductivity of sapwood (R_h) varies linearly with specific gravity (SG). As SG decreases, the actual conducting area increases proportionally. Puritch (1971) demonstrated that R_h (at a given SG) decreases exponentially as relative water content (RWC) decreases, for sapwood of Grand fir (*Abies grandis*). Waring and Running (1978) generalised Puritch's (1971) findings to predict Rk_h as a percentage of that value at saturation ($Rk_h sat$)) for Douglas fir (*Pseudosotsuga menziesii*). The relationship can be described by:

$$Rk_h/Rk_{h\,sat} = 0.4092\, e^{0.55 \times RWC^{napwc}} \qquad 2.22$$

This indicates that a decrease in RWC from 100 % to 90 % can reduce Rk_h to 58 % of that of saturation. A reduction in RWC from 70 % to 60 % represents a decrease in Rk_h from 19 % to 11 % of that of saturation. As RWC is reduced to the bound water level of approximately 20 %, Rk_h approaches 0. Such an exponential relationship is to be expected as a result of the pore size distribution of the wood studied. The larger diameter tracheids, common to the low SG wood laid down in the spring conduct more efficiently than predominantly smaller diameter tracheids laid down in later seasons.

In their work on stems of Doulas-fir, Waring and Running (1978) noted that under some conditions a diurnal change in RWC by as much as 25 % may be required to explain the observed decreases in Rk_h. They also noted marked hysteresis in the relation between Ψ_{leaf} and E at high RWC (90 %) but a lack of hysteresis at low RWC (56 %).

Embolisms resulting from cavitation are likely to reduce permeability by reducing the number of flow paths (Byrne, Begg and Hansen, 1977). Since the largest lumens will tend to cavitate first, one can deduce from the Hagen-Poisseuille law for fluid flow in capillaries that relatively few cavitations may cause substantial changes in permeability.

Edwards and Jarvis (1982) analysed a number of pressure-volume curves of fresh branchwood and stem sapwood of *P. contorta* and *Picea sitchensis* and concluded that the reduction in $Rk_h/Rk\,h\,sat$ at low water contents can only be the result of cavitation of tracheids.

Three phases in water loss, or the relationship between relative water content and applied pressure or osmotic potential, were discernable. In the initial phase at high water potentials (i.e. >-0.5 MPa), there was an exponential decline down to a water potential of about -0.5 MPa with a large capacitance,

long time constant, and large resistance to flow compared to intermediate water potentials (i.e. -0.5 to -1.5 MPa); followed by a linear slowly changing phase to about - 1.5 MPa, followed in some cases by a much steeper decrease in relative water content with decrease in potential (i.e. -1.5 to -3.0 MPa) where the time constant and resistance declined still further while the capacitance had a tendency to increase again.

They suggested that such a pattern reflects the size distributions of both the tracheid lumens and the margo (pit membrane) pores. The initial steep decline at high potentials are most probably associated with embolism in the large earlywood tracheids accounting for the large initial reduction in $Rk_h/Rk_{h\,sat}$. The second phase probably resulting from the embolism of smaller tracheids. At still lower potentials, a sufficient pressure gradient would exist to pass an air-water interface through the largest pores of the pit margo so that the third phase may reflect the pore size distribution of the margo. Nonetheless, their relationship between $Rk_h/Rk_{h\,sat}$ and relative water content was similar to that obtained by Puritch (1971) using small dowels (**Fig. 2.10**).

2.9.5 Tree hydraulic design

The hydraulic architecture of trees has been the subject of quantitative investigation since the pioneering work of Zimmermann (1978a; b). Zimmermann introduced the concept of leaf specific conductance (LSC) of stem segments. The LSC is defined as the absolute hydraulic conductance of a stem segment, k_h (mass of water per unit time), divided by the total leaf area fed by the stem segment. The LSC datum is of heuristic value because it can directly relate evaporative flux, E_t (kg m^{-2} s^{-1}), from leaves fed by a segment to the pressure gradient, dP/dx (MPa m^{-1}), within the segment, i.e., $ndP/dx = E_t/LSC$. A stem segment with a low LSC is less capable of supplying water to leaves fed by it than a stem segment with high LSC.

The LSC pattern throughout the crown of several hardwoods and softwoods has revealed a consistent pattern. The LSC of minor branches is 10 to 1000 times less than that of the bole of trees (*e.g.* Zimmermann, 1978 a; b; Ewers, 1985; Tyree, Graham, Cooper and Bazos, 1983; Thompson, Tyree, LoGullo and Salleo, 1983). This means that a decrease in Ψ through minor branches is very large compared to the gradients of Ψ in the bole, and could account for a substantial fraction of the total decrease in Ψ from the soil to leaves. Tyree (1988) shows that in cedar the main resistance to water flow resides in branches less than about 10 mm diameter. So the minor branches of cedar, and perhaps of all trees, might be better viewed as a collection of small independent plants each "rooted" in the bole.

2.9.6 Modelling

Modelling the dynamics of water flow through plants and trees has attracted continued interest for many years (Jarvis, Edwards and Talbot, 1981; Boyer, 1985). Such models can be divided into two major classes depending on whether they account for plant water storage capacity or not *i.e.*, whether they are (i) dynamic or (ii) steady state models, respectively.

Within each class, models can be further divided according to how the catena (chain) of plant resistances to water flow is accommodated. In the simplest models, the plant is reduced to a single resistance element (a one-link catena), or an unbranched catena of a small number of resistance elements *e.g.*, root resistance, stem resistance and leaf resistance in series. In other models the branching structure of the plant is explicitly taken into account. The plant is reduced to a larger number of resistance elements arranged in a branched catena pattern. Resistance measurements of portions of a

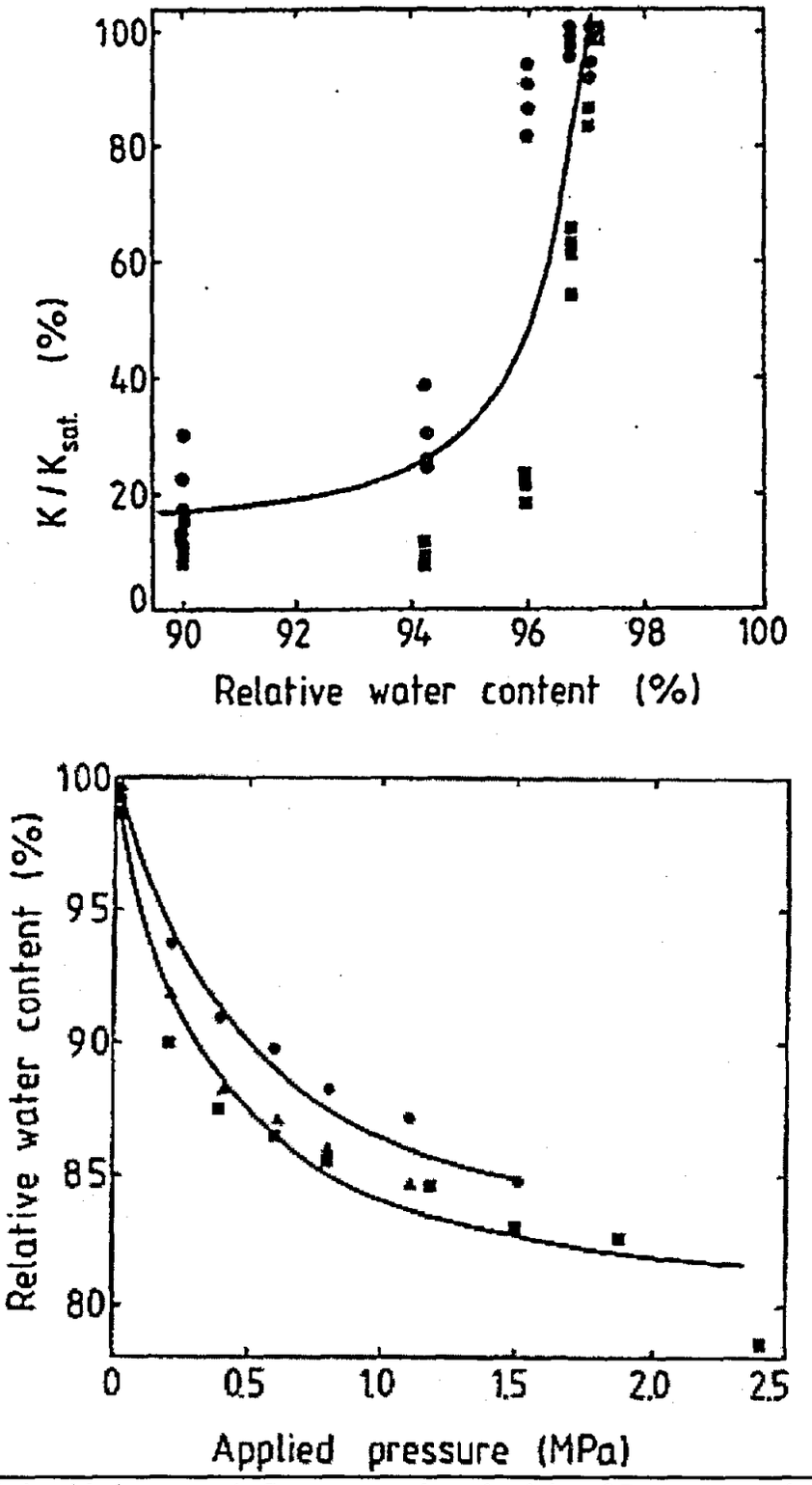

Fig. 2.10 The relationship between: A. Stem sapwood conductivity of *P. contorta* and sapwood relative water content where conductivity has been normalised relative to the value at saturation. Data are shown for a number of determinations on two separate stem sections. B. The relationship between stem relative water content and applied pressure for stemwood of *P. contorta* (triangle) and *Picea sitchensis* (■) at a height of 1.3 m, as well as at a height of 11 m just beneath the live crown (•) for the latter (Edwards and Jarvis, 1982)

tree may be more reliable than measurements of total plant resistance.

2.9.6.1 Single link catena

For a forest stand if the canopy is treated as a single leaf at a uniform water potential (Ψ_l), then the conductance for the entire pathway (g_p) ignoring branching may be given by (Richter 1973, Jarvis, 1975):

$$g_p = E_t/(\Psi_s - \Psi_l - h\rho g) \qquad 2.23$$

where Ψ_s is the soil water potential, E_τ is the transpiration rate from the canopy, $h\,\rho\,g$ is the gravitational pull on a column of water of density ρ and height h, and g is the acceleration due to gravity.

This forms a basis for describing the flux of water through parts of trees, whole trees, and forest stands. It identifies E_τ as the driving force for reducing the water potential in the leaves. The water potential gradient that results is related to the efficiency of the conducting system and is a function of the physical properties of the pathway. The conductance for the entire pathway, g_p, is considered to be uniform throughout the trees in the stand and linearly related to E_τ.

The assumption of uniform conductance may be adequate for models dealing with water flux from forest stands on a long term basis (Thorp *et al.*, 1978). However, departure from linearity implied in the above equation is often exhibited in the form of hysteresis in a diurnal relationship between E_τ and $(\Psi_s - \Psi_l - h\,\rho\,g)$ (Hinckley, Lassoie and Running, 1978). This apparent variation in G_p throughout the day is related, amongst other factors, to the lateral flux of water to the active xylem from stores within the tree.

To incorporate the additional effects of lateral movement of water from storage joining the transpiration stream, Landsberg, Blanchard and Warrit (1976) extended the electrical analog in Eq. 2.23 to include capacitance.

For the simplest case if it is assumed that the storage in the tree can be treated as a single reservoir with capacitance C, g_{sx} is the conductance between soil at water potential Ψ_s and the xylem in the leaves at water potential Ψ_x, then the total transpiration flux E_t is (Jarvis *et al.*, 1981):

$$E_t = (\Psi_s - \Psi_x)\cdot g_{sx} + C. \qquad 2.24$$

As an alternative to Eq. 2.23, water flux through tree stems may also be described in terms of physical properties of the sapwood by Darcy's equation. Considering the pathway from soil to leaves as one component, the volume flux of water passing through a single tree stem, q, with conducting area of xylem (sapwood) A_s and length (equivalent to tree height) h is given by:

$$g = \frac{k A_s}{h\,\eta}\cdot(\Psi_s - \Psi_l - h\rho g) \qquad 2.25$$

where k is the relative conductivity of the sapwood and η is the viscosity of water, which is dependent on temperature. This is more because of the introduction of sapwood basal area for a stand (nA_s) which is a property of the forest stand environment. By equating E_t in Eq. 2.24 with nq for a stand with n trees per unit area from Eq. 2.25, the definition of conductance for as forest stand is:

$$g_p = \frac{nkA_s}{h\,\eta}. \qquad 2.26$$

Whitehead, Jarvis and Waring (1984b) combined Eq. 2.25 with Eq. 2.10, which defines the driving

force for water movement in terms of canopy conductance $E_{imp} = g_c D_n / P$, ($g_c = g_s A_f$) where g_s is the average stomatal conductance and A_f is the leaf area for a tree, to give:

$$\frac{A_f}{A_s} = \frac{k(\Psi_s - \Psi_l - h\rho g)}{h\eta} \cdot \frac{P}{g_s D_m}. \qquad 2.27$$

This is a formal representation of the concepts presented by Hinckley and Ceulemans (1989) and provides a functional relationship that can be tested with a range of silvicultural treatments for different species growing at the same site, or at sites with different values of air saturation deficit. Some of these aspects have been investigated by Jarvis (1976), Whitehead *et al.* (1984b; c) and Espinosa Bancalari, Perry and Marshall (1987).

Potheir, Margolis and Waring (1989) suggest that increases in saturated k in relation to age for stands of *P. banksiana* can explain the observation that trees exhibit the same diurnal range in Ψ_{leaf} at different stages of stand development, while still maintaining similar maximum rates of transpiration per unit leaf area. Homeostatic adjustment in the cross-sectional areas of sapwood and heartwood in *abies balsamea* trees has been interpreted in relation to the degree of pruning.

2.9.6.2 Multiple link catena

In order to understand trees as whole and functional organisms, one needs to study their hydraulic architecture. This influences the movement of water from roots to leaves. Thus different designs could have different consequences for diverse species of trees. In trees with complicated branching patterns a complicated branched catena model may be more desirable than models further from closure in order to answer relevant questions, or the study of the comparative physiology of different tree species.

The entire pathway is comprised of a number of parallel-linked conductances for each of the components of the hydraulic pathway between the soil and the leaves. The locations of the points of limiting conductance within the pathway have been discussed in detail (Jarvis, 1975; Tyree *et al.*, 1975; Hinckley *et al.*, 1978; Landsberg and Jones, 1981; Whitehead and Jarvis, 1981). Richter (1973) has pointed out the errors that can result in models of water flow in trees when the consequences of branching structure are ignored.

Examples where steady-state branched catena models have correctly predicted the range of water potentials (Ψ) throughout tree crowns are those: (i) in cedar (*Thuja occidentalis)* by Tyree, Graham, Cooper and Bazos (1983), and (ii) in olive (*Olea europea* L.) by Thompson, Tyree, LoGullo and Salleo (1983).

Edwards, Jarvis, Landsberg and Talbot (1986) divided a tree into four compartments. The roots, branches, and leaves were each treated as a single compartment in which branching was not considered, but the stem was divided into a large number of thin slices. In the model, capacitance is defined for each compartment, and flow is described by Darcy's equation using relationships between relative conductivity and water content for the root, stem, and branch compartments. The model is driven by transpiration from the leaf using the Penman-Monteith equation. For each discrete time step, the model calculates changes in water content, flow, water potential and relative conductivity.

A model developed by Tyree (1988) is driven by transpiration and uses Darcy's equation in a similar manner to the model by Edwards *et al.* (1986). Hydraulic architecture is introduced by characterizing length, diameter, conductance, and leaf area for a branched catena of 4107 segments, although the root is considered as one compartment. The spatial variability of transpiration from

different quadrants of the crown is also considered. Capacitance effects are also included, but conductance does not vary with water content. Comparison of water potential simulated by the model, for different heights, with measurements in the lower part of a 6 m tall *Thuja occidentalis* tree showed good agreement.

2.10 List of terms

A (μmol m^2 s^{-1}) and E (mmol m^2 s^{-1}) represent the instantaneous rates of assimilation of CO_2 and of transpiration respectively, per unit area of a particular leaf at a particular instant of time. In the function $E = E(A)$, variation in A and E with space (s) and time (t): $\overline{A}$ could not conceivably be increased or decreased without increasing or decreasing E. The term $\delta E/\delta A$ is constant and $\partial^2 E/\partial A^2 > 0$ for any particular value of λ and corresponds to a particular optimal variation in *stomatal aperture* of an infinite number of optimal diurnal trajectories

λ = Lagrange multiplier, a constant which one might interpret as a physiological parameter that depends on the amount of plant available. When λ is large, marginal water cost is large and optimal variations in gas exchange do not deviate greatly from those which would occur if leaf conductance were constant. With decreasing λ, the deviations become relatively greater and gas exchange is increasingly confined to those periods early in the morning and late in the afternoon, when irradiance and temperature are appropriate for rapid photosynthesis but because the ambient vapour pressure deficit is relatively small, the potential rate of transpiration is also relatively small

Ψ = water potential (MPa); Ψ_w = plant tissue water potential; Ψ_p = pressure potential which describes the pressure against a cell wall and is determined by turgor in plant cells or tension in xylem elements; Ψ_π = solute or osmotic potential arising from osmotically active solutes dissolved in water; Ψ_τ = matric potential arising from capillary or colloidal forces by soil colloids or cell walls; Ψ_g = gravitation potential. Ψ_{leaf} = water potential of a single leaf at a uniform water potential. $\Psi_A - \Psi_B$ = water potential difference across a structure. Ψ_s = the soil water potential. Ψ_l = leaf water potential

L = measure of root abundance; L_v (m root m^{-3} soil), L_a (m root m^{-2} soil surface) or L_m (kg dry mass m^{-2}) are measures of root abundance

R = average rate of runoff (mm h^{-1})

F = average rate of drainage from the root zone (mm h^{-1})

P = average rate of rainfall (mm h^{-1})

E_t = average rate of transpiration from the dry tree canopy (mm h^{-1})

E_i = the average rate of evaporation from the tree canopy and stems wetted by rainfall (mm h^{-1})

$E = E_t + E_{ic}$ when $C = 0$ then $E = E_t$

E_u = average rates of understorey vegetation evaporation (mm h^{-1})

E_s = average rate of forest floor evaporation (mm h^{-1})

W = root zone water storage change ($W_j - W_{j-1}$) during the j_{th} period (mm h^{-1})

C_j = water stored on a tree (mm)

j = time period reference

p = proportion of rain falling through the tree canopy to the ground without being intercepted

E_{ic} = average rates of evaporation of tree intercepted rainfall during the period t (mm h^{-1})

H_c = average rate of drainage of tree intercepted rainfall during t (mm h^{-1}). Drainage of intercepted rainfall is expected to be zero when § , over a period of time, drainage is taken as the amount of water on the canopy after evaporation has taken place ($[(1-p)P - E_{ic}]\,\Delta t$)>

S = the tree surface water storage capacity (mm)

$c_{/S}$ = the fraction of the tree that is completely wet in the j_{th} period

E_I = evaporation rate of intercepted water (mol m^{-2} s^{-1})

s = slope of the relationship: saturation vapour pressure *vs* air temperature.

$\gamma = c_p P/\lambda$ *i.e.* psychometric constant (kPa K^{-1})

R_n = net radiant flux density (J m^{-2} s^{-1})

H = flux density of heat into storage (J m^{-2} s^{-1})

λ = molar latent heat of vaporization of water (J mol^{-1}).

g_{as} = surface conductance from the canopy to a mixed air layer above the canopy (mol m^{-2} s^{-1})

ρ = air density (kg m^{-3}).

C_p = molar heat capacity of air at constant pressure (J mol^{-1} K^{-1})

Ω = empirical coupling constant

A = the available energy flux density to the tree (W m^{-1})

g_A = bulk aerodynamic conductance for transfer of water vapour from the canopy surface to a reference height above (m s^{-1})

g_c = canopy conductance = $L \times g_s$, where L is leaf area and g_s is the median canopy leaf stomatal conductivity (mm s^{-1})

g_s = median or average stomatal conductance for the leaves in the canopy (mm s^{-1})

g = stomatal conductance (mmol m^{-2} total leaf area s^{-1})

L = leaf area for all surfaces (m^2)

E_q = equilibrium rate of transpiration (mm h^{-1})

E_{imp} = imposed rate of transpiration = $E_{imp} = g_c D_m/P$, where $g_c = g_s A_f$, (mm h^{-1})

ε = the change in latent heat content relative to the sensible heat content of saturated air (s/γ)

P = atmospheric pressure (kPa)

z = reference height above the canopy (m)

u = windspeed (m s^{-1})

z_o = roughness length of a forest surface (m)

d = zero plane displacement height (m)

m = von Karman's constant

PAR = photosynthetically active radiation (mol m^{-2} s^{-1})

P_n = photosynthesis

VPD = water vapour saturation vapour pressure deficit

D' = water vapour partial pressure difference

D = the air water vapour saturation deficit measured above tree height but within the canopy boundary layer (kPa)

D = diameter of the i th pipe (m)

D_i = is the water vapour saturation deficit of the planetary boundary air layer or at a reference height in the mixed layer well above the surface of the forest canopy (kPa)

ρ = density of the fluid (kg m^{-3})

η = dynamic viscosity of water, which is dependant upon temperature (MPa s^{-1})

n = a representative number

L_x = total leaf dry mass (kg) or area (m^2) supported by a tree above some height x (m)

p_x = permeability of the sapwood (m^2)

a = a parameter (kg m^{-4})

$p(x)$ = stem permeability

WSC = water storage capacity of a plant = $V(1 - \theta)$, the water storage capacity of a plant or tissue i.e., the quantity of water that can be lost without irreversible wilting (kg)

RWC = relative water content or relative turgidity (%)

SD = saturation deficit

SG = wood specific gravity = W_d/V_f(kg m^{-3})

$Flux$ = (kg s^{-1})

C = capacitance (kg MPa^{-1}). It is the relationship between water potential and water content ($dv/d\Psi$). The effect of capacitance is to cause the water flux into a region (F_A) to be unequal to the water flux going out (F_B) whenever Ψ is changing in the region. The magnitude of the differences in fluxes in and out depends upon the product of C_{AB} and the rate of change of Ψ with time ($d\Psi/dt$, MPa s^{-1})

dv/dt = derivative of the water content of a system with respect to time (kg s^{-1})

$d\Psi/dt$ = derivative of Ψ with time (MPa s^{-1})

W_f = fresh mass of wood (kg)

W_d = oven dry (70 °C) mass of wood (kg)

V_f = volume of wood (m^3)

V_s = volume of the solid (cell wall) material in wood (m^3)

V = quantity (volume or mass) of water in the tissue at full turgidity (m^3)

θ = critical relative water content leading to irreversible wilting (unitless fraction).

G_p = conductance for an entire pathway

G_{sx} = the conductance between soil at water potential Ψ_s and leaf xylem water potential Ψ_x

k_h = hydraulic conductance (kg m s^{-1} MPa^{-1}) = Flux/(dP/dx) i.e., conductance per unit pressure gradient (kg m s^{-1} MPa^{-1}). Note it differs from stem specific hydraulic conductivity k_s, where $k_s = k_h/A_s$ which is a measure of stem porosity (kg m^{-1} s^{-1} MPa^{-1})

$rk_h = k$, conductivity of the sapwood relative to that at wood saturation, which for any SG decreases exponentially with RWC

$rk_{h(sat)}$ = saturated conductivity

R = resistance which is the reciprocal of hydraulic conductance

LSC = leaf specific conductance of stem segments = k_h/A_s (kg m^{-1} s^{-1} MPa^{-1}). The LSC datum is of heuristic value because it can directly relate evaporative flux, E_t (kg m^{-2} s^{-1}) from leaves fed by a segment to the pressure gradient, dP/dx (MPa m^{-1}), within the segment, *i.e.*, $dP/dx = E_t/LSC$. A stem segment with a low LSC is less capable of supplying water to leaves fed by it than a stem segment with high LSC

h_g = is the gravitational pull on a column of water of density ρ in a tree at height h, and g is the acceleration due to gravity

q = the volume flux of water passing through a single tree stem (m^3)

h = length or tree height (m)

A_f = total leaf area distal to a tree stem segment (m^2)

$A_s = s_x$ = cross sectional conducting area of stem sapwood or xylem (m^2)

Chapter 3

Comparison between stem steady state heat energy balance (SSS), heat pulse velocity (HPV) and thermal dissipation sap flow measurement techniques

3.1 Abstract

The SSS and HPV techniques are frequently used in research within the fields of agrometeorology and plant physiology. Both techniques are however empirical and critically dependent on assumptions which, depending upon circumstance, may depart from reality to varying degrees. The theoretical and practical constraints in using each technique are presented in order to ascertain the validity of their application to different circumstances and to subsequent interpretation of measured data.

While a number of variants to the SSS technique exist, we focus on an application with a single constant output heater. This typically requires measurement of heat flux conducted through the plant limb and measurement assembly. Other variants apply for example single or multiple dynamic output heaters which potentially eliminate a need for dynamic measurements of conducted heat flux, and also reduce transient errors due to changes in heat flux to and from storage with plant tissue temperature changes.

Two empirical constants (K_{stem} and K_{gauge}) are required for inclusion in the SSS technique heat energy balance equations for conducted heat flux axially through (E_{axial}) and radially (E_{radial}) from the plant stem. The stem thermal conductivity K_{stem}, which is used in the calculation of E_{axial}, varies in and between plants with differences in plant stem anatomy (e.g. specific gravity, porosity and stem water content). Since E_{axial} is usually a small component of the heat energy balance it poses a relatively minor uncertainty to the accuracy of the technique. The term K_{gauge} is usually approximated, *in situ*, under zero sap flow conditions from a residual to the energy balance equation. However, determination of K_{gauge} is prone to error introduced from limited equipment precision, sampling procedure and model-error residuals which may be included in the energy balance equation. Since the E_{radial} term of the SSS technique can dominate the energy balance equation, the accuracy of the technique is sensitive to such errors. This poses a problem, which is more significant in larger plant species, where the confidence of obtaining a true K_{gauge} value at zero sap flow proves to be precarious (*e.g.* the incorrect appearance of temporal (daily) variations in K_{gauge}). A variable adjustment to the calculation of sap flow may also be necessary to account for diurnal temperature gradients, or different rates in stem temperature change, along the stem.

A number of variants to the HPV technique also exist. These differ in placement distance and arrangement of sensors, heater output, the method of calculating heat pulse velocity, the method of determining the ratio of the specific heat of conducting xylem wood to that of sap, and the method of scaling up from a sample measurement point to sap flow across the xylem.

Empirical constants which are fundamental to the HPV technique include a measurement of the specific heat capacity of the stem wood, which is a function of stem anatomy and water content, and plant specific adjustments for deviations from reality in the fundamental assumptions of the technique. The primary assumption made in applying HPV technique theory is that the stem is an infinite homogeneous, porous material with constant thermal conductivity. However heater and temperature probes are of finite size and have different thermal properties to the surrounding three dimensionally

anisotropic stem tissue in which they are usually inserted. Stem tissue borders, wounding resulting from sensor implantation, and a vascular anatomy exhibiting narrow growth rings of varying hydraulic conductivity, or otherwise an extremely diffuse porous wood with a relatively few large and widely dispersed vessels, are also important sources of departure from idealised theory. Together these tend to result in under-estimation of convective sap velocity. Consequently application of the HPV technique, which usually necessarily assumes that these practicalities have persistent effects, depends on empirical or numerical adjustment for such effects.

Comparison between the techniques is made by taking the following factors into consideration: plant vasculature, technique and sensor placement, localisation on efficiency and accuracy, and instrumentation.

The Granier (heat dissipation) method is an empirical method for determining sap flow in trees with diameters greater than 40 mm. Two cylindrical probes (about 2 mm in diameter) are inserted radially into the stem, each probe about 100 mm apart. The upper probe contains the sensing thermocouple and a heater. The temperature of the upper probe is referenced to the temperature sensed by the thermocouple in the lower probe. Constant power is applied to the heater and the temperature difference is empirically related to the sap flow. The temperature difference is measured under flow and no sap flow conditions and using values for the sap density and the area of the sap wood, the mass flow rate of sap is calculated. It is recommended that the technique be calibrated for species for which it has not been validated. The technique is relatively simple and requires few measurements and calculations.

3.2 List of terms

3.2.1 SSS technique

E_{sap} (W) = $E_{heater} - E_{axial} - E_{radial} - E_{storage}$

E_{heater} (W) = heat produced by the SSS gauge heater (W) = $I_{heater} \times V_{heater}$, where R_{heater} is V_{heater}/I_{heater} such that $E_{heater} = V^2_{heater}/R_{heater}$

E_{axial} (W) = $E_{upper} + E_{lower} = K_{stem} \times A_{stem} (dT_{upper}/dz_1 + dT_{lower}/dz_1)$ such that dT is temperature difference over the distance of dz between two points located upstream or downstream from the gauge heater respectively

E_{radial} (W) = radially conducted heat flux from a heated plant limb segment

$E_{storage}$ (W) = heat energy term to account for stem heating or cooling

$E_{residual}$ (W) = calculated voltage from a zero sum balance in the energy balance equation: $E_{heater} - E_{axial} - E_{radial} - E_{storage}$

C_w (J g^{-1} K^{-1} = specific heat of water (4.186 J g^{-1} K^{-1})

dT_{stem} (K) = the mean stem surface temperature difference between the junction pairs of thermocouples A and B (°C) used in practice to assume dT_{sap}

$dT_{stem\ natural}$ (K) = dT_{stem} values measured with the gauge heater switched off

K_{stem} (W m^{-1} K^{-1}) = stem thermal conductivity

A_{stem} (m^2) = stem cross sectional area

K_{gauge} (W mV^{-1}) = thermal conductance proportionality constant dependent on the gauge characteristics (such as installation of thermopile and insulation materials) and environment (J s^{-1} mV^{-1}). Typically it is calculated as: $(E_{heater} - E_{axial} - E_{sap})/V_{thermopile}$ under zero sap flow conditions

$K_{gauge\ apparent}$ (W mV^{-1}) = calculated value for K_{gauge} where with the assumptions: (i) steady state heat flux, (ii) zero or measured heat storage, (iii) accurate determinations of E_{heater}, E_{axial} and $V_{thermopile}$, and (iv) where sap flux has ceased such that $E_{sap} = 0$

M_{sap} (g s^{-1}) = sap flux

$V_{thermopile}$ (mV) = potential difference change produced in a thermopile due to temperature change between the outer surfaces of a layer of material surrounding the SSS technique heater (mV)

$V_{thermocouple\ A}$ (mV) = potential difference change with temperature between two sensing junctions in Thermocouple A

$V_{thermocouple\ B}$ (mV) = potential difference change with temperature produced between two sensing junctions in Thermocouple B

V_{heater} (V) = the measured voltage across a heater

R_{heater} (Ω) = heater resistance

S (V K^{-1}) = Seebeck coefficient for copper-constantan thermocouples

dz (m) = gap distance between thermocouples A and B

V (m^3) = heated segment volume

C_p (J kg^{-1} K^{-1}) = stem specific heat capacity

$\Delta T/\Delta t$ (K s^{-1}) = rate of stem temperature change

Ψ (MPa) = water potential

L (m) = length of flow path in the transfer medium (m)

T_{ha} (K) = temperature at the heater surface (K)

T_o (K) = temperature at the outside of the insulation material (K)

r_1 (m) = radius at the heater surface (m)

r_2 (m) = radius of the outside insulation material (m)

K_{radial} (W K^{-1}) = overall gauge radial thermal conductance, where $K_{gauge} = K_{radial}/S$ and $V_{thermopile}/S = (T_{hs} - T_o)$

t_c (s) = time constant

k_r (W m^{-1} K^{-1}) = thermal conductivity of the gauge insulation material

E_{regime} = stepwise pattern of voltage switching used

E_{sap}/E_{heater} = proportion of heat convected in sap to heat emitted by heater.

3.2.2 HPV technique

T = temperature (K), or departure from ambient temperature

t = time interval over which heat transfer is measured in determining heat fluxes (s)

k = thermal diffusivity (m^2 s^{-1})

K = thermal conductivity of a material (W^{-1} m^{-1} K^{-1}), is equal to the heat flux divided by the temperature gradient. This is numerically equal to the rate of heat flow (J s^{-1}) through a unit cube of material (1 m on a side) between two opposite parallel surfaces having a temperature difference of 1 K or °C

x, y, r = distance from heater (m)

a = fraction of any plane perpendicular to the x-axis occupied by sap streams

A = cross sectional area perpendicular to the direction of heat flow (m^2)

u = uniform velocity of sap streams (m s^{-1})

v = heat pulse velocity (m s^{-1})

ρ = density of a medium; ρ_s = density of sap (= water); ρ_w = density of combined wood-sap mixture = $\rho_b (1 + m_c)$; $\rho_b = \rho_{dry\ wood}$ = basic wood density = oven dry mass of wood /green volume of wood

C = specific heat capacity of a medium (J kg^{-1} K^{-1}); C_s = specific heat of sap (= water); C_w = specific heat of wood-sap mixture = $(C_b + m_c C_s)/(1 + m_c)$ (*e.g.*, 2.5 MJ kg^{-1} K^{-1} for soybean); $C_b = C_{dry\ wood}$ = specific heat of dry wood

q = average power applied per unit length of a sensor heater (W m^{-1})

Q = internally generated heat such that $Q = q/\rho C$, where ρC is the volumetric heat capacity of the medium

J = sap flow velocity (m s^{-1})

m_c = wood water content (Θ) = (wood-sap mixture mass - oven dry mass)/[oven dry mass]

σ = specific gravity (kg m^{-3}) = mass/[volume of water displaced by substance]

f_m = matrix fraction of bulk sample

f_l = liquid fraction of bulk sample

e = base of natural logarithms

$\pi \approx 22/7$

ln = natural log function

t_{max} = time (s) to peak temperature (*i.e.* $dT/d\Delta t = 0$)

t_{mo} = time (s) to peak temperature (*i.e.* $dT/d\Delta t = 0$) under the condition of zero sap flow

t_o = time (s) required for a temperature difference between two sensors to return to an initial value or an equal temperature subsequent to the release of a heat pulse in the sensing medium

ΔT_{mo} = peak temperature rise (K) resulting from a heat pulse, under the condition of zero sap flow

R = resistance of a conductor (K W^{-1}), which is directly proportional to its length in the flow direction and inversely proportional to its cross-sectional area perpendicular to the flow direction *i.e.* $R = (r \times L)/A$

r = resistivity (m K W^{-1}) which is resistance (K W^{-1}) of a cube as measured between two parallel surfaces.

3.3 Introduction

Transpiration may be defined as the loss of water-vapour by land plants, which occurs mainly from leaves and differs from simple evaporation in that it takes place from living tissue and is influenced by the physiology of the plant. Transpiration takes place chiefly through stomata and to a lesser extent through the cuticle. For a healthy plant transpiration is inevitable, particularly during interchanges of gasses between the plant and atmosphere in photosynthesis and respiration. Transpiration by trees growing in forests or plantations remains a difficult quantity to characterise.

Application of approaches to approximate transpiration from forest canopies and the rate at which water is released from these, through a measure of their evaporation, is frequently limited by the necessity for estimation of foliage area and certain physical and physiological properties of the foliage (*e.g.* stomatal conductance) for each component of the forest canopy (Monteith, 1965; Jarvis, 1975; Jarvis, James and Landsberg, 1976).

As an alternative approach, attempts at determining the rate (kg s^{-1}, mm s^{-1} and m^3 s^{-1}) at which water moves up the xylem of living plants and is subsequently lost to the surrounding atmosphere have led to the development of various techniques, which have been discussed by Denmead (1984).

The active xylem, sapwood, is the principle component of the tree in which water transport occurs and consists of several of the youngest growth rings, the number depending on the species and ranging from one to several years growth (Biddulph, 1959). After water has entered the roots it rises to most parts of the plant. This process is known as the ascent of sap. The ascent of sap is a result of transpiration, capillary rise and bulk flow all occurring simultaneously (Levitt, 1974). However sap flow in trees is known to lag behind transpiration by as much as 15 to 45 min (Hinckley, 1971; Veselkov and Tikhov, 1984). Differences between sap flow and transpiration are common in trees but not in many other plants.

Techniques which measure sap flux density (kg s^{-1} m^{-2}, mm s^{-1} m^{-2} and m^3 s^{-1} m^{-2} = m s^{-1}) remain the most economical and practical approach to the direct estimation of water use by individual trees. These techniques emphasise local measurement of sap flow which can be integrated or calibrated for an entire plant.

To scale up water use sampled from a small number of trees, the total cross-sectional area of a larger number of trees in a stand can be measured to develop a linear regression between total cross-sectional area and sapwood area. Subsequently sap flow could be calculated on a total sapwood per unit ground area basis.

Alternatively a survey of the trees' positions in the study area could be conducted. Subsequently

tessellation of the site could be performed, using the method of Dirichlet (1850), to apportion the study area among trees. This approach implies that each tree exploits all points closer to it than do other trees. This method is common to many investigations of ecology (Pielou, 1977; Mithen, Harper and Weiner, 1984; Hutchings and Discombe, 1986). Stand flux is calculated as the mean of each sampled tree's water use divided by its occupation area as determined by the tessellation (Cohen, Fuchs, Valkenburg and Moreshet, 1988).

Rein (1929), Huber (1932), Baumgartner (1934); Huber and Schmidt (1937) and Bloodworth, Page and Cowley (1955; 1956) laid the foundation for the use of heat to measure sap flux density. Currently the most widely applied techniques which use heat to measure sap flow are the steady state heat energy balance (SSS) and the heat pulse velocity (HPV) techniques (**Table 3.1** and **Table 3.2**). A notable advantage to these two approaches is that they allow practically continuous measurement of sap flow velocity over long periods of time, so that temporal variations can be followed. The data are produced in the form of an electrical signal, suitable for further processing and storage.

Table 3.1 List of frequently cited applications of the SSS technique

Honey mesquite (Prosopis glandulosa Torr. var. glandulosa, P. alba) - Dugas, Marcus and Mayeux (1992); Levitt, Simpson and Tipton (1992)

Corn (Zea mays L.) - Gavloski, Whitfield and Ellis (1992a; b;); Ishida, Campbell and Calissendorff (1991); Stockle, Kjelgaard and Campbell (1992); Cohen, Takeuchi, Nozaka and Yano (1993); Peressotti and Ham (1996)

Cotton (Gossypium hirsutum L.) - Ham, Heilman and Lascano (1990; 1991); Baker and Van Bavel (1987); Dugas, Heuer, Hunsaker, Kimball, Lewin, Nagy and Johnson (1994)

Cucumber (Cucumis sativus L.) - Kitano and Eguchi (1989)

Prairie grass (Andropogon gerardii Vitman and Sorghastrum nutans L.) - Senock and Ham (1995); Ham, Owensby, Coyne and Bremer (1995)

Sunflower (Helianthus annus L.) - Sakuratani (1981); Baker and Van Bavel (1987); Ham and Heilman (1990); Ishida, Campbell and Calissendorff (1991); Stockle, Kjelgaard and Campbell (1992)

Soybean (Glycine max. Merr.) - Sakuratani (1981); Sato and Sakuratani (1982); Sakuratani (1987); Cohen, Takeuchi, Nozaka and Yano (1993); Gerdes, Allison and Pereira (1994)

Sugarcane (Saccharum officinarum, S. spontaneum) - Sakuratani and Abe (1985); Saliendra, Meinzer, grantz, Neufeld and Goldstein (1992)

Rice (Orzea vulgare) - Sakuratani (1979; 1990)

Blue gum (Eucalyptus grandis) - Savage, Lightbody and Graham (1993)

Coffee (Coffea arabica L.) - Gutiérrez, Harrington, Meinzer and Fownes (1994)

Koa (Acacia koa Gray) - Gutiérrez, Harrington, Meinzer and Fownes (1994)

Black Spruce (Picea mariana) - Groot and King (1992)

Oak (Quercus virginiana) - Levitt, Simpson and Tipton (1992)

Jack Pine (Pinus banksiana Lamb.) - Groot and King (1992)

Potato (Solanum tuberosum L.) - Ishida, Campbell and Calissendorff (1991); Stockle, Kjelgaard and Campbell (1992)

Grape vines (Vitis vinifera L.) - Lascano, Baumhardt and Lipe (1992a; b)

Tropical deciduous forest vines (Entadopsis polystachya; Cyclanthera multifoliolata; Serjania branchycarpa) - Fichtner and Schulze (1990)

Peach (Prunus persica L.) - Shackel, Johnson, Medawar and Phene (1992)

Fig (Ficus benjamina, Ficus retusa L. Nitida) - Steinberg (1988); Steinberg Van Bavel and McFarland (1989)

Pecan tree (Carya illinoensis 'Wichita') - Steinberg, McFarland and Worthington (1990)

Bald cyprus (Taxodium distichum) - Steinberg, Van Bavel and McFarland (1990)

Crape myrtle (Lagerstroemia indica L.) - Zajicek and Heilman (1991)

Hibiscus (Hibiscus rosa-sinensis L.) - Steinberg, Zajicek and McFarland (1991b)

Privet or Wax Leaf Ligustrum (Ligustrum japonicum Thunb.) - Heilman, Brittin and Zajicek (1989); Heilman and Ham (1990); Steinberg, Zajicek and McFarland (1991a)

Croton (Croton melagocarpus) - Ong and Kahn (1993)

Apple (Malus sylvestris) - Valancogne and Nasr (1989).

Table 3.2 List of frequently cited applications of the HPV technique

Acacia (Faidherbia albida) - Ong, Singh, Kahn and Osman (1990)

Plane tree (Plantanus orientalis L.) - Cohen, Fuchs and Green (1981)

African hardwood (Albizia lebbeck) - Ong, Singh, Kahn and Osman (1990)

Willow (Salix fragilis) - Swanson (1962)

Grapevine (Vitis vinifera L.) -Schanderl (1956)

Citrus (Citrus sinensis L. Osbeck.) - Cohen, Fuchs and Green (1981); Cohen, Fuchs and Cohen (1983)

Citrus (grapefuit var Marsh seedless) - Cohen (1991)

Kiwifruit (Actinidia deliciosa) - Green and Clothier (1988)

Kiwifruit (Actinidia chinensis Planchon) - Edwards and Warwick (1984)

Apple (Malus sylvestris X Red delicious) - Marshall, 1958; Green and Clothier (1988)

Blue Gum (Eucalyptus grandis Hill ex Maiden) - Olbrich (1991)

Jarrah (Eucalyptus marginata) - Doley and Grieve (1966)

Mountain Ash (Eucalyptus regnans) - Dunn and Connor (1993)

Red River Gum (Eucalyptus camaldulensis) - Salama, Bartle and Farrington (1994)

Poplar (Populus alba L.) - Cohen, fuchs and Green (1981)

Poplar (Populus nigra var. italica Du Roi) - Closs (1958); Hein and Farr (1973)

Poplar (Populus deltoides) - Edwards and Booker (1984); Smith (1992)

Patula Pine (Pinus patula) - Dye, Olbrich and Poulter (1992)

Radiata Pine (Pinus radiataD. Don) - Swanson and Whitfield (1981); Hatton and Vertessy (1989; 1990); Hatton, Catchpole and Vertessy (1990)

Maritime Pine (Pinus pinaster) - Diawara, Loustau and Berbigier (1991)

Ponderosa Pine (Pinus ponderosa) - Lopushinsky (1986)

Aleppo Pine (Pinus halepensis Mill.) - Swanson (1972)

Sitka Spruce (Abies amabilis) - Hinckley and Ritchie (1970)

Douglas Fir (Pseudostuga menziesii) - Lassoie, Scott and Fritschen (1977); Lopushinsky (1986)

Norway Spruce (Picea abies (L). Karst) - Cermák, Cienciala, Kuera and Hällgren (1992)

Oak (Quercus spp.) - Miller, Vavrina and Christensen (1980); Cermák, Cienciala, Kuera and Hällgren (1992)

Engelmann spruce ( ) - Swanson (1967); Mark and Crews (1973)

Lodgepole pine (Pinus contorta) - Swanson (1967); Mark and Crews (1973)

Mountain Beech (Nothofagus solandri var cliffortoides (Hook. f.) Orst) - Swanson, Beneke and Havranek (1979)

Cotton (Gossypium hirsutum L.) - Cohen, Fuchs, Falkenflug and Moreshet (1988); Bloodworth, Page and Cowley (1955); Closs (1958); Stone and Shirazi (1975); Sakuratani (1981); Petersen, Fuchs, Moreshet, Cohen and Sinoquet (1992)

Soybean (Glycine max Merr. cv. tamahomare) - Cohen, Takeuchi, Nozaka and Yano (1993)

Corn (Zea mays cv. kakuteru 901) - Cohen, Takeuchi, Nozaka and Yano (1993).

3.4 Rationale

It is suspected that the SSS and the HPV techniques are critically dependent on assumptions which, depending upon circumstance, depart from reality to varying degrees and which consequently may render them both empirical in application. Selection for application of either technique depends upon the circumstances to which there is practical departure from reality in the over-riding assumptions for

each, and to which these can be accommodated.

Both the SSS and the HPV techniques are frequently cited (Tables 3.1 and 3.2) in research within the fields of agrometeorology and plant physiology. In order to ascertain the validity of application and subsequent interpretation of measured data using either technique, it is important that there is a theoretical and practical examination of each technique. This is necessary when the researcher is faced with a choice of applying either to a particular circumstance, particularly for the first time.

The null hypothesis to be tested is that each technique is equally appropriate and interchangeable in their application to plant species, irrespective of the circumstance, and secondly that neither is dependent upon circumstance specific empirical adjustment.

We present a comparative evaluation of the theoretical and practical constraints and implications in using the Steady State Heat Energy Balance (Sakuratani, 1981; 1984; Baker and Van Bavel, 1987; Ishida, Campbell and Calissendorff, 1991) and the Heat Pulse Velocity techniques (Cohen, Fuchs and Green, 1981; Swanson, 1983).

One would hope to learn from this the comparative extent to which each technique is necessarily prone to empirical adjustment, and under which circumstances application of either is preferable for research into the wide diversity in plant species growing under varying climatic conditions in South Africa.

In addressing this, specific factors which are to be considered for comparison concern (i) the suitability of each technique with regards to plant vasculature, and related to this, (ii) the implications of the degree of localisation of the techniques' sample measurement at the plant xylem on its efficiency and accuracy in determining of sap flow, and (iii) instrumentation.

3.5 Work plan and methodology

A literature review was conducted with initial installation and application of the two techniques. No data is presented in this chapter since this does not meet the rationale, hypothesis or objectives outlined above. Experimental work and data concerning the SSS technique follow in subsequent chapters. This thesis focusses on the application of the SSS technique, consequently no data using the HPV technique is presented.

3.5.1 SSS theory

The SSS technique was theorised by Vieweg and Ziegler (1960) and later developed further by Daum (1967), Saddler and Pitman (1970), Sakuratani (1981; 1984), Baker and Van Bavel (1987), Steinberg, Van Bavel and McFarland (1989; 1990) and many others.

By supplying a continuous constant heat energy flux (J s^{-1}) to a plant limb (using a surrounding heater) and accounting for its assumed component energy losses by: (i) conduction both vertically upwards and downwards (axially) through and radially from the stem, and (ii) heat stored in the plant limb, the heat component convected in sap can be determined (**Fig. 3.1**):

$$E_{sap} = E_{heater} - E_{axial} - E_{radial} - E_{storage}. \quad 3.1$$

Sap flow (kg s^{-1}) can be determined from the quotient of the sap convection energy component (J s^{-1}), and the product of sap specific heat capacity (J kg^{-1} K^{-1}) and the temperature difference (K) between above and below the heater (Fig. 3.1), such that:

$$\text{sap flow } M_{sap} = \frac{E_{heater} - E_{axial} - E_{radial} - E_{storage}}{C_w \times dT_{stem}} \quad 3.2$$

where

$$E_{sap} = C_w \times dT_{stem} \times M_{sap} \quad 3.3$$

and where: C_w is the specific heat capacity of sap which is assumed to be the same as that for water (4186 J kg^{-1} K^{-1}), dT_{stem} (K) is the mean sap temperature difference (frequently assumed from measurements at the stem surface) between the centre of two pairs of vertical points, separated by dz, each upstream and downstream of a heater respectively and M_{sap} is the sap flow (kg s^{-1}).

The heat energy flux supplied by the heater is determined by measuring the potential difference across the heater and the heater impedance:

$$E_{heater} = V^2_{heater}/R_{heater} \quad 3.4$$

where V_{heater} is the potential difference (V) across the heater and R_{heater} is its electrical resistance (Ω). The power applied to the heater is given by $E_{heater} = I_{heater} \times V_{heater}$ while from Ohm's law $R_{heater} = V_{heater}/I_{heater}$ so that $E_{heater} = V^2_{heater}/R_{heater}$. In practice the heater is powered by electronic circuitry connected to a battery, which facilitates a constant potential difference across the heater. Measurements and computations are facilitated by a datalogger.

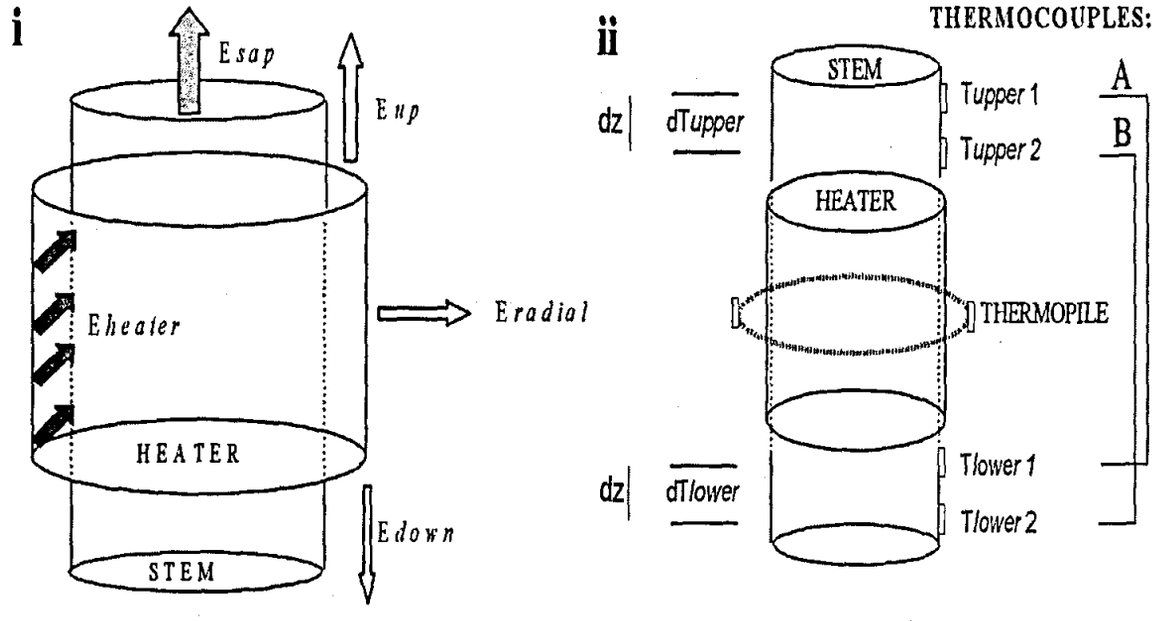

Fig. 3.1i Illustration of the steady state heat energy balance. Heat flux components are represented by arrows. The terms E_{heater}, E_{up}, E_{down}, and E_{radial} are determined directly using sensors and E_{sap} is determined by subtraction of the latter three terms from E_{heater} i.e.

$$E_{sap} = E_{heater} - E_{up} - E_{down} - E_{radial}.$$

ii. Diagram showing the conceptual and sensing components of the SSHB technique. Note the positions of thermocouples A and B used in the wiring procedure of Steinberg, Van Bavel and McFarland (1990) and the positions of the sensing junctions on the stem or plant limb surface. Each thermojunction is pair separated by the distance dz (m) such that combined temperature gradient in the stem away from the heater is given by:

$$[(dT_{upper}/dz) + (dT_{lower}/dz)]$$
$$= (T_{upper1} - T_{upper2})/dz + (T_{lower2} - T_{lower1})/dz = (T_{upper1} - T_{lower1})/dz - (T_{upper2} - T_{lower2})/dz$$

Most applications of the SSS technique use a heat transfer coefficient (K_{gauge} with unit W mV^{-1}), also referred to as the thermal conductance of the gauge, as the proportionality constant between the radial energy flux component E_{radial} (W) and the thermopile measured voltage difference between inner and outer surfaces of a cork layer surrounding the heater, such that:

$$E_{radial} = K_{gauge} \times V_{thermopile} \quad 3.5$$

The variable coefficient K_{gauge} can be derived clearly from heat transport theory. It is dependent on the thermopile design, the thermal properties of the gauge (*e.g.*, the nature and thickness of the insulating material used), and gauge size. Theoretically it is not a function of the environment. Further, it should not be a function of power, unless there is some type of model error in the heat balance.

Alternatively E_{radial} (W), based on the expression for radial heat flow in a cylinder of infinite length (Carslaw and Jaeger, 1959), may also be described by:

$$E_{radial} = 2 \pi k_r (T_{hs} - T_o) L / \ln (r_2/r_1) = K_{radial} (T_{hs} - T_o) \quad 3.6$$

where k_r is the thermal conductivity of the insulation material (W m^{-1} K^{-1}), T_{hs} is the temperature at the heater surface, T_o is the temperature at the outside of the insulation material, L is the length of the flow (m), r_1 is the radius at the heater surface, r_2 is the radius of the outside insulation material, and K_{radial} is an overall radial thermal conductance (W K^{-1}) (Ishida, Campbell and Calissendorff, 1991). The resultant simultaneous solution to the above two equations is $K_{gauge} = K_{radial}/S$, where S is the Seebeck coefficient (μV K^{-1}) for the thermocouple type used to measure $V_{thermopile}$ such that $V_{thermopile}/S = (T_{hs} - T_o)$.

Baker and Van Bavel (1987) show that for gauges with diameters between 8 and 18 mm, K_{radial} is approximately 0.03 W K^{-1}, meaning that the maximum temperature inside the heated segment at zero sap flow will exceed ambient temperature by 1 °C for every 0.03 W of heating. In this instance a heat input of 0.1 W was used resulting in a maximum temperature increase of slightly greater than 3 °C.

The voltage output from the thermopile is a function of the Seebeck coefficient and the number of junction pairs in the thermopile. The analysis of Baker and Van Bavel (1987) as presented in the above paragraph is incorrect since the increase in temperature in a heated stem segment at zero sap flow is also dependent upon axial heat conduction. This simplified analysis would cause an overestimate of stem heating, the significance of which would depend on the ratio of E_{axial} to E_{radial}.

The method for measuring E_{radial} described in Eq. 3.6 is impractical with regards to standard Dynamax gauge fittings and the assumed model dimensions around which the technique is based. It would either require measurement of the thickness, thermal conductivity and inner and outer surface temperature difference of the gauge insulation, or a measurement of the gauge thermal conductance (W K^{-1}). These measurements would destroy the sensor.

The heat energy balance term to describe heat storage, $E_{storage}$, is described by:

$$E_{storage} = V \rho C_p \Delta T/\Delta t \quad 3.7$$

where V is the heated segment volume (m^3), ρ is the density of the stem (kg m^3), C_p is the stem specific heat capacity (J kg^{-1} K^{-1}) and $\Delta T/\Delta t$ is the rate of temperature change in the stem (K s^{-1}).

A heat storage term has frequently been omitted from the assumed thermal energy balance *e.g.*,

Dynamax gauge design and assumptions of Baker and Van Bavel (1987) and Steinberg, Van Bavel and McFarland (1990). This would imply that it is assumed that the stem segment does not heat up or cool down significantly for any period during the application of the technique. While the influence of stored heat on the energy balance may be small, the assumption that the heated stem segment temperature will remain constant is unrealistic. Consideration of stored heat in the energy balance has been shown by Ham and Heilman (1990) and Groot and King (1992).

The vertically conducted (axial) energy flux component can be determined using two thermocouples, where potential difference (mV) changes with temperature between the two sensing junctions of these thermocouples (A and B), such that (Savage, Graham and Lightbody, 1993):

$$E_{axial} = [(V_{thermocouple\ A} - V_{thermocouple\ B})/(S \times dz)] \times A_{stem} \times K_{stem} \qquad 3.8$$

where S ($\mu V\ K^{-1}$) is the Seebeck coefficient for copper-constantan thermocouples, dz (m) is the gap distance between the two thermocouples, A_{stem} is the stem area (m^2), and K_{stem} is the stem thermal conductivity ($W\ m^{-1}\ K^{-1}$). This equation reflects the wiring procedure used by Steinberg, Van Bavel and McFarland (1990) which was introduced to reduce the number of datalogger channels required to operate the gauge *i.e.*, it allows the determination of three energy balance terms with the measurement of only two voltages. It does not not affect the accuracy of the gauges but does however not allow measurement of stem temperature (for calculation of $E_{storage}$), for which an extra thermocouple and channel would be required.

Practically dT_{stem} is recorded by a datalogger connected to the same thermocouples A and B as used to measure E_{axial} in the wiring manoeuvre used by Steinberg, Van Bavel and McFarland (1990) such that:

$$dT_{stem} = [(V_{thermocouple\ A} + V_{thermocouple\ B})/2]/S. \qquad 3.9$$

A two-dimensional mathematical analysis of the SSS procedure has been presented by Pickard and Puccia (1972). A variant of this technique in which, by varying the power of the heater, a constant temperature is maintained between the sensors above the heated stem segment has been presented by Cermák, Deml and Penka (1973), Cermák, Kuera, and Penka (1976), Cermák, Jenik, Kuera and Zidek (1984), Kuera, Cermák and Penka (1977); Schulze, Cermák, Matyssek, Penka, Zimmerman, Vasicek, Gries and Kuera (1985) and Fichtner and Schulze (1990).

A major criticism of the variable power constant temperature technique is that conductive heat loss has not been measured directly, which may cause significant errors. Ishida, Campbell and Calissendorff (1991) have combined the approaches of Sakuratani (1981; 1984) and Baker and Van Bavel (1987) with that of Cermák *et al.* (1973) and Fichtner and Schulze (1990) - to combine the advantages inherent in the two methodologies. Subsequent work using the combined technique has been presented by Stockle, Kjelgaard and Campbell (1992).

Some researchers have developed heat-balance gauges that use multiple heaters in combination with variable power techniques to eliminate some of the problems associated with more traditional, single heater approaches. Kitano and Eguchi (1988) used three heaters and three variable power controllers, which eliminate the need for dynamic measurements of radial and axial temperatures. Some workers have described multiple-heater gauge in which two tandem heaters are attached to the stem with a third, larger heater wrapped around the periphery of the gauge assembly. A new proto-type of multiple-heater sap flow gauge has been presented by Peressotti and Ham (1996). This gauge was

developed to eliminate the necessity of measuring radial heat flux from the gauge heater and reduce transient errors in the application of the technique.

3.5.2 HPV theory

The first widely accepted theoretical basis for the HPV technique was proposed by Marshall (1958). He suggested that the heat transfer mechanisms within a plant are conduction and convection (Eq. 3.10), the latter being proportional to sap velocity. It was first implemented, in a modified form, by Closs (1958):

$$\frac{\delta T}{\delta t} = k_x \frac{\delta^2 T}{\delta x^2} + k_y \frac{\delta^2 T}{\delta y^2} - au \frac{\rho_s C_s}{\rho_w C_w} \frac{\delta T}{\delta x} + \frac{Q}{\rho C} \qquad 3.10$$

where sap flow is in the axial direction (Marshall, 1958; Carslaw and Jaeger, 1959) and where T is temperature departure from ambient, t is time, u is sap speed, a is the fraction of xylem cross sectional area occupied by moving sap streams, ρ and C are density (kg m^{-3}) and specific heat capacity (J kg^{-1} K^{-1}) and subscripts s and w are for sap and the mixture of sap with the wood matrix, x and y are the axial and tangential thermal diffusivities of the mixture, respectively and Q is internally generated heat such that $q/\rho C = Q$, where ρC is the volumetric heat capacity of the medium and q is the average power applied per unit length of sensor (W m^{-1}).

The first two terms on the right hand side of Eq. 3.10 describe heat conduction and the third convection. Eq. 3.10 is of the same form as the equation for pure conduction in a medium in the axial direction (Jakob, 1949) *i.e.*, the stationary wood and the moving sap together act like a single medium moving at a speed defined by T. This speed is less than that of the sap itself; it is in fact a weighted average of the velocities of the sap and the stationary wood substance. This is not surprising when one considers that in the wood alone the heat pulse would remain stationary as it diffused, while in the sap alone the pulse would move at the same speed as the sap.

Marshall (1958) showed that if the sap and the woody matrix were considered as a homogeneous medium, then the ratio of sap velocity to heat pulse velocity could be written as:

$$\frac{u}{v} = \frac{a}{A} \times \frac{\rho_s C_s}{\rho_w C_w} \qquad 3.11$$

where u is the sap velocity within the lumens of the vessels, v is the heat pulse velocity, a and A are the lumen and total sapwood cross-sectional areas respectively, ρ (kg m^{-3}) is the density, C (J kg^{-1} K^{-1}) is the specific heat, and the subscripts $_s$ and $_w$ are sap and wood matrix plus sap (including gas) respectively.

Assuming the xylem to be infinite in extent so that surface effects could be ignored, heat released instantaneously along a straight line in the sap would diffuse gradually throughout the xylem by the process of conduction, until the temperature of all the xylem was raised by the same small amount. The temperature at any point would rise to a maximum and then fall much more slowly to the original value.

In this regard, for a given quantity of heat the temperature at a point at a given time would depend only on the xylem thermal diffusivity, k (m^2 s^{-1}), which depends on the thermal conductivity, K (W m^{-1} K^{-1}), and the volumetric heat capacity, ρC (J m^{-3} K^{-1}), where ρ is the density (kg m^{-3}) and C_p is the specific heat capacity (J kg^{-1} K^{-1}):

$$k = K/\rho C_p. \quad 3.12$$

Current HPV techniques follow Closs's implementation and detect times of arrival of a heat pulse upstream and downstream of a heater to determine convective heat pulse velocity:

$$\text{sap flow} = [\rho_w C_w/(\rho_s C_s)]\, \Sigma v_i A_{stem\,i}, \quad 3.13$$

where A_{stem} is the stem cross sectional area and the heat wave pulse velocity (v_i) is defined by:

$$v = \frac{\rho_s C_p}{\rho_w C_w} J \quad 3.14$$

such that:

$$J = \frac{a}{A} u = \left(\frac{\rho_w C_w}{\rho_s C_s}\right) v_i = \rho_b (C_w + m_c)\, v \quad 3.15$$

where J is the sap flow velocity (m s^{-1}), the term, ρ_b is wood density (oven dry mass / green volume), C_w is specific heat of wood-sap mixture, and $m_c(\theta)$ is wood water content *i.e.* (wood-sap mixture mass - oven dry mass)/(oven dry mass).

The specific gravity of sap (σ_s) is 1000 kg m^{-3}, and that of the solid woody matrix, excluding air, is 1530 kg m^{-3}. The latter value may be considered constant within and between species (Panshin and de Zeeuw, 1970; Edwards and Warwick, 1984). The specific heat of the woody matrix (C_m) may be taken as 1.38×10^6 kJ kg^{-1} K^{-1} (Skaar, 1972) and that of sap as equal to the specific heat of water (4.186 J g^{-1} K^{-1}).

Using the wood matrix (f_m) and liquid (f_l) component volume fractions of the stem, the bulk density (kg m^{-3}) of the tissue is given by:

$$C_w = 1530 f_m + 1000 f_l \quad 3.16$$

and its specific heat (kJ kg^{-1}) may be taken to be:

$$C_w = \frac{1530 f_m C_m}{1530 f_m + 1000 f_l} + \frac{1000 f_l C_s}{1530 f_m + 1000 f_l}. \quad 3.17$$

Volumetric heat capacity is linearly related to the inverse of Δt_{mo} (Campbell, Calissendorff and Williams, 1991) and can be measured at zero sap flow in a similar manner to that for measuring v_i:

$$\rho_w C_w = q/[e \pi r^2 \Delta T_{mo}]. \quad 3.18$$

The significance of measuring the volumetric heat capacity from Eq. 3.15 is that the water content of the plant tissue does not need to be monitored using Eq. 3.16 and Eq. 3.17 to solve Eq. 3.15.

3.5.2.1 Method A

The change in temperature (ΔT) measured at radial distance (r) from the heat source after a period of time (t) after the application of the heat pulse is given by (Carslaw and Jaeger, 1959; Cohen, Fuchs and Green, 1981):

$$\Delta T = \frac{q}{4\pi\rho C\, kt} \exp\left[-\frac{(r - v_i t)^2}{4kt}\right]. \quad 3.19$$

The exponent term $v_i t$ describes a convective influence on T where v is the heat wave convective velocity (m s^{-1}). The function described by Eq. 3.19 has a maximum occurring at time t_{max} when the first derivative of Eq. 3.19 is equal to zero ($dT/d\Delta t = 0$) such that:

$$v_i = \frac{\sqrt{r^2 - 4\,k\,t_{max}}}{t_{max}}. \qquad 3.20$$

For a given value of r, and with known physical and thermal properties of live wood, the measurement of t_{max} in Eq. 3.20 allows the computation of the sap flow velocity, J (m s^{-1}), from Eq. 3.15.

A property which is apparently difficult to determine is the thermal diffusivity, k (m^2 s^{-1}), of the live wood. With no sap flow, *i.e.* $v = 0$, Eq. 3.20 yields:

$$k = \frac{r^2}{4\,t_{mo}} \qquad 3.21$$

Substituting Eq. 3.21 into Eq. 3.20 yields an alternative equation whereby the heat pulse velocity can be measured from the time to peak rise in temperature from the heat pulse during sap flow relative to that at zero sap flow:

$$v_i = r\,\frac{\sqrt{1 - \frac{t_{max}}{t_{mo}}}}{t_{max}}. \qquad 3.22$$

3.5.2.2 Method B

Cohen, Fuchs and Green (1981) indicated that the temperature wave dissipation at a point upstream from the heater is obtained by replacing (r) with ($-r$) in Eq. 3.19. If the sensors are placed symmetrically above ($+r$) and below ($-r$) the heater, the differential temperature wave $T(+r) - T(-r)$ has a maximum occurring at a time t_{max} which also satisfies the first derivative of Eq. 3.19, provided that the sap velocity (v) differs from zero. With v equal to zero, $T(+x) - T(-x)$ is also zero, and its measurement can be used to check the absence of convective transport.

Fluctuations in the ambient temperature disturb temperature evolution described in Eq. 3.19, because herbaceous plants are thermally coupled to environment. The evaluation of the thermal diffusivity of stems is also difficult due to the uncertainty of getting zero flow. To overcome these difficulties, Closs (1958) and Swanson (1962) suggested using differential temperature measurement at two asymmetrically located points above and below the line heat source. Thus they considered two temperatures, one upstream (T_1) at a distance of $-x_1$ and the other downstream (T_2) at a distance $+x_2$ from the heater, and showed that for t_o, the time required for the temperature difference between the two sensors to return to an initial value (or indicate the same temperature:

$$v_i = \frac{x_1 + x_2}{2\,t_o}. \qquad 3.23$$

Using t_o one can determine v from Eq. 3.23 and invert Eq. 3.20 to determine k as:

$$k = \frac{x^2 - v^2\,t_{max}}{4\,t_{max}}. \qquad 3.24$$

Cohen, Fuchs, Falkenflug and Moreshet (1988) indicated that over the range of velocities between 0.17 and 0.22 mm s^{-1}, both t_o and t_{max} could be measured with reasonable accuracy so that k could be determined by solving Eq. 3.20 and Eq. 3.23 simultaneously ($t_o < 15$ s). The thermocouple configuration they suggested from their work on cotton (*Gossypium hirsutum*) is 9 mm above and 4 mm below the heater.

Cohen, Takeuchi, Nozaka and Yano (1993) questioned the validity of using simultaneously t_o and t_{max} to estimate k in personal communications with W.A. Dugas and S. Moreshet, since they were observing inconsistent results. They subsequently re-assessed the range of heat velocity for this procedure and concluded that k should be estimated only at $t_o \geq 13$ s since their data suggested errors in measurement of t_o at less than 13 s.

They noted that heat velocity in maize (*Zea mays*) was not measurable at sap flow rates of 7 g h^{-1} or below (heat velocity below 8×10^{-3} mm s^{-1}) as a result of inaccurate detection of temperature changes in the stem (low voltage signal). They concluded that temperature detection might be improved if the distance between the heater and sensors is reduced in order to shorten the time for t_o.

3.5.2.3 Method C

One may manipulate Eq. 3.19 in several ways to calculate velocity from the temperature variation with time at one or more points (x - direction) in the xylem. Marshall (1958) considered a single temperature sensor down-stream from the heater read at three times t_1, t_2, and t_3 such that $t_3 = 3\ t_1$ and $t_2 = 2\ t_1$, and derived:

$$V = r\left[\frac{t_1 \ln\left(\frac{T_1 t_1}{T_2 t_2}\right) - t_3 \ln\left(\frac{T_2 t_2}{T_3 t_3}\right)}{t_1 t_2 t_3 \ln\left(\frac{T_1 t_1 T_3 t_3}{T_2^2 t_2^2}\right)}\right]^{1/2}. \qquad 3.25$$

More generally, if the two sensors of the above configurations are sensed at any two times t_1 and t_2, such that $T_1 \neq T_2$ (Swanson, 1962):

$$V = (x_1 + x_2)\frac{\left(t_1 \ln\left(\frac{T_1}{T_2}\right)_{t_1} - t_2 \ln\left(\frac{T_1}{T_2}\right)_{t_2}\right)}{\frac{2\,t_1}{t_2} \ln\frac{\left(\frac{T_1}{T_2}\right)_{t_1}}{\left(\frac{T_1}{T_2}\right)_{t_2}}}. \qquad 3.26$$

3.5.2.4 Wound corrections to heat pulse velocity

Heisenbergs' Uncertainty Principle, philosophically, has been used to imply that the closer one is to the point of measurement, the more what one measures changes. Marshall's (1958) theory assumes that the heat pulse velocity probes play no role in the heat flow. The calculation of V from Eq. 3.23 is based on Marshall's (1958) idealized theory and assumes the heat pulse probes have no effect on the measured heat flow. Both the heater and the sensors occupy space in tissue and must therefore in some way alter the measured sap flow. It has been shown (Cohen *et al.*, 1981; Green and Clothier, 1988) that the influence of the probes and heat probe cause an underestimation in the measured heat pulse velocity. The general procedure to avoid this has been to apply an empirical correction for the effects of wounding. This correction can be done empirically (for example, Cohen, Fuchs and Green, 1981). Swanson and Whitfield (1981) derived correction coefficients from numerical solutions of Marshall's (1958) equations, for various wound sizes using an equation of the form:

$$V_c = a + b\ V + c\ V^2 \qquad 3.27$$

where V_c (cm h^{-1}) is the corrected heat pulse velocity and V is the raw heat-pulse velocity given by Eq. 3.23 and where a, b, and c are correction coefficients. The units of cm h^{-1} have been retained since the correction coefficients are for those units. The values for the correction factors for different wound widths are shown (**Table 3.3**). The use of Table 3.3 does not then involve empirical calibration of the technique except that the wound width has to be measured to within 0.4 mm. This method then avoids the use of an empirical calibration to obtain the best estimate V.

A first approximation of the wound size is the diameter of the drilled hole. Usually however, additional damage results and the wound size is larger and therefore unknown at the time of

Table 3.3 The values of the constants *a*, *b*, and *c* of Eq. 3.23 For the correction of the sap velocity for wounding (after Swanson and Whitfield, 1981)

Wound width (mm)	*a*	*b*	*c*
0.0	0.000	1.000	0.000
1.6	0.393	1.356	0.036
2.0	0.807	1.203	0.058
2.4	1.184	1.072	0.087
2.8	1.524	0.964	0.124
3.2	1.826	0.879	0.169
3.6	2.090	0.818	0.221

measurements.

A number of practical problems arise with regard to wound size corrections:

- 1. anatomical investigations by Barrett, Hatton, Ash and Ball (1995) indicated the total wound width is likely to extend about 0.3 mm on either side of the drill hole. So for a sensor with a 1.6 mm diameter, the typical wound width would be 2.2 mm;
- 2. the 0.3 mm extension may vary depending on species;
- 3. the wound size often increases with time. The rate of increase of wound size may vary between species and therefore independent verifications may be required to determine how long meaningful measurements may be obtained for a given set of probes;
- 4. insertion of the probes, if not carefully inserted and correctly aligned, may result in a higher wound size;
- 5. the corrected sap flow velocity is very sensitive to the wound factor so extra care needs to be taken when the probes are inserted or if the wound size is measured (**Fig. 3.2**).

3.6 Analysis and discussion

3.6.1 Biophysical evidence for empirical adjustment to technique theory

3.6.1.1 SSS technique

To date, determination of K_{gauge} has mostly been conducted either: (a) under conditions when E_{sap} is assumed to equal zero, or (b) by iterative selection using a lysimeter as the reference for true sap flow. The former is an empirical zero set and should not be confused with the latter which is a calibration response to known changes in sap flow rate. Thus the determination of K_{gauge} can be considered a form of empirical calibration.

The accuracy of both of these approaches would depend however on the extent of the model error in the heat balance. Assuming that the thermal conductivity of the stem is known and remains constant, or can be measured, all the other terms required for the calculation of sap flux are assumed to be either known constants or they are measured signals. Thus, re-arranging Eq. 3.1 from Eq. 3.5:

$$K_{gauge\ apparent} = \frac{E_{residual}}{V_{thermopile}} = \frac{(E_{heater} - E_{axial} - E_{sap} - E_{storage})}{V_{thermopile}} \qquad 3.28$$

such that $K_{gauge\ apparent} = K_{gauge}$ where (assuming steady state heat flux, measurable heat storage in the

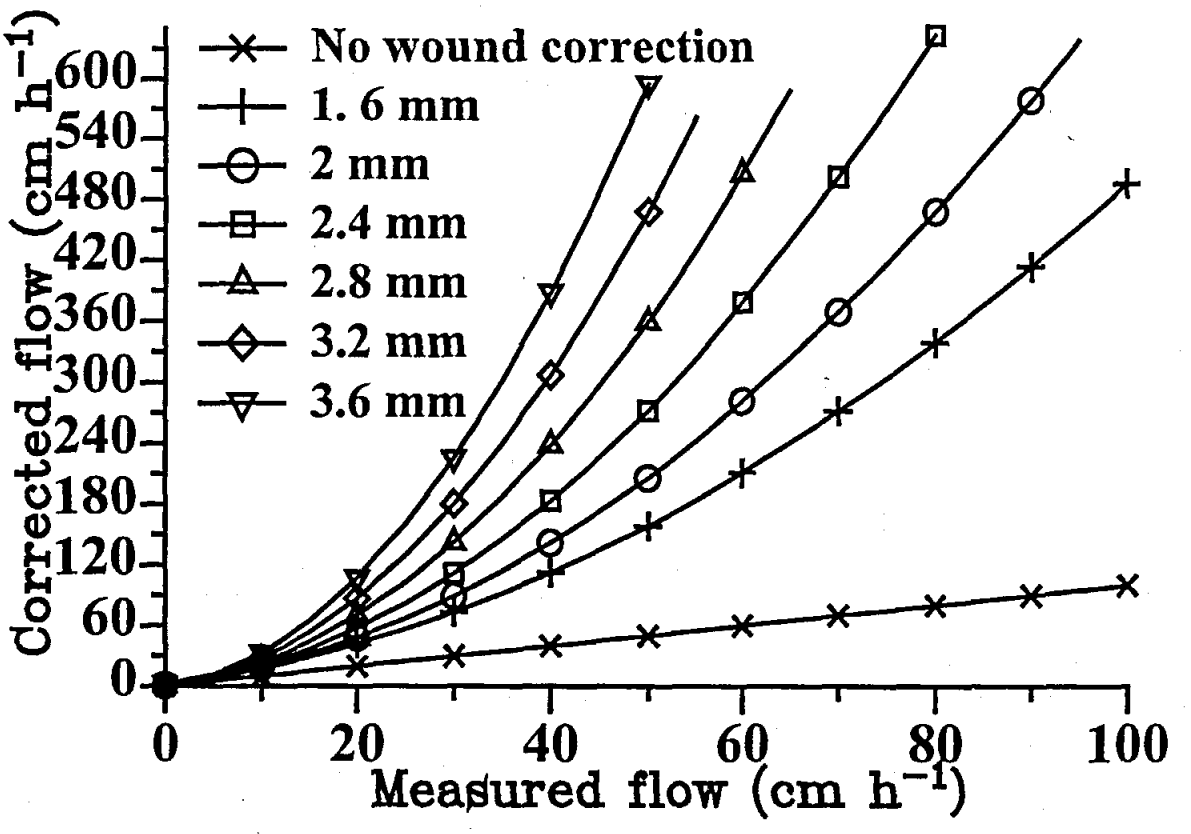

Fig. 3.2 The corrected flow for various measured flows and the various wound corrections. Typically, for a wound size of 2 mm, a measured flow of 60 cm h^{-1} is increased five fold and about six fold at a measured flow of 100 cm h^{-1}

gauge, and accurate determinations of E_{heater}, E_{axial} and $V_{thermopile}$) sap flux has ceased such that $E_{sap} = 0$.

Examples on the empirical determination of K_{gauge} include: (i) using a dowel rod consisting of wood, glass, bakelite or plastic to model a plant limb (Sakuratani, 1984; Savage, Graham and Lightbody, 1993), (ii) using excised sections of the plant limb (Baker and Van Bavel, 1987), (iii) using *in situ* predawn measurement under low evaporative conditions (Van Bavel and Van Bavel, 1990), and (iv) forcing low evaporative conditions by controlling radiation and temperature (Sakuratani, 1981; Baker and Van Bavel, 1987; Steinberg, Van Bavel and McFarland, 1989; Ham and Heilman, 1990; Heilman and Ham, 1990, Ishida, Campbell and Calissendorff, 1991).

Considering that E_{radial} can frequently be an order of magnitude larger than either E_{axial} or E_{sap} (*e.g.* low sap flow conditions), precision in the determination of K_{gauge} can necessarily dominate the accuracy of the sap flow calculation. Thus the technique is particularly vulnerable to deviation from assumptions of zero sap flow, model error, and measurement precision viz. the ratio of E_{sap} to E_{heater} (Sakuratani, 1981).When measured experimentally K_{gauge} often appears to change with time (Lightbody, Savage and Graham, 1994). This is caused by model or measurement errors. In fact temporal (daily) variations in K_{gauge} have been documented in many manuscripts cited in Table 3.1. Clearly the empirical determination of K_{gauge} is an important aspect to using this technique.

When measuring sap flux using the SSS sap flux technique, the thermal conductivity of the plant limb tissue (K_{stem}) in W m^{-1} K^{-1} is required for the calculation of the vertical (axial) conduction of heat

in Eq. 3.8. Over the years various techniques have been devised to measure K_{stem}. This value directly affects the determination of gauge conductance K_{gauge}. Thus a different combination of K_{stem} and K_{gauge} can result in the same determination of sap flow, M_{sap}. For this reason an assumed value of K_{stem} is required *a priori* for a particular plant limb prior to determining K_{gauge}.

Sakuratani (1981; 1984) assumed a thermal conductivity for a stem (90 % water) equal to that of water with acceptable errors. Frequently published averages for stem thermal conductivity are: 0.54 W m^{-1} K^{-1} (Sakuratani, 1981; 1984) for various herbaceous species and 0.42 to 0.47 W m^{-1} K^{-1} (Steinberg, Van Bavel and McFarland, 1989; Steinberg, McFarland and Worthington, 1990) for woody plant species, both of which are slightly less than 0.609 W m^{-1} K^{-1} for water at 300 K, thermal conductivity of water being dependent upon temperature (Weast, 1979), or 0.76 W m^{-1} K^{-1} for willow trees (Swanson and Whitfield, 1981).

In Chapter 4 we present details of the measurement of stem thermal conductivity. We measured a value of 0.34 W m^{-1} K^{-1} for a 28 mm diameter excised stem segment from a two year old *Eucalyptus grandis* seedling, using intrusive thermal conductivity probe sensors (Shiozawa and Campbell, 1990). The relatively low thermal conductivity value of the *Eucalyptus* trees can be attributed to the the high specific gravity and density of the wood sample taken. This is consistent with a trend of increasing thermal conductivity with increasing herbaceousness. The only cited anomaly to this trend is that the thermal conductivity value for willow, cited by Swanson and Whitfield (1981), is greater than that for pure water.

Clearly stem thermal conductivity essentially changes between different plant species and growth habits (*e.g.* with plant limb morphology, xylem hydraulic architecture and conduit specific gravity). The necessity for its measurement or alternatively assuming a fixed value axially conducted heat component of the energy balance of the SSS technique is empirical in nature.

Axially conducted heat loss is however frequently the smallest component of the energy balance in the SSS sap flux technique during the daytime hours. Consequently it is not surprising that sap flow rate, M_{sap}, may not be very sensitive to changes in tissue thermal conductivity - except at low flow rates (Sakuratani, 1979; Steinberg, Van Bavel and McFarland, 1989). Ishida, Campbell and Calissendorff (1991) calculated that a 10 % uncertainty in K_{stem} resulted in an uncertainty in E_{sap} less than 1 %. However, Steinberg *et al.* (1989) noted a 17 % error in measured sap flow when E_{axial} was omitted from the energy balance equation.

Critical to the SSS technique is the assumption of steady state. The heat energy flux (W) supplied by the heater (E_{heater}) is assumed to be fully accounted for according to the conservation of energy principle, such that $E_{heater} = E_{radial} + E_{axial} + E_{sap}$. This implies that no extraneous or unmeasured energy enters or departs the system other than by sap convection. To facilitate this it is usually necessary to insulate the heater and sensors from solar irradiance and wind effects. In circumstances where incident radiant energy may be large *e.g.*, in forests at times when the solar elevation is low, a highly reflective aluminium foil surrounding the thermal insulation is also applied.

A critical assumption implicit in the relation described in Eq. 3.2 is that the term dT_{stem} is solely a consequence of the displacement by sap of heat applied to the stem (usually mainly by a heater).

While several studies have reported a high degree of accuracy of the SSS sap flux method when compared with gravimetric measurements *e.g.*, Baker and Van Bavel (1987) and Ham and Heilman

(1990), or when subject to mathematical analysis *e.g.*, Baker and Nieber (1989) and Groot and King (1992), some have noted that serious transient errors in direction and magnitude of sap flow estimates, which may have occurred due to stem temperature gradients which violate the above assumption by imposing a bias in dT_{stem} *e.g.*, Cermák, Jeník, Kucera and Zídek (1984), Fichtner and Schulze (1990), Shackel, Johnson, Medawar and Phene (1992), Cohen, Takeuchi, Nozaka and Yano (1993). The details of this is discussed in Chapter 4.

Shackel, Johnson, Medawar and Phene (1992) have noted and attributed the occurrence of dT_{stem} values in the absence of heat input, to different rates of temperature change along the stem. Working on three year old peach trees (stems 60 to 75 mm in diameter) they observed the largest dT_{stem} values to occur under conditions of most rapid changes in stem temperature (dT/dt). Conversely the smallest dT_{stem} values occurred when all positions along the stem approached thermal equilibrium with the ambient. These observations were drawn from data pooled over 34 days while the gauge heater was switched off. In addition to a substantial degree of variability, their data exhibited that dT_{stem} was largely independent of dT/dt around solar noon (± 3 h).

By adjusting for a bias in dT_{stem}, Gutiérrez, Harrrington, Meinzer and Fownes (1994) noted a substantial increase in similarity between transpiration estimated by the SSS sap flux technique and gravimetric methods for koa (*Acacia koa* Gray) growing under greenhouse conditions (stems 9.5 to 11 mm in diameter).Thus it would appear that where it is necessary to adjust for a bias in dT_{stem}, the SSS technique is further dependent on empirical adjustment for measurement of sap flow.

3.6.1.2 HPV technique

The first quantitative treatment of the physical problem presented by pulsed heat from implanted sensors for estimation of sap flux was carried out my Marshall (1958). This work is theoretically sound for idealised situations but is not obtainable in practice. The technique is applied however on the assumption that practical deviations from the idealised theory have persistent effects. Numerical solutions are used to adjust for such problems based on *in situ* measurements (*e.g.*, *E. grandis* Hill ex Maiden (Olbrich, 1991); *Nothofagus solandri* (Hook. f.) Orst., *Pinus halepensis* Mill., and *Pinus Radiata* D. Don (Swanson and Whitfield, 1981).

Heater and temperature probes are of finite size and have thermal properties different from those of three-dimensionally anisotropic surrounding wood. In addition, sap flow tends to be interrupted by these sensors and their immediate neighbourhood (Leyton, 1969).

Sensitivity analyses have indicated that it is important to measure wound size accurately. Olbrich (1991) noted that wounding resulting from sensor implantation may be up to 48 % greater than the implied volume occupied by the sensor (resulting from tissue oxidation and resin deposition). The response to wounding depends on season (Lopushinsky, 1986), phenological state (Shigo and Hillis, 1973) and increases with time after probe implantation (Swanson and Whitfield, 1981; Olbrich, 1991). Clearly measurement errors in these will inevitably bias sap flux estimates.

The HPV technique is based on the assumption that the stem is a homogeneous and porous material. This implies that stem sapwood does not contain layers of non-convective material which may require appreciable time to reach thermal equilibrium with their surroundings. It also assumes that the heat moves uniformly through all the stem material and does not simply stream up a few large water-conducting channels. This implies that the convective heat pulse velocity coefficient is equal to the weighted average of the heat conducted through the woody matrix and that convected through the

sap; and implies a constant thermal conductivity through the woody matrix. This has been discussed by Hein and Farr (1973) after personal communication with D.C. Marshall.

Stem tissue borders are important sources of departure from idealised theory (Swanson, 1983) and deviation from ideal conditions tends to result in under-estimation of convective sap velocity. This was first shown by Marshall (1958) for sap-conducting elements surrounded by non-conducting tissue. Swanson (1983) has indicated that any non-convective thickness less than 0.4 mm would not cause significant departure from thermal homogeneity.

Hein and Farr (1973) established that ^{32}P radioisotope velocity was faster than the conducted heat pulse through the stationary wood combined with the convection of the heat pulse through the vessels containing sap, for Populus nigra var. italica Du Roi. Hein (1970) found that the xylem lumina for poplar (anatomically similar to willow) made up 20 % of the total xylem cross-sectional area and deduced that only 13 % of the lumina were involved in conduction.

Green and Clothier (1988) concluded that large vessels and substantial interstitial area of woody matrix affects the thermal homogeneity of kiwifruit (Actinidia deliciosa) and therefore affects the transmission and measurement of heat-pulse in kiwifruit; unlike that for apples (Malus sylvestris X Red delicious) where the vessels are small, short, closely packed and interconnected. They concluded that the HPV theory would need to be modified to take into account the inhomogeneous nature of plants with very large vessels *e.g.*, grape vines and kiwifruit.

In maize (typical herbaceous monocotyledon) the vascular bundles are scattered unevenly throughout the entire cross section of the stem, and their arrangement is related to the position of the various bundles of each leaf in the stem (Esau, 1965; Foster and Gifford, 1974). Sap velocity in the vascular bundles, traced by safranine, varied considerably between bundles but the average was ≈10 times higher than sap flux estimated by the heat pulse method (Cohen, Takeuchi, Nozaka and Yano, 1993).

Evidently, unadjusted, the HPV technique tends to underestimate sap flux systematically (Swanson, Beneke and Havranek, 1979; Cohen, Fuchs and Green, 1981; Green and Clothier, 1988; Olbrich, 1991). Consequently it is fundamentally based on a necessity for empirical adjustment to sap flow measurement since errors are caused by assumptions made (*e.g.* assuming instantaneous heat flow) in applying the transient heat flow equation. This limitation is counter-balanced by the opportunity for measurement continuity.

3.6.2 Extent of localisation

3.6.2.1 SSS technique

Non-intrusive placement of sensing junctions, *i.e.* where sensors are kept in contact with the plant limb, offer a significant potential advantage to applying the SSS technique over other procedures which do require sensor insertion into the xylem.

Whether the SSS technique is applied intrusively or non-intrusively, its application implies that temperatures are assumed to be constant throughout the plane of measurement and can be approximated by localised sample measurements for the determination of the stem temperature gradients: dT_{upper}, dT_{lower} and dT_{stem} (Fig. 3.1). Plant limb cross sectional area, and lateral and vertical thermal conductivities are also necessarily assumed to be constant throughout the plant stem section. In

reality however, one would expect all of these factors to vary systematically with radial profile differences in tissue type, water content and hydraulic conductance, from the centre to the surface of the stem. Clearly the size of plant under consideration is important when a non-intrusive approach to this technique is considered.

Since dT_{stem}, which appears in the denominator of Eq. 3.2, is used to calculate sap flux, very small dT_{stem} values result in M_{sap} approaching infinity. This situation is likely to occur at either very high sap flow rates or when sap flow has ceased (Fig. 3.3). Consequently the technique is particularly dependent on the sensor precision or accuracy for determining dT_{stem} at an upper and lower range of sap flow detection. Where measurement accuracy is compromised at low values for dT_{stem} relatively large errors can be anticipated. It is within this pretext that the technique is most vulnerable to extraneous temperature gradients ($^{o}C\ m^{-1}$).

Examples of conditions which contribute to extraneous temperature gradients in the stem include: (i) heat conduction down the limb when the sun is vertically overhead a species which presents a fairly large, horizontally closed canopy to incoming solar radiation, and (ii) heat conducted up the limb during night time when heat loss is frequently more rapid than the soil. This presents an inconvenience since the extent of such a predisposition to over or underestimate sap flow requires *in situ* evaluation.

Presented in **Fig. 3.3**, from left to right, are the possible thermocouple junction states under three different sap flow scenarios. (A.) Zero flow, (B.) Moderate flow (C.) Upper limit. During zero sap flow conditions (Fig. 3.3A) there should be no net temperature difference across the heater if the thermojunctions are evenly spaced relative to the heater. The E_{radial} and E_{axial} energy balance components would be at a maximum level. If the power to the heater is not decreased the stem section

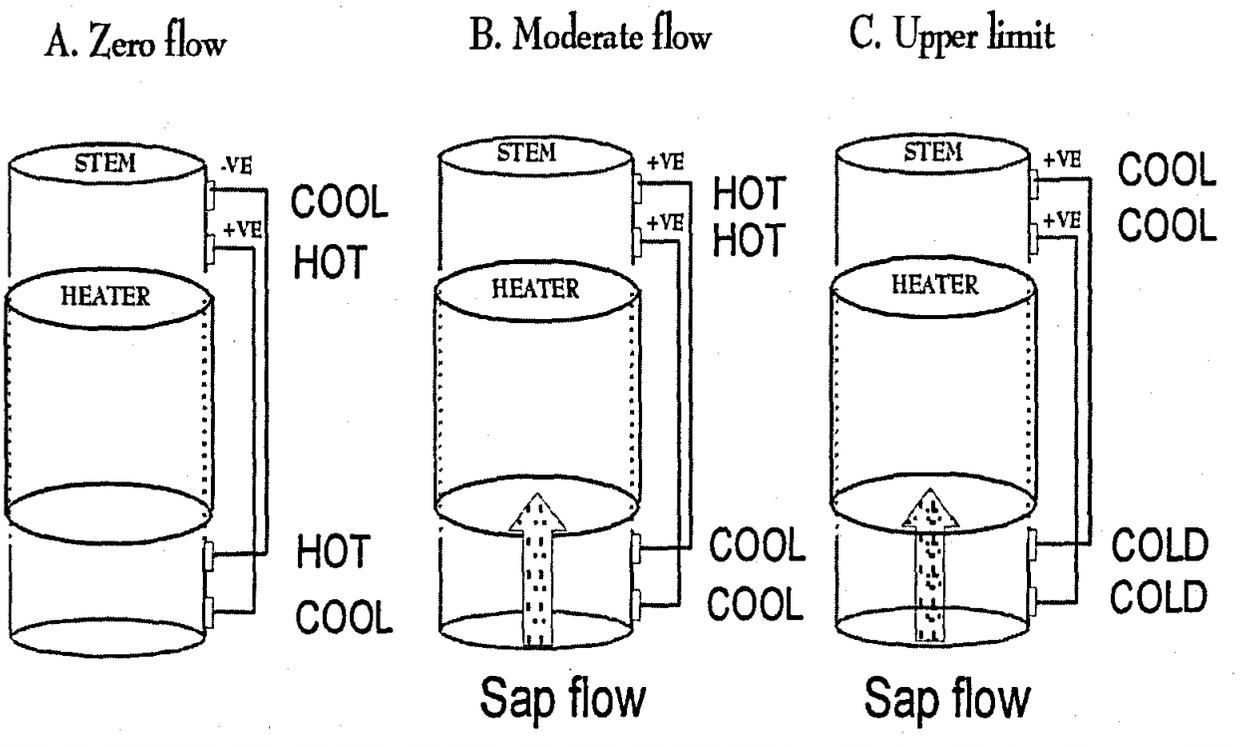

Fig. 3.3 Diagrams illustrating typical states of the gauge upper and lower thermocouples, during a typical day

under the heater would tend to heat up and be a source of heat over and above that of the heater upon resumption of sap flow (Fig. 3.3B). At low rates of change in sap flow, dT_{stem} recorded may be considerable. During this period the assumption of steady-state is violated and significant error introduced into calculated sap flow. Consequently it is necessary to regard the technique lower limit to be where steady-state heat flow is re-established following this event. With the transition from zero flux (Fig. 3.3B), as the heated section moves over the upper thermocouple junctions, dT_{stem} increases considerably. The magnitude of this depends upon the extent to which the stationary sap in the stem segment under the heater increased in temperature before the re-commencement of sap flow. Practically the extent to which this is recorded depends on the datalogger interrogation (sampling) interval, and the rate of change in sap flow. At the upper limit to sap flux most of the input heat is removed by sap convection (Fig. 3.3C). At this point one would expect E_{axial} and E_{radial} approach zero with the approach of E_{sap} towards E_{heater}. The temperature difference across the heater (dT_{stem}) also approaches zero resulting in an infinity error due to division by zero in Eq. 3.2.

Shackel, Johnson, Medewar and Phene (1992) showed that under natural conditions there were substantial measurement errors in sap flux of young peach trees (*Prunus persica* L.), because the surface temperature was not equivalent to the temperature in the cross section. Their results suggested that the stem surface temperature differential was not simply a consequence of the dissipation of heat supplied by the gauge, but was affected by environmental conditions.

A distinct limitation to the SSS sap flux technique is (i) the likelihood of tissue damage, without prior knowledge of the plants specific tissue sensitivity, and (ii) stimulation of nodal bud growth, from increases in stem temperature and impaired stem respiration in the region under heater and insulation. Where non-dynamic heat input systems are used, risk of significant plant tissue damage limits the application of the technique on any single limb to a period of only a few weeks. In this circumstance effects are likely to be greatest under low sap flow conditions *e.g.*, conditions of low evaporative demand and at night. However under day-time conditions much of the heat flux from the heater can be removed by sap flow. Such dynamic changes in heat requirements can prove challenging.

The SSS technique requires the establishment of steady-state heat flux conditions. A time constant is a measure of time taken for re-establishment of steady state conditions *i.e.*, lag response time to a rapid change *e.g.*, in sap flow or heater power, due to the thermal inertia of the system. This has been described (Kuera, Cermák and Penka, 1977; Baker and Van Bavel, 1987).

The dynamic response of the system can be improved by either reducing the dimensions of the heated segment or increasing the thermal conductance of the system. There are however practical limitations in both cases. If the heated segment selected is very small, the heat input must be reduced to avoid physiological plant damage. The result is that the various outward fluxes and corresponding signals diminish, increasing the relative error of the measurement. If the thermal conductance is too large, the implied assumption of one-dimensional conduction in the stem becomes increasingly tenuous for a given gauge installation and heater setting.

Published time constants of Dynamax gauges (Van Bavel and Van Bavel, 1990) suitable for fitment on stems between 10 and 19 mm diameter, ranges from 4 to 9 minutes at a sap flow rate of 10 g h^{-1}. Similarly for gauges between 25 and 100 mm diameter, the time constant ranges from 15 to 55 minutes. These time constants typically decrease to zero as sap flow increases (Sakuratani, 1981).

Sakuratani (1981) evaluated the heat flux by the energy balance components: E_{axial}, E_{radial} and E_{sap}

with increased sap velocity in 13 mm diameter sunflower (*Helianthus annus*) stems. As the mean stem sap velocity increased, the magnitude of the heat energy flux removed by sap convection (E_{sap}) increased with a proportional decrease in the contribution by the other components, particularly E_{axial}. With increased sap velocity (m s^{-1}), the stem thermal conductivity radially into the stem remained greater than that in the axial direction. While not detected, heat storage in active sapwood probably decreased with increasing sap velocity *i.e.*, the stem cools down with increased sap flux.

Sakuratani (1981) showed that the relative error of E_{sap} typically increases in an exponential manner with a reduction in the proportion of supplied heat conducted to sap. For a given sap flow accuracy level the proportion of heat conducted to sap must necessarily increase with decreased precision in the $E_{sum} = E_{axial} + E_{radial}$ measurement (**Fig. 3.4**). This example illustrates that for an E_{sap} accuracy of between 80 and 90 % (*i.e.* $1 - e_f$) the proportion of heat conducted to sap should be between 20 and 30 %. Consequently, under ideal conditions it is expected that the accuracy of the technique will increase with increased sap flow. The limits imposed are by the magnitude of the heater power setting. As E_{sap}/E_{heater} decreases, a point may be a chosen as the technique lower limit. It is also quite conceivable that with increased sap flow a point is reached where E_{sum} approaches zero and e_q and e_f increase to infinity as measurement precision limits are approached *i.e.*, E_{heater} is insufficient (Fig. 3.4). Consequently a value for the ratio E_{sap}/E_{heater} could also be selected as the technique upper limit.

Using the notation E_{sum} to represent the sum of E_{axial} and E_{radial}, rather than the residual difference between E_{heater} and E_{sap}, Sakuratani (1981) described the following procedure in order to evaluate errors in the determination of E_{sap}. Firstly he defined the relative errors: (i) e_f as the error fraction of E_{sap} (ie., $e_f = (E_{sap} - E'_{sap})/E'_{sap}$) and (ii) e_q as the error fraction of E_{sum} (ie., $e_q = (E_{sum} - E'_{sum})/E'_{sum}$)

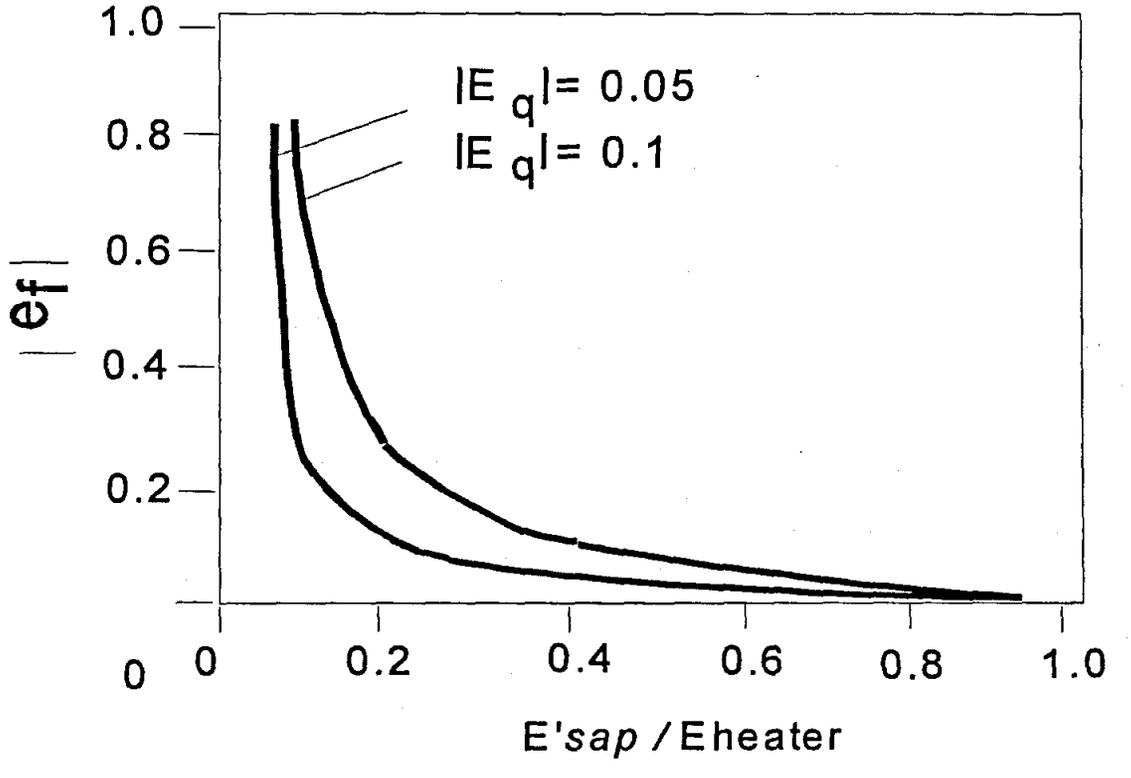

Fig. 3.4 Illustration of the dependence of e_f on the magnitude of $E'sap/E_{heater}$ as influenced by the value of e_q

where E'_{sap} is the true value of the heat energy flux transported in the sap, and E'_{sum} is the true value of E_{sum}.By combining the above equations and assuming $E_{heater} = E'_{heater}$ where E'_{heater} is the true value of E_{heater}, a relation for e_f is obtained such that the % error in E_{sap} = the % error in E_{sum} × (fraction E'_{sum} is of E_{heater}/fraction E'_{sap} is of E_{heater} (ie., $e_f = e_q \times [E'_{sap}/E_{heater}) - 1]/(E'/E_{heater})$. Thus the term $|e_f|$ is the absolute value of the relative error in the determination of convected heat with sap flow. E'_{sap}/E_{heater} is the ratio of the true value of convected heat to the heat energy supplied to the stem segment. $|e_q|$ is the absolute value of the relative error in the determination of heat loss due to conduction and convection. To evaluate the magnitude heat energy flux into sap convection at an accuracy higher than the relative error of 20 % then: $E'_{sap}/E_{heater} = -0.2$ at $|e_q| = 0.05$ or $E'_{sap}/E_{heater} = -0.35$ at $|e_q| = 0.10$ (Sakuratani, 1981).

The phenomenon presented in Fig. 3.4 is reflected in the temperature difference across the heater (dT_{stem}). A maximum and minimum dT_{stem} value is associated with the applied gauge's lower and upper limits respectively, where 'cut-off' sap flow rates can be selected from the relationship between sap flow rate and dT_{stem} **(Fig. 3.5)**. Data is from four Dynamax SGB19 gauges fitted to 20 mm diameter Phragmites stems. Most of the calculated night-time sap flow rates fall below 5 g (15 min)$^{-1}$, except for those associated with a very small dT_{stem} value (Circle A). During the day data associated with a dT_{stem} value less than 1.5 °C would also require exclusion for a valid data set. In this case a sap flow rate of 55 g (15 min)$^{-1}$ constituted the technique upper limit where $E_{sap}/E_{heater} = 0.1$. The limits of this function are indicated where dT_{stem} tends towards zero in each case but remain within measurable

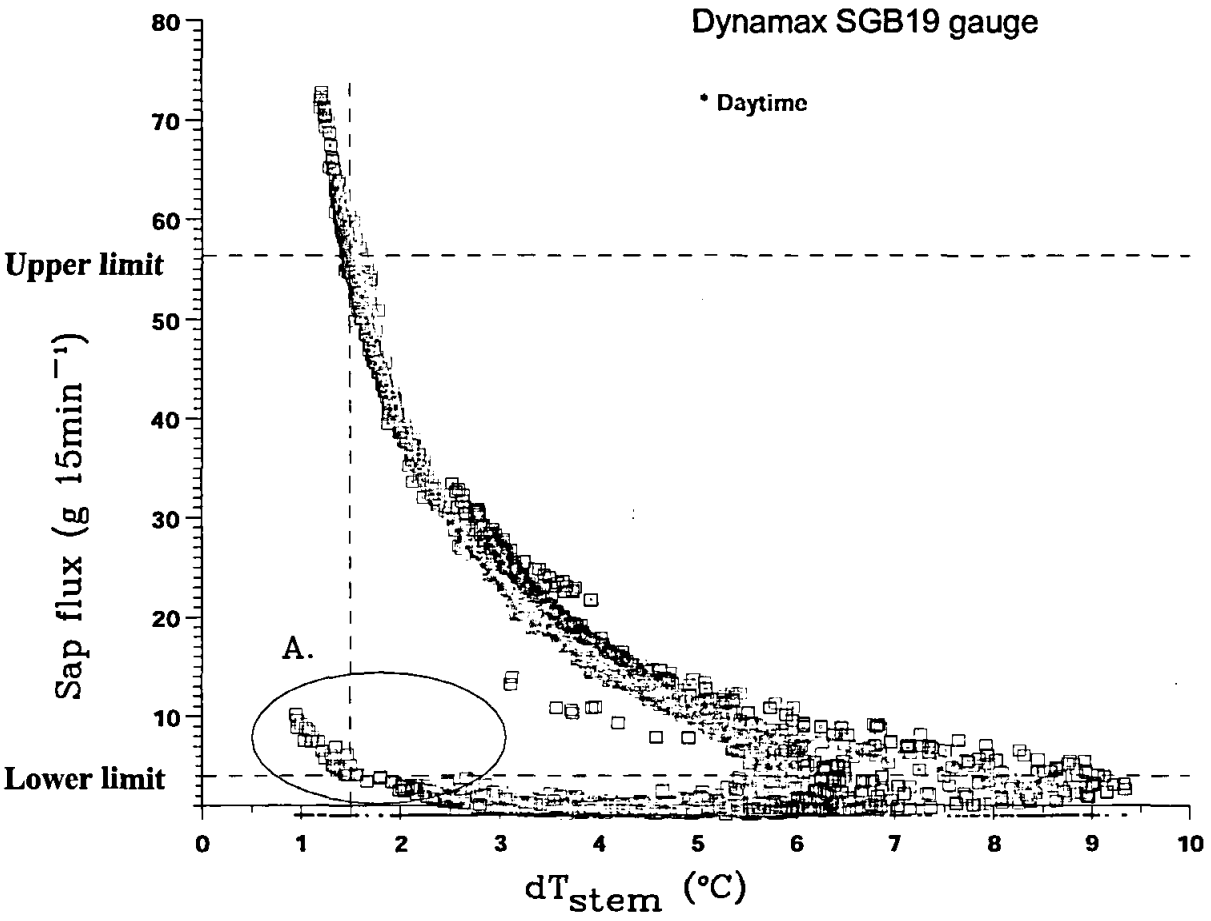

Fig. 3.5 Relationship between sap flow vs. dT_{stem} during steady state-conditions, and the night-time deviation from this function when the steady state assumption is compromised

precision limits. Since E_{sap} = sap flow (g) × dT_{stem} ×C_p, the slope of sap flow *vs* dT_{stem} = (C_p/E_{sap}). For a heater flux of 0.4 W, data is rejected (10 % accuracy) where the above slope is greater than 116 *i.e.*, $C_p/(E_{heater} \times 0.1)$, or (20 % accuracy) where the above slope is greater than 52.25 *i.e.*, $C_p/(E_{heater} \times 0.2$.

3.6.2.2 HPV technique

Assuming that the sap moves with uniform parallel motion perpendicular to the straight line heater, the pulse of heat would also depend on conduction and convection in the bodily movement of sap. Consequently the temperature at a point directly downstream from the heater would rise to a greater maximum than if the sap were stationary and at an earlier time (**Fig. 3.6**). It would also return to its original value more quickly for a given quantity of heat. The temperature at a point at a given time would thus depend on both the diffusivity of the sap wood and the sap velocity (Eq. 3.10).

Typically two points have been used along the temperature curve following the heat pulse (ca 0.2 seconds for herbaceous species, ca 8 seconds for woody species). For low flow rates, it is suggested that convective heat velocity (v = 0 to 0.22 mm s^{-1}, t_o > 20 s) be estimated by Eq. 3.23. At such low flow rates the t_o datum can be measured with precision to accurately estimate sap velocity. However at velocities greater than 0.22 mm s^{-1} the initial differential temperature change is too small and evolves too rapidly to detect when temperature returns to its initial value, but the temperature wave does have a well defined maximum that is related to sap velocity (**Fig. 3.7**). In such circumstances v should be estimated by Eq. 3.20 (Cohen, Fuchs, Falkenflug and Moreshet, 1988).

Two sensor-heater probe arrays are possible (**Fig. 3.8**). One uses a heater coupled to a single sensor probe, forming a couplet, and is only suitable for one method of heat pulse velocity measurement (Method A); while the other, which uses a heater and two sensor probes to form a triplet, is suitable for all three methods (Method A, Method B and Method C). Sensor probe separation is typically set at approximately 10 mm above and 5 mm below the heating probe. Frequently exact spacings are determined following implantation and these values used subsequently in the heat pulse velocity calculations (Swanson, 1983; Cohen, Fuchs, Falkenflug and Moreshet, 1988; Olbrich, 1991).

Method B is frequently named the Compensation Heat-pulse Technique. This involves the time delay for an equal temperature rise to be sensed at the locations upstream and downstream of the heater, following the release of a heat pulse (Green and Clothier, 1988). Probes are connected in a Wheatstone bridge configuration and adjusted to zero output before heat pulse generation. Usually the time taken for the bridge to return to the initial balance point after the heater is pulsed is recorded (Olbrich, 1991).

Since sap flow velocity usually varies with depth into a stem, to calculate volumetric flow rates it is necessary to measure sap flux density at different depths into the stem. Spacings of one probe per 2.5 × 10^3 mm^2 sapwood in young trees and one probe per 4.5 × 10^3 mm^2 in older trees have been recommended (Swanson, 1983; Olbrich, 1991). Some examples of sample probe depths used include (i) 4, 10, 17 and 23 mm (Olbrich, 1991) and (ii) 5, 12, 18 and 24 mm (Smith, 1992).

The sensors located in different positions along each probe are used to derive a sample of convected heat pulse velocity. Each sample position is considered to represent sap flux at the corresponding position in the sapwood. The sapwood area associated with each sensor is then calculated on the basis of concentric rings, with their limits midway between successive sensors. Total sap flow is calculated as the sum of these partial areas multiplied by their associated sap flux densities. This procedure is

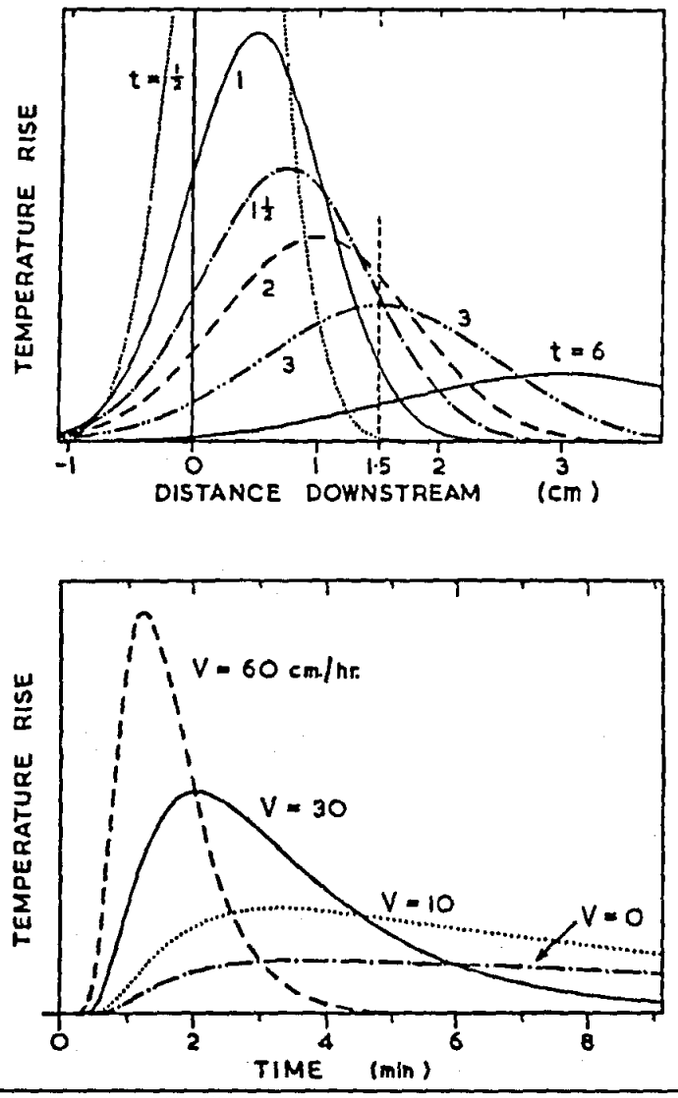

Fig. 3.6A Theoretical temperature distribution at particular times, t (min) after release of a heat pulse. Heat pulse velocity, V = 0.3 m h^{-1}. Diffusivity, k = 0.25 × 10^{-6} m^2 s^{-1}. B. Theoretical curves of temperature rise against time at the point 15 mm downstream from the heater, for heat-pulse velocities, V = 0, 0.1, 0.3, 0.6 m h^{-1}. Diffusivity, k = 0.25 × 10^{-6} m^2 s^{-1}

termed the "step function" by Swanson (1983) and Olbrich (1991) respectively. Alternatively a second order least squares regression equation may be fitted to the sap flux density measurements. The resulting flux profile could then be integrated over the sapwood cross-section to calculate volume flux (Green and Clothier, 1988).

Probes are usually placed below the bark. The location of the cambium and sapwood interface is determined by examination of colour changes along a stem cross section from sample cores. Heartwood my be distinguished from sapwood by application of a methyl-orange stain. This results in development of a crimson colour in the more acidic heartwood and a more neutral colour in sapwood. Where R_x represents the radius of the tree at the sapwood bark interface, and R_h represents the tree radius at the sapwood heartwood interface, the conductive area is calculated as $\pi (R_x)^2 - \pi (R_h)^2$. Consider a probe with a sensor spacing of 10 mm. The area of the outer most ring 15 mm ring is given by $\pi [(R_x)^2 - (R_x - 15)^2]$, the area of the next ring 10 mm ring is given by $\pi [(R_x - 15)^2 - (R_x - 25)^2]$

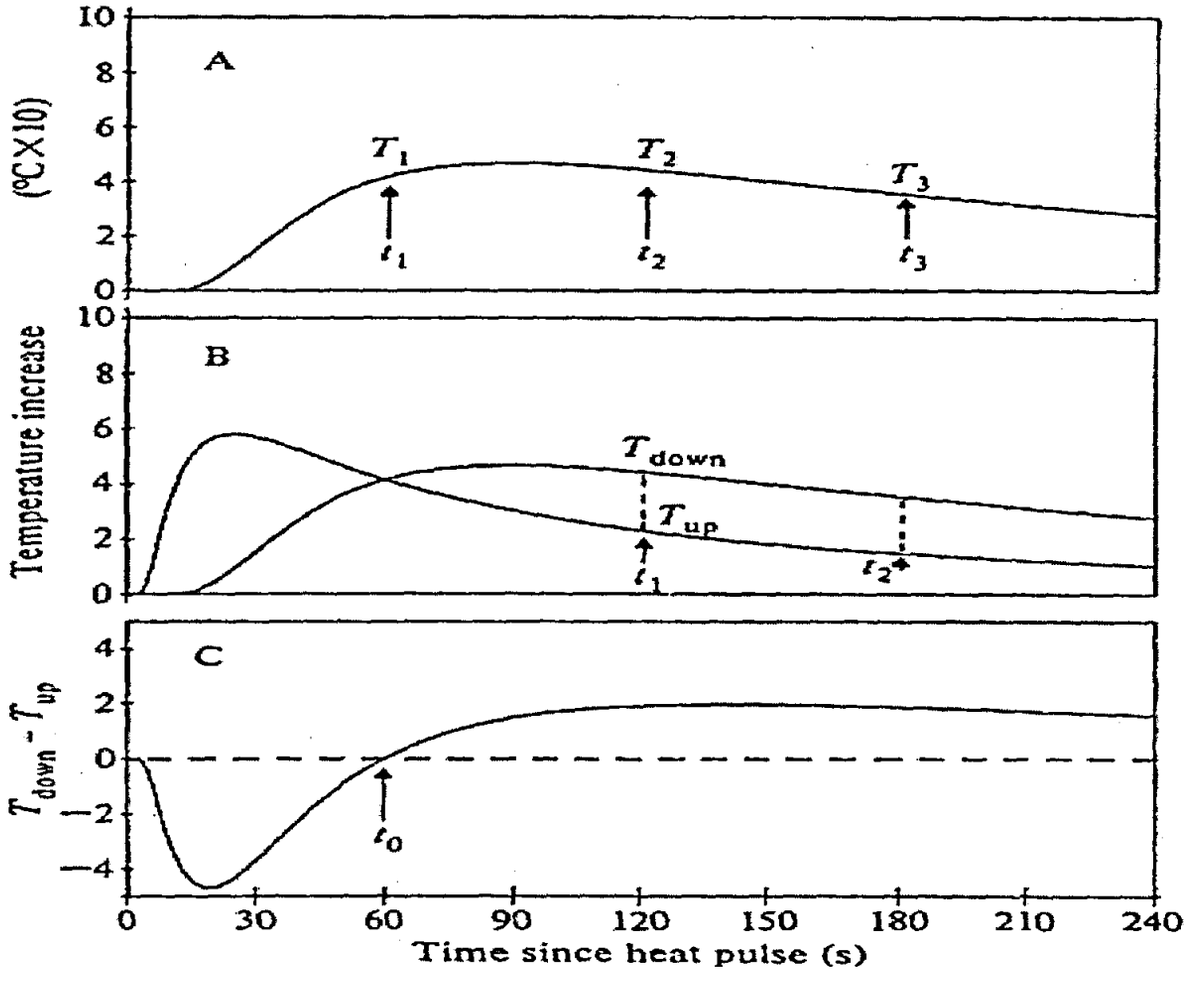

Fig. 3.7 Plots of time *vs* temperature rise for the various solutions to Eq. 3.19. Heat pulse velocity = 0.15 m h^{-1}. A. Temperature rise at one sensor located 10 mm downstream from the heater. B. Temperature rise at the downstream sensor and a second at 5 mm upstream. C. Temperature difference at 10 mm downstream, 5 mm upstream

and so on (**Fig. 3.9**).

Several studies on a variety of species have shown that sap velocity is not uniform throughout the sapwood but for example may peak 10 to 20 mm from the cambium for some tree species (Swanson, 1967; Mark and Crews, 1973; Lassoie, Scott and Fritschen, 1977; Miller, Vavrina and Christensen, 1980; Cohen, Fuchs and Green, 1981). This has led to the generalization of a parabolic sap flow distribution. Several workers advocate the fitting of a least squares polynomial (quadratic) function to stem flux measurements and subsequent integration to derive a measurement of sap flux, from point estimates within the sapwood (Cohen, Fuchs and Green, 1981; Edwards and Warwick, 1984; Green and Clothier, 1988).

Cermák, Cienciala, Kuera and Hällgren (1992) confirmed the radial profile of flow velocity in mature Norway spruce (*Picea abies* (L). Karst) to be symmetrical *i.e.*, maximum flow velocity was in

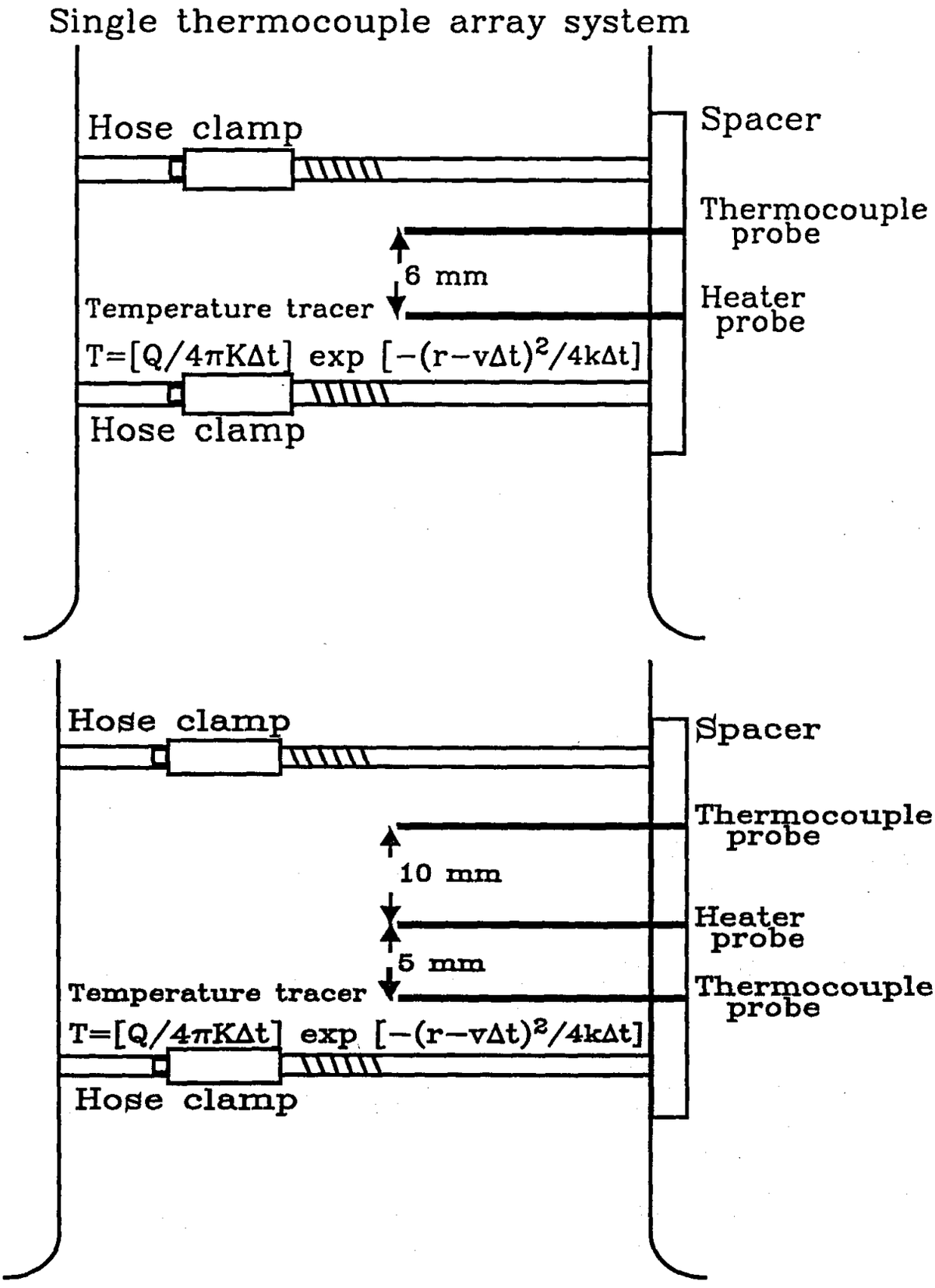

Fig. 3.8 Sensor and heater probe arrays used in the application of the HPV technique, an intrusive sap velocity system. The thermocouple probe consists of three thermocouples embedded in a stainless steel tube (length 35 mm, diameter 1.3 mm). The thermocouples are spaced 10 mm apart with one thermocouple 5 mm from the tip of the tube

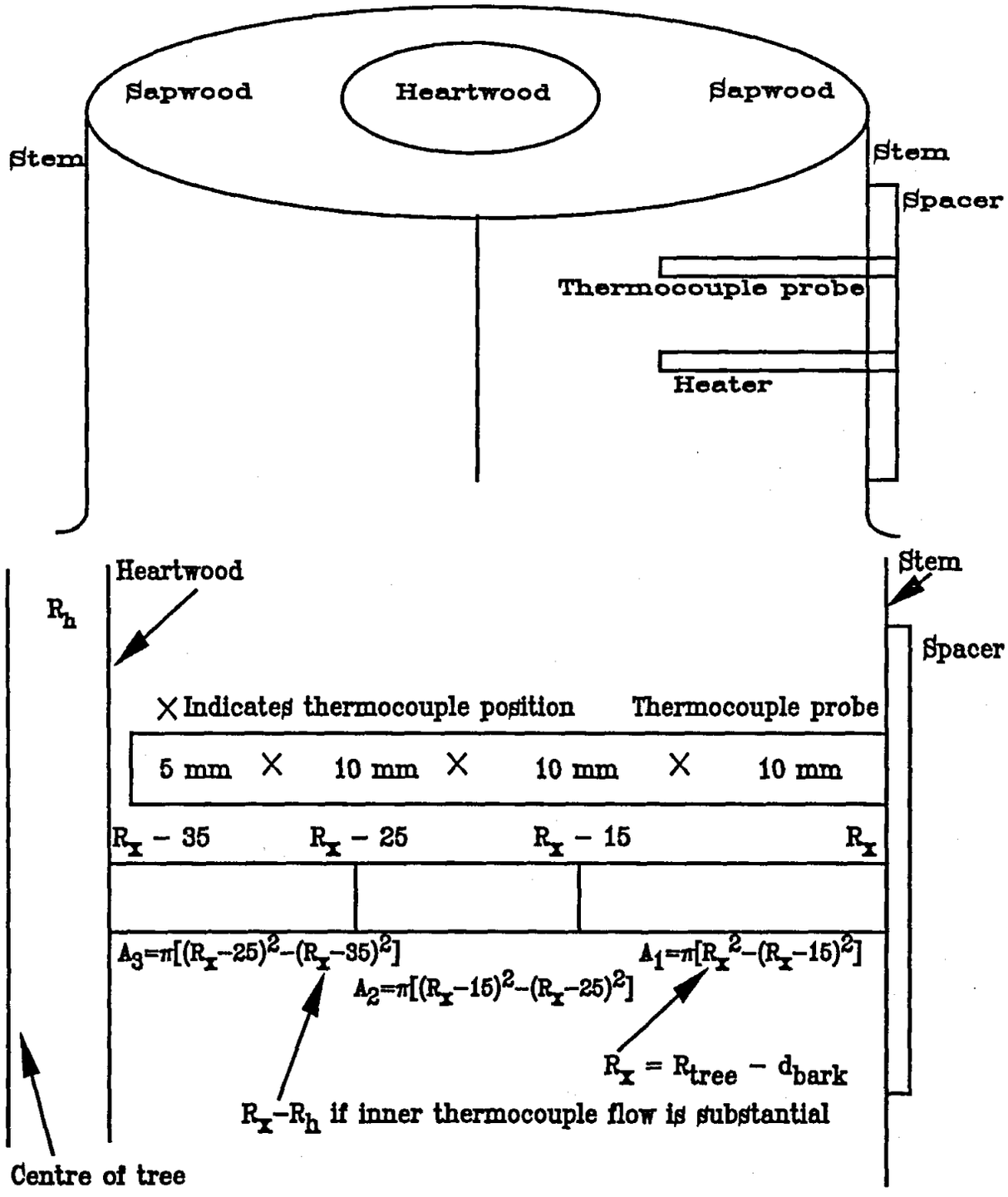

Fig. 3.9 Diagrammatic representation of single thermocouple probe iserted into the sapwood of a stem. The non-conducting heartwood region is shown. The spacer facilitates the insertion of the probes into the stem and allows accurate positions at know distances. Conducting sapwood area determination: R_h is the radius of the heartwood. If there is no heartwood $R_h = 0$. The distance R_x is the radius of the tree at the sapwood bark interface. The thermocouple probe consists of three thermocouples embedded in a stainless steel tube (length 35 mm, diameter 1.3 mm). The thermocouples are spaced 10 mm apart with one thermocouple 5 mm from the tip of the tube. If the inner thermocouple detects little or no flow, R_h can be taken as $R_x - 35$ with little error. If the flow at the inner thermocouples substantial, it will be necessary to determine R_h by doing an increment boring on the tree and measuring R_h directly. The radius of the xylem, R_x is calculated from the tree radius R_{tree} minus the bark thickness d_{bark}

the centre of the conducting xylem and tailed with low amplitude in the direction of the cambium and heartwood, but was highly variable around the trunk. In contrast they noted that in pedunculate oak (Quercus robur L.) the radial profile of flow velocity was highly asymmetrical in the youngest growth ring and tailing centripetally for about 10 growth rings, but that variability around the trunk was less.

Non-conducting tissue *e.g.*, annual growth rings in Douglas fir (Pseudostuga menziesii), radiata pine (Pinus radiata) and patula pine (Pinus patula), may also invalidate the assumption of a parabolic radial sap flux distribution (Hatton and Vertessy, 1989; Dye, Olbrich and Poulter, 1992).

The width of wood influenced by the pulse of heat is usually 7 to 8 mm (Swanson, 1974) and therefore, if the widths of annual rings are substantially narrower than this, the resulting averaging effect reduces between-ring variation. Should the rings be wider than this, clearly between-ring variation may be revealed in sampled point measurements. If differences in sap velocities through the sapwood occur as a result of growth rings, it will have an important bearing on the sampling strategy and the estimation of mean sap velocity for the species.

Sap flow velocities tend towards zero across the sapwood profile at night and profile curvature, if it develops, generally increases with increasing flux. Hatton, Catchpole and Vertessy (1990) used a weighted average approach to the sampled sapwood area of *Pinus radiata*, with sensor spacing determined from a theorem to determine equal areal weighting of each sensors data, to obtain flux from the sap flow velocity estimates with depth into the bole. This approach is less sensitive to artifacts arising from small measurement errors or random variation in sap flow velocity than the least square polynomial technique.

No growth ring effect has been observed in *Populus deltoides* and *Eucalyptus grandis*. Both profiles were in the form of a skewed parabolic function, with velocities highest at approximately 10 mm inside the cambium, declining to zero at the heartwood interface (Olbrich, 1991; Smith, 1992). This facilitates easy sampling procedure in terms of probe placement.

3.6.3 Construction

3.6.3.1 SSS technique

Typically a flexible heater (Heater Designs Inc. or Fantech Corp., U.S.A.) is installed completely surrounding a portion of stem. In larger gauges, heaters are typically constructed from silicone rubber impregnated fibre glass with Nichrome wire, while smaller gauge heaters are etched from 0.25 mm Inconel foil on 0.05 mm Kapton and then coated with varnish (Baker and Van Bavel, 1987; Baker and Nieber, 1989). The heater is completely surrounded by a 2 to 3 mm thick cork / neoprene gasket substrate layer, subsequently enclosed by a polyurethane foam insulation material which has a thermal conductivity much lower than that of plant tissues. These three components are secured to each other using flexible silicone, isocyanurate or cyanoacrylate adhesive (Superglue).

In order to estimate the radial heat flux density, a number of 0.01 to 0.38 mm diameter teflon insulated thermocouples (Omega Engineering, U.S.A.) joined together to form a thermopile equal in width to the heater, are used to measure the temperature difference between the inner and outer surfaces of the cork-layer. The thermopile is typically constructed by joining equal lengths, alternately of copper and constantan wire, beginning and ending with copper wires. Alternate junctions are glued to opposite surfaces of the cork layer. A thumbtack is used to punch holes for wire insertion between surfaces (Steinberg, Van Bavel and McFarland, 1989).

A further two, either: (i) copper-constantan (type T) or (ii) chromel-constantan (type E), thermocouples are used to determine the mean temperature difference across the heater *i.e.*, between points upstream and downstream of the heater (Eq. 3.9), and also to determine conducted heat flux away from the heater through the plant limb (Eq. 3.10). The junctions are placed at the inner surface of the cork layer, while all the leads run through the outer cork surface proximal to the insulation material. One junction pair, one junction each from two thermocouples paired together, separated by a distance *dz* (m), is placed upstream from the heater. The two remaining junctions of the thermocouple pair are placed downstream from the heater. The junction separation distance of a particular thermocouple is typically equal to the stem diameter plus half the heater width (Ishida, Campbell and Calissendorff, 1991). Two to four thermocouple pairs (**Fig. 3.10**) wired in parallel may be used to achieve a better sample around the plant limb (Mitchell, 1983).

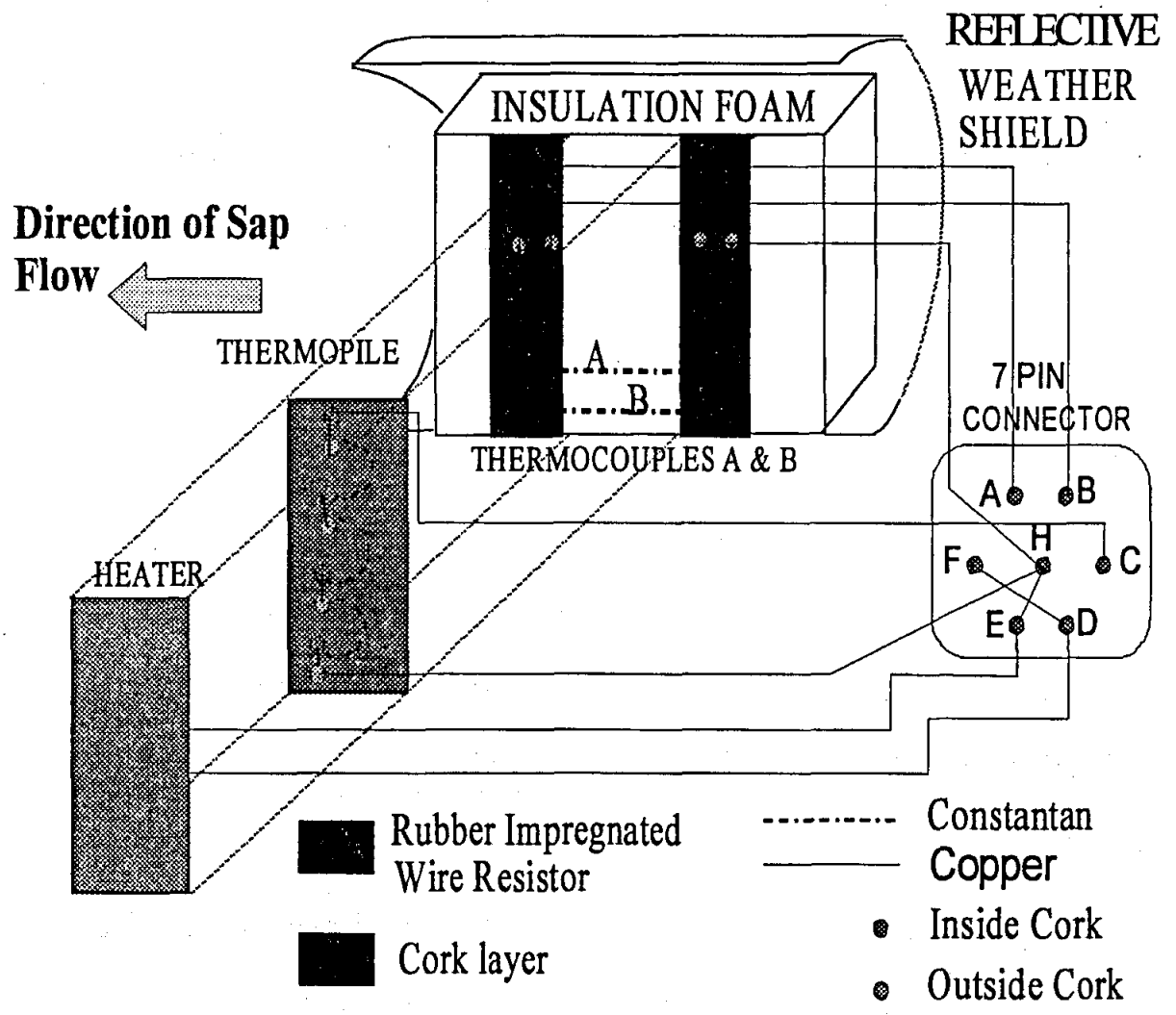

Fig. 3.10 Schematic of the construction and wiring of a typical 4-channel Dynamax SSHB sap flux technique gauge positioned horizontally. The four finely dotted lines show where the thermopile and heater fit sequentially between the two junctions of a thermocouple pair, A and B respectively. Letters A, B, C, D, E, F, and H on the 7 pin connector represent the pins connected to wires coded by colour (green, brown, blue, red, black, orange and white respectively) for connection to a data logger. An 8 th pin may also be used when using cables 25 m or longer to connect a sense lead (yellow) to the heater for more accurate determination of actual potential difference across the heater

Gauges can be supplied with power by an external power source (Elanco Electronics Inc. model XP750) calibrated to deliver a set voltage (Gavloski, Whitfield and Ellis, 1992a; b; Ishida, Campbell and Calissendorff, 1991).

3.6.3.2 HPV technique

Different approaches are frequently used to apply the HPV technique. Typically two types of sensor used: (i) thermocouples, and (ii) thermistors.

A heater probe is paired with one or more sensor probes. Often these are constructed into stainless steel or teflon tubes (35 to 120 mm in length; 0.5 to 2.1 mm in diameter). The sensor probes are embedded with thermocouples (copper-constantan 0.05 to 0.1 mm) while heater probes are embedded with heating elements. These are tipped at one end with silver solder. The spherical junction is near the tip of the probe (Cohen, Fuchs, Falkenflug and Moreshet (1988).

As an alternative to thermocouples, microbead thermistors (GB 43 J1; Fenwal electronics, Farmingham Massachusetts) may be used. For example, Cohen, Fuchs and Green (1981) mounted these on phenol fibre strips 0.8 mm thick, 3 mm wide and 65 mm long, spaced 10 mm apart. The probe was moulded in epoxy to form a cylindrical rod. At the thermistor locations the epoxy was replaced by aluminium segments over a length of 1.5 mm to improve thermal contact between wood and sensors.

Using a 0.36 Ω heater coupled to a 12 V heat source Cohen, Fuchs and Green (1981) controlled the pulse width with a 555 timer (Signetics, Sunnyvale, California) from 0.25 s to 1.5 s in steps of 0.25 s. The corresponding heat outputs were from 100 J to 600 J.

Different kinds of heat pulse recorders have been used. "Old style" pen recorders, typically have a sensitivity of 4 $\mu V\ mm^{-1}$ (Heine and Farr, 1973). Differential output is amplified and recorded on a potentiometric recorder with accurate chart speed control. Subsequently the time elapsed between heat pulse release and maximum signal can then be read off the chart (Cohen Fuchs and Green, 1981). Customised commercial heat pulse recorders (Aokautere Soil Conservation, P.O. Box 8041, Palmerston North, New Zealand) are currently available. These record sensed data and automatically trigger heat pulses with a duration of 0.7 to 0.8 seconds (Cohen, Fuchs, Falkenflug and Moreshet, 1988; Olbrich, 1991).

Versatile scientific dataloggers (Campbell Scientific, Logan, UT) are also suitable. For example, using a Campbell Scientific 21X datalogger, Cohen, Takeuchi, Nozaka and Yano (1993) applied a heat pulse of 0.2 s. The temperature difference between the two thermocouples was monitored at 0.4 s intervals for a period of 450 s after the heat pulse. To correct temperature readings, the temperature difference was monitored over a duration of 60 s before the heat pulse application to compute stem temperature drift.

3.7 The thermal dissipation method

The Granier (1985, 1987) method is an empirical method for determining sap flow in trees with diameters greater than 40 mm. Two cylindrical probes (about 2 mm in diameter) are inserted radially into the stem, each probe about 100 mm apart. The upper probe contains the sensing thermocouple and a heater. The temperature of the upper probe is referenced to the temperature sensed by the thermocouple in the lower probe. Constant power is applied to the heater and the temperature difference is empirically related to the sap flow. The temperature difference is measured under flow

(ΔT) and no sap flow conditions (ΔT_o) and related to sap flow u_v in $m^3\ m^{-3}\ s^{-1}$:

$$u_v = 119 \times 10^{-6}\ [(\Delta T_0 - \Delta T)/\Delta T]^{1.231}.$$

The mass flow is then calculated using:

$$F_w = \rho_s\ u_v\ A_{sw}$$

where ρ_s is the sap density and A_{sw} is the area of the sap wood. It is recommended that the technique be calibrated for species for which it has not been validated.

The technique is relatively simple and requires few measurements and calculations.

3.8 Discussion and conclusion

Any work plan for the application of the SSS technique for research purposes would require the determination of the extent to which empirical measurement of K_{gauge}, k_{stem} and dT_{stem} would be possible for adjustment of measured sap flow so that it approximates actual sap flow within an acceptable level of accuracy. Both techniques require experimentation to know peak sap flow before designing and applying a gauge. The size of plant and potential for tissue damage is important.

The morphology, air filled lacunae, sensitivity to damage (*e.g.* fungal infection, gumming) are important issues in the case of heat pulse velocity technique.

The SSS is theoretically based, only dependent on knowledge of the gauge conductance K_{gauge} and the stem thermal conductivity K_{stem}.

Chapter 4

Use of a stem steady state heat energy balance technique for the *in situ* measurement of transpiration in *Eucalyptus grandis*: theory and errors

4.1 Abstract

The stem steady state heat energy balance (SSS) technique for the *in situ* measurement of transpiration rate is non-intrusive and dynamic. Application of heat around a stem and measurement of temperature differentials at various points allows sap flow rate to be calculated under steady state conditions. Problems in assuming steady state under field conditions that are not steady state are discussed. The magnitude of stem differential temperatures was maintained as large as possible during the day-time hours through the application of heater power. Two gauges on the same *Eucalyptus grandis* tree yielded very similar data although there was some evidence that the upper gauge measurements were being affected by heating from the lower gauge. Good comparisons between flow rates and lysimetric evaporation rates for 30-min data were obtained. Standard deviations of all component energy terms increases dramatically at sunrise and sunset.

The SSS technique is critically dependent on the value of the continuous power supplied to the heater and the resultant stem temperature differential dT_{stem} measured. The expression used for calculating the sap flux M_{sap} has dT_{stem} in the denominator. If heater power is too low and/or transpiration rates are high, then dT_{stem} tends to zero with the M_{sap} value calculated becoming unstable when compared with lysimeter values. The influence of stem thermal conductivity K_{stem} and gauge conductance K_{gauge} on calculated M_{sap} values is discussed.

Theory associated with the correction of naturally occurring stem temperature gradients was developed and used to correct measurements. Naturally occurring vertical temperature gradients in the stem of *E. grandis* may affect the measurement accuracy of the calculated M_{sap} values. Corrections may be performed based on actual stem temperature gradients in the absence of heat applied to the heater. It is advisable to measure these stem gradients, in the absence of any heating, for a range of environmental conditions. The error may be much larger for the larger diameter gauges (diameters greater than 35 mm). A method could be developed to switch off the heater power on various days, measure the stem temperature gradients, and correct the measured gradients for those days when the power to the heater was on. The errors in M_{sap} are large negative (corresponding to an overestimation in M_{sap} by the gauge) before 11h30 when the sap flow is increasing with the errors then becoming increasingly positive after this time. At night, the large errors are often of no consequence since M_{sap} is small. If the data were integrated for a complete day, the overestimation in M_{sap} before noon would not cancel with the underestimation after noon.

For the large Dynamax SGB-100ws sap flow gauges, a reduction in the power supplied to the gauge heater may require up to six hours before steady state thermal equilibrium is achieved, the duration of this period being influenced by the magnitude of the voltage change. Different magnitudes in power supplied to the gauge require the use of different K_{gauge} values for the determination of E_{radial}. A linear model allows gauge conductance K_{gauge} to be determined for different heater voltages. This procedure is useful when batteries become progressively discharged or due to changes in gauge heater resistance.

The field use of the largest sized (120 mm diameter) stem steady state heat energy balance gauges is

discussed. Measurements were performed at Kwa-Mbonambi, Zululand and at Bloemendal near Pietermaritzburg. The technique was validated using a cut-stem technique. Measurements were performed at Kwa-Mbonambi on fertilised and unfertilised trees. Aspects addressed in this study include: diurnal stem and gauge temperature gradients; stem heating; a mathematical determination of the influence of stem gauge conductance and stem thermal conductivity on gauge accuracy, using the cut-stem technique for verification of sap flow. Our data suggested that a storage term in the heat energy balance for the 120-mm diameter gauges is necessary. In the cut-stem experiment, a gauge conductance of between 1.6 and 1.8 W mV^{-1} resulted in an adequate comparison with the day-time cumulative sap flow, measured using a portable lysimeter. The maximum daily sap flow was more than 35 kg (for an unfertilised tree) compared to 24 kg maximum for a fertilised tree.

4.2 Introduction

Given the scenario of the establishment of commercial forests, there can be no doubt of the impact of this on limited and unpredictable water supplies. Traditional agricultural practices (such as the growing of maize, soybeans), for which there is a reasonable knowledge of plant water utilization, will be displaced by forest production with little knowledge of its water utilization.

Eucalyptus spp., for example, are often planted in ecologically sensitive areas not suited to their high water usage or in areas dominated by traditional crop production where irrigation would be used to supplement rainfall. There is therefore a need to determine the water usage of trees in order to establish which areas are not suited to growth with respect to rainfall, soil form, water holding capacity and soil depth. The stem steady state heat energy balance technique (SSS) for the measurement of sap flow is applied and compared against lysimetrically measured evaporative losses.

4.3 Theory

4.3.1 Determination of gauge thermal conductance K_{gauge}

The K_{gauge} term in the radial energy flux E_{radial} is calculated under conditions wherein $E_{sap} = 0$ and hence $M_{sap} = 0$ (Eqs 3.2 and 3.5). For these conditions, where $E_{axial} = E_{upper} + E_{lower}$ are the conductive energy fluxes:

$$E_{radial} = K_{gauge} V_{thermopile} = E_{heater} - E_{upper} - E_{lower} - E_{storage}. \quad 4.1$$

Hence

$$K_{gauge} = (E_{heater} - E_{upper} - E_{lower} - E_{storage})/V_{thermopile}, \quad 4.2$$

under conditions of zero mass flow rate, allow E_{radial} to be determined. On large diameter trees, the K_{gauge} term may be determined for an excised trunk.

Three methods have been used for determining K_{gauge}, the value of which is necessary for the calculation of M_{sap}:

1. the gauge is mounted on the stem of the species and K_{gauge} determined under low evaporative conditions (for which $M_{sap} = 0$);

2. the gauge is mounted on an excised stem, of similar size to that used for calculation of M_{sap}. After 2 h, K_{gauge} is determined;

3. the gauge is mounted on a wooden dowel rod of similar size to that used for the calculation of M_{sap}.

An incorrect K_{gauge} value, K_{gauge}' say, may result in non-zero E_{sap} values. Theoretically, one may correct for this. For if E_{sap}' is the measured (incorrect and non-zero) minimum sap flow, then:

$$E_{sap}' = E_{heater} - E_{upper} - E_{lower} - E_{storage} - K_{gauge}' V_{thermopile} \quad 4.3$$

where

$$E_{sap} = 0 = E_{heater} - E_{upper} - E_{lower} - E_{storage} - K_{gauge} V_{thermopile}. \quad 4.4$$

Solving Eqs 4.3 and 4.4 simultaneously results in:

$$K_{gauge} = K_{gauge}' + E_{sap}'/V_{thermopile} \quad 4.5$$

where $K_{gauge} > K_{gauge}'$ if $E_{sap}' > 0$ and $V_{thermopile} > 0$. Equation 4.5 provides a method for calculating the correct K_{gauge} value in terms of the incorrect K_{gauge}' and E_{sap}' values and the measured $V_{thermopile}$ values.

The other energy balance components may then be calculated as follows:

$$E_{radial} = (K_{gauge}/K_{gauge}')\cdot E_{radial}', \quad 4.6$$

$$E_{sap} = E_{heater} - E_{upper} - E_{lower} - E_{storage} - E_{radial}$$

and

$$M_{sap}\,(\mathrm{g\ h^{-1}}) = 3600\, E_{sap}/(dT_{stem}\cdot c_p).$$

4.3.2 Stem thermal conductivity K_{stem} (W m^{-1} K^{-1})

The other parameter that is required for the calculation of M_{sap} is the stem thermal conductivity K_{stem} (W m^{-1} K^{-1}). Suppose that an incorrect value for the stem thermal conductivity, designated K_{stem}', is used. If the correct thermal conductivity is known later, designated K_{stem}, the stem energy balance components may be corrected as follows:

$$E_{upper} + E_{lower} = (K_{stem}/K_{stem}')\cdot(E_{upper}' + E_{lower}') \quad 4.7$$

and

$$E_{sap} = E_{heater} - E_{upper} - E_{lower} - E_{storage} - E_{radial}.$$

A numerical simulation of a temperature-controlled heat balance method showed that inserting thermocouples into the stem to provide radial averaging of stem temperature resulted in a significant reduction in error of the flow measurement, especially for species with scattered vascular bundles (Ishida *et al.*, 1991).

4.3.3 Technique assumptions

The assumption of steady state may not apply at certain times of the day for experiments in the field or in controlled environments. At times when the solar elevation is low, large radiant energy may be incident on the stem of the plant. Under these conditions, steady state may not apply. Furthermore, in controlled environments, particularly if artificial heating or cooling is used, steady state conditions may not be applicable.

The elegance of the stem flow energy balance technique, compared to other techniques, is that no calibration appears necessary (Baker and van Bavel, 1987). Therefore the main assumptions of the technique needs critical investigation. The primary assumptions of the technique may be summarized as follows:

1. steady state must prevail. Thermal insulation of the sensors and the heater is therefore a necessary requirement. In the case of some plants, for example maize, this insulation would substantially reduce stem transpiration which would presumably occur under normal circumstances;

2. under conditions of zero mass flow rate, Eqs 3.2 and 3.5 are used to calculate K_{gauge} and it is this value that is assumed to apply under conditions of zero or non-zero mass flow rates;

3. alternatively, in the case of plants maintained under controlled environmental conditions, the plant and its container could be weighed at two different times. The gauge conductance K_{gauge} is the value obtained by equating SSS and lysimetric mass differences between the two times. It is assumed that the soil evaporation is negligible.

The temporal variation in K_{gauge} does not seem to have been investigated. Under field conditions, for species with a trunk diameter greater than 100 mm, zero mass flow may never be achieved as even the low evaporative demand flows may exceed 0.2 kg h^{-1}. Under these conditions, it may not be possible to accurately determine K_{gauge}. Therefore, K_{gauge} would have to be determined using a wooden dowel rod of similar diameter. It is unclear, in this case, whether K_{gauge} determined on a wooden dowel rod as opposed to the actual stem influences the *in situ* calculations.

4.3.4 Technique limitations

The technique is based upon the fact that, under steady state conditions, the energy flux terms E_{radial}, E_{upper}, E_{lower} and E_{sap} all account for E_{heater}. Heat energy flux not part of E_{upper}, E_{lower} or E_{radial} will automatically contribute to E_{sap} whether it is rightly sap energy flux or not. Since the heater surrounds the plant stem and not just the sap stream of the stem, there may be other energy fluxes included in the residual term E_{sap} (Eq. 3.1). These energy fluxes could possibly be undetected or could already be included in the temperature differentials (Shackel *et al.*, 1992) used to calculate E_{upper}, E_{lower} or E_{radial}. The storage term $E_{storage}$ is usually ignored for smaller diameter stems but cannot be ignored for larger daimeter stems such as those approaching 100 mm.

In order to compare sap flow rate in kg s^{-1} with evaporation rate from aerodynamic techniques or Penman type evaporation calculations, knowledge of the leaf area index (*LAI*) is required. Furthermore, different plants with differing *LAI* cannot easily be compared unless the individual *LAI* values are known. Even for the same rapidly growing plant, with a rapidly increasing *LAI*, flow rates are not easily compared between time periods too far apart.

Another disadvantage of the stem heat energy balance technique must be due to the fact that a fairly large increase in temperature occurs in the region of the heater. The effect of the increase is unknown. Ideally, the temperature increase should be kept as low as possible. The manufacturers of Dynamax gauges recommend that the increase should always be less than 8 °C. During the day, much of the heat flux from the heater is removed by the sap flow. Under conditions of low evaporative demand, this is not the case and the heat flux heats the epidermis to temperatures that may cause irreversible physiological damage. One may partly avoid this problem by decreasing the power supplied to the heater during times of low evaporative demand.

Since dT_{stem} appears in the denominator of Eq. 3.2 used to calculate M_{sap}, care has to be taken ensure that its value does not become too small for accurate measurement. Such small values would result in M_{sap} approaching infinity and could occur under conditions of high flow rates.

Another disadvantage of the technique lies in the fact that different diameter plants may require different diameter gauges. While the gauges can be constructed to stem diameter size (Ham and Heilman, 1990), the various Dynamax (Houston, Texas) gauges currently commercially available may be used on stems within a narrow diameter range: 9 to 13 mm; 12 to 16 mm; 15 to 19 mm; 18 to 23 mm; 24 to 32 mm; 32 to 45 mm; 45 to 65 mm and 100 to 125 mm (**Table 4.1**). Some workers have compared trunk and branch sap flow (Steinberg *et al.*, 1989). The sensor model number and voltage and power specifications are shown in **Table 4.2.**

4.3.5 Technique verification

4.3.6 An error analysis of the stem steady state heat energy balance technique

The sap flow using the SSS technique is calculated using measurements from a number of other measurements each of which may have an error component that influences the error in the calculated sap flow. Mathematical combination of data is necessary in order that other quantities are calculated. Measurements that are added, subtracted, multiplied or divided are simple examples that occur often. As a more complex example, we consider the determination of the population standard deviation $\sigma_n(M_{sap})$. The statistical results for the scale factor case, the linear combination case, the general product will be stated here but will not be proved.

4.3.6.1 Scale factor

The n measurements $x_1, x_2, ..., x_n$, yield n values of z:

$$z_1 = \alpha x_1, z_2 = \alpha x_2, ..., z_n = \alpha x_n.$$

The mean of the z values, $\bar{z}$, is given by $\bar{z} = \alpha \bar{x}$. The sample variance $\sigma_n^2(z)$ is:

$$\sigma_n^2(z) = \alpha^2 \sigma_n^2(x).$$

4.3.6.2 Sum

Suppose that we have n measurements of $x_1, x_2, ..., x_n$, and m measurements of $y_1, y_2, ..., y_n$ of y. If the

Table 4.1 Dynagage sensor model number and physical specifications

Model number	Stem diameter (mm) and area range (mm^2)						Thermocouple separation distance *dz* (mm)	Gauge height (mm)
	Typical		Minimum		Maximum			
	Diameter	Area	Diameter	Area	Diameter	Area		
SGA10-ws	10.0	78.5	9.0	63.6	13.0	132.7	4.0	70
SGA13-ws	13.0	132.7	12.0	113.1	16.0	201.1	4.0	70
SGB16-ws	16.0	201.1	15.0	176.7	19.0	283.5	5.0	70
SGB19-ws	19.0	283.5	18.0	254.5	23.0	415.5	5.0	130
SGB25-ws	28.0	615.8	24.0	452.4	32.0	804.2	7.0	110
SGB35-ws	41.0	1320.3	32.0	804.2	45.0	1590.4	10.0	255
SGB50-ws	50.0	1963.5	45.0	1590.4	65.0	3318.3	10.0	305
SGA100-ws	110.0	9503.3	100.0	7854.0	125.0	12271.8	15.0	460

Table 4.2 Dynagage sensor model number and voltage and power specifications

Model number	Heater voltage (V)			Heater power (W)			Heater resistance (Ω)		
	Typical	Minimum	Maximum	Typical	Minimum	Maximum	Typical	Minimum	Maximum
SGA10-ws	4	3	5	0.1	0.05	0.15	170	150	190
SGA13-ws	4	3	5	0.15	0.07	0.2	120	105	135
SGB16-ws	4.5	3	5	0.2	0.1	0.25	100	50	120
SGB19-ws	4.5	3	5	0.3	0.15	0.4	65	50	75
SGB25-ws	4	3	5	0.4	0.25	0.5	43	38	47
SGB35-ws	6	4	7	0.9	0.4	1.2	40	35	45
SGB50-ws	6	4	7	1.4	0.6	2	25	21	29
SGA100-ws	8.5	6	10	4	2	5.5	18	16	20

two measurement sets are independent, then we define $z_{ij} = x_i + y_j$ with a mean value defined by

$$\bar{z} = \bar{x} + \bar{y}.$$

The sample variance $\sigma^2_{nm}(z)$ is given by:

$$\sigma^2_{nm}(z) = \sigma^2_n(x) + \sigma^2_m(y).$$

4.3.6.3 Linear combination

Suppose that x, y, ... are sets of data with x being a set of one observation, y another, etc., each data set having a corresponding mean $\bar{x}$, $\bar{y}$, etc., and sample variance $\sigma_n(x)$, $\sigma_m(y)$, etc. Then, applying the results of the scale factor and sum of functions, we have, if $z = \alpha x + \beta y + ...$, $\bar{z} = \alpha \bar{x} + \beta \bar{y} + ...$

$$\text{Also, } \sigma^2_{nm....}(z) = \alpha^2 \sigma^2_n(x) + \beta^2 \sigma^2_m(y) + ...$$

4.3.6.4 General function

Suppose n measurements of x have been obtained, with the resulting mean being $\bar{x}$ and the sample variance $\sigma^2_n(x)$. What would be the mean and variance if the measurements were mathematically transformed from x to z, say? If $z = f(x)$, where x has a sample variance of $\sigma^2_n(x)$, then, to first order approximation and assuming that the function and its derivatives are well-behaved:

$$\bar{z} = f(\bar{x}).$$

If all terms involving higher than second order terms are neglected $\sigma^2_n(z) = [f'(\bar{x})]^2 \sigma^2_n(x)$.

4.3.6.5 General product

Suppose that $z = \alpha x^a y^b .....$

$$\text{Then } \sigma^2_n(z) = (\partial z/\partial x)^2 \cdot \sigma^2_n(x) + (\partial z/\partial y)^2 \cdot \sigma^2_m(y) + ...,$$

where the terms in brackets () are, respectively, evaluated at the mean of $\bar{x}$, $\bar{y}$,.....

4.3.6.6 Error in M_{sap}

The expression:

$$M_{sap} = [V^2_{heater}/R_{heater} - K_{stem} A_{stem} (\Delta T_1 - \Delta T_2)/dz - K_{gauge} V_{thermopile}] \cdot (dT_{stem} \cdot c_p)^{-1}$$

based on

$$E_{sap} = E_{heater} - E_{upper} - E_{lower} - E_{storage} - E_{radial}$$

will be used to determine the sample variance $\sigma^2_n(M_{sap})$. For simplicity, the storage term $E_{storage}$ will be ignored. For convenience, we have defined:

$$\Delta T_1 = (T_{upper\,1} - T_{lower\,1})$$

$$\text{and } \Delta T_2 = (T_{upper\,2} - T_{lower\,2})$$

As mentioned in the general product case, all terms are evaluated at their means. Since M_{sap} is the product of the term enclosed in square brackets [] and $(dT_{stem} \cdot c_p)^{-1}$, we use the General Product rule to obtain the sample variance $\sigma^2_n(M_{sap})$:

$$= [V^2_{heater}/R_{heater} - K_{stem} A_{stem} (\Delta T_1 - \Delta T_2)/dz - K_{gauge} V_{thermopile}]^2 \cdot \sigma^2_n [(dT_{stem} \cdot c_p)^{-1}]$$
$$+ (dT_{stem} \cdot c_p)^{-2} \cdot \sigma^2_n [V^2_{heater}/R_{heater} - K_{stem} A_{stem} (\Delta T_1 - \Delta T_2)/dz - K_{gauge} V_{thermopile}].$$

Invoking the General Function rule, we have:

$$\sigma^2_n [(dT_{stem} \cdot c_p)^{-1}] = \sigma^2_n (dT_{stem})/[c_p^2 \, dT^4_{stem}].$$

Using the Linear Combination rule, we have:

$$\sigma^2_n [V^2_{heater}/R_{heater} - K_{stem} A_{stem} (\Delta T_1 - \Delta T_2)/dz - K_{gauge} V_{thermopile}]$$
$$= \sigma^2_n (V^2_{heater}/R_{heater}) + \sigma^2_n [K_{stem} A_{stem} (\Delta T_1 - \Delta T_2)/dz] + \sigma^2_n (K_{gauge} V_{thermopile}).$$

Using the General Product and General Function rules, we have:

$$\sigma^2_n (V^2_{heater}/R_{heater})$$
$$= \sigma^2_n (V^2_{heater} R^{-1}_{heater}) = (4V^2_{heater}/R^2_{heater}) \sigma^2_n (V_{heater}) + (V^4_{heater}/R^4_{heater}) \sigma^2_n (R_{heater}),$$
$$\sigma^2_n [K_{stem} A_{stem} (\Delta T_1 - \Delta T_2)/dz] =$$
$$A^2_{stem} [(\Delta T_1 - \Delta T_2)^2/dz^2] \, \sigma^2_n (K_{stem})$$
$$+ K^2_{stem} [(\Delta T_1 - \Delta T_2)^2/dz^2] \, \sigma^2_n (A_{stem}) + K^2_{stem} A^2_{stem} \sigma^2_n [(\Delta T_1 - \Delta T_2)/dz],$$
$$\sigma^2_n (K_{gauge} V_{thermopile}) = K^2_{gauge} \sigma^2_n (V_{thermopile}) + V^2_{thermopile} \sigma^2_n (K_{gauge}),$$
$$\text{and } \sigma^2_n [(\Delta T_1 - \Delta T_2)/dz] = [\sigma^2_n (\Delta T_1) + \sigma^2_n (\Delta T_2)]/dz^2 + \sigma^2_n (dz) \, [\Delta T_1^2 + \Delta T_2^2]/dz^4.$$

Consolidating all the expressions, we have:

$$\sigma_n^2(M_{sap}) = [V_{heater}^2/R_{heater} - K_{stem}A_{stem}(\Delta T_1 - \Delta T_2)/dz - K_{gauge}V_{thermopile}]^2\sigma_n^2(dT_{stem})/[c_p^2 dT_{stem}^4]$$
$$+ (dT_{stem}\cdot c_p)^{-2}\cdot\{[(4V_{heater}^2/R_{heater}^2)\,\sigma_n^2(V_{heater}) + (V_{heater}^4/R_{heater}^4)\,\sigma_n^2(R_{heater})]$$
$$+ A_{stem}^2\,[(\Delta T_1 - \Delta T_2)^2/dz^2]\,\sigma_n^2(K_{stem}) + K_{stem}^2\,[(\Delta T_1 - \Delta T_2)^2/dz^2]\,\sigma_n^2(A_{stem})$$
$$+ K_{stem}^2 A_{stem}^2 + [\sigma_n^2(\Delta T_1) + \sigma_n^2(\Delta T_2)]/dz^2 + \sigma_n^2(dz)\,[\Delta T_1^2 + \Delta T_2^2]/dz^4$$
$$+ K_{gauge}^2\,\sigma_n^2(V_{thermopile}) + V_{thermopile}^2\,\sigma_n^2(K_{gauge})\}. \qquad 4.8$$

4.4 Materials and methods

4.4.1 Field measurements

The location for this research was at the University of Natal, Pietermaritzburg. A *E. grandis* tree, about 18 months of age, was transplanted directly into a 167 litre drum with minimal disturbance to soil adjacent to the roots. As much of the field soil (a sandy loam) as possible was placed in the drum.

The tree was then immediately placed in a confined environment for a period of eight weeks following which it was placed in the open environment. Measurements on the tree were first obtained some ten weeks after transplanting. The tree was watered daily with fertilizer applied every five weeks.

The tree was placed directly on the lysimeter and half-hourly (manual) measurements were obtained during daylight hours. For a four day period, manual lysimeter measurements were also obtained at 20h00 and at midnight.

A Kubota Ltd.[1] (Japan) KA-10 battery operated scale with a range mass of 0 to 300 kg and a sensitivity of 0.05 kg was used for the purpose of comparing lysimeter and gauge sap flow rates. For the sensors used for the current research (model number SGB25-ws), the diameter may be within the range 24 mm to 32 mm with the typical stem diameter being 28 mm. The sensor was applied to the base of the stem. The procedures for gauge application are:

preparation involves removing rough areas (including bark material) using very fine abrasion. The stem is then coated with electrical insulating compound (Dow Corning number 4). This improves contact between stem and sensor. Contact is critical for correct operation of the technique;

following the application of the insulating compound, the stem is covered with cling wrap material. The cling wrap material prevents the electrical components of the sensor from being smeared with the compound. The cling wrap also prevents water from the stem from entering and corroding the sensor;

the sensor is applied to the stem under high evaporative demand conditions when stem diameter is likely a minimum. The sensor and areas above and below the heater are thermally in- sulated to ensure that steady state conditions are even more likely to apply. The plastic cover ensures that no water can enter the sensing region. Reflective material is used as the final cover.

If the gauge were applied higher up the stem, then no account of stem transpiration, if any, can be made. The sensor consists of a heater embedded in a thin sheet of cork, with a pair of

1 The mention of commercial products does not imply endorsement or otherwise by the authors or their sponsors

copper-constantan thermocouples placed above and below the heater. In order to determine the radial heat flux density, thermocouples are used to measure the temperature difference between inner and outer layers of the cork substrate mounted to surround the stem. In one experiment, in order to compare sap flow measurements on the same tree but using different sensors, a SGB25-ws gauge was connected to the base of the tree stem with another SGB25-ws sensor connected to the same stem but some 80 mm from the top of the sensor below. Both sensors were powered from the same battery. Measurements in the field were also obtained using a wooden dowel rod for which it was not possible for M_{sap} to be anything other than 0 g h^{-1}.

The Dynagage (Houston, Texas, USA) sensors were connected to a 21X datalogger (Campbell Scientific, Logan, Utah, USA) containing the program used to determine M_{sap} as well as other energy balance components. The data recorded by the datalogger was transferred directly to a portable computer using an optically isolated serial interface (Campbell Scientific SC32A). The TERM program allowed one to view the input and output storage locations on a real time basis. The input storage data was generated every 15 seconds whilst the output storage data usually consisting of the 30-minute averages, was generated every half hour. This conveniently allowed for real-time checking of the gauge data with the lysimetric data. The datalogger was also used to determine the half-hourly standard deviation of the following 15-s measurements: V_{heater}, V_{upper}, V_{lower}, $V_{thermopile}$ and dT_{stem}, the first four terms expressed in mV and the last in °C. An extended precision datalogger instruction was used for all standard deviation measurements to allow for a voltage resolution of 0.33 μV on the 21X datalogger. The 21X datalogger currently only allows at most two gauges to be connected at a time (Steinberg *et al.*, 1990). Compared to the 21X, the CR7X datalogger has better thermal stability, better accuracy, more internal memory (optional) and allows a maximum of 24 gauges to be connected simultaneously (assuming that all of the voltage card slots are occupied; roughly three gauges per voltage card is possible).

The connection of sensors to the datalogger is dependent on cable length. For short sensor connecting cables there is little voltage decrease, due to the length of connecting cables, between the power supply and heater. In this case, the battery voltage need only be measured once for a group of sensors using a single-ended or a differential voltage measurement. For cable lengths exceeding 6 m, wires from the power supply to the heater are separated from those wires used by the datalogger to monitor the voltage supplied to the heater. Since the impedance of the datalogger is practically infinite, there can be no electrical current carried in the connecting wires from the heater to datalogger and therefore no voltage drop in these wires.

The voltage supplied by the battery to the heater was connected to electronic circuitry to allow for manually adjustable voltages. Once the voltage adjustment had been made, the circuitry ensured that the voltage was extremely stable. Initially the electronic circuitry consisted of a three terminal LM317T transistor (designed for a 12 to 13 V direct current input and a 1.2 V to 12 V output) together with resistors to allow for manual switching from 5 to 11 V was employed.It was necessary to attach a heat sink to the LM317T transistor. A voltage divider circuit was used to ensure that the voltage V_{heater} sensed by the datalogger was never greater than 5 V. Subsequent to this initial work, the datalogger program we used automatically controls the switching using a digital control output port of the datalogger and a Darlington pair to decrease the current drain on the logger from 800 mA to 300 mA. A LZ12HE relay coil was then wired to the heat sunk LM317T transistorised voltage regulator with the gauge heater powered from this output. Weather data from an automated weather station within 200 m of the site included solar irradiance, air temperature, relative humidity, and windspeed. All weather data were logged

using a Campbell Scientific CR10 or CR10X datalogger powered from a battery charged by a solar panel.

4.4.2 Power supply and datalogger considerations

The connection of sensors to the datalogger is dependent on cable length. For short sensor connecting cables there is little voltage decrease, due to the length of connecting cables, between the power supply and heater. In this case, the battery voltage need only be measured once for a group of sensors using a single-ended or a differential voltage measurement. For cable lengths exceeding 6 m, wires from the power supply to the heater are separated from those wires used by the datalogger to monitor the voltage supplied to the heater. Since the impedance of the datalogger is practically infinite, there can be no electrical current carried in the connecting wires from the heater to datalogger and therefore no voltage drop in these wires.

The Campbell range of datalogger have the necessary accuracy and programming capabilites for the real-time calculation of sap flow. While these dataloggers may be somewhat more expensive than the other types of dataloggers, there are certainly a good deal more powerful and they are sufficiently accurate. The CR10 datalogger and a multiplexer can also be used for sap flow measurements. The 21X datalogger currently only allows at most two gauges to be connected at a time so usually a multiplexer is used in addition. Compared to the 21X, the CR7X datalogger has better thermal stability, better accuracy (allowing use with thermocouple psychrometers but not so with the 21X), more internal memory (optional) and allows a maximum of 24 gauges to be connected simultaneously (assuming that all of the voltage card slots are occupied; roughly three gauges per voltage card is possible). The CR7X has two types of voltage cards. The 723 voltage card is the less expensive card but does not allow for the measurement of the internal reference temperature of the datalogger. Only the 723-T card allows this option. When using stem flow gauges, absolute temperature measurements are not required for the calculation of any of the sub-component energy flux terms. Hence, the 723-T card is not necessary for such measurements unless one also requires the simultaneous measurement of air or stem temperature. Generally, it is assumed that the datalogger used is the CR7X with a 723-T card and a 723 card (allowing for the simultaneous use with 5 gauges), unless otherwise specified.

4.4.3 Stain techniques applied to Eucalyptus stems

A double stain technique similar to that described by Newbanks, Bosch and Zimmermann (1983) and Sauter (1984) was used to examine transverse sections of *Eucalyptus* stems. Typically after staining, cellulose and cytoplasm are identified by a blue/green colour, lignin by a red colour, suberin by a red/orange colour, cutin by a green colour, and tannins by a red/brown colour.

Tissue was fixed in an FAA (10 ml 37 % formaldehyde, 50 ml 96 % ethanol, 5 ml acetic acid, 35 ml distilled water) solution for 48 h. Tissue was then dehydrated by passing it sequentially through a graded series of mixtures of water:ethanol: tertiary-butanol. The sample was then left at 40 °C in a 1:1 tertiary butanol:liquid paraffin solution for 24 hours, liquid paraffin for 12 hours, liquid parrafin with a few wax pellets for 12 hours and finally a solution of liquid parrafin with more wax pellets added for a further 24 hours. A specimin tube was half filled with melted paraffin wax and left until the top solidified. The material in solution was then poured on top of the wax and placed in an embedding oven at 60 °C while the material slowly sank into the wax and the solvent was driven off. Following this, the wax impregnated sample was poured with the molten wax into a mould and orientated with a hot needle. The mould was then lowered into a dish of ice-cold water to cool and set.

The blocks were trimmed to a suitable thickness and orientation. Thin sections of the sample were cut using a microtome. Subsequently these were mounted on glass microscope slides which had been coated with a chrome-glatin-alum adhesive. A drop of 3 % FAA was placed on each slide. These were dried at 40 °C.

The sections were dewaxed in two three minute rinses of xylene, washed twice in a 1:1 xylene/alcohol mixture for 10 minutes, washed in a 95 % alcohol solution for 5 minutes and then a 70 % alcohol solution for 5 minutes. The samples were placed in a safranin stain for 2 to 24 hours, washed in clean water and then placed in 0.5 % picric acid solution in 95 % alcohol, for dehydration and colour differentiation. Subsequently they were soaked in 95 % alcohol for up to two minutes and then in absolute alcohol for up to ten minutes. Following this a fast green/clove oil counter stain was applied for 30 seconds. The sample was washed three times in xylene for a few seconds each. Sections were then mounted in Canada balsam.

4.5 Results from the staining techniques

Initially 100 mm Eucalyptus stems were cut and placed standing in a dye solution for 5 min. Subsequently they were re-cut. The absorbed dye resulted in some clear patterns. The stem is clearly diffusely prorous. An even distribution of vessels in areas shaped into concentric rings in the readily conducting sapwood is easily distinguishable **(Plate 4.1)**.

Subsequently tissue was sampled from a young sapling tree with a 40 mm diameter stem. The vascular anatomy in transverse section of this stem is shown in **(Plate 4.2)**. The medullary rays, which traverse the xylem radially and pass through the vascular cambium and spread out into the phloem layer beyond, function to transport water radially through the stem. These present channels for water and heat transport from the outside to the inside of the stem.

The thick walled fibrous cells which are most evident in the phloem pose a particular restriction to heat flow. However the existance of the dilated phloem rays would act as a sink and relatively large channel for heat to the axilliary rays for subseqent transfer to convection in the vessels which intersperse the xylem.

If not actively turned over, the water in these expanded phloem rays could be involved in heat storage. In comparison to the xylem the phloem appears to be quite spongy. While it is considered to be a small water store on the whole plant scale, it is known to be one of the most available and actively turned over sources of stored water during periods of supply deficits from roots. This explains considerable shrinkage and the angular stem which develop in eucalypts under drought conditions. Interestingly the angular shape assumed by the droughted stems follow a similar pattern to the core.

Should the heat not be conducted efficiently from the stem surface to the convective influence of the vessels, one would expect the tissue external to the vascular cambium to heat up relative to the xylem. However the vasculature does appear to lend itself to an even distribution of heat from the outside to the inside of the stem and subsequent convection, with the exception of the phloem bark continuum. While motivation for the placement of thermocouples on the stem surface may be tenuous, keeping in mind the thick nature of the fibres which predominate in the phloem, the presence of numerous axilliary rays offers suitable rationale to facilitate this.

Should an invasive approach to thermocouple placement be deemed necessary to accurately monitor convected sap temperature changes, holes would be required for their location under the phloem to be

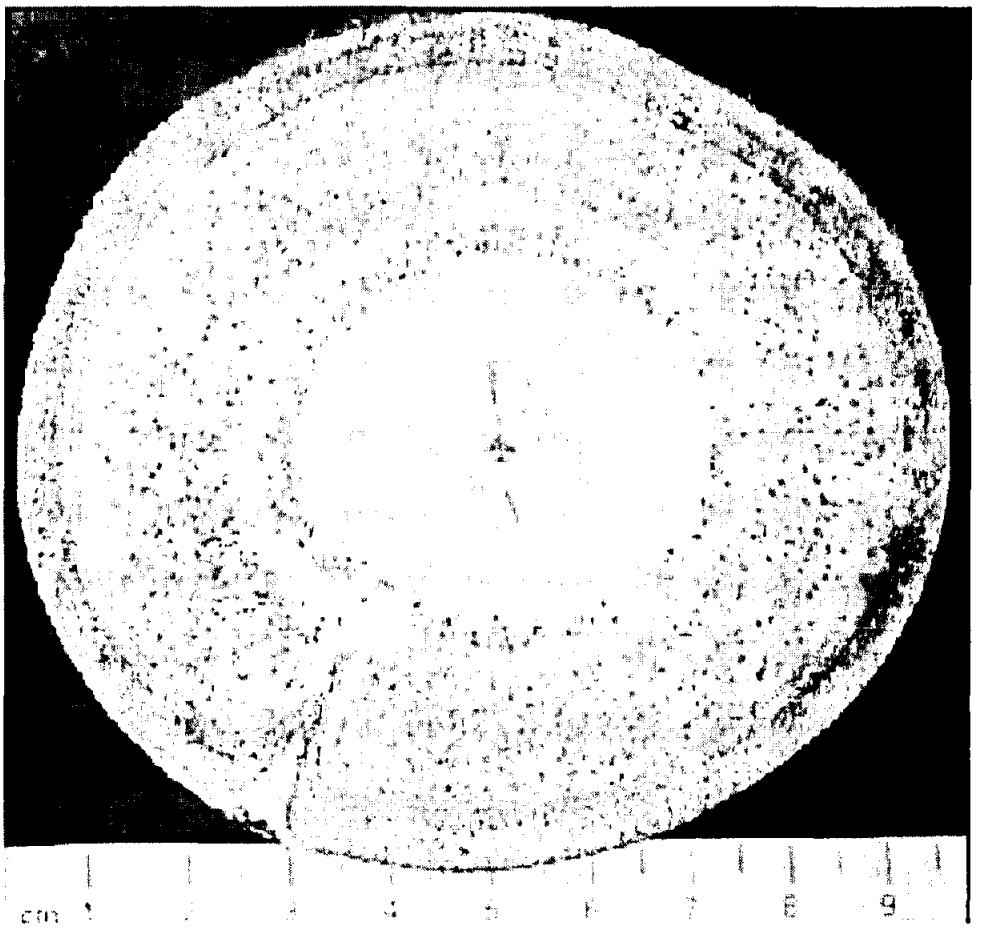

Plate 4.1 The dye solution was absorbed resulting in a diffuse pattern of blue spots. These show concentric rings of uneven absorption and exhibit regions of more readily conductive sapwood. The stem is clearly diffusely porous

in contact with the xylem vessels where most of the convection occurs. Considering the closeness of the vessel distribution this could compromise the flow measurement due to vessel damage. This would however be influenced by the size of the probe used in relation to the stem under consideration.

4.6 Field use of the 25 mm^2 and 100 mm gauges[3]

4.6.1 Introduction

Our aim was (a) to compare mass flux measured using using SSS techniques and those evaporation measurements obtained using lysimetric techniques; (b) to obtain *in situ* measurements of the diurnal stem flow rate and the transpiration rate; (c) determine the error of each component of the SSS technique as well as the overall error in the sap flux; (d) determine if half-hourly M_{sap} measurements are accurate estimates of tree transpiration and (e) investigate the time response of the sap flow measurements by abruptly shading portions of the canopy.

2 Based on the paper by Savage, Graham and Lightbody (1994)

3 Emphasis in this chapter is on the 25 mm gauges

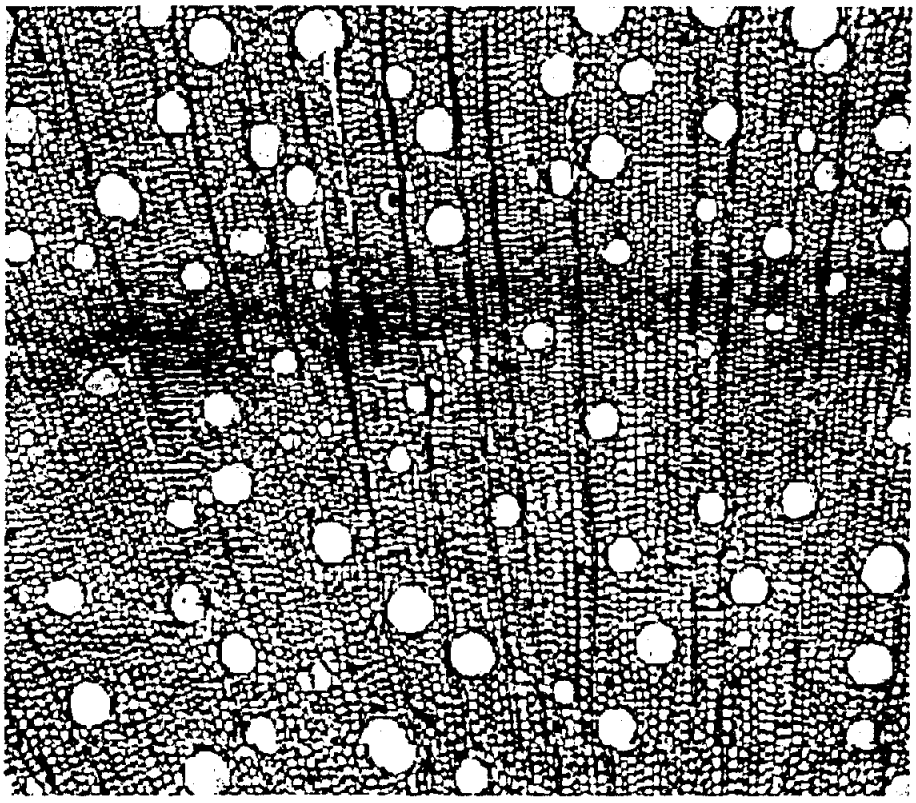

Plate 4.2 Secondary xylem is arranged radially showing an annual growth ring. Internally to the secondary xylem is a small core of thin walled pith cells

4.6.2 Results and discussion

4.6.2.1 Weather conditions

Comparisons between stem steady state heat energy balance (SSS) M_{sap} and lysimeter M_{lys} measurements were performed for a five day period with hot and relatively cloudless days (**Fig. 4.1**). On all of the days, windy conditions caused fluctuations in the manual lysimeter measurements to exceed 100 g for M_{sap} exceeding 400 g h^{-1}. On Day 313, rain occurred at 20h00 and the experiment was terminated the next afternoon.

4.6.2.2 A comparison of M_{sap} for two gauges on the same stem

The two SSS sensors were placed 80 mm apart. It was not possible to position the sensors closer together so that the heat from the heater of the bottom sensor did not affect the measured energy balance components of the upper sensor. For both sensors we used K_{gauge} = 1.565 W mV^{-1} and K_{stem} = 0.54 W m^{-1} K^{-1}. The comparison between the two sensors as well as the solar irradiance is shown (**Fig. 4.2**). Even for the 30-min data, there is very good agreement between the two sensors. A pleasing aspect is the fact that the night-time M_{sap} values for both sensors are practically 0 g h^{-1}, an indication that the correct K_{gauge} was used.

The regression for the bottom M_{sap} value against the top sensor is also shown (**Fig. 4.3**). Much of the scatter in these data is due to a phase shift in M_{sap} of the one sensor compared to the other, probably due to radiative exposure differences. This phase shift can be seen by close examination of the data for the afternoon of Day 321 (Fig. 4.2). In spite of this problem, the correspondence is good. Both sensors had similar diurnal variations in the standard deviations of the voltage terms (**Figs 4.4 and 4.5**).

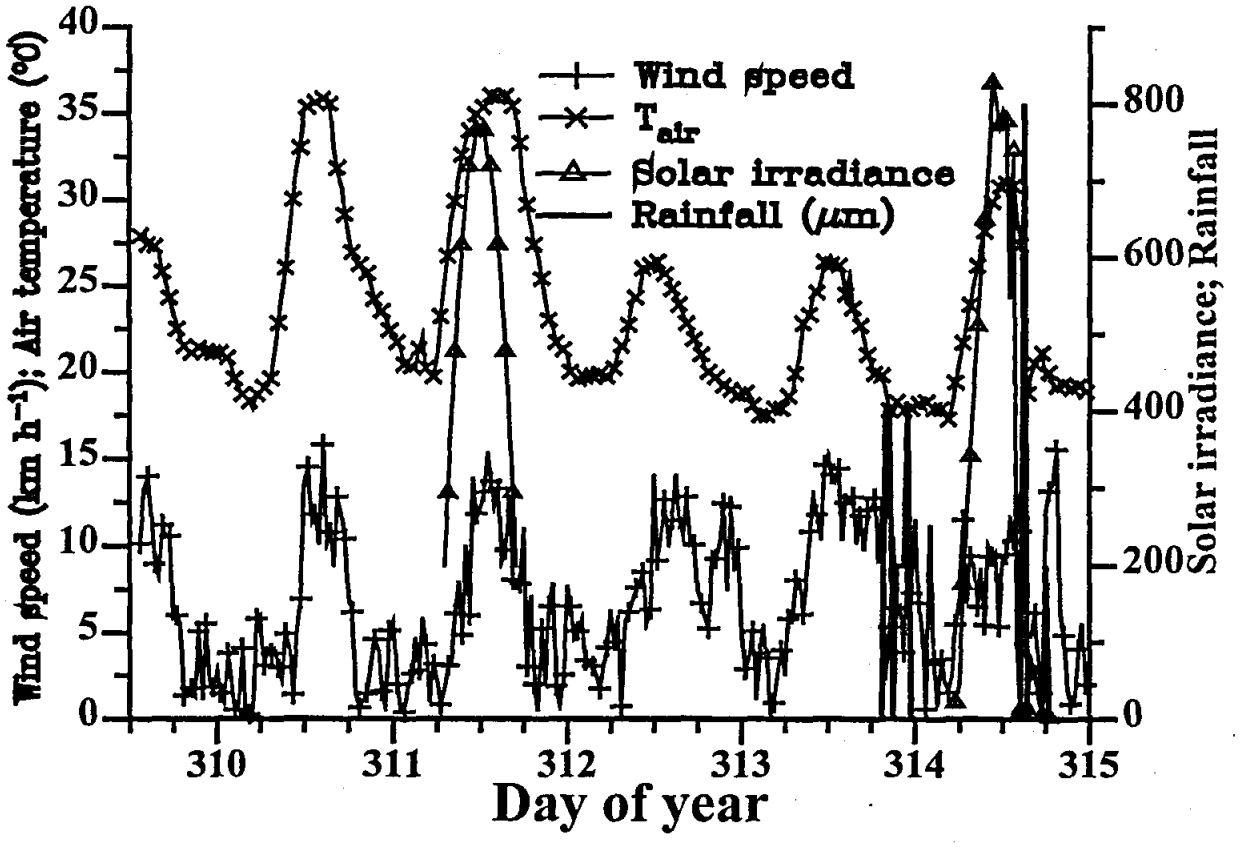

Fig. 4.1 The diurnal variation in a number of the measured weather parameters for the duration of the experiment. Each day indication corresponds to a local time of midnight. Plotted on the left-hand y-axis is the average wind speed at a height of 10 m above ground. The variation in T_{air} (°C) is plotted on the same system of axes. Plotted on the right-hand y-axis is the solar irradiance (W m^{-2}) and rainfall (in μm). Rainfall only occurred on Days 313 and 314, 1991. Each point represents the average 30 min value

The effect of increased solar irradiance at sunrise results in increased M_{sap} values almost immediately, or at least within the same half-hour. The diurnal course M_{sap} values during the day-time is anti-symmetrical with the increases corresponding to sunrise rapid whereas the decreases corresponding to sunset are less rapid. This may be due to the resistance to water loss in storage tissue being lower than that at night.

4.6.2.3 Comparisons between lysimeter flow rates M_{lys} and gauge flow rates M_{sap}

Comparisons between stem steady state heat energy balance (SSS) M_{sap} and lysimeter M_{lys} measurements were performed for a five day period with hot and relatively cloudless days. On all of the days, windy conditions caused fluctuations in the manual lysimeter measurements to exceed 100 g for M_{sap} exceeding 400 g h^{-1}. The flow rates M_{sap} and M_{lys}, independently determined, compare favourably for the half-hourly time intervals (Fig. 4.3). The good comparisons between the lysimeter 30 min values and the M_{sap} values is also reflected in the good comparisons between the time integrated values (**Table 4.3**). Also shown in Table 4.3 are the integrated M_{sap} values (kg) for a K_{gauge} value of 0.8 W mV^{-1} and 1.565 W K^{-1}. The mean and standard deviation for K_{gauge} so computed was used in the error analysis performed on the M_{sap} calculations (based on other measurements, Section 4.6.2.4).

The thermal conductance (K_{gauge}) for a particular SSS gauge installation must be pre-determined. Most workers have used the pre-dawn M_{sap} value of roughly 0 g h^{-1} to determine K_{gauge}. The

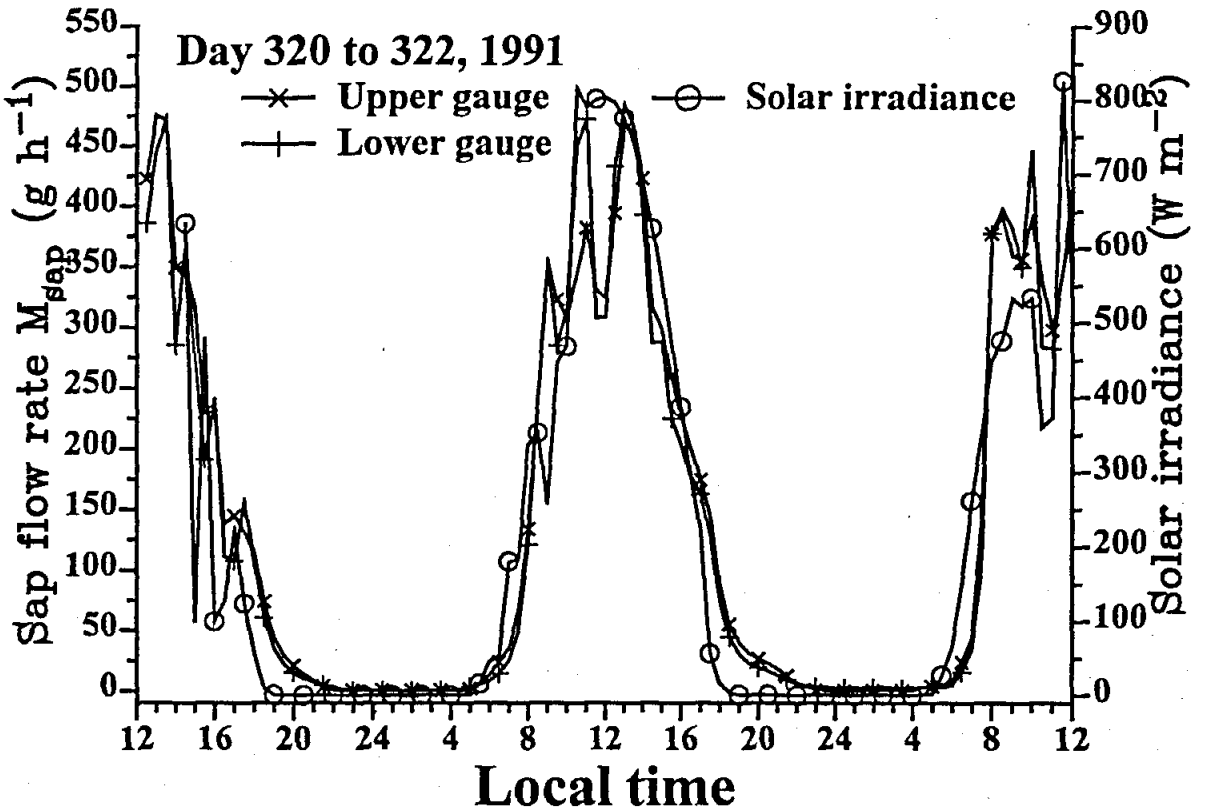

Fig. 4.2 The diurnal variation in M_{sap} (g h^{-1}), left-hand y-axis, for two gauges connected to the same tree for 1991 Day 320 to 322. Also shown is the solar irradiance (W m^{-2}), right-hand axis. In general, there was a concomitant change in M_{sap} with change in solar irradiance. Unstable dT_{stem} values (Fig. 4.8) at sunrise cause large increases in M_{sap}. Some workers attribute this to sap flow heating

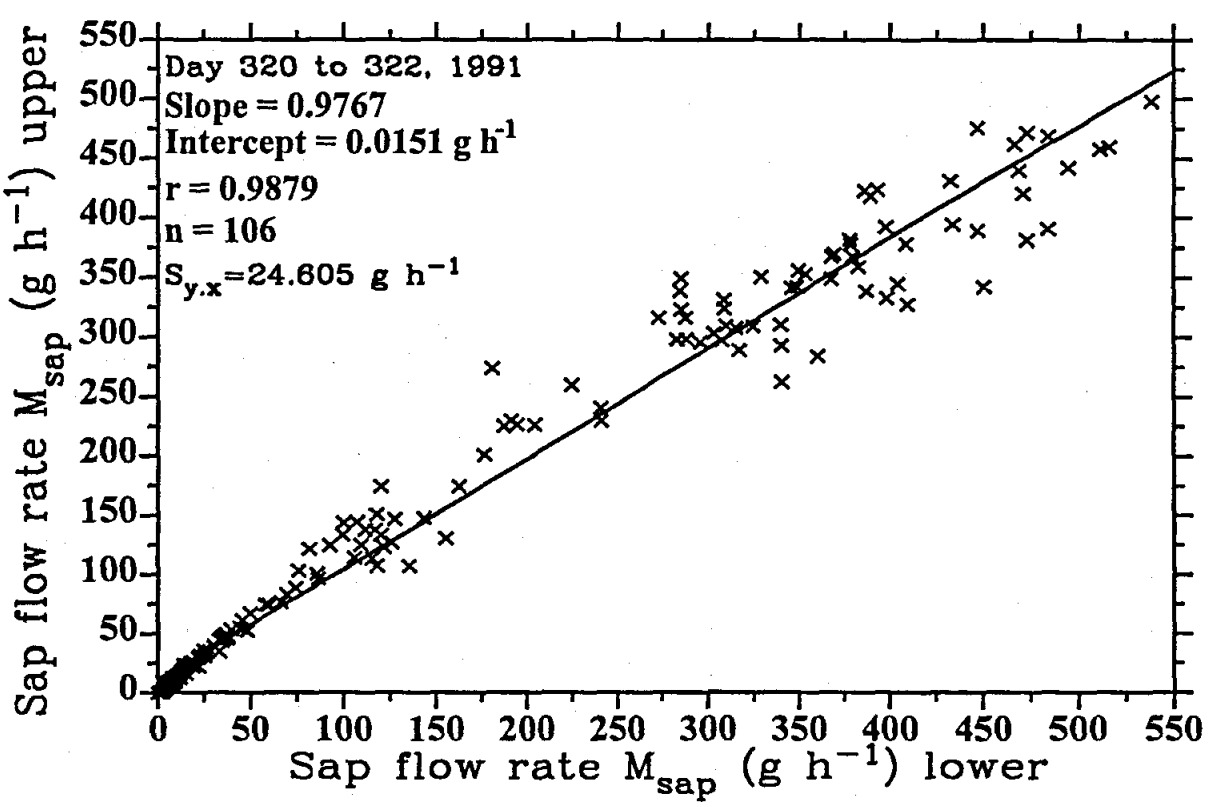

Fig. 4.3 The comparison between the upper and lower gauges placed on the same tree

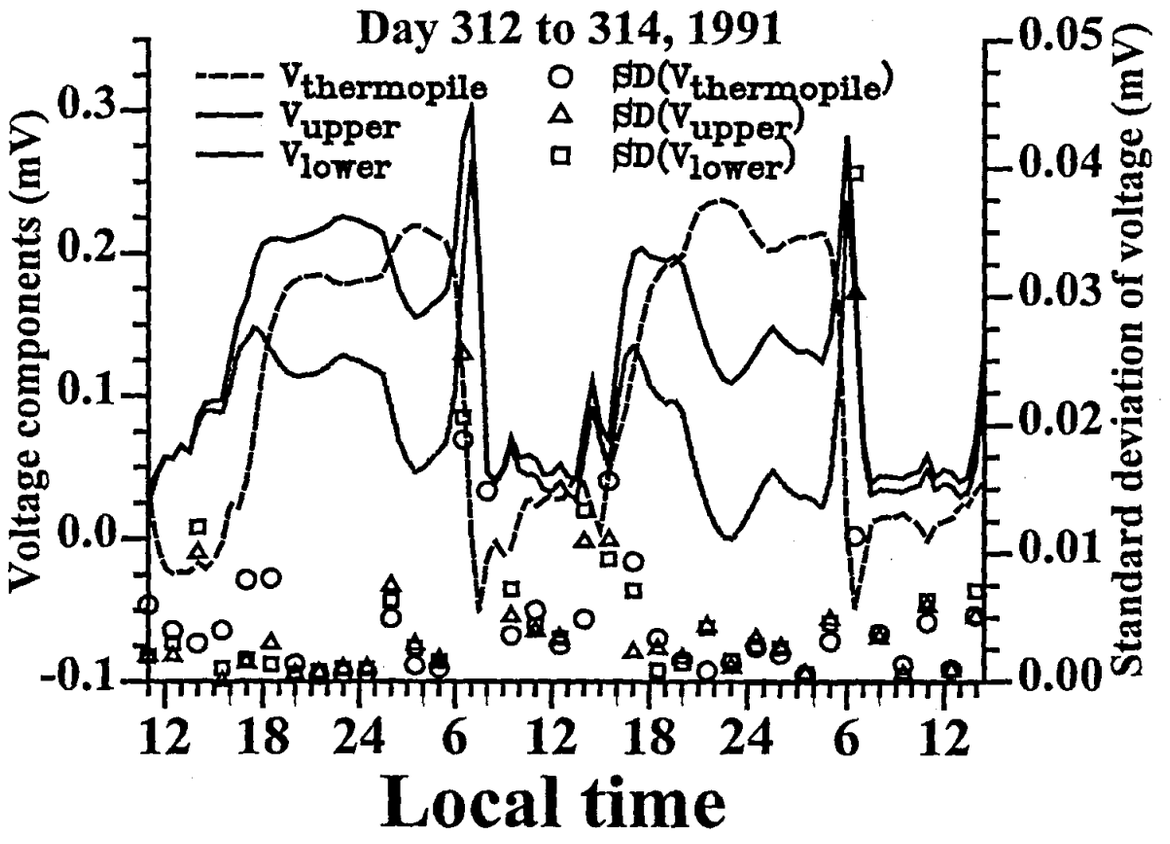

Fig. 4.4 Diurnal variation in the mean (left-hand y-axis) and standard deviation (right-hand y-axis) of $V_{thermopile}$, V_{upper} and V_{lower} for 1991 Day of year 312 to 314. During day-time, the mean voltages resulted in $E_{thermopile}$, E_{upper} and E_{lower} being small compared to residual term E_{sap} (used to calculate $M_{sap} = E_{sap}/(c_p\, dT_{stem})$ (see Eqs 3.1 and 3.2)

assumption that $M_{sap} = E_{sap}/(dT_{stem}\ c_p) = 0$ must imply that $E_{sap} = 0$. However, the sap flow energy flux E_{sap} may never equal zero as one might expect, because flow during the night may in fact not cease; that is, $M_{sap} \neq 0$. However, we have noticed a variation in K_{gauge} during the night with slow convergence to a minimum value as the minimum flow conditions are approached. We averaged the K_{gauge} values under the night-time minimum flow conditions for a number of consecutive nights. For the remainder of the study, we used $K_{gauge} = 1.565$ W mV^{-1}.

The dT_{stem} values (left-hand y-axis of Fig. 4.5) are usually a minimum around the solar noon times corresponding to maximum flow rates, increasing towards a maximum at sunset with a gradual decrease to a secondary minimum at midnight. Large increases in dT_{stem} occur at sunrise. This increase could be due to the transpiration of overnight-heated sap or it could be due to the sudden increase in heat energy external to the gauge from the increased solar irradiance. The day-time minimum of dT_{stem} was between about 0.8 and 1.5 °C (Fig. 4.5) indicating that the preset V_{heater} value of around 4.5 V was just sufficient to produce sufficient heating of the sap that could be detected by the thermocouples (Fig. 3.1). During the night-time, dT_{stem} increased to around 7 °C and less. It should be remembered that the temperature increase dT_{stem} is dynamic, occurring whenever measurements are performed. Certainly then there must be a compromise between the level of heating applied during night-time hours of relatively low E_{sap} conditions and the magnitude of dT_{stem} during day-time hours. We believe that our data shows an adequate compromise (Fig. 4.6). The value of V_{heater} we chose had the added advantage

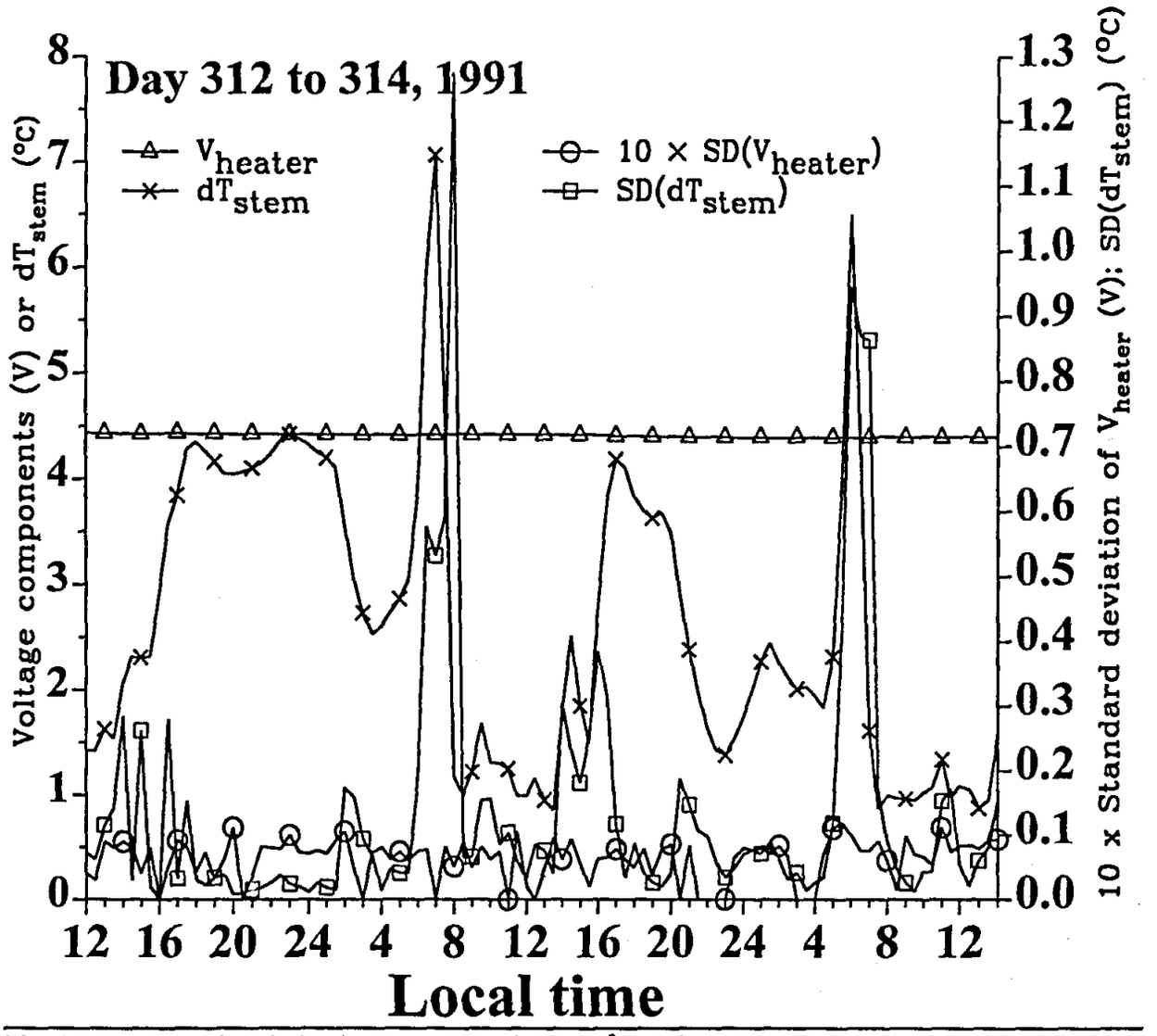

Fig. 4.5 The diurnal variation in V_{heater} (V)and dT_{stem} (°C) (left hand y-axis) for a thermal conductivity K_{stem} of 0.42 and 0.54 W m^{-1} K^{-1} for Days 312 to 314, 1991. Also shown (right hand y-axis are the standard deviations in V_{heater} (V) and dT_{stem} (°C) measured for each 30-min period. The dT_{stem} value seldom decreased below 1 °C in magnitude during day-time hours. It is a denominator term (Eq. 3.2) and therefore critical in determining M_{sap}. It should always be examined to ensure that it results in realistic M_{sap} values

Table 4.3 Integrated lysimeter transpiration totals and gauge totals for various parameters (day-time hours only). The mean and standard deviation of K_{gauge} was calculated from midnight to 04h00

Day of year	Lysimeter daily total (kg)	Gauge total (kg) (K_{gauge} = 0.8, K_{stem} = 0.34)	Gauge total (kg) (K_{gauge} = 1.565,K_{stem} = 0.34)	Mean K_{gauge} (W mV^{-1}) for K_{stem} = 0.34	Standard deviation K_{gauge} (K_{stem} = 0.34)
309	3.20	3.90	3.80	1.690	0.0607
310	6.59	4.88	5.03	1.582	0.1384
311	8.27	9.73	9.33	1.809	0.4463
312	8.26	7.49	7.69	1.826	0.0806
313	2.43	2.63	2.52	2.583	0.1760
314		6.82	5.93	1.673	0.0499

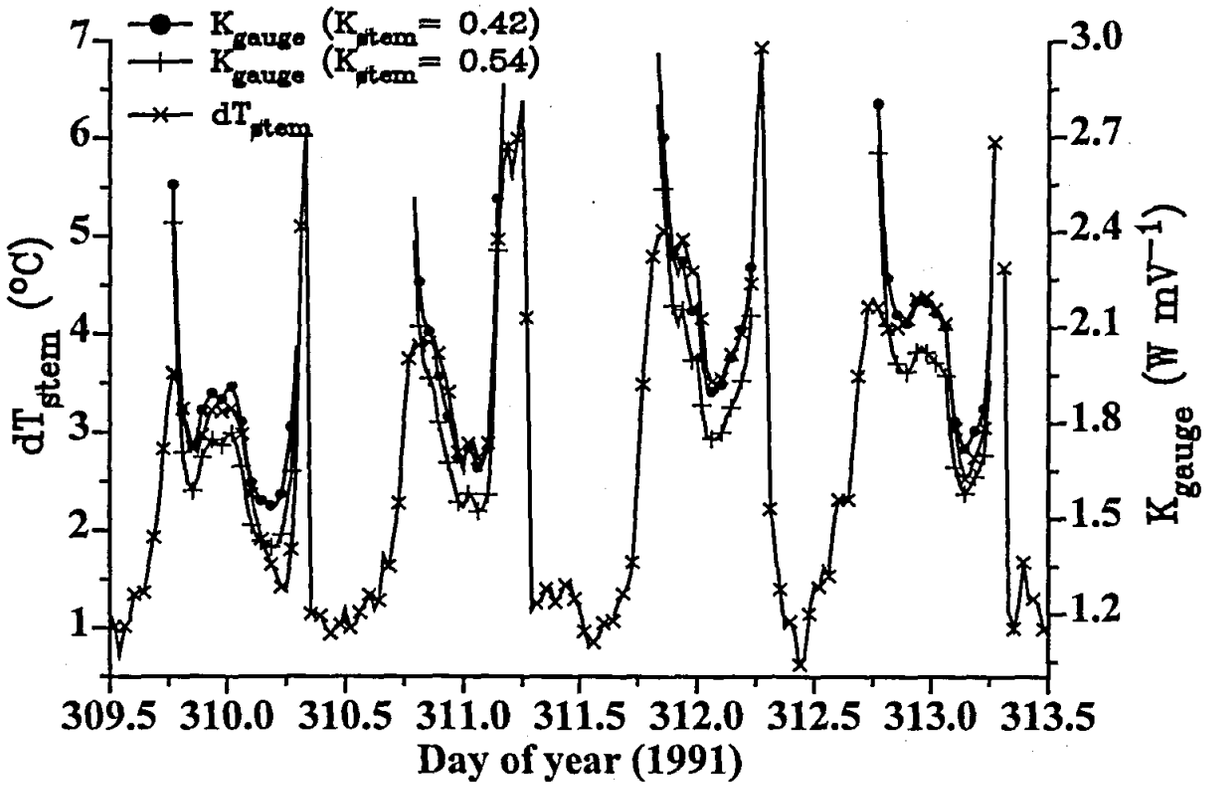

Fig. 4.6 The diurnal variation in dT_{stem} (°C), left hand y-axis and K_{gauge} (W mV^{-1}) for a thermal conductivity K_{stem} of 0.42 and 0.54 W m^{-1} K^{-1}

that it could be measured directly by the data logger without voltage division using a potential divider circuit.

4.6.2.4 Calculation of the standard deviation of M_{sap} for each half-hourly period

The theory associated with the calculation the standard deviation of the component energy balance terms has been presented (Section 4.3.6). The relevant equation (Eq. 4.8) may be used to calculate the standard deviation of the sap flow rate (g h^{-1}). The standard deviation (right-hand y-axis) and means (left-hand y-axis) of all the voltage measurements are shown (Figs 4.4 and 4.5). The standard deviation of all the voltage terms increases dramatically around sunrise and around sunset but more so at sunrise. The largest standard deviation occurs in the dT_{stem} term.

4.6.2.4.1 Error analysis

The mean and standard deviations for the constants utilized in the calculation of the sap flow rate using the stem steady state heat energy balance technique are illustrated in **Table 4.4.** A standard deviation in the thermocouple gap distance was obtained by measuring the thermocouple gap distance for at least three gauges. Most of the terms were insignificant when calculating the standard deviation of M_{sap}. Hence Eq. 4.8 could be reduced to a much simpler equation without loss in accuracy:

$$\sigma_n^2(M_{sap}) = [(\sigma_n^2(dT_{lower}) + \sigma_n^2(dT_{upper}))/dx^2 + (\sigma_n^2(dx)\cdot(dT_{lower}^2 + dT_{upper}^2)/dx^4]/(dT_{stem}\cdot c_w)^2. \quad 4.9$$

The specific heat capacity of the sap c_w is assumed to be constant with no variance. The smaller the stem temperature differential dT_{stem}, the larger the variance in the sap flux. Conversely, the larger the upper and lower thermocouple temperature differences, dT_{upper} and dT_{lower} respectively, and their respective variances, the larger the variance in the sap flux. Lastly, the smaller the thermocouple gap

Table 4.4 The means and standard deviations (SD) of the constants required for the calculation of the standard deviation of the sap flux (Eq. 4.8). The covariances (CV) of all the so-called constants are also presented as a percentage

Parameter	dx (m)	K_{stem} (W m^{-1} K^{-1})	K_{gauge} (W mV^{-1})	A_{stem} (m^2)	R_{heater} (Ω)
Mean	0.007	0.34	1.676	0.000674	40.01
SD	0.00035	0.04	0.1	0.00005	0.02
100 × CV (%)	5	11.8	5.97	7.4	0.005

distance, the larger the variance in sap flux, while the larger the variance in the thermocouple gap, the larger the variance in sap flux.

The sap flux was measured and compared with the standard deviation of the sap flux calculated using Eq. 4.8, for Day 321, 1991 (**Fig. 4.7**). During the day when the sap flow rate reached about 120 g/15 min, the standard deviation of M_{sap} was about 7 g/15 min. The standard deviation can be expressed more perceptively as a percentage error (**Fig. 4.8**). The percentage error in the sap flux was also calculated using Eq. 4.9 from sunrise to sunset for Day 321, 1991, by dividing the standard deviation of the sap flux by the actual sap flux and then multiplying by 100 (Fig. 4.8).

The percentage error of the sap flux exceeded 100 % at sunrise, which coincides with the sunup event. However, the sap flux during this time period may be interpolated. During the day the percentage error decreased to about 8 % and then increased in the evening when sap flow was low (Fig. 4.8).

The percentage error of the thermocouple gap distance dx was also calculated as this was the only

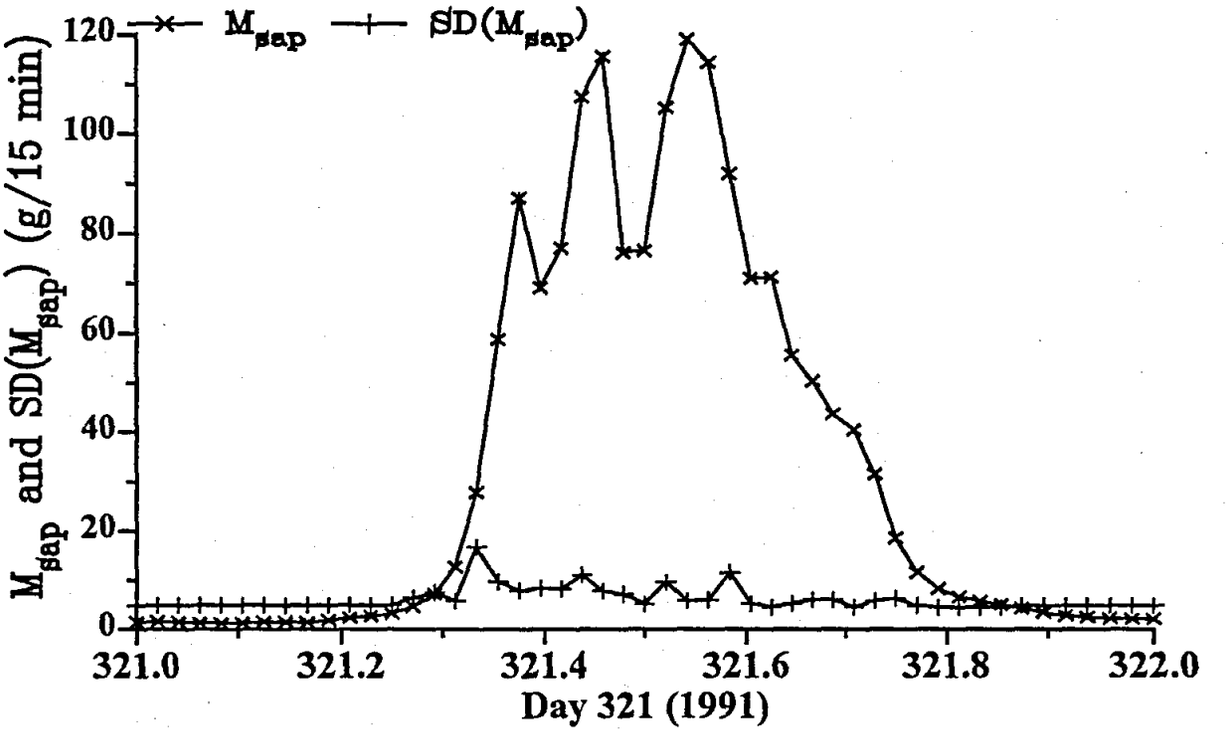

Fig. 4.7 Comparison of the sap flow rate M_{sap} and its standard deviation SD(M_{sap}) as calculated using Eq. 4.8, for Day 321, 1991

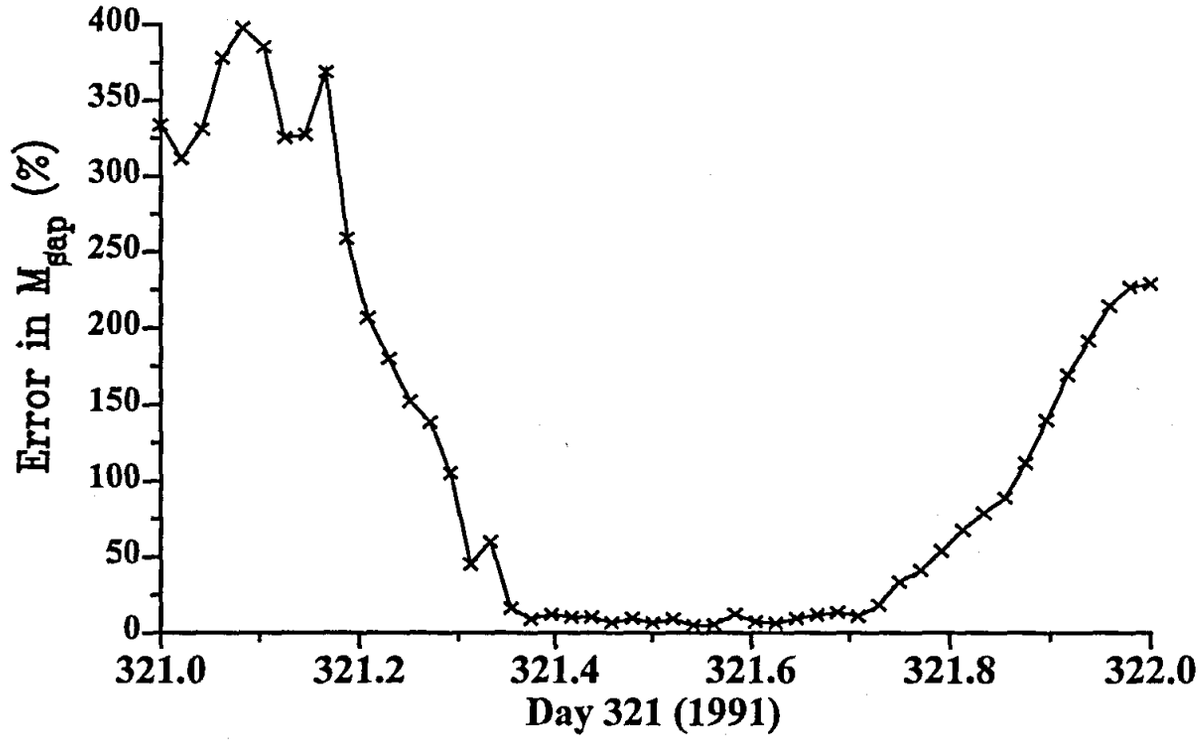

Fig. 4.8 The percentage error in M_{sap} as a function of time from sunrise to sunset, Day 321, 1991. At sunrise the error in M_{sap} exceeded 100 %

constant that had a significant effect on the variance in M_{sap}. It was calculated for a 0 to 10 % standard deviation of dx. The respective standard deviations of the sap flux were then calculated at midday, Day 321, 1991, when the sap flow rate was 76.7 g/15 min. A comparison of the percentage error in M_{sap} and the percentage error in dx are illustrated (**Fig. 4.9**). It is seen that a 10 % increase in the standard deviation of the thermocouple gap can result in an increase of over 100 % in the percentage error of the sap flux (about 3.6 % to 7.2 %).

Therefore, if the thermocouple gap distance can be measured accurately, then the standard deviation of the sap flux will decrease significantly. The thermocouple gap constants for the SGB25-ws and SGA100-ws gauges are 7 mm and 15 mm respectively. If the standard deviations of both gauges can be measured to be the same, then the percentage error in dx will be larger in the SGB25-ws compared to the SGA100-ws gauge because of the smaller thermocouple gap distance. Therefore, in terms of the standard deviation of the thermocouple gap constant, the smaller (SGB25-ws) 25-mm diameter gauge will measure sap flux less accurately relative to the larger (SGA100-ws) 100-mm diameter gauge.

With no error in the thermocouple gap distance dx, the percentage error is 3.5 % due to the stem temperature differential dT_{stem}, $\sigma_n^2(dT_{lower})$ and $\sigma_n^2(dT_{upper})$ (Eq. 4.9). The stem temperature differential will only increase the standard deviation of the sap flow during the day when it decreases to a very low value due to it being in the denominator (Eq. 4.9). This confirms that the stem temperature differential must be kept above about 0.75 °C during the day, which in turn implies that the power supplied to the heater must be quite high during the day, but within the specified limits of the specific gauge (Table 4.1). The variances of the upper and lower thermocouple temperatures dT_{upper} and dT_{lower} respectively are once again low at night and high during the day. Similarly for their respective temperatures.

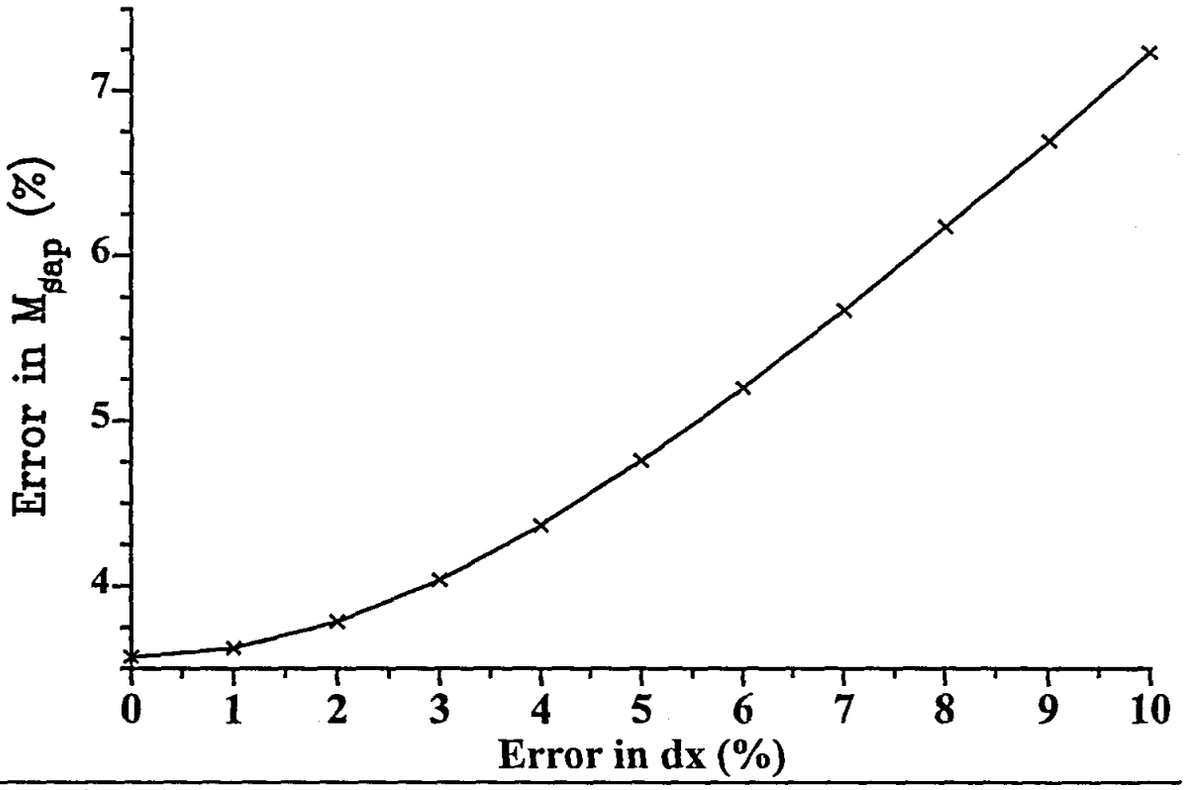

Fig. 4.9 Effect of increasing the standard deviation of the thermocouple gap between 0 and 10 % on the percentage error of the sap flux. The sap flux was constant at 76.7 g/15 min which is the midday value for Day 321, 1991. A typical percentage error in dx, used in the experiment, was 5 % which implies a standard deviation of 0.35 mm for $dx = 7$ mm

4.6.2.5 Gauge conductance and stem thermal conductivity aspects

The value of the stem thermal conductivity K_{stem} directly affects the gauge conductance K_{gauge}. Thus, a different combination of K_{stem} and K_{gauge} can result in the same M_{sap}. For this reason, we set the stem thermal conductivity K_{stem} to 0.54 W m^{-1} K^{-1} and calculated the K_{gauge} value accordingly. We resolved this problem as follows: we kept constant the stem thermal conductivity K_{stem} and using Eqs 3.1 and 3.5 changed K_{gauge} to roughly half the value determined from examination of the minimum night-time flow, *viz.* K_{gauge} (*actual*) = 1.565 W mV^{-1}. We also used a K_{gauge} double that of K_{gauge} (*actual*). Too high a $K_{gauge} = 2\,K_{gauge}$ (*actual*) value resulted in significant negative M_{sap} values during the night-time (**Fig. 4.10**, curve with lowest values and negative during the night-time). Conversely too low a $K_{gauge} = ½\,K_{gauge}$ (*actual*) value resulted in significant positive M_{sap} values (calculated from Eq. 3.2) during the night-time. During the day-time however, the most crucial time in terms of the use of the technique, the effect of increasing K_{gauge} within the $½\,K_{gauge}$(*actual*) to $2\,K_{gauge}$ (*actual*) range had only a slight affect on the calculated M_{sap}.

The problem of the interplay between K_{gauge} and K_{stem} is not serious for the 25 mm gauges used. The sap flow rate M_{sap} was recalculated for K_{gauge} = 0.8 W mV^{-1} for two K_{stem} values (0.40 W m^{-1} K^{-1} and 0.54 W m^{-1} K^{-1}). The effect of this change during the day-time and night-time hours is insignificant; the overriding influence of using the incorrect K_{gauge} = 0.8 W mV^{-1} is to cause positive M_{sap} flow rates when the M_{lys} values are known to be 0 g h^{-1}(**Fig. 4.11**). Steinberg *et al.* (1989) showed, using a sensitivity analysis, that a 4 to 9 % error in M_{sap} would result if K_{gauge} were in error by 10 to 20 %. However, their calculations assumed that there was no error in K_{stem}, the thermal conductivity of the stem.

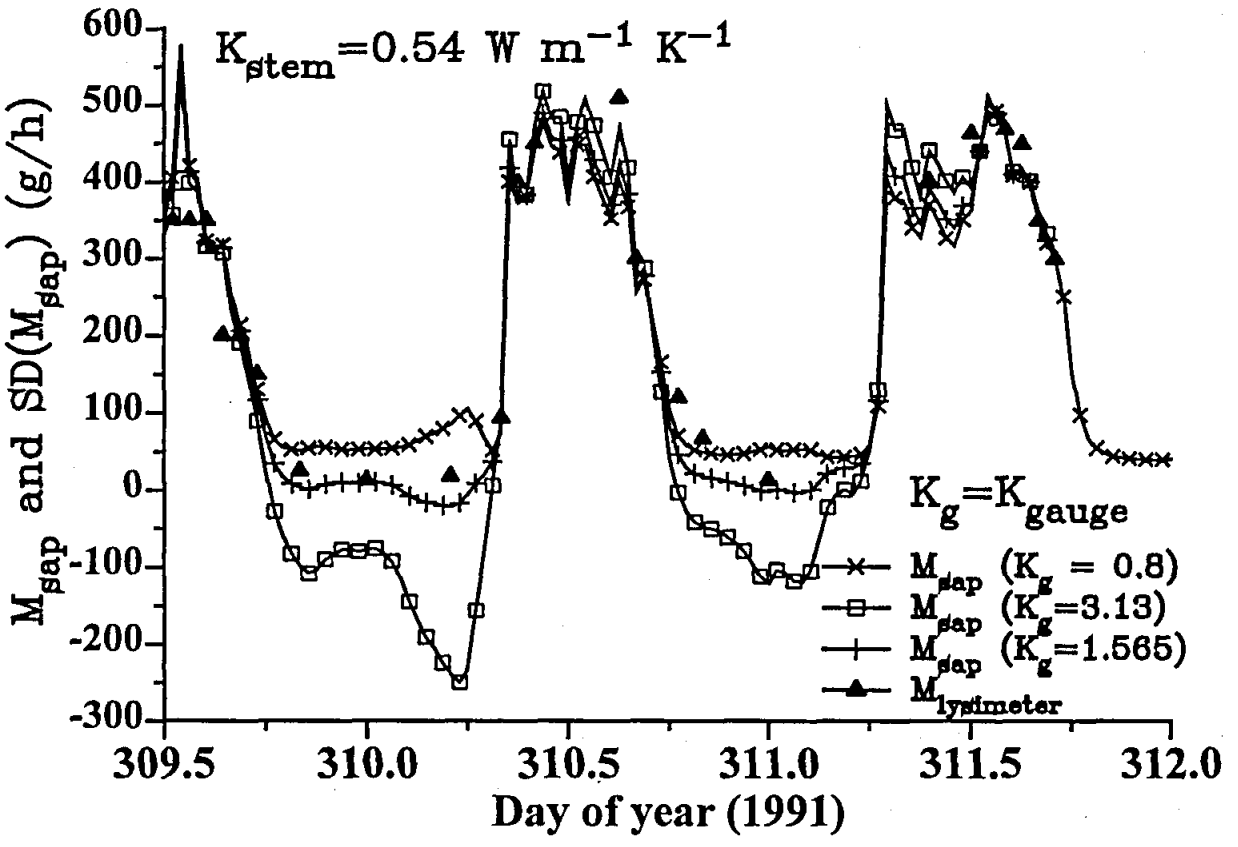

Fig. 4.10 The diurnal variation in M_{sap} (g h^{-1}) for three K_{gauge} (abbreviated K_g in the figure) values. Also shown are the lysimeter mass flow rates

It was apparent that the 30-min gauge flow rates compare quite well with the 30-min lysimeter values. Based on other work in the literature, this was not expected as most workers have used an integrated time scale of four to 24 h.

4.6.2.6 Energy balance components

The diurnal variation in E_{sap} (W), M_{sap} (g h^{-1}) and the lysimeter flow rate M_{lys} (g h^{-1}) are shown for Days 310 to 312 assuming a stem thermal conductivity (K_{stem}) of 0.54 W m^{-1} K^{-1} and a SSS gauge conductance (K_{gauge}) of 1.565 W mV^{-1} which is equivalent to 0.0626 W K^{-1} **(Fig. 4.12)**. The thermal conductivity of the stem, K_{stem}, must be known prior to measurement. Most workers have assumed a fixed value of 0.54 W m^{-1} K^{-1} for herbaceous species, independent of stem water content or temperature. Also shown in Fig. 4.12 are the M_{lys} values for Day 309 to 311 as confirmation of these conclusions. The data for Day 311 are shown **(Fig. 4.13)**.

The term E_{sap} is the dominant term (Fig. 4.12) of the SSS energy balance terms (but obviously excluding E_{heater}). Occasionally, we noted negative E_{radial} values (Fig. 4.13). Since $E_{upper} + E_{lower}$ was practically 0 g h^{-1}, this meant that *Esap* actually exceeded E_{heater}. The negative E_{radial} amount implied that instead of the heat from the heater being conducted radially outward through the cork insulation surrounding the heater, heat must have been conducted inwards from the outside where the radiative load is high. We therefore assumed that the steady condition was not being met because of a lack of insulation surrounding the heater. Equation 3.1 cannot apply as there is an unspecified residual term. We therefore decided to further insulate the gauge with 50 mm thick waterproof insulation (Fig. 4.13).

The implication then is that the act of further insulating the sensor surrounding the stem ensured

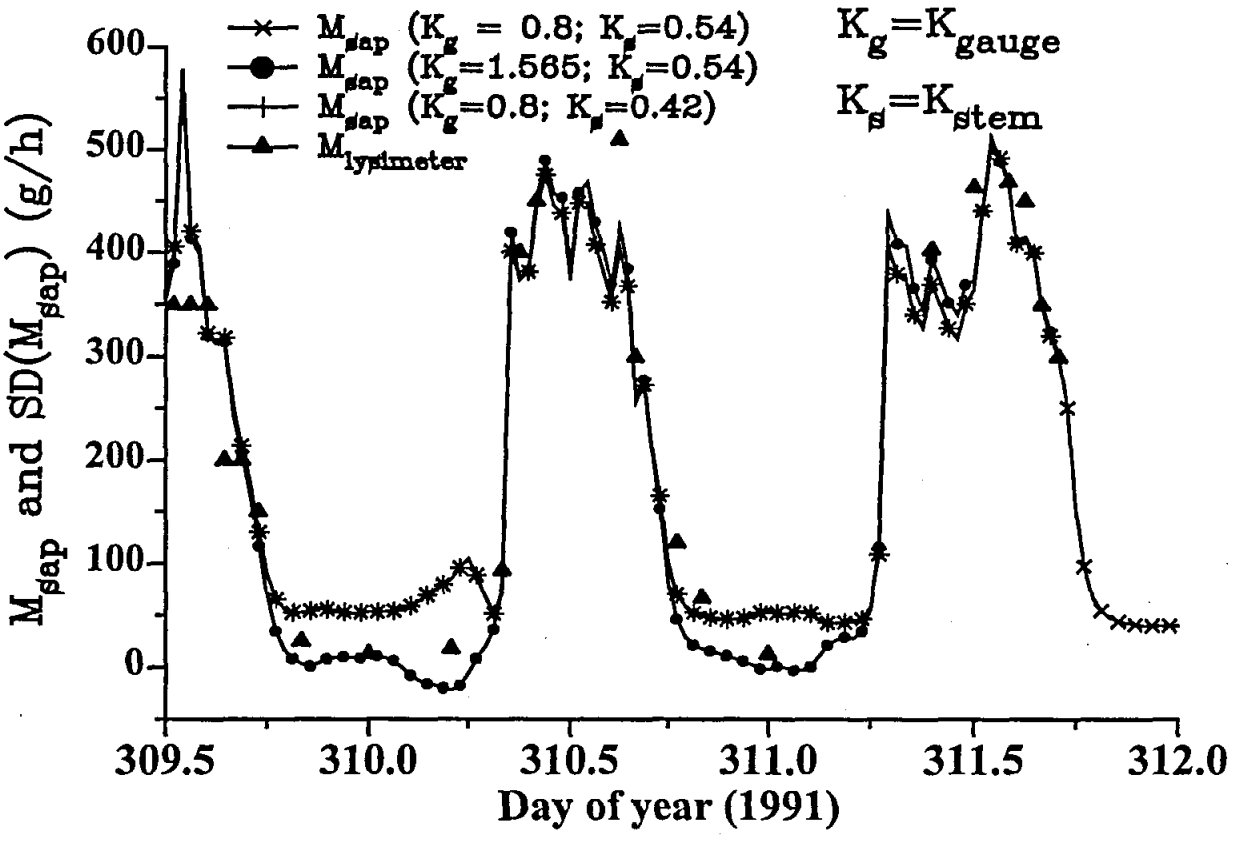

Fig. 4.11 The diurnal variation in M_{sap} (g h^{-1}) for various combination of K_{stem} and K_{gauge} values. Also shown are the lysimeter mass flow rates

that E_{radial} was practically 0 W or at least > 0 W. An examination of the value of E_{radial} after 12h00, Day 311 (Fig. 4.13) showed that E_{radial} was usually positive except for:

(a) times associated with sunrise (**Fig. 4.14**);

(b) times associated with irrigation (Fig. 4.12, Day 312, local time about 12h00).

Also of interest in Fig. 4.14 is the number of times E_{sap} exceeded E_{heater} prior to the addition of the insulation on Day 311 at 12h15 (Fig. 4.13) and the relatively few times $E_{sap} > E_{heater}$ after insulating. In fact, as was the case for the positive E_{radial} values, $E_{sap} > E_{heater}$ for times associated with sunrise or when there was an irrigation.

4.6.2.7 The effect of heater voltage on sap flow measurements

The experiment described in Section 4.6.2.3 was repeated in 1992. For 1992 the sap flux measured using the two techniques followed a slightly similar pattern (**Fig. 4.15**). However, there were two problems associated with the sap flow rate measured using the SSS technique for 1992.

Firstly, soon after sunup, the sap flow rate suddenly increased for a very short period and then decreased to reasonable proportions, referred to as a sunup event. The reasoning for this is a subject of much concern. The sap that had been heated overnight, suddenly moved past the upper thermocouples, while the heated sap adjacent to the thermocouples below the heater, was suddenly replaced with cool, fresh sap from below. This caused a sudden peak in dT_{stem} (**Fig. 4.16**) until all the heated sap had been convected past the upper thermocouples, and then it decreased rapidly.

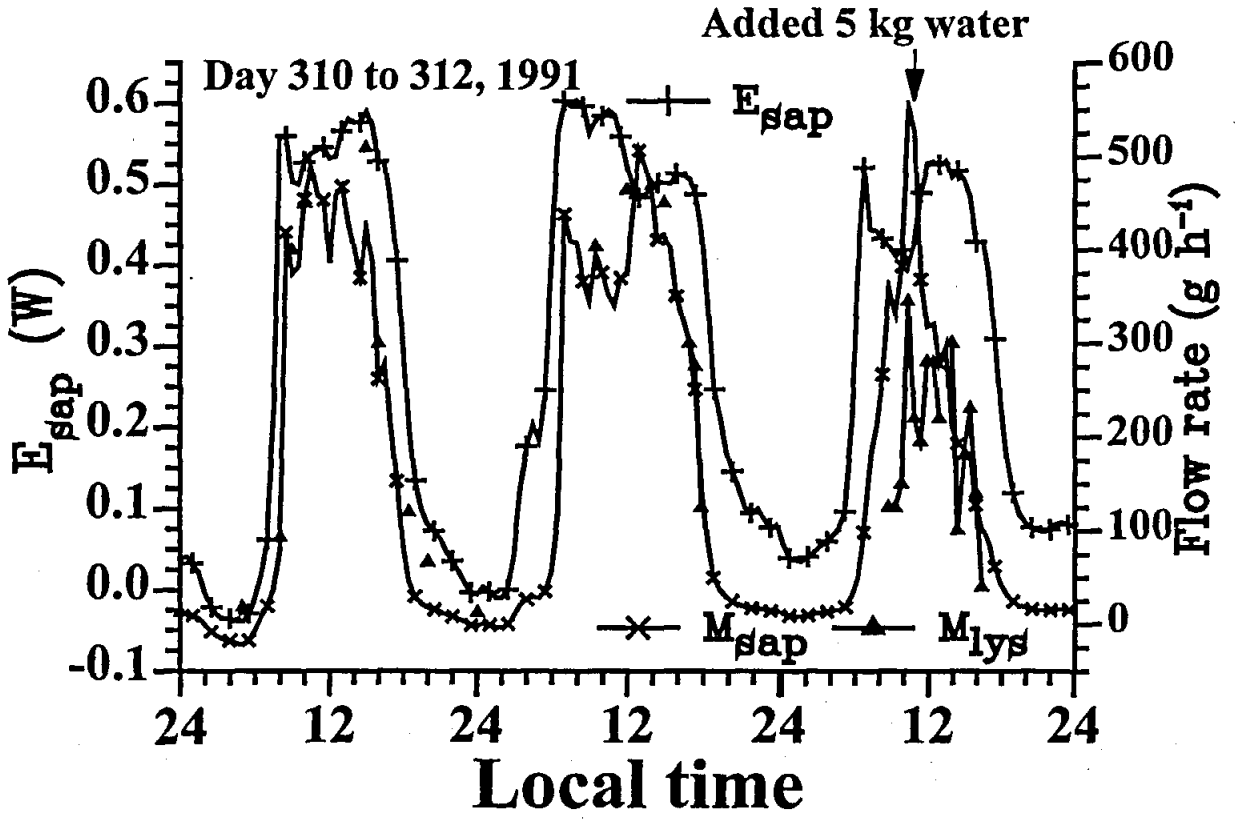

Fig. 4.12 The diurnal variation in E_{sap} (W), left hand y-axis and the mass flow rates (g h^{-1}), right hand y-axis as measured using a lysimeter M_{lys} and M_{sap} measured using a SSS 25 mm gauge (SGB25-ws) for Days 310 to 312, 1991. On Day 312 (the third of the three daily time courses), high wind speeds resulted in variable lysimeter flow rates M_{lys}. These M_{sap} are associated with a gauge conductance of 1.565 W mV^{-1} (equivalent to 0.0622 W K^{-1}) and a stem thermal conductivity K_{stem} of 0.54 W m^{-1} K^{-1}

Secondly, the sap flux during the day for 1992 was overestimated using the SSS technique. This overestimation occurred as a result of the temperature differential dT_{stem} approaching too close to zero during the daylight hours (Fig. 4.16), because the voltage being supplied to the heater was too low. The power supplied to the heater was too low during a period of high evaporative demand, and consequently the heat energy flux being supplied by the heater was too low (**Table 4.5**). Since dT_{stem} is a term in the denominator in the equation used to calculate M_{sap} (Eq. 3.2), if it reaches too small a value, then M_{sap} will tend to infinity. It is essential in a case such as this, that a high flow rate filter be used to establish a maximum sap flux.

To eliminate these two problems, it is imperative that the voltage supply to the heater be decreased or disconnected at night if K_{gauge} determinations are not required, and that the heater power output be increased within the limits of the gauge during the day. Unfortunately, the power was not reduced during the subsequent experiments.

On Day 312, 1991, at midday the sap flux suddenly increased causing a peak (Fig. 4.12). This would have been due to the heater voltage being too low during a period of high flow, resulting in the stem temperature differential being too small. At the same time however, the tree was irrigated.

When M_{sap} and M_{lys} are compared for 1992 (Fig 4.15), it can be seen that the sap flux is overestimated when using the SSS technique relative to 1991 (Fig. 4.12).

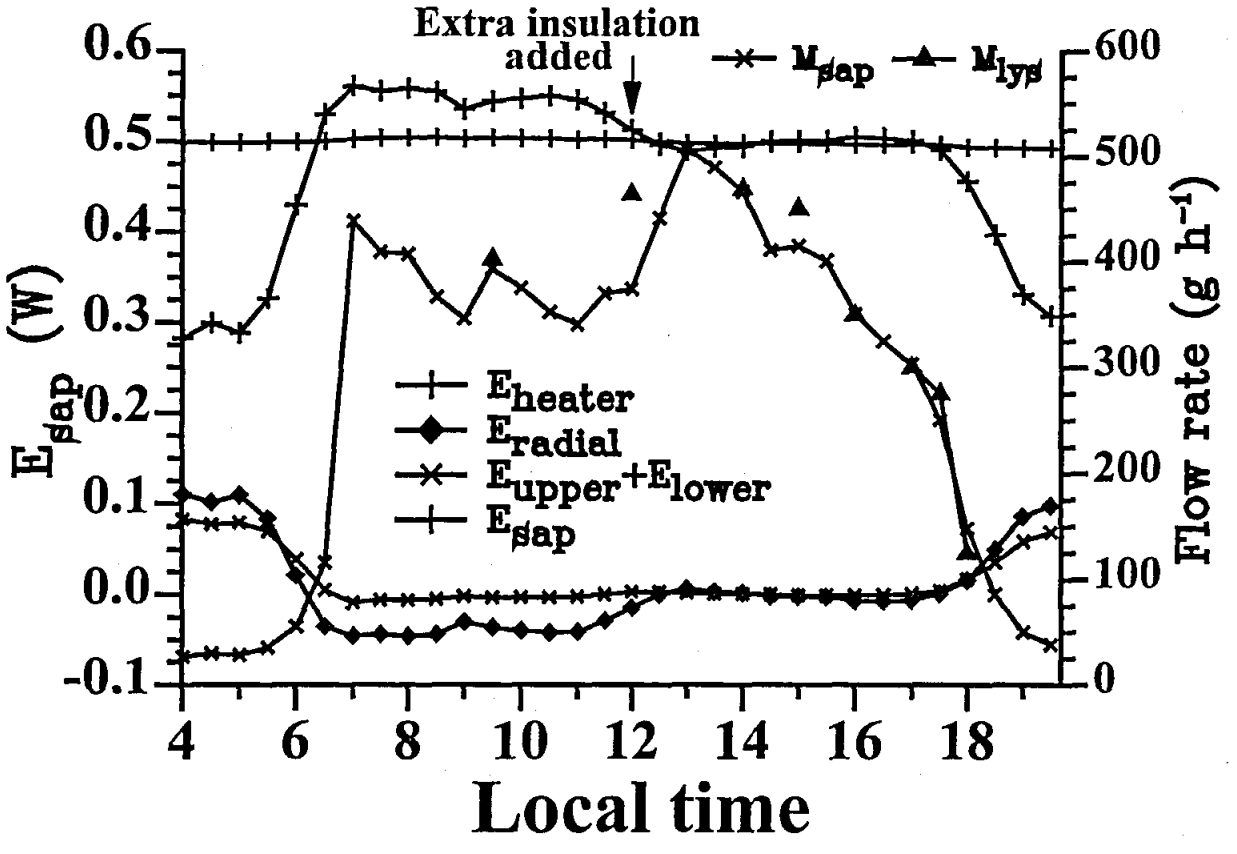

Fig. 4.13 The diurnal variation in the component energy fluxes as well as the mass flow rate measured using the gauge and the lysimeter for Day 311. The effect of extra insulation applied to the sensor is shown

The stem differentials dT_{stem} were averaged for the three days for 1991 and 1992 and then compared (Fig. 4.16). At 09h30, dT_{stem} for 1992 decreased much lower than that in 1991. It remained lower until 13h30 and then decreased again from 14h00 until 15h30 (Fig. 4.16). These times correspond with the overestimation of M_{sap} measured for 1992 using the SSS method (Fig. 4.15).

If the voltage supplied to the heaters are averaged for the three days and compared for the two experiments, it can be seen that in 1992 the voltage was decreased by about 0.2 V (Table 4.6). This had a detrimental 10 % decrease in E_{heater}, and consequently a significant decrease in dT_{stem} during hours of high evaporative demand (Table 4.6). As discussed earlier, when dT_{stem} approaches zero during periods of high evaporative demand, M_{sap} approaches infinity. Extreme care needs to be exercised in ensuring that, under conditions of high evaporative demand, the dT_{stem} value is greater than 0.75 °C. If this is not the case, the M_{sap} value will be an overestimate of the true value. Under these conditions, the voltage applied to the heater should be increased but not beyond 5.0 V for the SGB25-ws gauge and not beyond 10.0 V for the SGA100-ws gauge for no damage to the heater to occur.

4.6.2.8 Comparison with Class-A pan evaporation with sap flow measurements

A comparison between gauge measured sap flow and potential evaporation was made to ensure that the gauge was not measuring values greater than potential. A sample of 62 leaves were taken from a branch that had been removed to allow space for a gauge to be attached. Sap flow was measured on this tree. The length and breadth of each leaf was measured, as well as the corresponding leaf area measurements using a LI 3000 leaf area meter. The product of the length and breadth of the 62 leaves

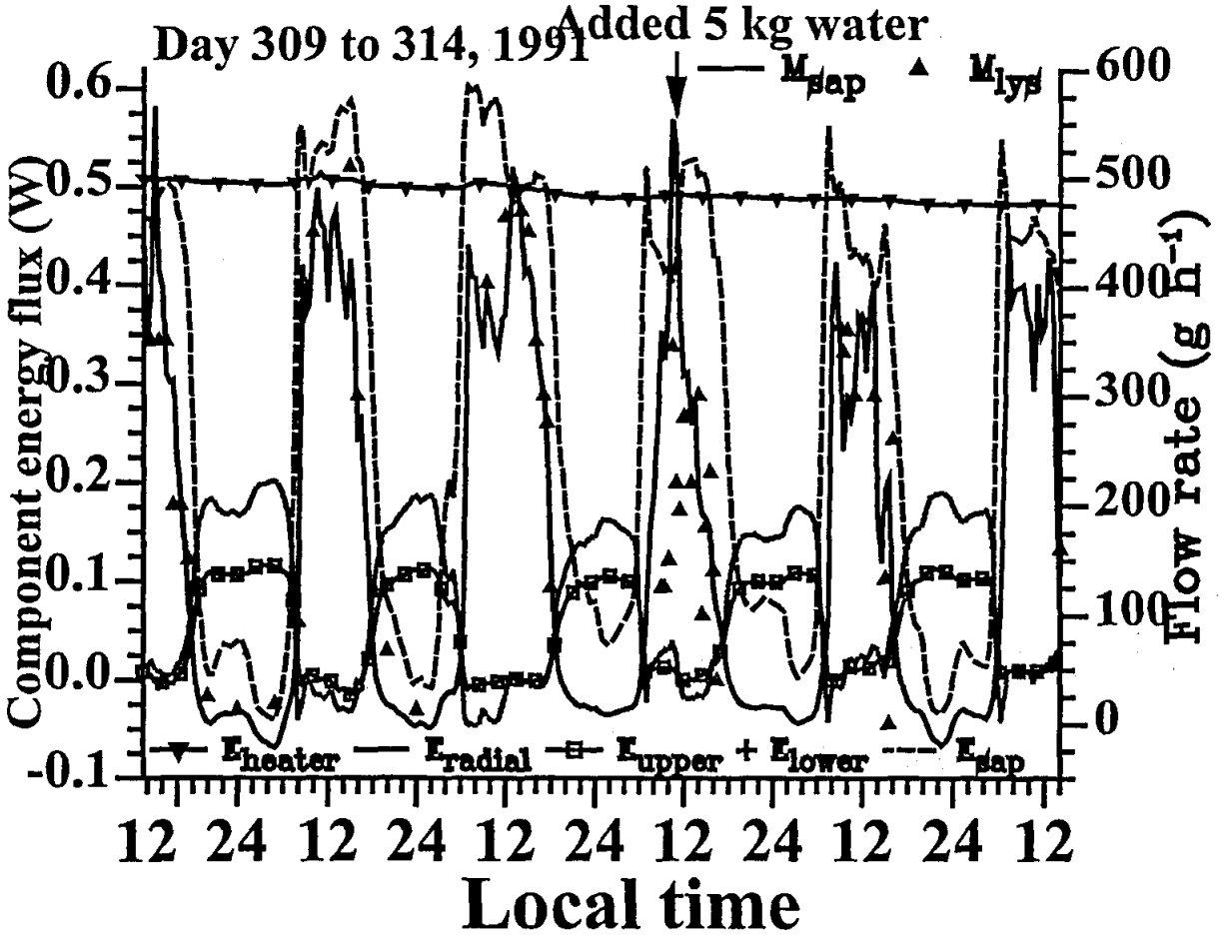

Fig. 4.14 The diurnal variation in energy balance components (W), left hand y-axis and the mass flow rates (g h^{-1}), right hand y-axis as measured using a lysimeter M_{lys} and M_{sap} measured using a SSS 25 mm gauge (SGB25-ws) for Days 309 to 314, 1991. On Day 312 (the third of the three daily time courses), high wind speeds resulted in variable lysimeter flow rates M_{lys}. These M_{sap} are associated with a gauge conductance of 1.565 W mV^{-1} (equivalent to 0.0626 W K^{-1}) and a stem thermal conductivity K_{stem} of 0.54 W m^{-1} K^{-1}

was calculated as 0.1866 m^2, while the area of the leaves was measured as 0.1379 m^2 using the leaf area meter.

A comparison of the area as measured by the leaf area meter (independent axis) against the product of the length and breadth (dependent axis) for the 62 leaves, resulted in a very strong correlation (data not shown). The regression, with a forced zero intercept, resulted in an r-value of 0.998. A slope of 1.36 was calculated by dividing the product of length and breadth by the measured leaf area. The total leaf area of the tree was then calculated as 1.5719 m^2 by dividing the product of the length and breadth of all the leaves (1042 leaves) on the tree (2.1378 m^2) by the slope constant of 1.36.

The soil surface area of the drum was measured to be 0.4608 m^2. The total leaf area was then divided by the soil surface area to calculate a leaf area index (LAI) of 3.4135. The latent heat energy flux density of the sap (W m^{-2}) was calculated at half-hourly intervals for Days 310 to 312, 1991, using the measured sap flux and the leaf area index. The total latent heat energy density for Day 311, 1991 was calculated by summing the individual latent heat flux density values (Day 310) to midnight (Day 311) and multiplying the result by the increment of time (30 min = 1800 s). Hence the total latent heat

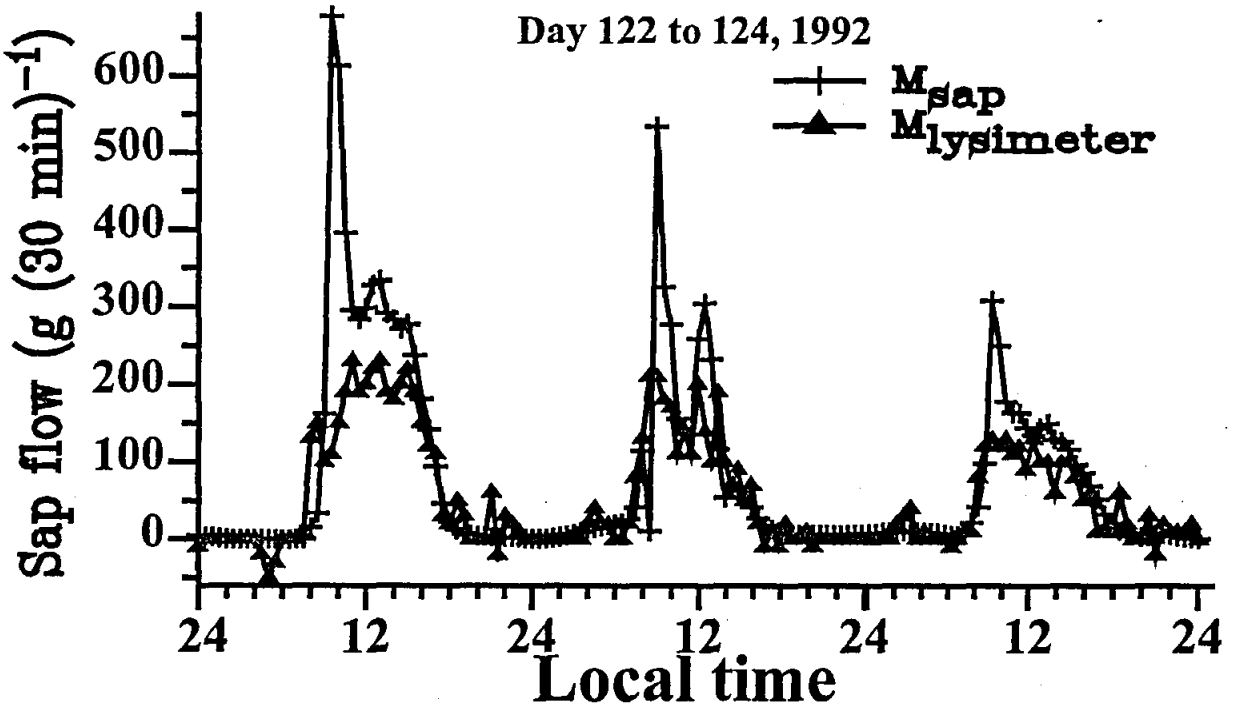

Fig. 4.15 Comparison of sap flow rates (g/30 min) in a 26-month old Eucalyptus tree using the SSSHEB and lysimetric techniques for Days 122 to 124, 1992. The average heater voltage was 4.25 V

energy density for Day 311, 1991, was calculated to be 14.66 MJ m^{-2}. The Class A-pan evaporation was measured as 11.4 mm for Day 311, 1991. Therefore the total latent energy density for the Class A-pan for the day was calculated as 27.70 MJ m^{-2} by multiplying the evaporation by the specific latent heat of vaporization Lv and the density of the sap (1000 kg m^{-3}). As was to be expected, since the Class A-pan represents potential evaporation, the total gauge latent energy density (14.66 MJ m^{-2}) was calculated to be less than the Class A-pan latent energy density (27.70 MJ m^{-2}) for Day 311, 1991. The ratio of plant latent heat density to class-A pan latent heat density was 0.53. The main disadvantage of the procedures described here is that the tree leaf area index is required. However, it is possible to make similar calculation from tree population density (- see Chapter 5 (Eq. 5.1) for more details of this application). It would be expected that the ratio we have calculated is temporarily and spatially dependent and influenced by tree stress and condition.

4.6.2.9 Tree response by shading a branch using sap flow measurements

Plants must contend with fluctuations in solar irradiance caused by partly cloudy skies and shading from adjacent plants and buildings. To accurately measure water use in landscapes, using the stem steady state heat energy balance technique, the gauges must quickly respond to large changes in transpiration produced by a dynamic environment. Hinckley (1971) reported that sap flow can lag behind transpiration by as much as 15 to 45 min in Douglas-fir. If it can be assumed that there is only a brief lag at high flow rates for small *E. grandis* trees, then by shading a portion of the tree, the response of the tree to a change in leaf area can be calculated. When the shading occurs, it will take the SSS gauge a short period to respond to the decrease in transpiration depending on the response of the tree to a change in the leaf area. The same should apply when the shading is removed.

When determining the response of a tree to changes in solar irradiance due to shading, it is important to take into consideration which side of the tree is to be shaded. Steinberg *et al.* (1990a)

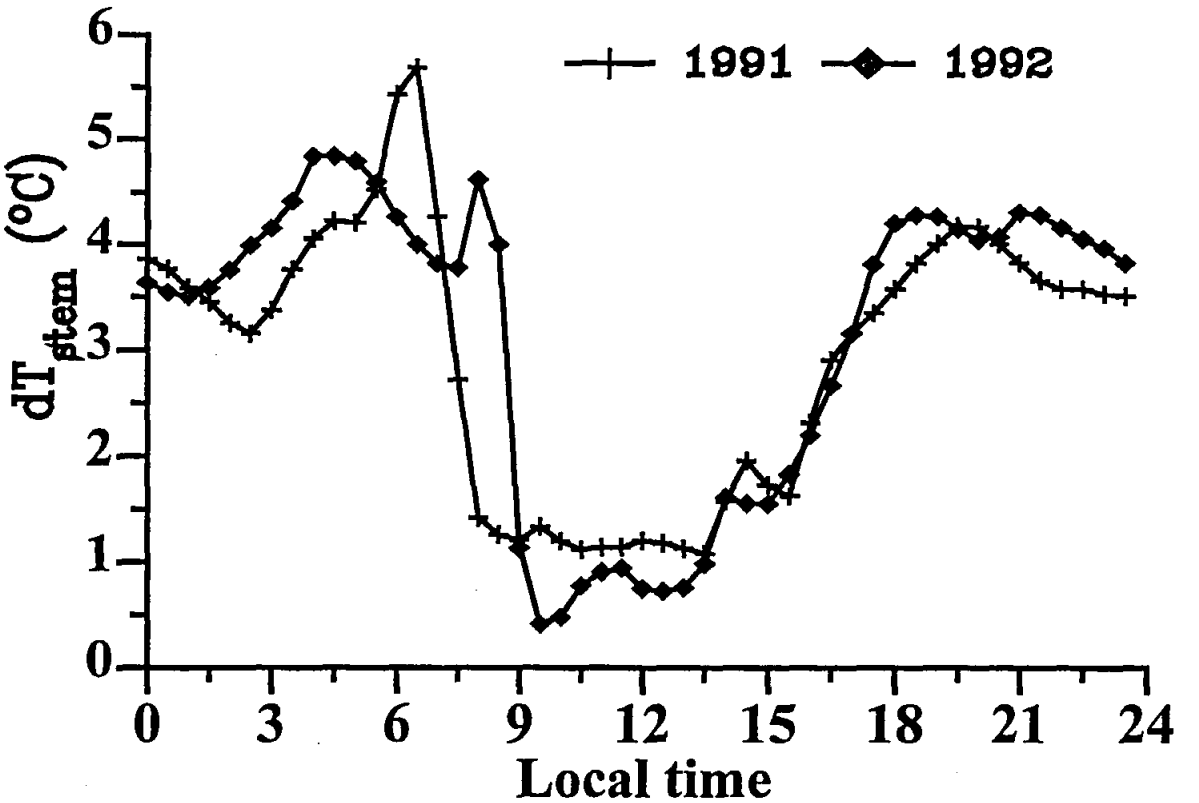

Fig. 4.16 Comparison of the stem temperature differentials (°C) measured using the SSS technique for 1991 (average heater voltage = 4.46 V) and 1992 (average heater voltage = 4.25 V). Each point is an average for the three days for the respective years shown in Fig. 4.15

Table 4.5 The voltage supplied to the SSS heaters, the heat energy flux and dT_{stem} are each an average of three data points for each half hour (Days 310 to 312 for 1991, and Days 122 to 124 for 1992) between 09h30 and 13h30

Local time	April 92			Nov 91		
	V_{heater} (V)	E_{heater} (W)	dT_{stem} (°C)	V_{heater} (V)	E_{heater} (W)	dT_{stem} (°C)
930	4.248	0.450	0.414	4.449	0.495	1.337
1000	4.246	0.450	1.337	4.450	0.495	1.197
1030	4.243	0.449	0.782	4.449	0.495	1.123
1100	4.243	0.449	0.908	4.447	0.494	1.140
1130	4.241	0.449	0.945	4.447	0.494	1.145
1200	4.239	0.448	0.755	4.446	0.494	1.205
1230	4.232	0.447	0.726	4.442	0.493	1.179
1300	4.228	0.446	0.761	4.439	0.492	1.130
1330	4.230	0.446	0.988	4.438	0.492	1.082

found that sap flux in the southern branches of a pecan tree was 41 % higher than in the northern branches of the same diameter, caused by the difference in exposure to radiation. Examples of different water use rates between irradiated and shaded branches within a tree canopy have been documented elsewhere. Daum (1967) cited a case where sap flow direction was reversed in a shaded branch, to supply the irradiated crown. Furthermore, the cumulative sap flow pattern in the trunk resembled that in a sunlit branch (Steinberg *et al.*, 1990a). These findings demonstrate that the xylem flux rate in the main trunk is driven primarily by the steepest potential gradient between soil and leaf.

A SGB25-ws gauge was attached to the stem of the same *E. grandis* tree using procedures described in Section 4.4. However, sap flux measurements were obtained every two minutes for a sunny cloudless day. At 10h40 on Day 345, 1991, a large white polythene bag enclosed two branches (approximately 10 % of the tree) on the south side of the tree so that it was air-tight. At 11h29 the bag was removed so that the entire tree was exposed. The shaded branches were 600 mm above the upper thermocouple of the gauge.

When the polythene bag was placed over the two branches at 10h40, the sap flux immediately decreased from 675 g/15 min to 545 g/15 min (**Fig. 4.17**). The tree continued transpiring but at a decreasing rate until 10h54. The shading was removed at 11h30 and the tree, as measured by the gauge, required two minutes before it responded by showing an increase in the measured sap flow rate (Fig. 4.20). The suprising aspect of this experiment is the speed at which the sap flow decreased after shading given that the shaded branches were above the upper thermocouple of the gauge!

At high flow rates of say 675 g/15 min, the SGB25-ws gauge therefore measured a very quick response of the tree to a change in the incident solar irradiance. Due to the sudden response of the measured sap flux to the shading, one may conclude that tree capacitance does not affect M_{sap}, especially at high flow rates.

When a portion of the tree was shaded from the incident solar irradiance, there was an immediate decrease in sap flow rate implying a rapid response to physiological events. When the shading was removed, the sap flow almost immediately increased. In conclusion therefore, tree water capacitance does not affect the measurement of M_{sap} at high flow rates.

4.6.2.10 Artificial verification of stem gauges

Experimentation with an artificial system to test the functionality and precision of Dynamax-SGB19 (diameter of 19 mm) gauges on *Eucalyptus* stems was conducted (acknowledgments to Professor Norman Pammenter, University of Natal, Durban). A system was used where water was supplied under pressure (0 to 250 kPa) to an excised stem segment with a Dynamax-SGB19 gauge fitted. The flow rate was monitored gravimetrically using a precision mass balance. After excision, the stem sections were coated with silicon grease and wrapped in plastic film sheeting to prevent water loss while in transit to the laboratory. The stem ends were recut and joined to water filled transparent plastic tubing, submerged in water. Pressure was applied to the column of water feeding the one end of the excised stem using both a natural water pressure head and a gas controlled pressure chamber. The system used was limited to use on stems with diameters less than 25 mm.

Gauge component voltages were monitored using a Campbell Scientific 21X datalogger, and sap flow rates determined subsequently. Gravimetric sap flow rate did not compare well with that measured by the SSS technique. This was attributed to the use of an incorrect value for K_{gauge}, the constant used in determining the techniques radial heat flux component, E_{radial}; and the influence of

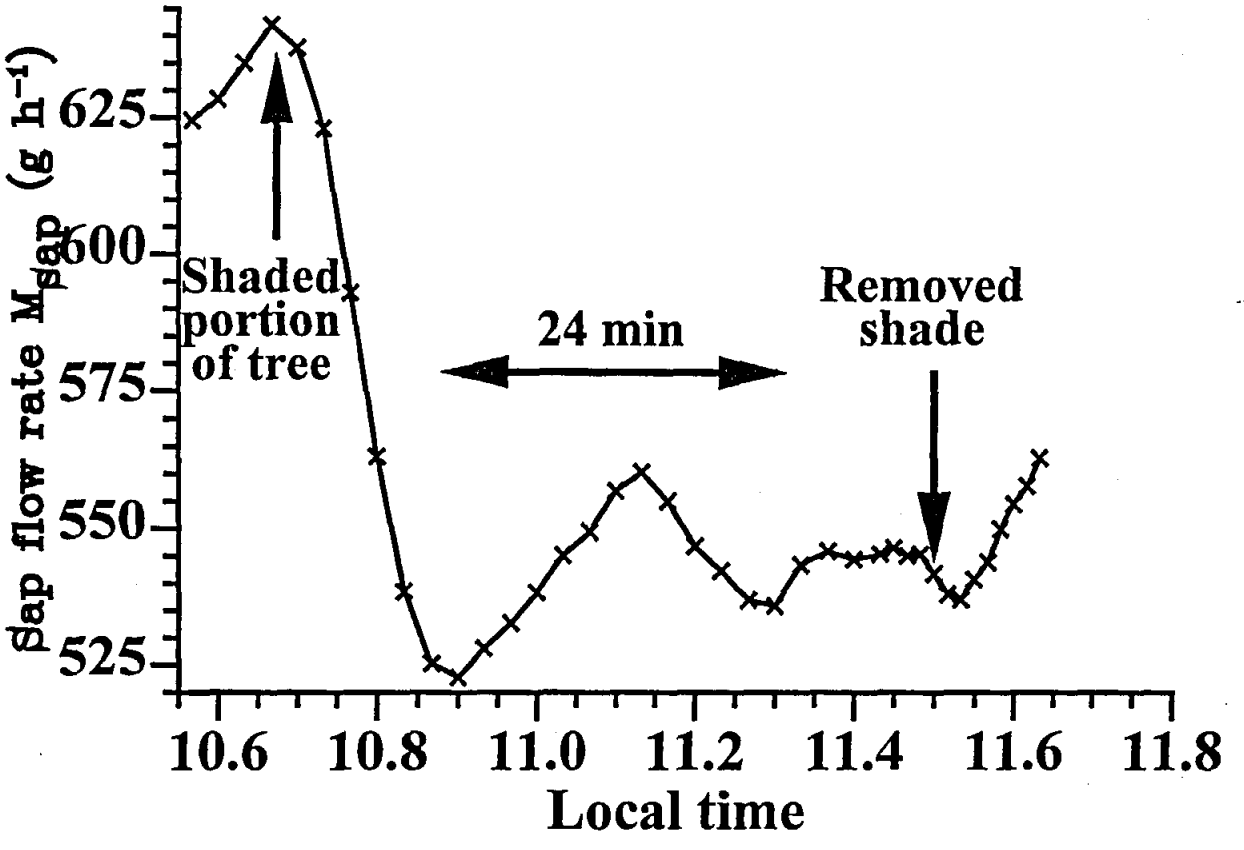

Fig. 4.17 The effect of shading a portion of the tree immediately decreases the sap flux indicating rapid response to physiological events and little effect of tree stem conductance on sap flow measurements. About 10 % of the total tree leaf area (two branches) was shaded (that is, totally enclosed) with plastic for 50 min. The area shaded was about 0.6 m above the upper thermocouple of the stem flow gauge. The tree was shaded and then unshaded 50 minutes later (Day 345, 1991)

interfering naturally occurring temperature gradients in the system. It was concluded that K_{gauge} most likely changes with power (J s^{-1}) supplied to the gauge heater. From this cursory investigation, it was evident that: (i) experimentation to determine the influence of naturally occurring temperature gradients upon sap flow rate detection, and (ii) the determination of possible relationships between power supply to the gauge heater and K_{gauge}, for gauges of different size and insulating material, was necessary before full verification of the SSS technique was possible using this methodology.

4.6.2.11 Effect of heater voltage V_{heater} on gauge conductance K_{gauge} using SGB-100ws gauges

To investigate the influence of different measured voltages across the gauge heater on K_{gauge}, two excised sections (110 mm diameter) of a *E. grandis* tree stem were each fitted with a Dynamax SGB-100ws gauge, and K_{gauge} determined, using a Campbell Scientific CR7X data logger, while the voltage across the heater was stepped every three hours (**Table 4.6**). Four of the switched mode power supply units were wired in parallel to effect the switching. These were powered by a constant power supply regulator operating from mains power. The gauges were wrapped in an extra layer (approximately 30 mm thick) of foam insulation. The excised stem sections with the gauges installed were sealed in plastic to prevent water loss from the stems. Data was collected at intervals of 10 minutes over a period of three days for three different voltage setting regimes (Table 4.6).

Table 4.6 Voltage applied across gauge heater over different time intervals, using the switched mode power supply

Local time	0 to 3	3 to 6	6 to 9	9 to 12	12 to 15	15 to 18	18 to 21	21 to 24
Regime 1	6.5	10.0	6.0	9.5	5.5	8.5	7.5	7.5
Regime 2	4.5	9.0	4.0	8.0	3.5	7.0	6.0	6.0
Regime 3	9.0	9.0	8.0	8.0	7.0	7.0	6.0	6.0

At a voltage step time interval of 3 hours (regime 1 and regime 2 in Table 4.7), K_{gauge} tended to increase linearly with voltage supplied across the gauge heater **(Fig. 4.18)**. However it is evident from the data that the time to achieve steady state thermal equilibrium i.e. gauge transient response time, upon changing the heater voltage is longer than 3 hours. It is also apparent that this time changes with change in voltage upon switching. By extending the voltage step time interval to 6 hours and reducing the magnitude of the voltage change between steps (regime 3 in Table 4.6), steady state thermal equilibrium was achieved and a linear relationship between gauge heater voltage and K_{gauge} identified. Using the linear model: $Y = mX + c$, a slope (m) of 0.00132 was obtained for the relationship between the independent variable, applied heater voltage (mV), and the dependent variable, K_{gauge} (W mV^{-1}), for both of the gauges tested. The constant (c) differed however for each of the gauges, ranging from -1.9 to -1.75 (Fig. 4.18).

From these results one can conclude that for the large Dynamax SGB-100ws sap flow gauges, a reduction in the power supplied to the gauge heater may require up to six hours before steady state thermal equilibrium is achieved, the duration of this period being influenced by the magnitude of the voltage change. Further, different magnitudes in power supplied to the gauge require the use of different K_{gauge} values for the determination of E_{radial}. By applying the linear model presented above, these results also provide a basis to facilitate a modification of K_{gauge} with changes in source voltage. Changes in battery voltage are a frequent occurrence as batteries become progressively discharged. Also, there could be changes in gauge heater resistance due to the application of voltage to the heater or due to changes in the environmental temperature.

4.6.3 The influence and measurement of naturally occurring vertical temperature gradients on stem steady state heat energy balance flow rates

The stem heat energy balance technique (Fig. 3.1) relies upon applying continuous heat energy, under steady state conditions, to a section of the stem of a plant over a vertical distance. The technique does not involve the implanting of sensors into the stem but rather has sensors in contact with the stem. A heater completely surrounding the stem, is used as the source of continuous heat energy. In order to attain the steady state condition, it is usually necessary to insulate a portion of the stem and the sensors from external heating or cooling, usually solar irradiance and wind effects, as well as removing the possibility of water entering the stem with possible corrosion of the sensors. The heat energy flux (J s^{-1} = W) supplied by the heater (E_{heater}) must be accounted for according to the conservation of energy. We assume that the components of heat energy flux are as follows: heat energy flux may be conducted radially outward (E_{radial}), conducted vertically upward through the stem (E_{upper}), conducted vertically downward through the stem (E_{lower}), and may be convected with the vertical ascent of sap flow (E_{sap}) (Fig. 3.1) and that no other energy terms are involved. Hence

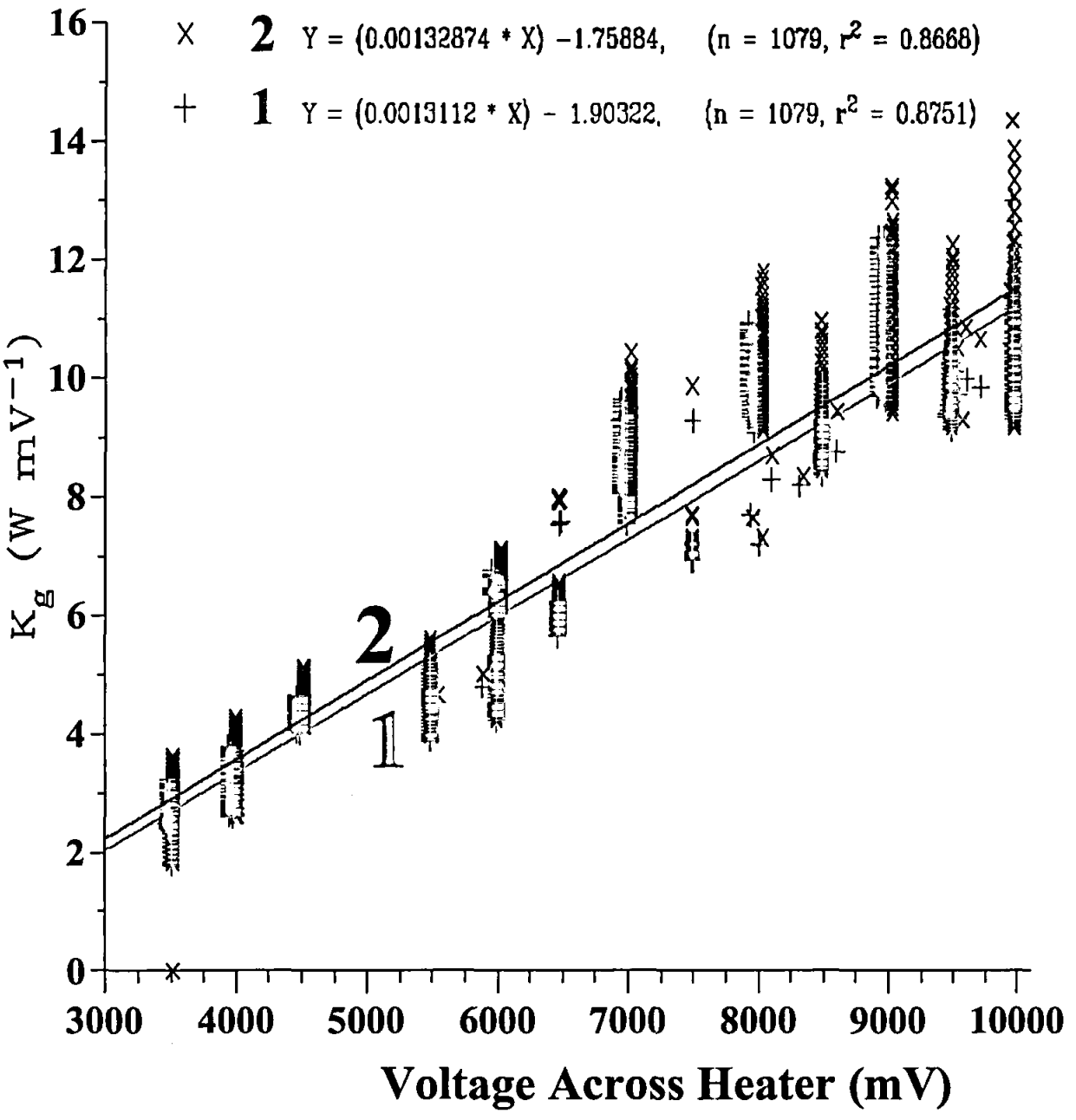

Fig. 4.18 Relationship between gauge conductance as a function of voltage applied to heater for two stem gauges

$$E_{heater} = E_{radial} + E_{upper} + E_{lower} + E_{sap}$$

If each of these terms, except E_{sap}, can be calculated, one has a method for calculating E_{sap} *in situ*.

The energy flux transported by sap flow (W) is assumed to be given by:

$$E_{sap} = M_{sap}\, dT_{stem}\, c_p$$

where M_{sap} is the mass flux of sap (kg s^{-1}), dT_{stem} is the measured stem temperature difference (obtained by measuring the temperature difference between two vertical point pairs above and below the heater, Fig. 3.1) and c_p is the specific heat capacity of water (J kg^{-1} K^{-1}). The temperature increase dT_{stem} of the stem is calculated by averaging the temperature differences $T_{upper\,1} - T_{lower\,1}$ and $T_{upper\,2} - T_{lower\,2}$ denoted $T_{u1} - T_{l1}$ and $T_{u2} - T_{l2}$ (Fig. 3.1):

$$dT_{stem} = [(T_{u1} - T_{l1}) + (T_{u2} - T_{l2})]/2.$$

Suppose that h is the distance between the top thermocouple of the upper pair and the top thermocouple of the lower pair shown (Fig. 3.1). The theoretical development of the stem steady state heat energy balance technique requires the determination of stem temperature gradients created by the application of heat to the stem by a heater that completely surrounds the stem. For the calculation of the energy flux terms conducted above and below the heater (E_{upper} and E_{lower} shown in Fig. 3.1), the stem temperature gradient is:

$$(dT_{upper}/dz) + (dT_{lower}/dz) = [(T_{u1}-T_{l1})/dz] - [(T_{u2}-T_{l2})/dz]$$

If the gauge heater alone creates vertical temperature gradients in the stem, we have:

$$dT_{stem} = [(T_{u2} - T_{l2}) + (T_{u1} - T_{l1})]/2$$

where T_{u1}, T_{u2}, T_{l1} and T_{l2} are the temperatures, measured in the absence of a naturally occurring temperature gradient, at the upper positions $u1$ and $u2$, and at the lower positions $l1$ and $l2$ respectively.

If there is a naturally occurring vertical temperature gradient γ (°C m^{-1}) (that is, this gradient would occur even if there were no heat supplied from the heater), then the measured stem temperature differential $T_{u2} - T_{l2}$ and $T_{u1} - T_{l1}$ have the temperature difference γh included in their measurement. Since γh is not due to the application of heat from the heater, it needs to be subtracted from the $T_{u2} - T_{l2}$ and $T_{u1} - T_{l1}$ measurements. Hence, the actual dT_{stem} term is given by:

$$dT_{stem} = [(T_{u2} - T_{l2} - \gamma h) + (T_{u1} - T_{l1} - \gamma h)]/2$$

$$\text{or } dT_{stem} = [(T_{u2} - T_{l2}) + (T_{u1} - T_{l1}) - 2\gamma h]/2. \qquad 4.10$$

The naturally occurring vertical temperature gradient γ (°C m^{-1}) would not affect the determination of $E_{upper} + E_{lower}$ (Fig. 3.1) since they cancel:

$$(dT_{upper}/dz) + (dT_{lower}/dz) = [(T_{u1}-T_{l1} - \gamma h)/dz] - [(T_{u2}-T_{l2} - \gamma h)/dz]$$

$$= [(T_{u1}-T_{l1})/dz] - [(T_{u2}-T_{l2})/dz].$$

What are the options for reducing the error?

(a) One could decrease the vertical distance h. There may be other problems with this option as if the distance h is decreased, the temperature differences would be smaller and more difficult to measure with accuracy.

(b) One could attempt to reduce the magnitude of γ using extra insulation. Usually extra insulation is required anyway. For larger gauges (greater than 30 mm in diameter), even more insulation would be required. However in view of the discussion on E_{radial} *via* K_{gauge} (Section 4.6.2.6 and Fig. 4.13), the amount of insulation used should always be standardized.

(c) One could increase the power to the heater to increase the temperature differences $(T_{u2} - T_{l2})$ and $(T_{u1} - T_{l1})$ in comparison to the temperature γh. Switching off the heater at night and at times when the flow rate is low therefore becomes even more important. However, we showed (Section 4.6.2.11) that about 4 h is required for steady state condition be achieved.

(d) One could make sure that the gauge is always about 0.5 m above ground. Presumably the naturally occurring temperature gradient would be greater close to ground than that at 0.5 m above

ground where the flow of air around the stem would dissipate naturally occurring temperature gradients.

(e) In view of these problems, it is essential that there is good contact between the sensing thermocouples and the stem of the tree.

(f) One could measure γh in the absence of heat supplied to the heater and attempt to correct the heated gauge temperature differentials according to:

$$dT_{stem} = [(T_{u2} - T_{l2}) + (T_{u1} - T_{l1}) - 2\gamma h]/2$$

Switching on and off the power would have to be performed on different days if only one gauge is available. Alternatively, an unheated gauge could be attached to the stem and below that of a heated gauge. It is more important that, at the least, the naturally occurring temperature gradient be measured in the early hours of the morning (sunrise to say 11h00) as it is during this period when these gradients are likely to be significant compared to the measured stem temperature gradient dT_{stem} for a heated gauge.

(g) The use of gauges in artificial environments where a large vertical gradient in the absence of heat from the heater can be created should be avoided.

4.6.3.1 Analysis for naturally occurring vertical temperature gradient γ

The analysis here assumes that there is a diurnally varying naturally occurring temperature gradient γh measured within the gauge with no power connected to the heater. Fitting a cubic relationship to the data of Shackel *et al.* (1992, Fig. 5 top), yields the relationship:

$$\gamma h = [(\text{SAST} - 15.222)/7.333]^3$$

in the absence of any heat supplied by the heater. Since Shackel *et al.* (1992) used a 50 mm diameter gauge with a top and bottom thermocouple distance of 160 mm compared to 60 mm for the 25 mm gauge, their stem gradients are multiplied by 60/160 = 0.375 and this result added to the measured dT_{stem} values to yield:

$$dT_{stem} = [(T_{u2} - T_{l2}) + (T_{u1} - T_{l1}) - 2\gamma h]/2 \text{ where:}$$

$$\gamma h = (60/160)\cdot[(SAST - 15.222)/7.333]^3$$

where $SAST$ is the South African Standard Time and

$$[(SAST - 15.222)/7.333]^3$$

is the dT_{stem} temperature gradient measured by Shackel *et al.* (1992) for a 50 mm diameter gauge with a 160-mm thermocouple distance between upper and lower thermocouples.

Between the times 23h00 and 08h00, we assumed that the naturally occurring stem temperature gradient was 0.40 °C for a 50 mm gauge. Converting this value to that for a 25 mm gauge, we used a stem temperature gradient of 0.15 °C for the 50 mm gauge between 23h00 and 08h00.

The calculated M_{sap} values were corrected for the naturally occurring stem temperature gradients, as a function of time of day, for *E. grandis* measurements. The data shown include a column for the environmental γh values of Shackel *et al.* (1992), the environmental γh values corrected for the 25 mm gauge (used for the *E. grandis* measurements). These data are depicted in **Figs 4.19 to 4.23**. The

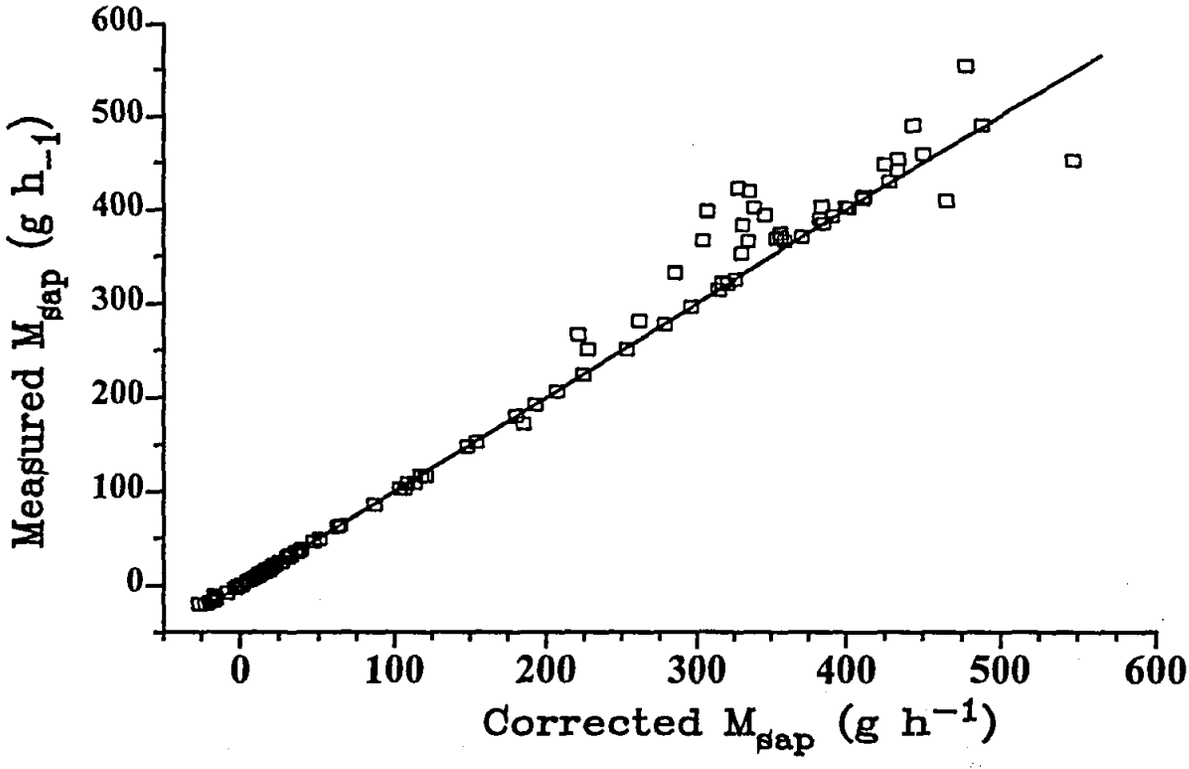

Fig. 4.19 The corrected M_{sap} as a function of the uncorrected (measured) M_{sap} values for *E. grandis* using a 25 mm gauge. The solid line is the 1:1 line

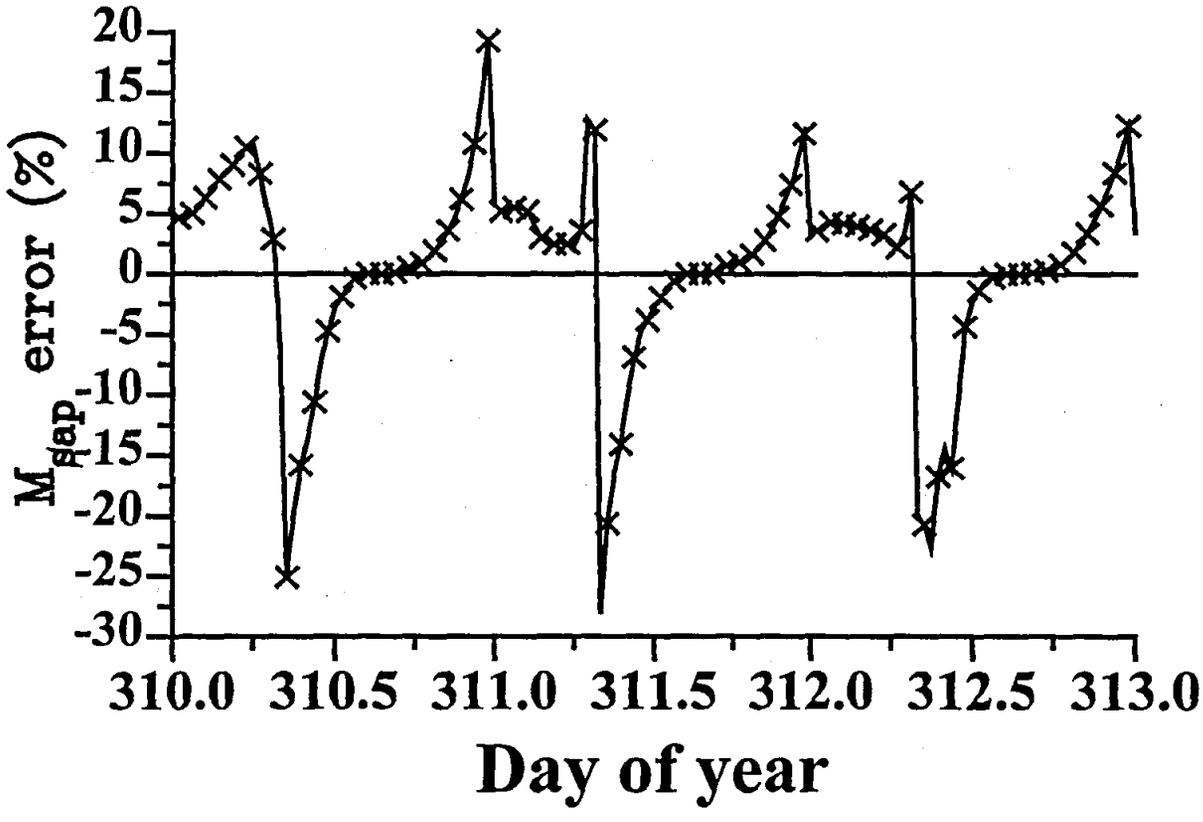

Fig. 4.20 The error in the measured M_{sap} values, $100 \times (M_{sap\ corrected} - M_{sap\ measured})/M_{sap\ corrected}$, relative to the corrected values, as a function of time of day for 5 to 10 November 1991

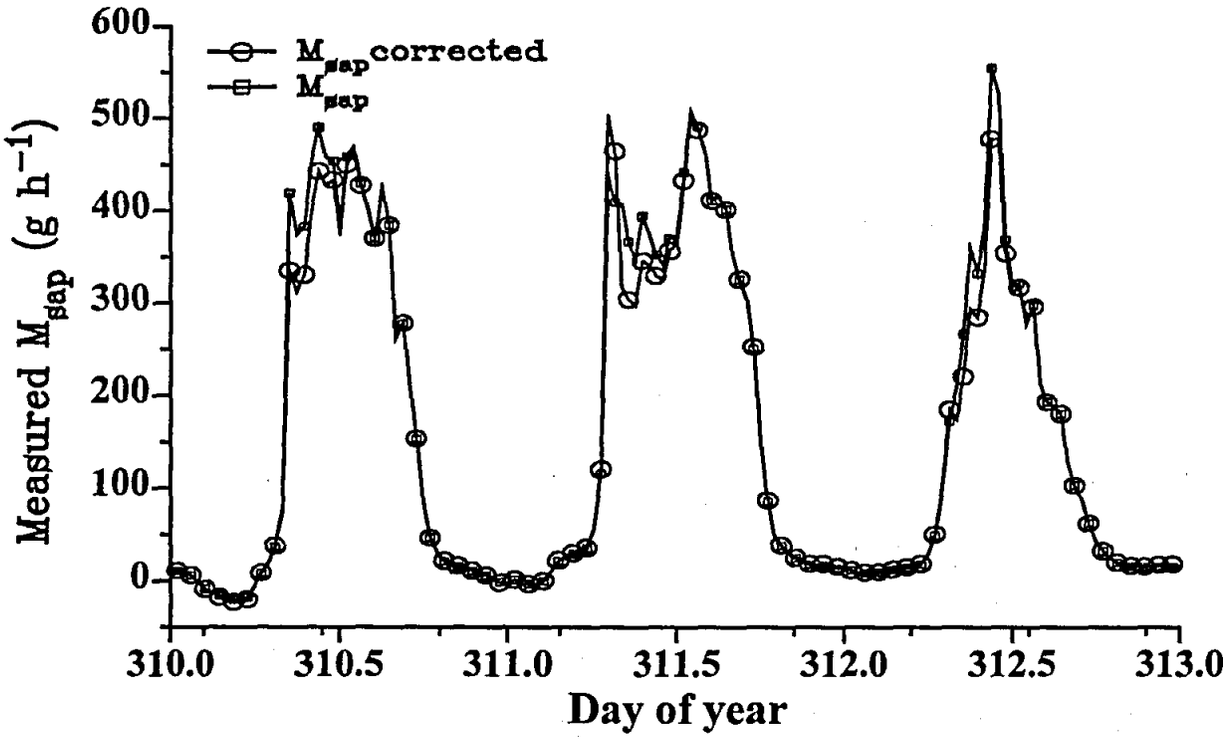

Fig. 4.21 Diurnal variation in measured and corrected M_{sap} values (left-hand y-axis). Corrected values were calculated by measuring naturally occurring stem temperature differences ΔT_{stem} in an unheated gauge and then offsetting these values from the measured vertical temperatures dT_{stem} with power supplied to the heater. The diurnal variation in the measured and corrected M_{sap} values is for 6 to 8 November 1991

errors shown in Fig. 4.25 show large negative errors in M_{sap} (corresponding to an overestimation in M_{sap} by the gauge) before 11h30 when the sap flow is increasing with the errors then becoming increasingly positive. The error values should be regarded with caution as stem temperature gradients in the gauge were taken from Shackel *et al.* (1992) and are not those measured for *E. grandis*. At night, the large errors are often of no consequence since M_{sap} is small (Fig. 4.23). If the data were integrated for a complete day, the overestimation in M_{sap} before noon would not cancel with the underestimation after noon.

It appears then that the errors can be corrected and are certainly much smaller than anticipated by Shackel *et al.* for the gauges we used (25 mm diameter). The errors are largest under conditions of high flow rates in the early morning to before noon hours. It remains to be seen (Section 4.6.3.2) what the γh temperature difference value, the actual temperature difference in the stem in the absence of heating, are for our measurements using *E. grandis*.

4.6.3.2 Measured naturally occurring temperature gradients using Dynamax-SGB100 (100 mm diameter) and SGB25 (25 mm) gauges

Two Dynamax-SGB100 gauges were attached to the same tree (stem diameter of 100 mm) in order to compare the rate of sap flow measured by gauges placed at different heights in the tree. The experiment was conducted at Bloemendal near Pietermaritzburg. One gauge (Gauge #2) was installed approximately 1 m above ground level and the other (Gauge #1) at a height of approximately 4 m above ground level. Both gauges were wrapped in an extra layer (approximately 30 mm) of insulating material. Gauge component voltages were monitored every 10 minutes, for five days using a Campbell

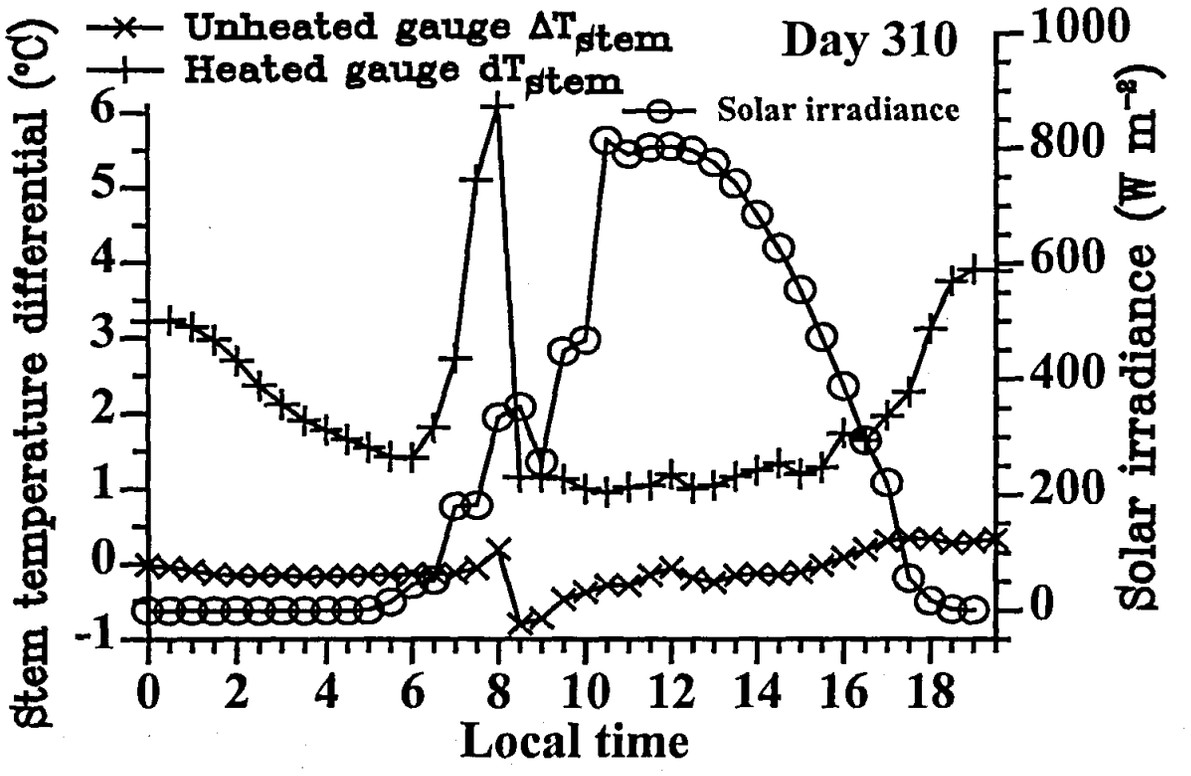

Fig. 4.22 The diurnally varying vertical stem temperature differential ΔT_{stem} for an unheated stem 25-mm gauge. Vertical temperature differentials occur due to natural conduction of heat from soil to plant stem. A negative temperature differential is due to a relatively warmer region at the lower thermocouple compared to the upper region. The ΔT_{stem} value offsets dT_{stem} in calculating M_{sap} (Eq. 4.17). The curves represent the average diurnal curves for a period of a week for three gauges

Scientific CR7X datalogger. The gauge conductance K_{gauge} was modified according to the power supplied to the gauge's heater. Sap flow rates detected by each gauge compared poorly. The upper gauge consistently overestimated sap flow rate relative to the lower one during the day. Speculatively, this could be attributed to a difference in dT_{stem} between the gauges or differences in the naturally occurring temperature gradients between the two positions.

To investigate the influence of naturally occurring stem temperature gradients, an extra gauge (Gauge # 3) was placed below the lower gauge (gauge #2). The heaters to gauges #1 and #3 were switched off. The data indicates that naturally occurring stem temperature gradients potentially influence dT_{stem} more in positions higher up the stem during the day than lower down, and *vice versa* during the night. Typically, day-time temperature gradients were in an up tree direction, from the soil to the tree canopy, and from the inside to the outside of the gauge. Night-time gradients were in the opposite directions.

Typical data for stem and root naturally occurring gradients are presented (**Figs 4.24 and 4.25**). Of note is the larger naturally occurring gradients for stems (Fig. 4.24) than for roots (Fig. 4.25) although in the case shown, the 100 mm diameter gauges were used on the stems and the 25 mm diameter gauges were used on the roots in this experiment conducted in Pietermaritzburg. It is clear then that dT_{stem} measurements need to be corrected. It may be possible to apply these corrections without the need for a second (unheated) gauge on the same stem.

Naturally occurring stem temperature gradients are likely to result in a day-time overestimation and

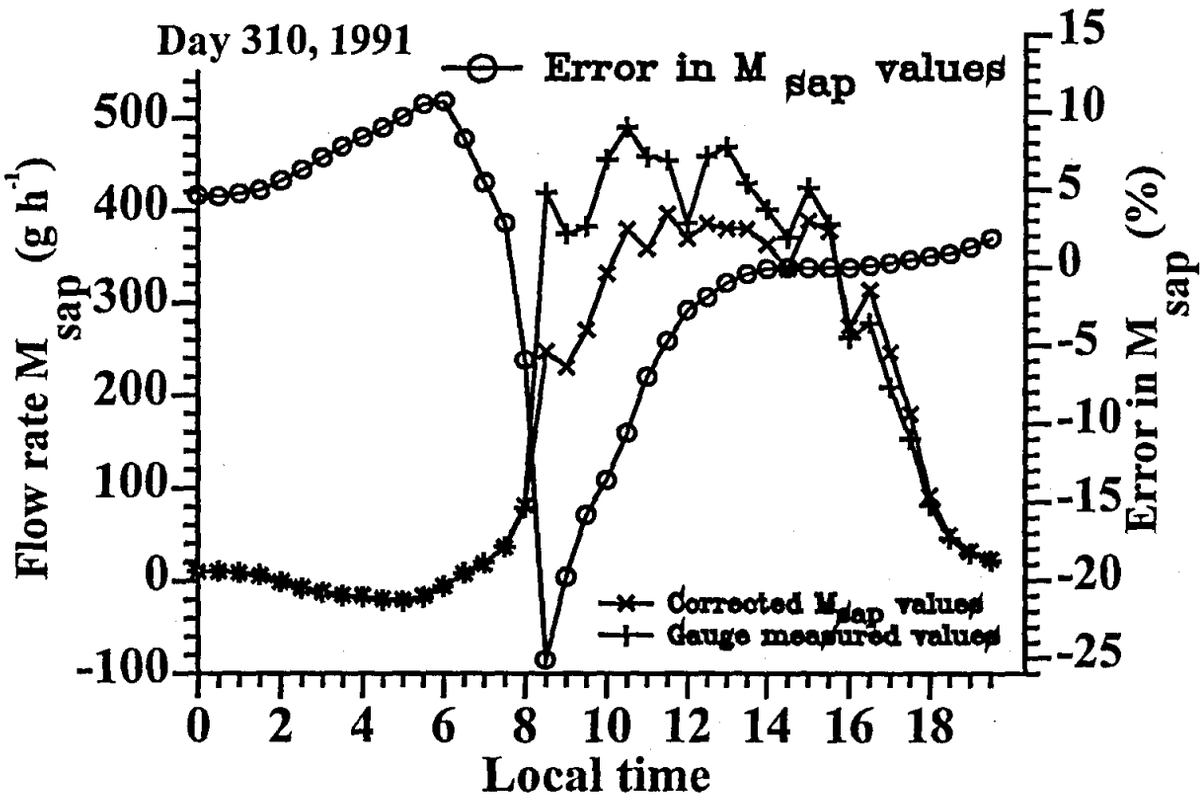

Fig. 4.23 Diurnal variation in measured and corrected M_{sap} values (left-hand y-axis) for 25-mm gauges. Corrected values were calculated by measuring naturally occurring stem temperature differences ΔT_{stem} in an unheated gauge and then offsetting these values from the measured vertical temperatures dT_{stem} with power supplied to the heater. Also shown (right-hand y-axis is the diurnal variation in the error in M_{sap}

a night-time underestimation of sap flow rate by the SSS technique, due to an underestimation of dT_{stem} during the day and an overestimation of dT_{stem} at night. Naturally occurring stem temperature gradients measured by gauges #1 and #3 followed a diurnal pattern. The difference (%) between dT_{stem} (gauge #2) before and after compensation for temperature gradients measured by gauges #1 and #3 peaked at 30 % during the day and night respectively. The potential therefore exists to extend the gauge design to measure naturally occurring temperature gradients for adjustment of dT_{stem}.

SAST in decimal hours	Shackel's γh (for 50 mm diameter gauges)	Shackel's γh corrected for 25 mm gauges)	Measured dT_{stem}	Corrected dT_{stem} ($dT_{stem} - \gamma h$)	Old M_{sap} value	M_{sap} corrected for γh	Error (%)
Day 310: 6 November 1991							
0.0	0.40	0.15	3.22	3.07	10.4	10.9	4.7
0.5	0.40	0.15	3.24	3.09	10.8	11.3	4.6
1.0	0.40	0.15	3.15	3.00	9.1	9.6	4.8
1.5	0.40	0.15	2.98	2.83	6.3	6.6	5.0
2.0	0.40	0.15	2.70	2.55	-0.6	-0.6	5.6
2.5	0.40	0.15	2.37	2.22	-7.7	-8.3	6.3
3.0	0.40	0.15	2.12	1.97	-12.5	-13.4	7.1
3.5	0.40	0.15	1.91	1.76	-15.8	-17.1	7.8

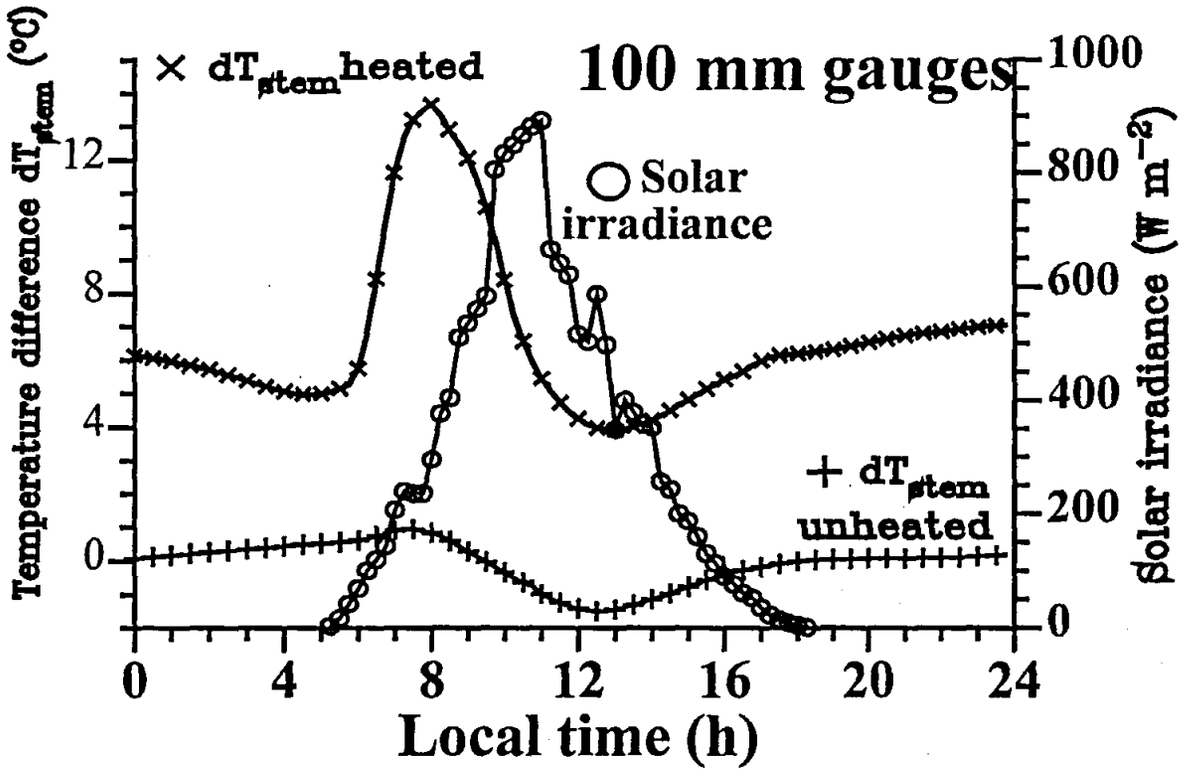

Fig. 4.24 The diurnal variation in dT_{stem} for an unheated gauge and a heated gauge (100 mm diameter) applied to the stem of three *E. grandis* trees in September in Pietermaritzburg.. Also shown (right-hand y-axis) is the solar irradiance. The curves represent the average diurnal curves for a period of a week for three gauges

SAST in decimal hours	Shackel's γh (for 50 mm diameter gauges)	Shackel's γh corrected for 25 mm gauges)	Measured dT_{stem}	Corrected dT_{stem} $(dT_{stem} - \gamma h)$	Old M_{sap} value	M_{sap} corrected for γh	Error (%)
4.0	0.40	0.15	1.78	1.63	-17.1	-18.6	8.4
4.5	0.40	0.15	1.66	1.51	-20.3	-22.4	9.0
5.0	0.40	0.15	1.55	1.40	-21.8	-24.1	9.7
5.5	0.40	0.15	1.43	1.28	-17.5	-19.6	10.5
6.0	0.40	0.15	1.41	1.26	-5.9	-6.6	10.7
6.5	0.40	0.15	1.81	1.66	8.5	9.3	8.3
7.0	0.40	0.15	2.72	2.57	19.7	20.8	5.5
7.5	0.40	0.15	5.10	4.95	36.8	38.0	2.9
8.0	-0.96	-0.36	6.08	6.44	79.1	74.7	-5.9
8.5	-0.77	-0.29	1.15	1.44	419.2	335.0	-25.1
9.0	-0.61	-0.23	1.16	1.39	374.7	312.7	-19.8
9.5	-0.48	-0.18	1.13	1.31	382.7	330.4	-15.8
10.0	-0.36	-0.14	1.00	1.13	455.0	400.6	-13.6
10.5	-0.27	-0.10	0.95	1.05	489.8	442.9	-10.6
11.0	-0.19	-0.07	1.02	1.09	458.0	427.9	-7.0
11.5	-0.13	-0.05	1.04	1.08	453.9	433.3	-4.7
12.0	-0.08	-0.03	1.19	1.22	386.1	376.1	-2.7
12.5	-0.05	-0.02	1.00	1.02	458.4	449.8	-1.9
13.0	-0.03	-0.01	1.04	1.05	468.2	463.6	-1.0
13.5	-0.01	-0.00	1.16	1.17	429.4	427.7	-0.4
14.0	-0.00	-0.00	1.24	1.24	400.7	400.1	-0.1

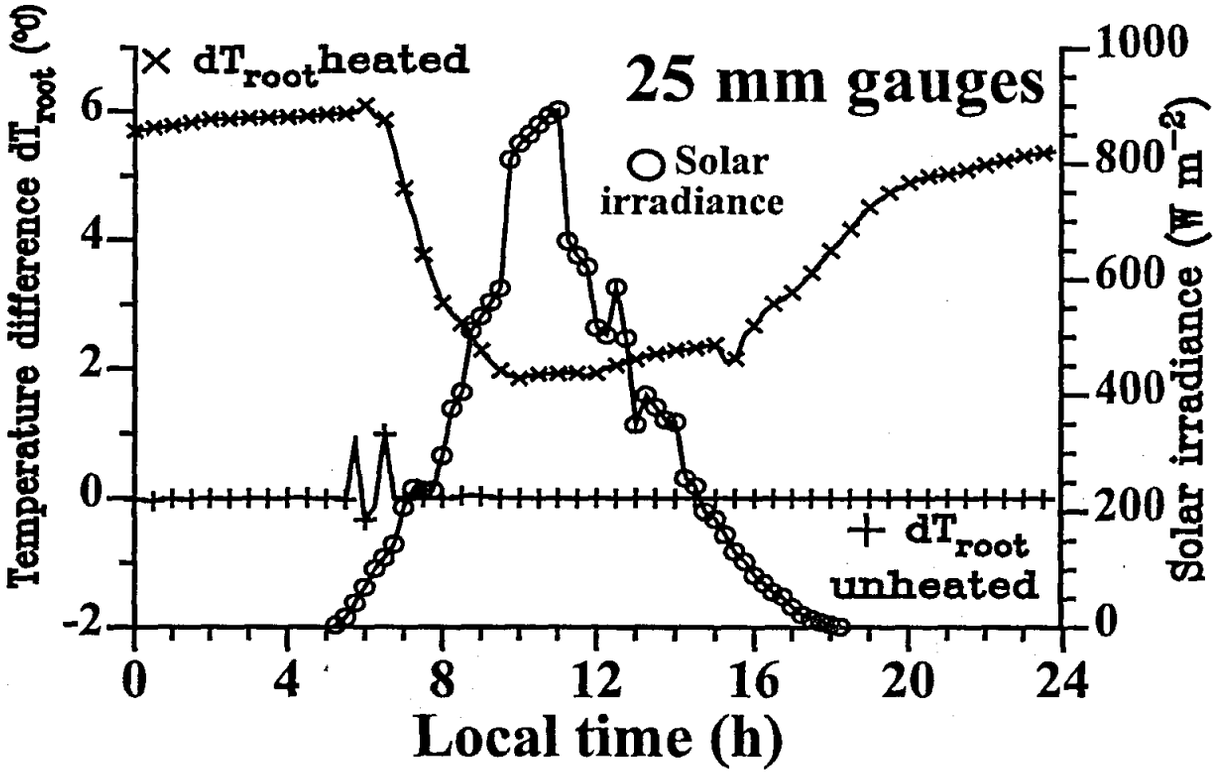

Fig. 4.25 The diurnal variation in dT_{stem} for an unheated gauge and a heated gauge (25 mm diameter) applied to roots of three *E. grandis* trees in September in Pietermaritzburg. Also shown (right-hand y-axis) is the solar irradiance. The curves represent the average diurnal curves for a period of a week for three gauges

SAST in decimal hours	Shackel's γh (for 50 mm diameter gauges)	Shackel's γh corrected for 25 mm gauges)	Measured dT_{stem}	Corrected dT_{stem} ($dT_{stem} - \gamma h$)	Old M_{sap} value	M_{sap} corrected for γh	Error (%)
14.5	-0.00	-0.00	1.34	1.34	370.5	370.4	-0.0
15.0	-0.00	-0.00	1.19	1.19	424.7	424.7	-0.0
15.5	0.00	0.00	1.28	1.28	384.7	384.8	0.0
16.0	0.00	0.00	1.73	1.73	262.3	262.4	0.0
16.5	0.01	0.00	1.64	1.63	277.7	278.0	0.1
17.0	0.01	0.01	1.96	1.95	208.8	209.4	0.3
17.5	0.03	0.01	2.28	2.27	153.1	153.9	0.5
18.0	0.05	0.02	3.11	3.09	82.3	82.8	0.7
18.5	0.09	0.03	3.75	3.72	46.3	46.8	0.9
19.0	0.14	0.05	3.90	3.84	29.9	30.3	1.3
19.5	0.20	0.07	3.89	3.81	21.9	22.3	1.9
20.0	0.28	0.10	3.89	3.78	17.9	18.4	2.7
20.5	0.37	0.14	3.91	3.77	16.0	16.6	3.6
21.0	0.49	0.18	3.93	3.75	14.1	14.8	4.7
21.5	0.63	0.24	3.81	3.57	10.9	11.6	6.2
22.0	0.79	0.30	3.65	3.35	8.4	9.2	8.1
22.5	0.98	0.37	3.41	3.04	5.8	6.5	10.8
23.0	1.19	0.45	3.11	2.66	2.5	2.9	14.4
23.5	1.44	0.54	2.80	2.26	-1.1	-1.3	19.3
Day 311: 7 November 1991							
0.0	0.40	0.15	2.63	2.48	-1.8	-1.9	5.7

SAST in decimal hours	Shackel's γh (for 50 mm diameter gauges)	Shackel's γh corrected for 25 mm gauges)	Measured dT_{stem}	Corrected dT_{stem} ($dT_{stem} - \gamma h$)	Old M_{sap} value	M_{sap} corrected for γh	Error (%)
0.5	0.40	0.15	2.89	2.74	1.2	1.3	5.2
1.0	0.40	0.15	2.90	2.75	-0.5	-0.5	5.2
1.5	0.40	0.15	2.74	2.59	-2.9	-3.1	5.5
2.0	0.40	0.15	2.71	2.56	-3.0	-3.1	5.5
2.5	0.40	0.15	2.89	2.74	0.4	0.5	5.2
3.0	0.40	0.15	3.73	3.58	10.2	10.7	4.0
3.5	0.40	0.15	4.97	4.82	21.6	22.2	3.0
4.0	0.40	0.15	5.71	5.56	26.6	27.3	2.6
4.5	0.40	0.15	5.92	5.77	29.5	30.2	2.5
5.0	0.40	0.15	5.62	5.47	28.3	29.0	2.7
5.5	0.40	0.15	6.00	5.85	35.3	36.2	2.5
6.0	0.40	0.15	6.38	6.23	55.4	56.7	2.4
6.5	0.40	0.15	4.16	4.01	116.1	120.5	3.6
7.0	0.40	0.15	1.18	1.03	438.1	501.7	12.7
7.5	0.40	0.15	1.26	1.11	409.1	464.6	11.9
8.0	-0.96	-0.36	1.28	1.63	407.2	317.9	-28.1
8.5	-0.77	-0.29	1.40	1.69	366.6	303.9	-20.6
9.0	-0.61	-0.23	1.40	1.63	346.2	297.6	-16.4
9.5	-0.48	-0.18	1.27	1.44	393.9	345.3	-14.1
10.0	-0.36	-0.14	1.34	1.47	375.3	340.8	-10.1
10.5	-0.27	-0.10	1.44	1.54	352.3	329.5	-6.9
11.0	-0.19	-0.07	1.48	1.55	340.9	325.1	-4.8
11.5	-0.13	-0.05	1.30	1.35	369.8	356.4	-3.8
12.0	-0.08	-0.03	1.21	1.24	374.0	364.4	-2.6
12.5	-0.05	-0.02	0.97	0.99	441.4	432.8	-2.0
13.0	-0.03	-0.01	0.82	0.83	506.5	500.1	-1.3
13.5	-0.01	-0.00	0.86	0.86	489.7	487.0	-0.6
14.0	-0.00	-0.00	0.91	0.91	466.3	465.4	-0.2
14.5	-0.00	-0.00	1.05	1.05	411.0	410.8	-0.0
15.0	-0.00	-0.00	1.04	1.04	415.1	415.1	-0.0
15.5	0.00	0.00	1.07	1.07	401.1	401.1	0.0
16.0	0.00	0.00	1.26	1.26	350.6	350.7	0.0
16.5	0.01	0.00	1.35	1.35	325.1	325.5	0.1
17.0	0.01	0.01	1.44	1.43	302.9	304.0	0.4
17.5	0.03	0.01	1.67	1.66	250.9	252.6	0.7
18.0	0.05	0.02	2.56	2.54	148.1	149.3	0.8
18.5	0.09	0.03	3.49	3.45	86.1	86.9	1.0
19.0	0.14	0.05	4.23	4.18	50.2	50.8	1.2
19.5	0.20	0.07	4.80	4.72	38.1	38.7	1.6
20.0	0.28	0.10	4.97	4.87	29.8	30.4	2.1
20.5	0.37	0.14	5.06	4.92	24.8	25.5	2.8
21.0	0.49	0.18	5.00	4.82	21.5	22.3	3.7
21.5	0.63	0.24	4.87	4.64	18.1	19.0	4.8
22.0	0.79	0.30	4.86	4.57	16.8	17.9	6.1
22.5	0.98	0.37	4.97	4.60	17.4	18.8	7.4
23.0	1.19	0.45	4.81	4.36	15.7	17.3	9.3
23.5	1.44	0.54	4.64	4.10	14.4	16.2	11.6
Day 312: 8 November 1991							
0.0	0.40	0.15	4.62	4.47	15.0	15.5	3.2
0.5	0.40	0.15	4.16	4.01	11.7	12.1	3.6
1.0	0.40	0.15	3.66	3.51	9.4	9.8	4.1

SAST in decimal hours	Shackel's γh (for 50 mm diameter gauges)	Shackel's γh corrected for 25 mm gauges)	Measured dT_{stem}	Corrected dT_{stem} ($dT_{stem} - \gamma h$)	Old M_{sap} value	M_{sap} corrected for γh	Error (%)
1.5	0.40	0.15	3.52	3.37	9.0	9.4	4.3
2.0	0.40	0.15	3.50	3.35	8.9	9.3	4.3
2.5	0.40	0.15	3.55	3.40	9.8	10.2	4.2
3.0	0.40	0.15	3.67	3.52	11.3	11.8	4.1
3.5	0.40	0.15	3.79	3.64	12.5	13.0	4.0
4.0	0.40	0.15	3.88	3.73	13.3	13.8	3.9
4.5	0.40	0.15	4.01	3.86	14.5	15.1	3.7
5.0	0.40	0.15	4.15	4.00	15.6	16.2	3.6
5.5	0.40	0.15	4.52	4.37	18.5	19.1	3.3
6.0	0.40	0.15	6.04	5.89	29.7	30.4	2.5
20.0	0.28	0.10	4.04	3.94	17.6	18.1	2.6
20.5	0.37	0.14	4.07	3.93	16.2	16.8	3.4
21.0	0.49	0.18	4.10	3.92	15.4	16.1	4.5
21.5	0.63	0.24	4.15	3.92	15.0	15.9	5.7
22.0	0.79	0.30	4.24	3.94	15.2	16.4	7.0
22.5	0.98	0.37	4.36	3.99	16.1	17.6	8.4
23.0	1.19	0.45	4.42	3.97	16.3	18.1	10.1
23.5	1.44	0.54	4.38	3.84	16.0	18.2	12.3
Day 314: 11 November 1991							
0.0	0.40	0.15	1.74	1.59	1.1	1.2	8.6
0.5	0.40	0.15	1.99	1.84	8.1	8.8	7.5
1.0	0.40	0.15	2.27	2.12	12.0	12.8	6.6
1.5	0.40	0.15	2.44	2.29	13.7	14.6	6.1
2.0	0.40	0.15	2.26	2.11	11.3	12.1	6.6
2.5	0.40	0.15	2.12	1.97	9.8	10.6	7.1
3.0	0.40	0.15	2.01	1.86	8.2	8.8	7.5
3.5	0.40	0.15	2.02	1.87	8.4	9.0	7.4
4.0	0.40	0.15	1.94	1.79	7.2	7.8	7.7
4.5	0.40	0.15	1.83	1.68	5.5	6.0	8.2
5.0	0.40	0.15	2.31	2.16	12.1	13.0	6.5
5.5	0.40	0.15	3.91	3.76	25.1	26.1	3.8
6.0	0.40	0.15	6.49	6.34	54.5	55.8	2.3
6.5	0.40	0.15	4.32	4.17	109.3	113.2	3.5
7.0	0.40	0.15	1.61	1.46	270.6	298.5	9.3
7.5	0.40	0.15	0.87	0.72	452.1	546.6	17.3
8.0	-0.96	-0.36	0.99	1.35	387.7	284.7	-36.2
8.5	-0.77	-0.29	0.97	1.26	398.0	306.5	-29.9
9.0	-0.61	-0.23	0.96	1.19	399.7	322.8	-23.8
9.5	-0.48	-0.18	0.95	1.12	401.9	338.3	-18.8
10.0	-0.36	-0.14	1.02	1.16	379.6	335.1	-13.3
10.5	-0.27	-0.10	1.07	1.17	365.9	334.5	-9.4
11.0	-0.19	-0.07	1.33	1.41	304.8	289.3	-5.4
11.5	-0.13	-0.05	0.98	1.02	402.8	383.5	-5.0
12.0	-0.08	-0.03	1.09	1.12	356.6	346.4	-2.9
12.5	-0.05	-0.02	1.06	1.08	365.6	359.1	-1.8
13.0	-0.03	-0.01	0.87	0.88	427.3	422.3	-1.2
13.5	-0.01	-0.00	0.95	0.95	392.4	390.4	-0.5
14.0	-0.00	-0.00	1.55	1.56	225.8	225.5	-0.1
14.5	-0.00	-0.00	3.03	3.04	108.4	108.4	-0.0

4.6.3.3 Conclusions

Naturally occurring vertical temperature gradients in the stem of *Eucalyptus grandis* may affect the measurement accuracy of the calculated sap flux (M_{sap}) values. Corrections may be performed based on actual stem temperature gradients in the absence of heat applied to the heater. It is advisable to measure these stem gradients, in the absence of any heating, for a range of environmental conditions. It would appear that the error is much larger for the larger diameter gauges (diameters greater than 35 mm) but this has yet to be fully determined. A method could be developed to switch of the heater power on various days, measure the stem temperature gradients, and correct the measured gradients for those days when the power to the heater was on. The errors in M_{sap} are large negative (corresponding to an overestimation in M_{sap} by the gauge) before 11h30 when the sap flow is increasing with the errors then becoming increasingly positive after this time. At night, the large errors are often of no consequence since M_{sap} is small. If the data were integrated for a complete day, the overestimation in M_{sap} before noon would not cancel with the underestimation after noon.

It appears then that the errors can be corrected and are certainly much smaller than anticipated by Shackel *et al.* (1992) for the gauges we used (25 mm diameter). The errors are largest under conditions of high flow rates in the early morning to before noon hours.

4.6.4 Storage correction

We have assumed that the energy balance of the gauge is defined by Eq. 3.1. This analysis usually excludes a storage term in the energy balance. As is the case for the Bowen ratio technique (Savage *et al.*, 1998), the storage flux may be calculated from $E_{storage} = V \rho c_p \Delta T/\Delta t$ where V is the stem volume segment, ρ is the density of the stem, c_p is the stem specific heat capacity and $\Delta T/\Delta t$ is the rate of temperature change in the stem (between two measurement time intervals). The calculation is simple to perform given that the absolute temperature at one point of the stem is measured. The results of these calculation, as compared with the correction for naturally occurring stem temperature gradients are shown (**Fig. 4.26, bottom set of curves**). Fortuitously, for the times shown, the storage and naturally occurring temperature gradients oppose each other (top set of curves) with the measurement error in M_{sap} being about 15 % during peak flow times. The measured, adjusted and natural stem temperature differences are shown (**Fig. 4.27**, middle set of curves) with the lower set of curves showing the energy balance component curves, including the E_{sap} value corrected for storage and the storage term $E_{storage}$.

4.6.5 Technique verification and application

4.6.5.1 Review of literature on cut-stem technique

Descriptions of water movement through plants at the soil-plant-atmosphere continuum (SPAC) level, often make use of Ohm's law analogue equations even though the limitations of this approach have been demonstrated by Richter (1973) and Jarvis (1975). The problems associated with their use have been traced primarily to non-steady state flow resulting from dynamic water exchange (capacitance) and variable flow resistances developed in different parts of the plant.

To combat these difficulties, present research has redefined the SPAC system. Rather, the plant water flow system constitutes a summation of flows and resistances through small segments incorporating the plant's hydraulic architecture. This provides a significant theoretical improvement in that resistance at different points in the system can be dealt with individually: where q is the flux through the entire plant Ψ, is component water potential and R the component resistance. Operationally, measurement of $\Delta\Psi$ and q within functioning plants has proven challenging.

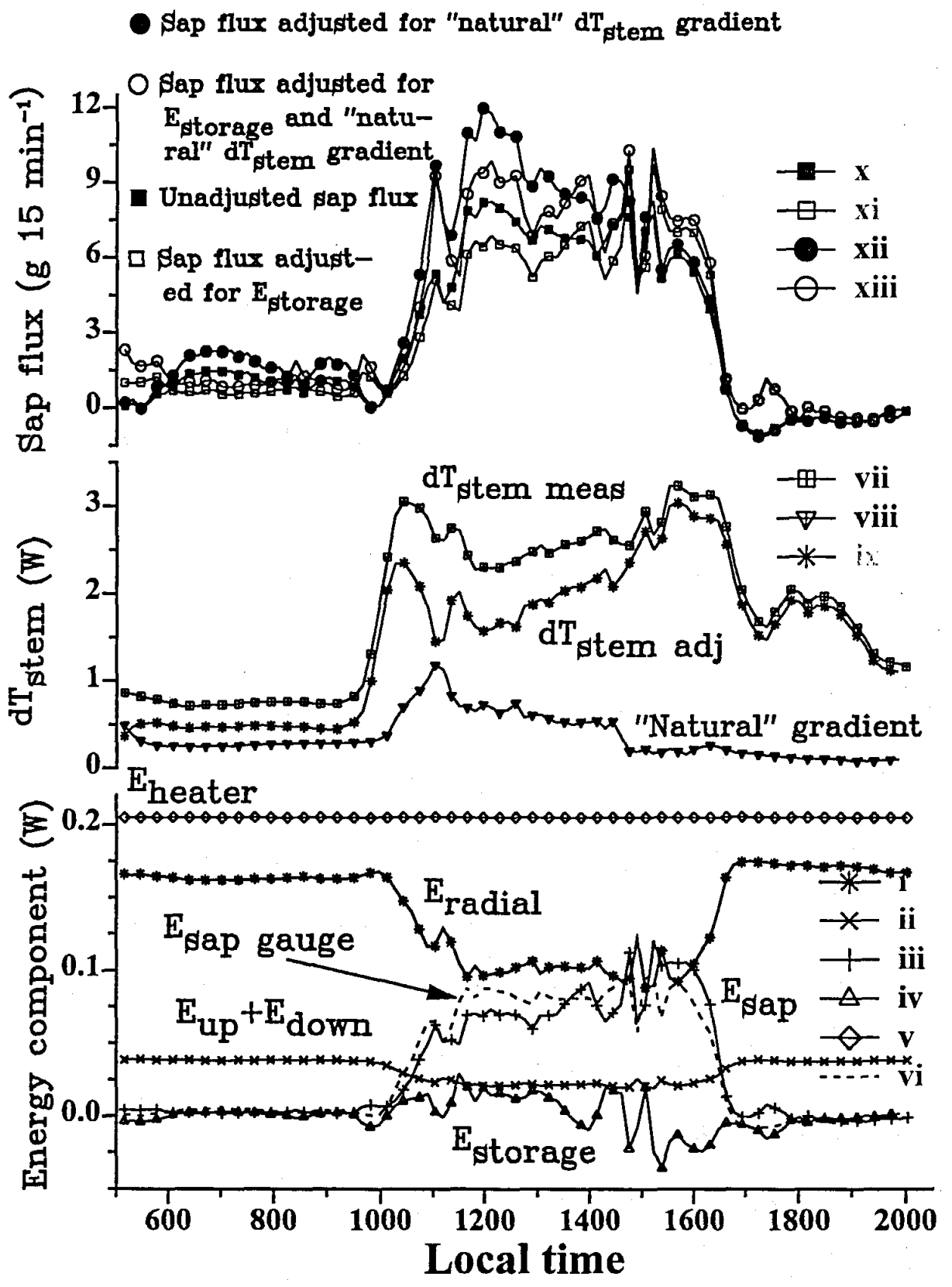

Fig. 4.26 Top: Sap flux adjusted for storage and naturally occurring temperature gradients;
middle: measured, adjusted and natural stem temperature differences;
bottom: energy balance component curves, including the E_{sap} value corrected for storage and the storage term $E_{storage}$

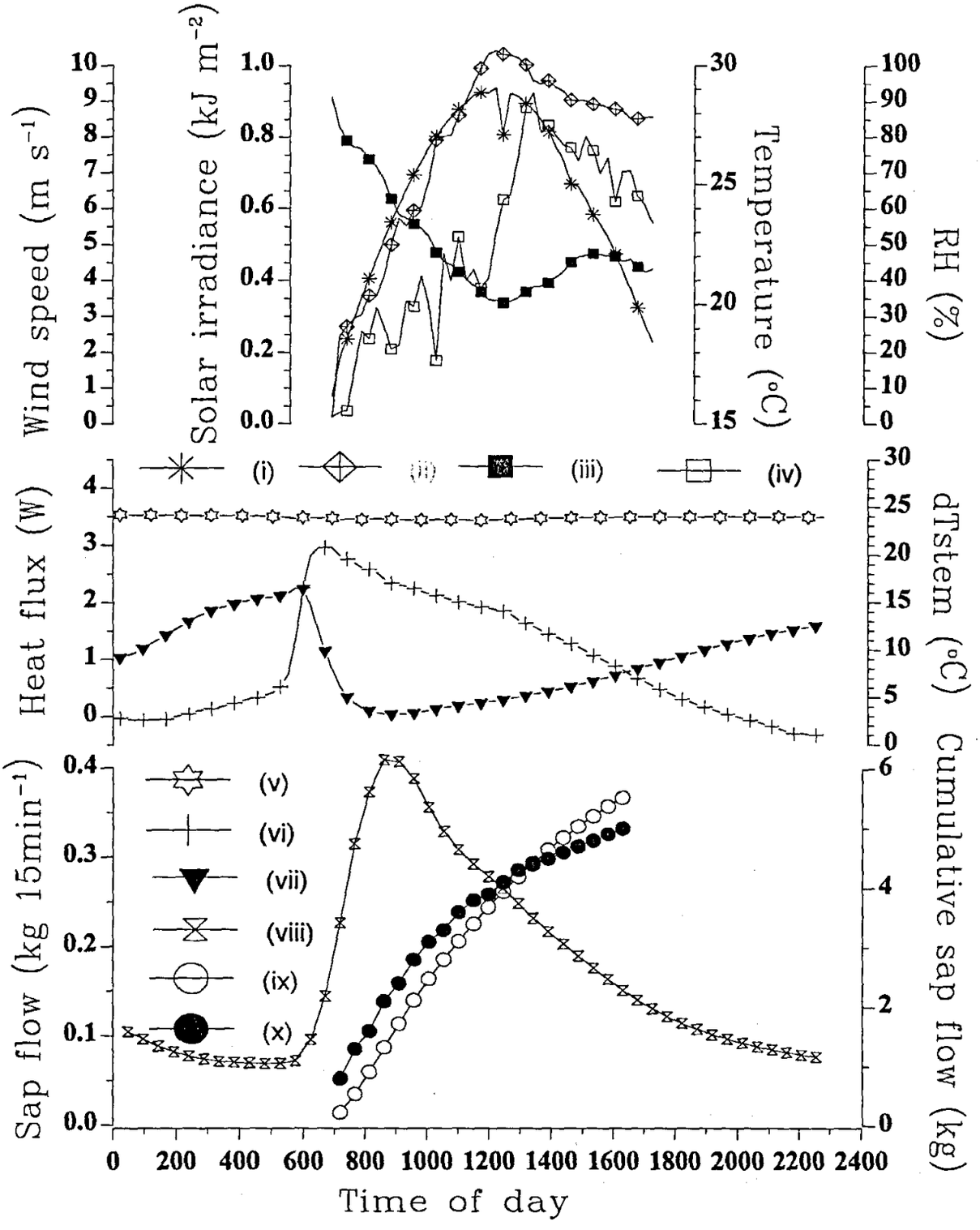

Fig. 4.27 Graph depicting the data from the cut stem technique experiment used to verify the SSHB technique on a relatively large stem. Cumulative sap flow data from the application of a Dynamax SGB100 gauge (18.7, K_{stem} = 0.1W m^{-1} K^{-1}; K_{gauge} = 1.6 W mV^{-1}; V_{heater} = 8 V) to a Eucalyptus tree stem (diameter 98.8 mm) are compared to water lost by transpiration measured using a weighing lysimeter. (i) = solar irradiance (kJ m^{-2}). (ii) = temperature (°C). (iii) = relative humidity (%). (iv) = windspeed (m s^{-1}). (v) = E_{heater} (W). (vi) = E_{sap} (W). (vii) = dT_{stem} (°C). (viii) = sap flow (kg 15min^{-1}). (ix) = Cumulative sap flow measured by Dynamax SGB100 gauge (kg). (x) = Cumulative transpiration measured by weighing lysimeter (kg)

$$q = \frac{\Delta\Psi_{soil-root}}{R_{soil-root}} + \frac{\Delta\Psi_{root-xylem}}{R_{root-xylem}} + \frac{\Delta\Psi_{xylem-leaf}}{R_{xylem-leaf}} + \frac{\Delta\Psi_{leaf-air}}{R_{leaf-air}}$$

While good progress has been made in analysing leaf-air resistance in many trees, study of other sources of flow resistance has lagged. Attempts to measure R_{plant} or R_{xylem} have followed three methodologies. One method has been under laboratory conditions to measure flux and Ψ gradients through excised tissue or small plants. A second approach has been to measure *in situ* in various ways and transpiration as an estimate of sap flow (q). Finally a number of workers have used tree excision at ground level to measure flow resistance by difference.

The use of tree cutting techniques for the examination of plant water relations has been described for a number of trees including Scots Pine (*Pinus sylvestris* L.) by Rutter (1966) and Roberts (1976; 1977), apple trees (*Pyrus malus*) by Landsberg, Blanchard and Warrit (1976), Norway Spruce (*Picea abies* L. Karst.) by Roberts (1978), Lodgepole Pine (*Pinus contorta* Dougl ex. Loud.) by Running (1980), a mallee eucalypt (*Eucalyptus behriana* F. Muell.) by Myers, Küppers and Neales (1987), and Mexican Patula Pine (*Pinus patula*) by Dye, Christie, Olbricht, Ferreira and Tallon (1990). Cutting a stem under water truncates the catenary system of hydraulic resistances and capacitances that makes up the normal path of water flow from soil to atmosphere in an intact tree. Cutting the stem under water therefore abruptly connects a source of water ($\Psi = 0$) with that of the stem and its attached leaf canopy.

Running (1980) found that excision of *Pinus contorta* at mid-day always resulted in rapid recovery of leaf water potential when water was supplied to the cut stem, suggesting a high soil-root resistance. Transpiration was unaffected if leaf water potential before cutting was not limiting leaf conductance. He noted that trees under stress at the beginning of the excision procedure resulted in artificially high water uptake rates after cutting particularly where the trees exhibited significant stem storage.

Similarly, Myers *et al.* (1987) noted that upon cutting under water at mid-day, uptake by the cut stem over the following hour was approximately six times the estimated transpiration rate from the E. behriana canopy. This was attributed to an increase in stemwood water content. Unlike that of any of the other authors cited above, the canopy bulk water potentials were initially between -4.4 and -3.4 MPa. Accompanying the period of rapid water uptake was a 2.3 MPa increase in Ψ. The dried stemwood mass in their experiment was 35.84 kg and its density was 980 kg m^{-3}. The capacitance of the stemwood was 0.007 g^{-1} MPa^{-1}. An increase in by 2.3 MPa corresponded to an increase in water volume by 452 ml (0.1 mm of evapotranspiration Ψ). This is 71 % of the total observed uptake of 636 ml. Only 103 ml of the water lost over this period was attributable to transpiration (16 %).

Other examples include water storage in the stem sapwood of Pseudostuga menziesii (Waring and Running; 1978) which may be withdrawn and replenished at the rate of of 1.7 mm day^{-1} from a total of 27 mm. Likewise over 2 weeks the water content change in Pinus sylvestris was equivalent to 5 mm of water (Waring, Whitehead and Jarvis; 1979). Contrary to these observations, Landsberg *et al.* (1976) and Roberts (1976; 1977; 1978) observed that the alleviation of low Ψ by stem-cutting resulted in a rapid decrease in leaf conductance associated to rapid and prolonged stomatal closure.

It is reasonable to conclude therefore that comparing sap flow using heat tracer techniques and that using graviemtric water displacement using the cut stem technine would differ from a concomitant measurement of transpiration. A large change in scale of the sap flow magnitude could also be anticipated after cutting the stem.

4.6.5.2 Methods and materials

To investigate the validity of Eq. 3.1, the influence of different measured voltages across the gauge heater on $K_{gauge\ apparent}$ were determined. Two excised sections (110 mm diameter) from a Eucalyptus grandis tree stem were each fitted with a Dynamax SGB-100 gauge (18 Ω heater). Measurements were recorded using a Campbell Scientific CR7X data logger. The heater voltage was stepped every three hours (Table 4.6). Data was collected at intervals of 10 minutes over a period of three days for three different voltage setting regimes (Table 4.6). Four switch mode power supply units were wired in parallel to control switching. These were powered by a low impedance constant power supply regulator. The gauges were wrapped in an extra layer (ca. 30 mm thick) of foam insulation. The excised stem sections with the gauges installed were sealed in plastic to prevent water loss.

The site chosen to apply the SSS technique to Eucalyptus grandis trees with stem diameters ca 110 mm is located at Amangwe Zululand (Kwa-Mbonambi, coastal Kwa-Zulu Natal).The map reference is: SOUTH AFRICA 1:50 000 sheet 2832CA KWA-MBONAMBI, Lat. 28° 30'- 28° 45'; Long. 32° 00'- 32° 15', altitude 60 m. This area is characterised by a flat to undulating aspect and sandy eutrophic soil (Clovelly form, Setlagole family, on the S.A. binomial soil classification system). Geological surveys in the area have indicated that while spatially very variable, the sands extend to a depth of 50 m above an aquifer consisting of sandstone conglomerate. Perched water tables caused by compacted siltstone and mudstone layers are frequently present as shallow as 6 m in depth. The soils at the time of site selection exhibited cracks, were very dry and near depletion of stored water. At the time, E. grandis trees growing there were 15 to 20 m high in their second rotation. Stumps from the first rotation had been chipped and disk-ploughed back into the soil. Many trees exhibited crown thinning, slowed growth rates and trunks with an angular form, often associated with stem shrinkage due to water depletion. Some trees show symptoms of stress related fungal infection, similar to tree decline scenarios reported from Australia (Heatwole and Lowman, 1986).

Concern had been expressed that while well suited to rapid Eucalyptus biomass production in the short term, this area may prove to be marginal for sustained production in the long term at the present concentration and activity, in the absence of water supplementation. The mean annual precipitation is approximately 1100 mm (51 year average) and the climate falls into the humid moist region as classified by Schulze (1958). From August to December potential evaporation is greater than rainfall. The potential for transpiration is likely to follow a similar pattern. It is significant to note however that healthy mature Eucalyptus trees tend to be more aerodynamically resistant and present a greater surface area for evaporation than the apparatus used to measure potential evaporation at most weather stations. The potential for these trees, after a certain stage of growth, to transpire more water than that supplied by rainfall alone, and their subsequent dependence on soil stored water in the long term, is evident.

In June 1992 a Dynamax SGB100 gauge was attached to each of a number of E. grandis trees (28 months from establishment) growing in the ICFR fertiliser experiment number C51 (spacing was 3 m between rows and 2 m within rows) to test the range efficiency of a Dynamax SGB100 SSS gauge using the cut stem technique. Sap flow was monitored for a period of a few days. Following this sample trees were connected to surrounding trees using three pulleys connected to the stem base 0.5 m above ground level. Another three pulleys were connected 8 m above ground-level. The sampled trees were sequentially cut at mid-night using a chain-saw, and suspended in a drum of water situated on a portable lysimeter. Following this the trees were re-cut under water using a wood planeing blade as a chisel.

This initial experiment was repeated on 7 November 1992 on trees situated at the ICFR's Bloemendal research station (Crammond, Natal). An automatic weather station was erected 10 m from the Bloemendal research site during the cut-stem verification of the SSS technique on 110 mm Eucalyptus stems. This included a 207 air temperature and relative humidity sensor (Phys-Chem Scientific corporation, New York, New York, USA), a LI200S silicon pyranometer (Li-Cor, Lincoln, Nebraska, USA), a TE525 tipping bucket raingauge (Texas Electronics, Dallas, Texas, USA) and an ECO model WS/D86 wind speed and direcion sensor (ECO Pretoria, RSA) for the measurement of air temperature and relative humidity, solar irradiance, rainfall, wind speed and wind direction, respectively.

In March 1993 the ICFR fertiliser experiment number C51 site was revisited. Two Dynamax SGB100 gauges were fitted to *E. grandis* trees growing in a control plot which had received no fertiliser, and two were fitted to trees growing in an experimental plot which received a split fertiliser application (half at planting and half three months later). The fertiliser comprised of N (LAN (28) @ 500 kg ha^{-1}), P (SUPERPHOSPHATE (10,5) @ 760 kg ha^{-1}), K (K_2SO_4 @ 100 kg ha^{-1}) and fritted trace elements (FRIT @ 120 kg ha^{-1}). The aim was to determine whether there was any response to fertilisation in depletion of the stored water reserve, and how this compared to potential evaporation for the region. On the day of arriving at the site the drought conditions were interrupted when the site received 90 mm of rainfall. Some rain had also been received a week earlier. Prior to this it had experienced an unusually long four month dry period.

4.6.5.3 Results

In the initial investigation of the validity of Eq. 3.1 by studying the influence of different measured voltages across the gauge heater on K_{gauge} apparent, it was observed that K_{gauge} apparent changed in proportion to heater voltage. The time to equilibrium increased with the step magnitude in heater voltage to as much as four hours. Within this time period the slope of the relationship between heater voltage and K_{gauge} apparent also changed with the magnitude in the voltage step. The time constant after stepping down the voltage was greater than for stepping it up. One of a number of possible regressions is presented in Fig. 4.17. When the heater voltage was stepped up K_{gauge} apparent increased rapidly then drifted down towards an asymptote approximated by the regression line. Similarly when the voltage was stepped down the opposite occurred.

This data does not take stored heat into consideration, since the thermocouple arrangement used with commercial SSS technique gauges (Dynamax) designed by Steinberg, van Bavel and McFarland (1989) precludes this. When E_{heater} and E_{radial} (assuming unitary K_{gauge} i.e., $E_{radial} = V_{thermopile}$) were plotted and regressed against heater voltage (Fig. 3.8), E_{radial} and E_{axial} increased with heater voltage. These were minuscule however compared to the change in E_{heater} implying that in order to include the residual difference between E_{heater} and $(E_{radial} + E_{axial})$ i.e., the numerator of Eq. 3.1, into the energy balace, K_{gauge} would necessarily have to change in a similar manner to E_{heater} in order to validate those equations.

These observations are attributed to the omission of the heat storage term of Eq. 3.1 in the assumed thermal energy balance, the numerator component of Eq. 3.2.

This indicates that the stem section necessarily heated up and cooled down depending upon whether heat was added or removed from storage respectively. If heat storage or the rate of stem section heating or cooling is not proportional to changes in $V_{thermopile}$, V_{upper} and V_{lower} for a given heater input, as

might be the case under dynamic ambient environmental and sap flux conditions, it would be appropriate to measure $E_{storage}$. Alternatively, if $E_{storage}$ were to be constant one could account for the residual by adjusting E_{heater} by some factor.

The observed change in K_{gauge} apparent with added heat implies that this factor served the dual function of modulating both E_{radial} and $E_{storage}$ together so as to set sap flow to zero in the excised segment. This is not unreasonable since E_{axial} did not change appreciably with an increase in E_{heater} ($E_{axial} < 15\%$ of E_{radial}). Clearly if $E_{storage}$ were included in Eq. 3.1, $K_{gauge\ apparent}$ would have approximated K_{gauge} and would not have changed with the change in E_{heater}.

Dynamax SGB100 measured sap flow (Eq. 3.1) showed reasonable agreement with water uptake measured gravimetrically using a lysimeter. Only if the value for K_{gauge} was reduced from 5.5 ($K_{gauge\ apparent}$) to 1.6 was it possible to calibrate for day-time sap flow (Fig. 4.27). Night-time sap flow in this circumstance measured gravimetrically was 60 g 30 min^{-1}. This has little value to non-cut stem applications but does show that by calibrating day-time sap flow, nighttime sap flow was not zero yet very closely approximated that measured by the scale.

Considering the premise for applying $K_{gauge\ apparent}$ i.e., where nocturnal sap flow is assumed to be zero, it was deemed necessary to examine $E_{storage}$ and possible interferences to dT_{stem}. Using $K_{gauge} = K_{gauge\ apparent}$ and without correcting for a bias in dT_{stem}, the Dynamax SGB100 gauge under-estimated measured sap flow by 25.20 % (**Fig. 4.28**).

Naturally occurring dT_{stem} gradients (heater switched off) were measured at two locations, one higher up the stem than the other. The gauge at the higher position recorded a greater dT_{stem} value than the other. When these naturally occurring gradients were subtracted from dT_{stem} measured when the heater was switched on, Dynamax measured sap flow closely approximated that measured gravimetrically by the lysimeter (Fig. 4.28). The naturally occurring dT_{stem} gradient at the upper (further downstream) position had an earlier and greater influence on the mid-day sap flow calculation than the gradient measured further down the stem, but of shorter duration. The area under these two curves did not differ markedly, however. When the upper and lower naturally occurring dT_{stem} gradients were applied to account for a bias in dT_{stem}, cumulative day-time sap flow only deviated by ±2.8 % from that measured gravimetrically (5.0 kg).

The naturally occurring dT_{stem} gradients were in an upstream direction i.e., down the stem, between midnight and the onset of sap flow. Subsequently they followed an inverse pattern to sap flow, with full reversal in direction at mid-day. This may be explained by a convective cooling influence of sap flow on the stem temperature downstream compared to that upstream of the heater.

Sap flow was not adjusted for a bias in dT_{stem} in applying the technique to fitted SGB100 gauges on the two E. grandis trees growing in a control plot which had received no fertilizer and those which had received the split fertilizer application. In a similar manner to the June 1992 visitation (data not presented), sap convected heat flux distinctly exceeded the heater energy flux during the first half of the morning from 06h00 to 10h00 (**Fig. 4.29**). During this period E_{radial} and E_{axial} approached zero and became negative. This was not attributed to insufficient input heat since dT_{stem} was not sufficiently small to invalidate the data between those times, but rather to heat coming out of storage as the system cooled down.

This can suitably be explained as follows. With the onset of sap flux, cold sap displaced sap that

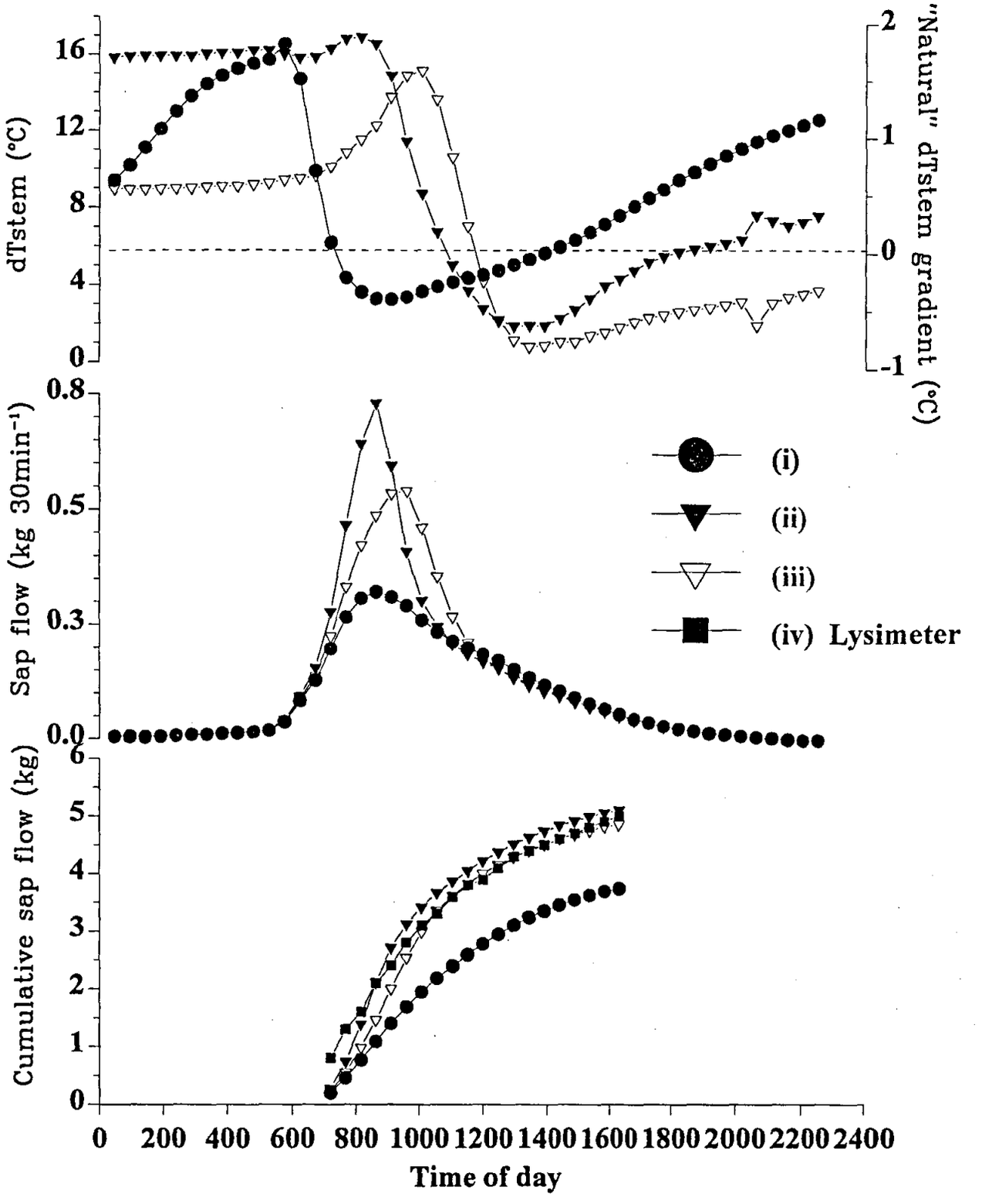

Fig. 4.28 Graph illustrating the correction of sap flow by γ, the natural dT_{stem} gradient. Sap flow was underestimated by 25.20 % without being corrected. Two gradients were measured. One higher uper up the stem than the other. The further up the tree the gauge was positioned the greater the influence of the natural dT_{stem} measured on the mid-day sap flow calculation. In comparison, the gradient measured at a position futher down the tree resulted in a later and smaller calculated peak sap flow. The area under these two curves did not differ markedly, however. Cumulative adjusted sap flow was not very different from transpiration measured gravimetrically. (i) Unadjusted data. (ii) Data adjusted for upper natural dT_{stem} measurement. (iii) Data adjusted for upper natural dT_{stem} measurement. (iv) Lysimeter

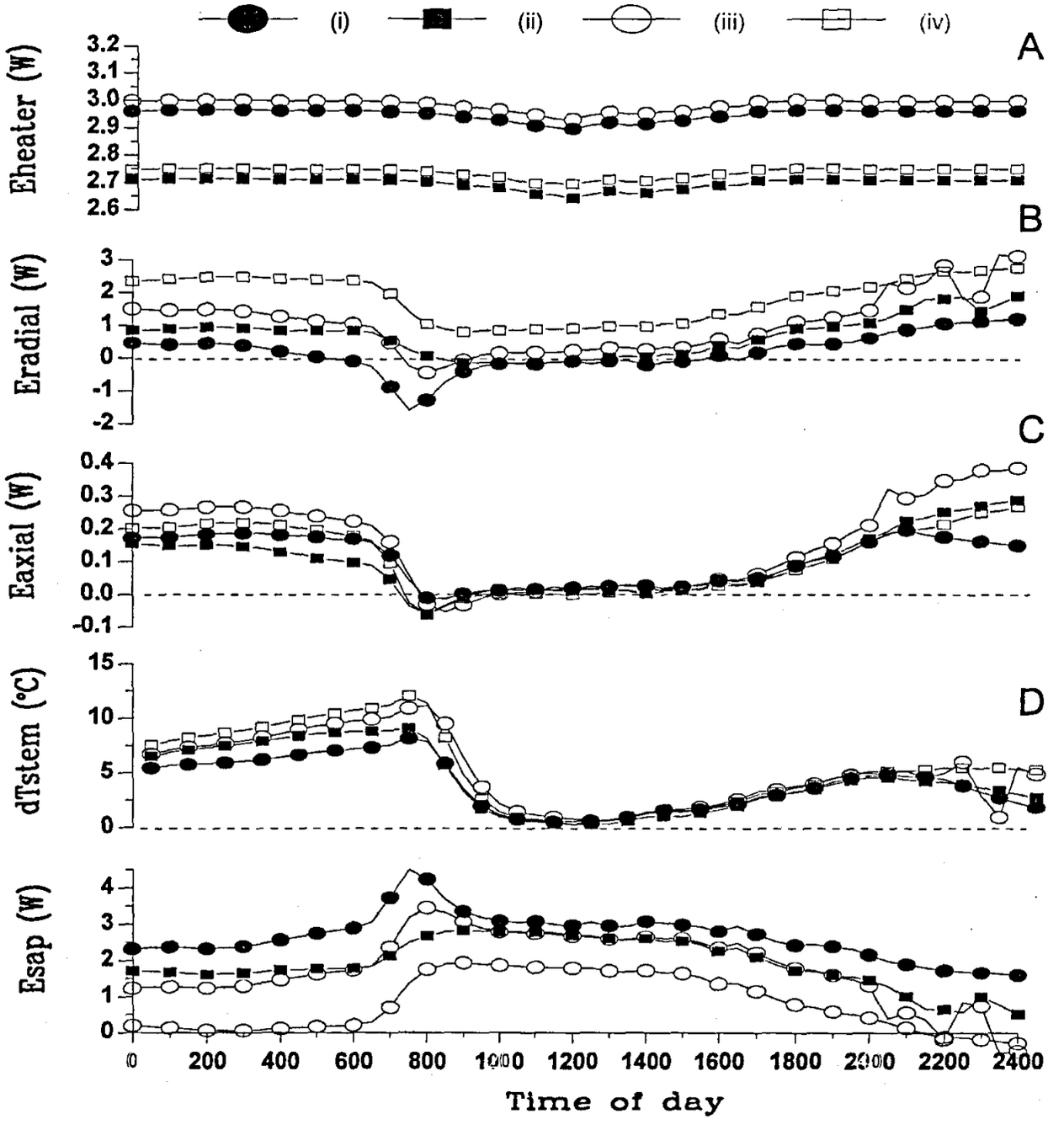

Fig. 4.29 Graph showing the partitioning of the input heat flux E_{heater} (A) on E_{radial} (B), E_{axial}(C), E_{sap} (E) and the change in stem temperature either side of the heater associated with the displacement by sap convection, dT_{stem} (D), during the application of a Dynamax SGB100 SSHB gauge (dz = 15 mm, 18 ; $K_{gaugeapparent}$ = 6.5) on a 100 mm *Eucalyptus* stem. Data (i) and (ii) are for the unfertilised trees, while (iii) and (iv) are for fertilised trees. In this circumstance there is a period (between 06h00 and 10h00) where sap convected heat flux distinctly exceeded the heater energy flux. During this period E_{radial} and E_{axial} approached zero and became negative. This is not attributed to insufficient input heat, since dT_{stem} was not sufficiently small to invalidate the data over this period. This can be attributed to heat coming out of storage as the system cooled down. With the onset of sap flux cold sap replaced sap warmed overnight. Heat from the warmed insulation material and outer regions of the stem flowed to the cooler displacing sap, resulting in a reversal of the modal direction of conducted heat through the stem and thermopile. The net result would be an over-estimation of sap flux during this period. This effect was strongest during cold winter mornings

had been warmed overnight. Perceivably, heat from the warmed insulation material and outer regions of the stem then flowed to the cooler displacing sap. This would have resulted in a reversal of the modal direction of conducted heat through the stem and thermopile, in turn causing is an over-estimation of sap flux. This effect was strongest during cold mornings, particularly when bark had been removed from the stem before fitment of the gauge. As a consequence the upper limit data filter value of 0.8 for the E_{sap}/E_{heater} ratio was not a suitable data rejection statistic, since extraneous heat from storage introduced artifact into its calculation **(Fig. 4.30)**.

The upper limit (80 % accuracy) sap flow rate (Fig. 4.30) was ca.3 kg 30 min^{-1}. This is considerably less than the peak flow rate of 15 kg h^{-1} recorded in 80 mm diameter Pecan (Carya illinoensis) stems by Steinberg, McFarland and Worthington (1990), where a heater power of 1.2 W had been applied. There was a greater range in gauge performance in their application compared to Fig. 4.30 due to the greater heater power used compared to Fig. 4.29A (2.7 to 3 W). By applying a voltage from 6V up to 10 V the Dynamax SGB100 heater (18 Ω) supplies 2 to 5.5 W of power. Clearly there is considerable scope to have increased the upper limit range of the gauge. However this would be done at he risk of increasing the nigh-time sap flow. The heated sap could detrimentally effect cell function below the heater. With the current application the peak temperature difference between incoming and outgoing sap was as high as 12.5 °C. However, in this case there was continued night-time sap flow. This value was observed to increase to as much as 30 °C when sap flow had ceased completely.

Sap flow through the unfertilised trees consistently exceeded that through the fertilised trees. The comparison is not influenced by the manitude of E_{heater} since two heater settings were used for each treatment (Fig. 4.29). The value of dT_{stem} did decreased however to below the 0.24 °C limit recommended by van Bavel and van Bavel (1990). The sap flow upper limit was ca. 3.0 kg 30 min^{-1} or 1.7 g s^{-1} (Fig. 4.30). Where calculated sap flow exceeded the range limitation of the gauge, the upper value of 1.7 g s^{-1} was assumed. The sap flow results of the experiment are summarized in **Table 4.7**.

It is apparent that under the conducive conditions present at the time, the daily sap flow far exceeded the mean daily A-pan reading for the month and the maximum mean daily rainfall for the year. This indicates that if the sap flow levels measured over the six days were to be sustained for a considerable length of time, the trees would inevitably be dependent on soil stored water at the current espacement and in the absence of water to supplement the current rainfall pattern.

Interestingly, it appears that the unfertilized trees tended to constantly transpire more water over the test period that the fertilized trees. Unfortunately it was not possible to measure leaf area or extent of rooting in the respective trees at the time, as this would have interfered with the pre-existing fertiliser experiment. Subsequently in 1994 these trees were excavated after they had been felled. The fertilised trees had a considerably more extensive fine root system than the unfertilised trees. However the unfertilised trees had a more developed deep rooting system. In both cases the tap root was restricted to a depth of 5 m by a clay layer.

One may speculatively explain the differences between the unfertilised and fertilised trees as follows. At the onset of the dry period (November 1991 to March 1992) the fertilised trees utilised available water more rapidly than unfertilised trees due to differences in growth response to nutrient availability. Consequently they experienced drought related stresses earlier and more severly than unfertilised trees with the progression of the dry period. The differences in recovery of the transpiration level after the good rains may be associated to differences in the stress intensities experienced. Alternatively, the fertilised trees could have been exhibiting a greater photosynthetic efficiency than

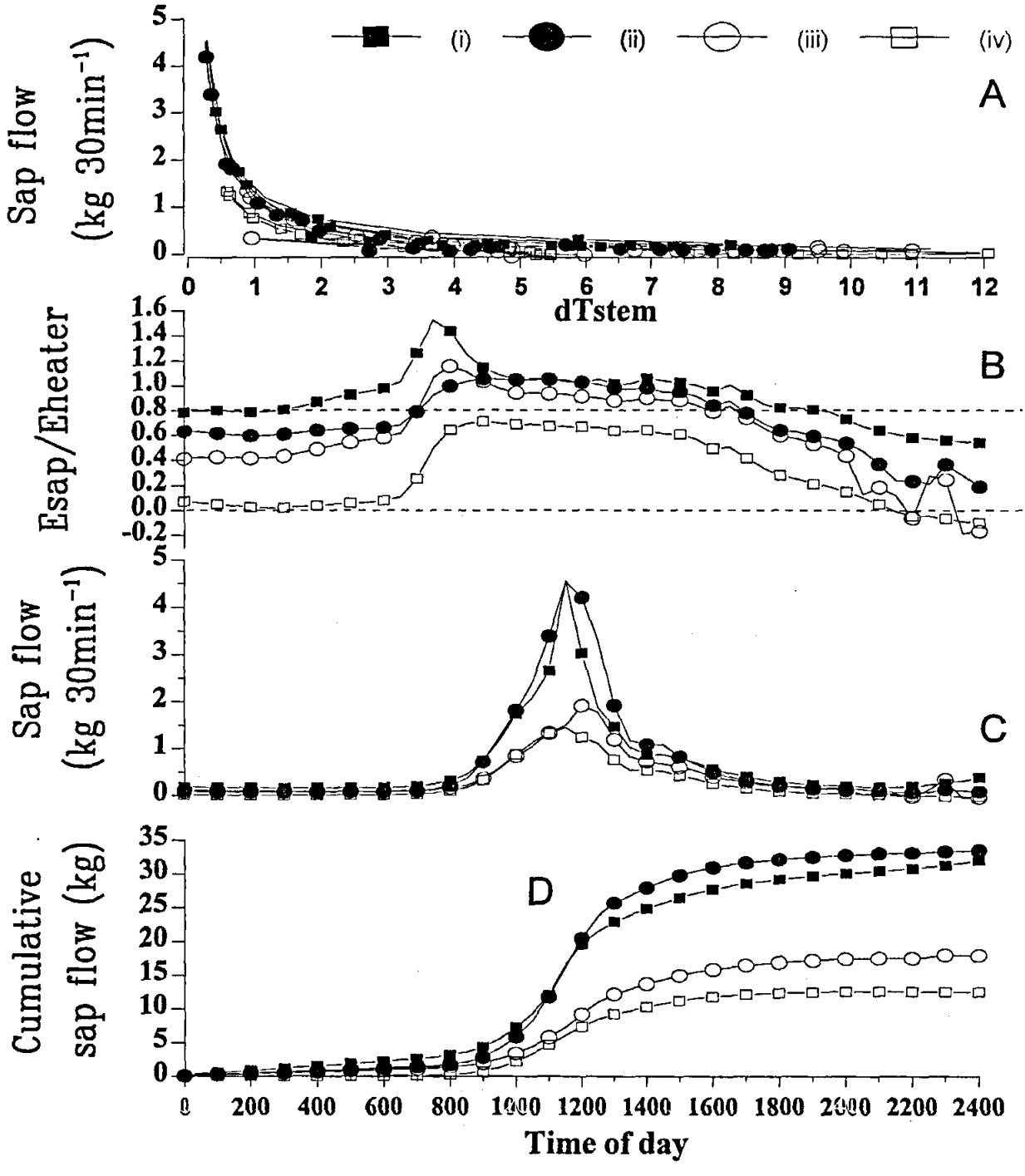

Fig. 4.30 Graph showing the relationship between sap flow and dT_{stem} (A); and the diurnal courses of E_{sap}/E_{heater} (B), sap flow (C) and cumulative sap flow (D) during the application of a Dynamax SGB100 gauge (dz = 15 mm, 18 Ω) on a 110 mm *Eucalyptus* stem. Peak flow rate is ca 4.5 kg 30 min^{-1}. The suggested upper limit data filter value of 0.8 for the E_{sap}/E_{heater} ratio was not a suitable data rejection statistic, since extraneous heat from storage introduced artifact into its calculation. Normally maximum measurable sap flow rate is determined by instrument sensitivity, ignoring the estimated limits imposed by thermal noise on the precision of dT_{stem}. In practice dT_{stem} might be measured within ca 0.1 °C accuracy. The accuracy of the datalogger is within 1μV. van Bavel and van Bavel (1990) recommended a value of 0.24 °C as the minimum acceptable for dT_{stem} for valid data, within the technique upper limit boundary. For their data this corresponded to a sap flux peak of 1.52 m h^{-1}. However with deviation from the assumptions of the technique eg., non-representative sampling of sap temperature at the stem's surface, these criteria would necessarily need to be increased

Table 4.7 Daily sap flow (7th to 12th March 1992) measured on four trees[1] growing at the ICFR's Amangwe field site number C51, KwaMbonambi, coastal northern Zululand.

	Total daily sap flow (kg or litres)				Total daily sap flow (mm)			
Day	Tree 1	Tree 2	Tree 3	Tree 4	Tree 1	Tree 2	Tree 3	Tree 4
66	16.89	17.98	12.10	11.54	11.26	11.99	8.02	7.69
67	32.16	24.30	8.95	7.75	21.44	16.20	5.97	5.17
68	35.14	25.92	24.26	16.62	23.43	17.28	16.17	11.08
69	32.39	30.47	21.52	19.27	21.59	20.32	14.35	12.85
70	29.23	22.45	21.51	18.68	19.49	14.97	14.34	12.45
71	17.70	10.97	12.15	10.92	11.80	7.31	8.10	7.28
Mean	27.25	22.02	16.74	14.13	18.17	14.68	11.16	9.42

[1]Trees were approximately 15 m high and 110 mm in diameter. Trees were sampled in March 1993 at the ICFR fertiliser experiment number C51. Trees 1 and 2 had been fertilised at pre-plant and three months post-plant, while trees 3 and 4 were unfertilised control trees. The mean March daily A-pan evapotranspiration value for the region is 5.3 mm equivalent head. Total daily sap flow (kg) was converted to mm equivalent head by divding by the area produced by half the row spacing and converting to mm equivalent head by dividing by ρ, the density of water. (Where mid-day peak flow rate exceeded the range limit of the gauges, data points were transformed to a half hour mean upper level reading of 1.7 g s^{-1}). It is apparent that, under the conducive conditions present at the time, the sap flow per day far exceeded the mean daily A-pan reading for the month (March) and the maximum mean daily rainfall for the year. This indicates that if the levels of sap flow measured over the six days were to be sustained for a considerable length of time, the trees would inevitably be dependent on soil stored water where, at the current espacement, water supplementation might be necessary to avoid almost certain decline in productivity and a perceived increase in risk to fatality

the unfertilised trees. Convergence in the transpiration level between the fertilised and unfertilised trees would then be expected twith decreasing available light or an increased necessity for temperature control.

4.6.6 Stem thermal conductivity

4.6.6.1 Field determination of K_{stem} using a stem steady state method

We have shown that a K_{gauge} value of 1.565 W mV^{-1} could be used for both gauges on the same stem, the choice of the correct K_{gauge} value being that under night-time minimum flow conditions M_{sap} = 0 g h^{-1}. Since K_{gauge} is the proportionality constant between the radial heat energy flux density component E_{radial} and the measured temperature difference between inner and outer layers of the cork substrate mounted to surround the stem, why should K_{gauge} not be the same for a plant stem and a dowel rod? For the same environmental conditions as the previous measurements, we placed a gauge around a dowel rod of unknown thermal conductivity. In the datalogger program we used a value of K_{gauge} of 1.565 W mV^{-1} and K_{stem} = 0.54 W m^{-1} K^{-1}. After the data collection period the data was imported into a spreadsheet from which the value of K_{stem} could be altered from its original K_{stem} = 0.54 W m^{-1} K^{-1} value to another and the effect of this change on the E_{sap} observed (using Eqs 3.1 and 3.5). This process was continued until the night-time E_{sap} value was regarded as 0 W (**Fig. 4.31**), which it must be for a system such as a dowel rod. The components of the energy balance are shown for a thermal conductivity of 0.215 W m^{-1} K^{-1} for Day 311 to 314 arrived at using the iterative procedure described. The value of $K_{stem} = K_{dowel\,rod}$ must be compared with other values found in the literature: K_{balsa} = 0.11

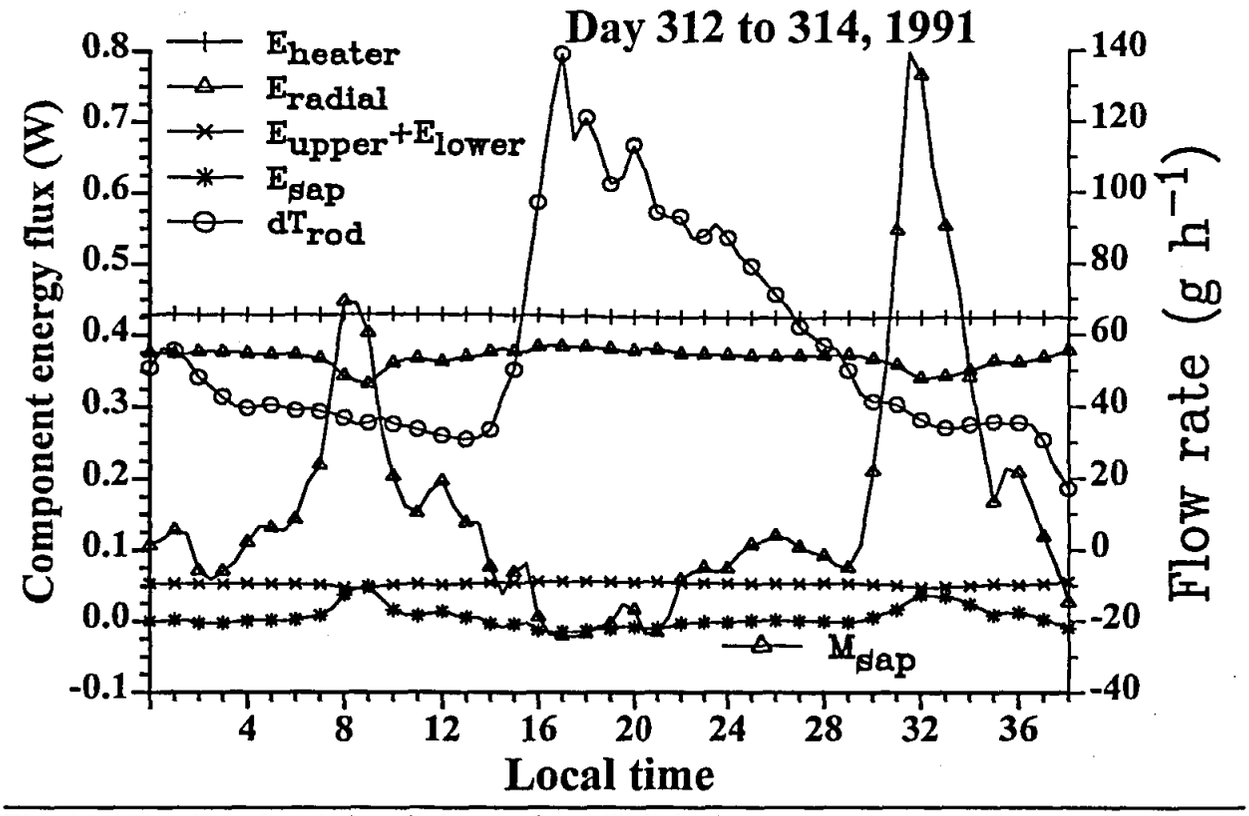

Fig. 4.31 The diurnal variation (in hours after 16h30) in the component energy fluxes as well as the mass flow rate measured using a 25-mm gauge attached to a dowel rod in the open environment (Day 312 to 314, 1991) containing no water. The influence of the early morning temperature disequilibrium is evident in the increased mass flux approaching 100 g h^{-1} for a system containing no water at all. There is no reason why similar temperature disequilibrium conditions should not occur on stems. Also shown is the diurnal varaiiation in dT_{rod}. At times associated with sunrise, there is a rapid increase in dT_{rod} followed by a gradual decline during the rest of the day and night. This confirms the data depicted in Fig. 4.24 for 100-mm stems except that in the case of the 100-mm stems, the dT_{stem} values are much larger (approaching 15 °C) and the decline in is much more rapid for stems

W m^{-1} K^{-1}, K_{fir} = 0.54 W m^{-1} K^{-1}, K_{pine} = 0.45 W m^{-1} K^{-1}, and K_{walnut} = 0.65 W m^{-1} K^{-1} (Gray, 1972).

4.6.7 Laboratory determination of stem gauge conductance

4.6.7.1 Introduction

Usually, the gauge conductance K_{gauge} (W mV^{-1}) of a stem steady state heat energy balance sensor is determined in the field by assuming that negligible sap flow occurs during the night and therefore that the energy flux transported in the sap stream, E_{sap} (W) is close to zero. The gauge conductance directly determines the radial heat flux E_{radial} (W) which is then iteratively altered to force the sap flux, defined as the residual energy flux divided by c_p dT_{stem} (where c_p is the specific heat capacity and dT_{stem} is the stem temperature difference), to zero. The disadvantage of this technique is that it assumes that the sap flux is zero whether it is or not. We propose a method based on laboratory measurements. *A priori* knowledge of stem thermal conductivity is required for the determination of gauge conductance. We also discuss the use of the measurement of the thermal conductivity of plant stems.

Thermal conductivity probes have been used for laboratory measurements of soil thermal conductivity. The thermal conductivity probe placed in porous media measures the thermal conductivity of that media. In this study, we use these probes for the measurement of stem thermal

conductivity K_{stem} (W m^{-1} K^{-1}). The operation of the thermal conductivity probe involves heating it at a constant rate and determining its temperature, using a thermocouple, at predetermined times. In a short time period t_2 - t_1 for which a temperature difference T_2 - T_1 results, $(T_2 - T_1) = [\overline{q}/(4\,\pi\,K)] \cdot \ln(t_2/t_1)$ where $\overline{q}$ is the average power applied to the sensor per unit sensor length and K is the media thermal conductivity (W m^{-1} K^{-1}). Hence a plot of T_2 - T_1 *vs* $[\overline{q}/(4\,\pi)] \cdot \ln(t_2/t_1)$ (since $\ln(t_2/t_1)$ is the independent variable) has a slope of $1/K$. The power per unit length of probe is the average power applied per unit length from just after the probe is heated until a few minutes later. Hence, K = 1/slope. The initial temperature increase due to the application of heating current should not be used as the measured temperature is affected by the probe during this time and does not represent media thermal conductivity. The y-intercept of relationship T_2 - T_1 *vs* $[\overline{q}/(4\,\pi)] \cdot \ln(t_2/t_1)$ is zero. For if not, the temperature of the porous media during measurement may have altered.

The stem thermal conductivity is an important parameter that affects the calculation of gauge conductance K_{gauge} in stem gauge measurements. We wanted to directly determine the thermal conductivity of *E. grandis* stems as well as that of a dowel rod which could then be used as a reference. These measurements would then assist in the determination of stem gauge conductance, an important factor in the measurement of stem flow rate. The stem thermal conductivity directly affects the gauge conductance.

4.6.7.2 Materials and methods

Four dowel rods, supplied with the Dynamax (Houston, Texas, USA) SGB25-ws stem gauges were initially used for the thermal conductivity determinations and subsequently also used for the determination of stem gauge conductance. Each rod was drilled with a single hole to accept a probe inserted axially in the rod. The sensors were connected to a Campbell Scientific (Logan Utah, USA) CR7X datalogger. The rods and sensors were placed in an insulated box in an office. The datalogger was programmed to power each sensor every four hours and, at the same time, measure the temperature of each probe during heating, and the power supplied to the heater from 4 s after the start of heating until 201 s.

The probe (available from Decagon, Pullman, Washington, USA) is heated at a constant rate and its' temperature determined, using a thermocouple placed inside the probe, at predetermined times on a logarithmic scale. The heating is accomplished by applying a 5 V continuous analogue output voltage from the datalogger to the heater wire placed inside the sensor. The power used was the average power from 4 to 211 s after the application of the heat. The initial temperature increase due to the application of the heating current was not used since during the first 4 or so seconds, the measured temperature was affected by the probe itself and for this period did not represent the thermal conductivity of the porous media. Hence, we chose t_2 = 4 s.

The thermal conductivity of *E. grandis* stems were also measured. Following removal of stems from the trees, the 300-mm long stems were covered with cling wrap to prevent water loss. After the thermal conductivity measurements, the stems were weighed, oven-dried and reweighed for calculation of stem water content.

Following the thermal conductivity measurements, three gauges were attached to three separate dowel rods. The 25-mm diameter rods, with attached gauges, were placed in an insulated box. For almost a week, a voltage of between 4.34 and 4.65 V was applied to three stem gauges and the normal temperature differences and voltages associated with stem gauge measurements were monitored using

a CR7X datalogger. For each 30-minute interval, energy fluxes associated with the radial, vertical and heater terms were calculated. The E_{sap} (or residual) values for the dowel rod were calculated for each 30-min period as $E_{heater} - E_{vertical} - E_{radial}$ where the radial flux was calculated as the product of the thermopile voltage $V_{thermopile}$ and the gauge conductance K_{gauge}. The E_{sap} values were converted into sap flux M_{sap} by dividing E_{sap} by $c_p\, dT_{stem}$ where c_p is the specific heat capacity of water and dT_{stem} is the stem temperature difference. This procedure was repeated by varying the gauge conductance K_{gauge} values from 1.00 to 2.50 W mV^{-1}. Since the sap flux M_{sap} for the dowel rod should ideally be zero, we calculated the mean of all of the M_{sap} values for a six day period for the dowel rod as a function of K_{gauge}. The actual gauge conductance corresponded to that for which $M_{sap} = 0$ kg h^{-1}.

4.6.7.3 Results and discussion

4.6.7.3.1 Thermal conductivity measurements for dowel rod and stems

A typical plot of the temperature difference $T_2 - T_1$ vs $[\overline{q}/4\,\pi] \cdot \ln(t_2/t_1)$ for a wooden dowel rod is shown (**Fig. 4.32**). For this relationship, the slope was 9.8624 m K W^{-1} resulting in a dowel rod thermal conductivity of 0.1014 W m^{-1} K^{-1}. The measurement of the thermal conductivity for four dowel rods was performed during a four-day period. The data are shown in **Table 4.8**. There were significant statistical differences in $K_{dowelrod}$ between rods (at the 95 % level of significance). For this reason, the individual $K_{dowelrod}$ values were used in the subsequent measurements of stem gauge conductance K_{gauge}.

A typical plot of the temperature difference $T_2 - T_1$ vs $[\overline{q}/4\,\pi] \cdot \ln(t_2/t_1)$ for the stem of a *E. grandis* tree is shown (**Fig. 4.33**). For this relationship, the slope was 2.4704 m K W^{-1} resulting in a

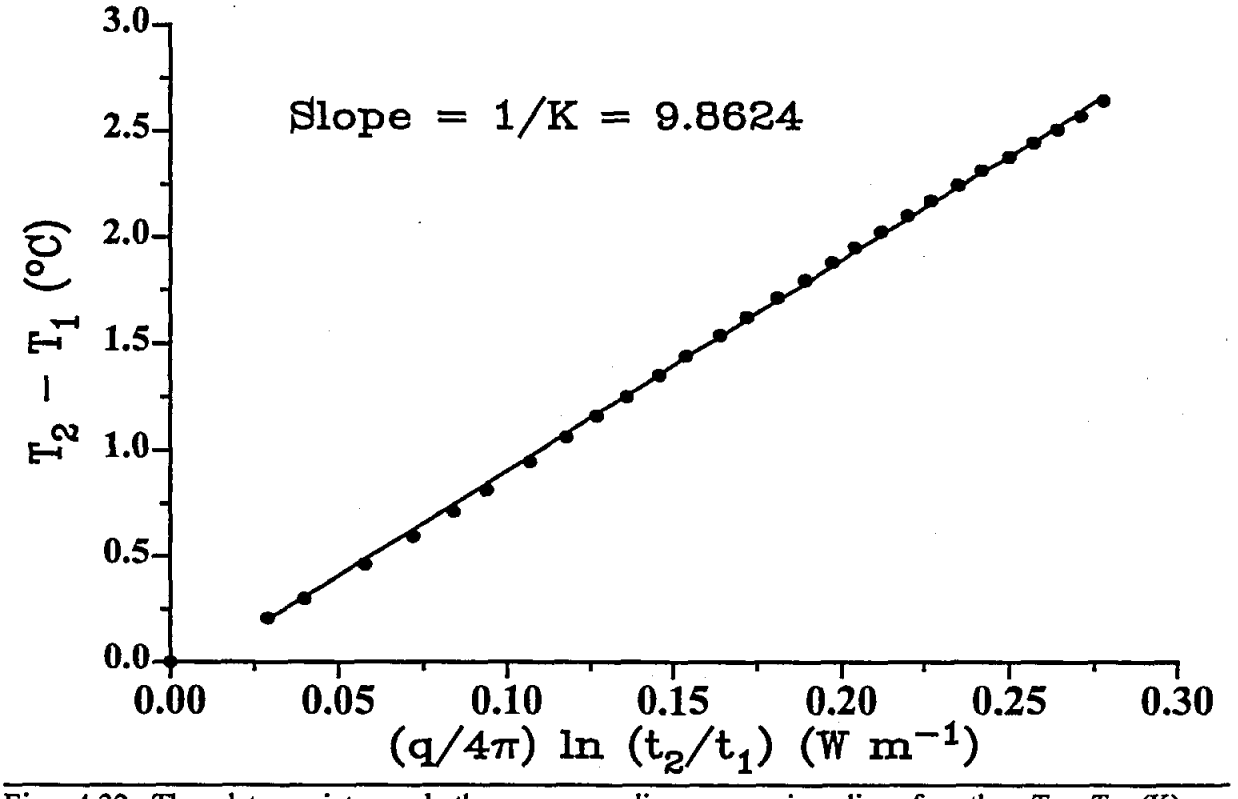

Fig. 4.32 The data points and the corresponding regression line for the $T_2 - T_1$ (K) *vs* $[\overline{q}/4\,\pi] \cdot \ln(t_2/t_1)$ (W m^{-1}) relationship for a wooden dowel rod

Table 4.8 The measured thermal conductivity values for the four wooden dowel rods $K_{dowelrod}$ (W m^{-1} K^{-1}) obtained during a three-day period using four thermal conductivity probes. During this time period, temperature varied between 27 and 32 °C

Day (1991) and time	$K_{dowelrod}$ W m^{-1} K^{-1}			
	Sensor #1	Sensor #2	Sensor #3	Sensor #4
Day 348, 12h00	0.10107	0.09250	0.12286	
16h00	0.10127	0.09273	0.12303	0.11765
20h00	0.10112	0.09278	0.12306	0.11752
Day 349, 00h00	0.10129	0.09271	0.12305	0.11776
04h00	0.10139	0.09281	0.12305	0.11777
08h00	0.10101	0.09262	0.12292	0.11749
12h00	0.10107	0.09267	0.12296	0.11758
16h00	0.10107	0.09267	0.12281	0.11787
20h00	0.10117	0.09277	0.12309	0.11832
Day 350, 00h00	0.10129	0.09287		
04h00	0.10131	0.09288	0.12326	0.11781
08h00	0.10124	0.09278	0.12323	0.11786
12h00	0.10119	0.09281	0.12313	0.11775
16h00	0.10120	0.09275	0.12304	0.11777
20h00	0.10141	0.09287	0.12338	0.11797
Day 351, 00h00	0.10123	0.09280	0.12317	0.11789
04h00	0.10127	0.09291	0.12304	0.11777
08h00	0.10107			
Mean	0.10120	0.09276	0.12308	0.11779
SD	0.00011	0.00010	0.00014	0.00019
n	18	17	16	16
Overall mean		0.1081		
SD		0.0122		
n		67		

stem thermal conductivity of 0.4048 W m^{-1} K^{-1}. The measurement of the conductivity for two stems was performed during a two-day period. The data are shown in **Table 4.9**. There were significant statistical differences in K_{stem} between stems (at the 95 % level of significance). The average value shown in Table 4.8 (*viz.* 0.3435 W m^{-1} K^{-1}) was used as the stem thermal conductivity for *E. grandis* for all subsequent stem gauge measurements.

4.6.7.3.2 Gauge conductance measurements

We wished to determine gauge conductance by applying gauges to wooden dowel rods. For these rods, the condition that M_{sap} = 0 kg h^{-1} must clearly be satisfied at all times. We had previously attempted such measurements in the field environment but we were unable to maintain the necessary temperature control, particularly after sunrise. We therefore resorted to determining the energy flux components on a dowel rod, under isothermal laboratory conditions, for which the thermal conductivity was known. Measurements of the various temperature differences and voltages were performed for a six-day period. Typical data for Day 351 to 353 (1991) are shown (**Fig. 4.34**). As expected, the $V_{thermopile}$, V_{upper} and V_{lower} voltages are all reasonably constant. Although the V_{heater} voltage appears variable, due to the scale used, there is less than a 1 % variation at all times. The dT_{stem} varied in sympathy with the changes in V_{heater}.

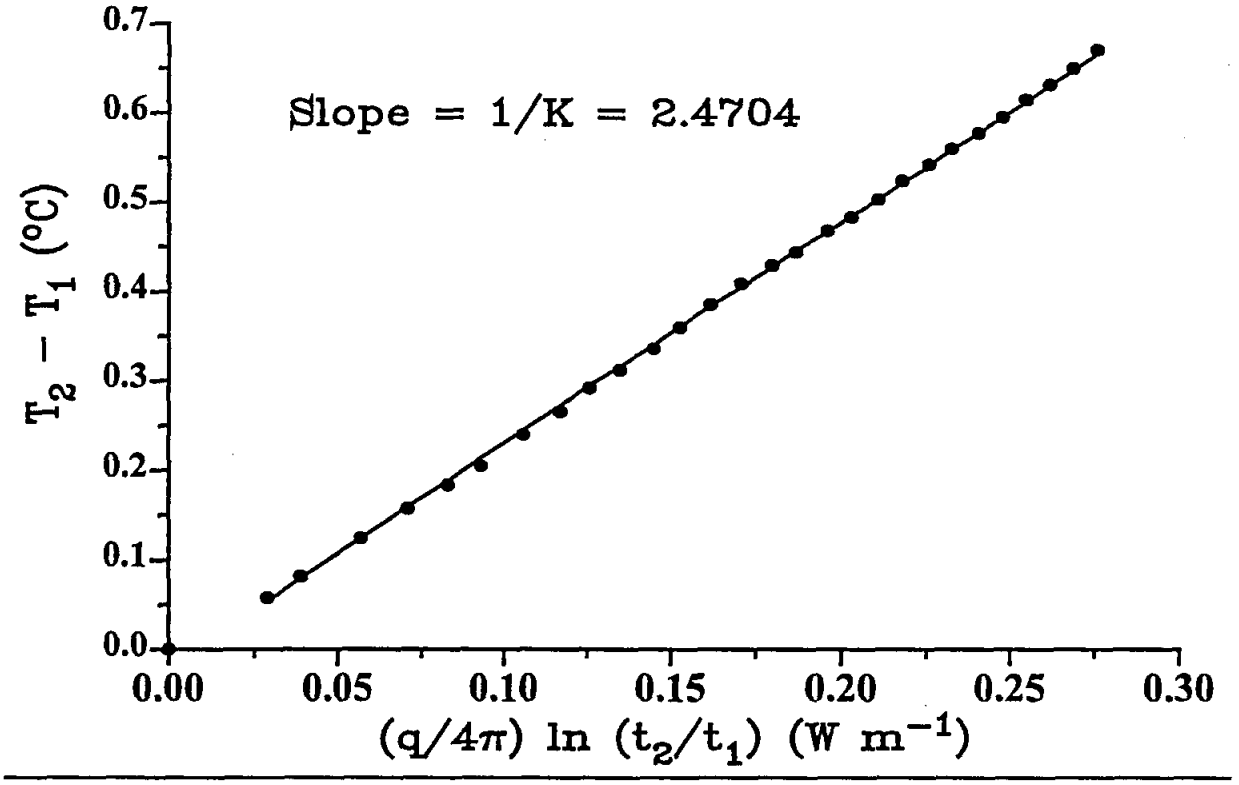

Fig. 4.33 The data points and the corresponding regression line for the $T_2 - T_1$ (K) *vs* $[\bar{q}/4\,\pi] \cdot \ln(t_2/t_1)$ (W m^{-1}) relationship for an *E. grandis* stem

Table 4.9 The measured thermal conductivity K_{stem} (W m^{-1} K^{-1}) values for two *E. grandis* stems for a two-day period. During this time period, temperature varied between 28 and 32 °C. The average stem water content was 58.5 %

Day (1991) and time	K_{stem} (W m^{-1} K^{-1})	K_{stem} (W m^{-1} K^{-1})
359, 08h00	0.2995	0.4048
359, 00h00	0.2974	0.4046
359, 04h00	0.2939	0.4040
359, 08h00	0.2883	0.3957
359, 12h00	0.2850	0.3882
359, 16h00	0.2842	0.3895
359, 20h00	0.2858	0.3977
360, 00h00	0.2856	0.4028
360, 04h00	0.2858	0.4043
360, 08h00	0.2815	0.3977
360, 12h00	0.2812	0.4013
360, 16h00	0.2815	0.4030
Averages	0.2875	0.3995
SD	0.005591	0.005945
Overall mean	0.34346	
Overall SD	0.056293	

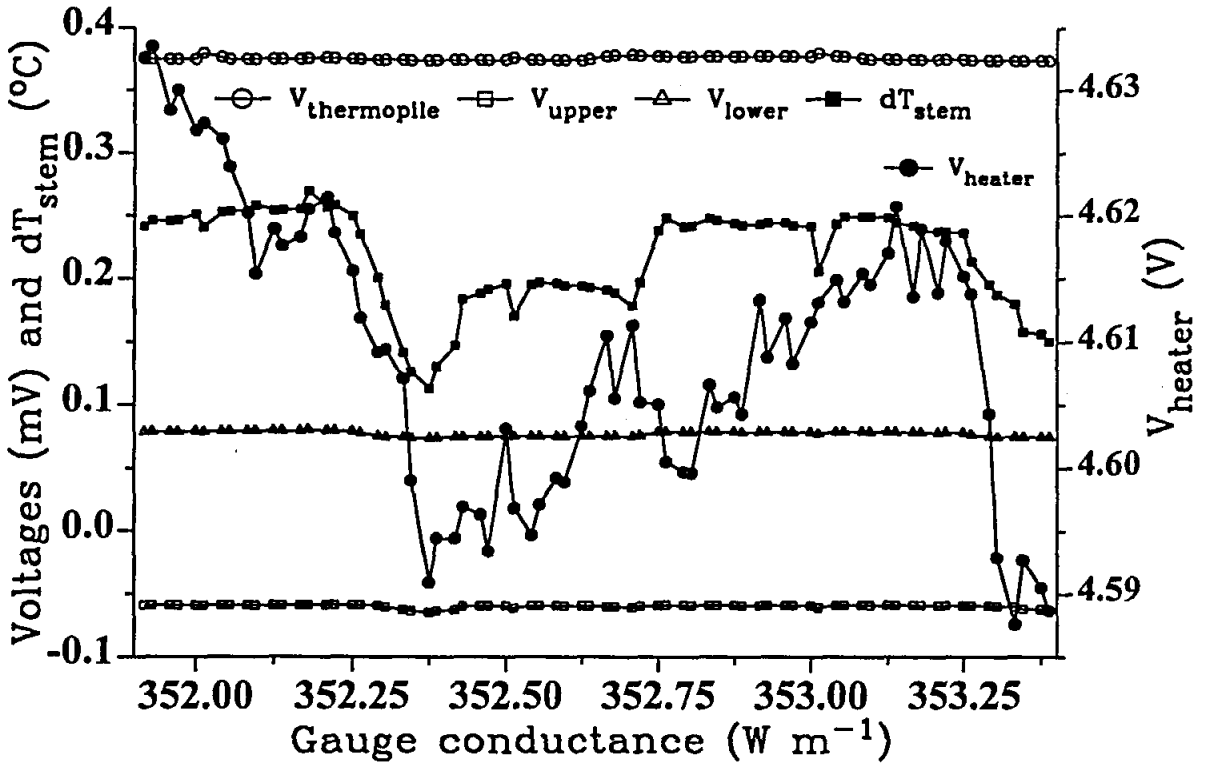

Fig. 4.34 The variation in the voltage components $V_{thermopile}$, V_{upper}, and V_{lower} and the temperature dT_{stem} with local time for stem gauge # 1 attached to a wooden dowel rod. Measurements were performed in an office on Day 351 at 21h00 until Day 353 at 11h00 (1991)

From the data collected, it was possible to recompute M_{sap} for the three gauges for K_{gauge} arbitrarily varying between 1.0 and 2.5 W mV^{-1}. This range was chosen to yield both negative and positive sap fluxes. The relationship between calculated sap flux M_{sap} and gauge conductance K_{gauge} was determined for each gauge (**Fig. 4.35**). For the three gauges chosen, three different K_{gauge} values result in a zero sap flux. The computed gauge conductance was 1.32, 1.18 and 1.91 W mV^{-1} for gauges #1, #3 and #4 respectively. The standard deviation in M_{sap} as a function of K_{gauge} varied considerably (Fig. 4.35), approaching a minimum value around the correct K_{gauge} value. It would appear that the K_{gauge} value can vary between gauges and would therefore need to be determined for each gauge.

4.6.7.4 Conclusions

Laboratory measurements of the thermal conductivity of 25-mm diameter *E. grandis* stems averaged 0.3435 W m^{-1} K^{-1}. This value is lower than the value of 0.54 W m^{-1} K^{-1} used by many workers for herbaceous plants. Dowel rod thermal conductivity averaged 0.1081 W m^{-1} K^{-1} (with a standard deviation of 0.0122 W m^{-1} K^{-1}). Stem gauge conductance was determined by measuring the component energy fluxes with gauges applied to dowel rods (with known thermal conductivity values). These data allowed the sap flux to be calculated as a function of gauge conductance varying between 1.0 and 2.5 W mV^{-1}. The gauge conductance corresponding to a zero sap flux was 1.32, 1.18 and 1.91 W mV^{-1} for gauges #1, #3 and #4 respectively. We conclude then that it is necessary to determine the gauge conductance, in the manner described, for each gauge used.

Chapter 5

Sap flow and aerodynamic evaporation techniques for the separation of total evaporation into canopy transpiration and soil evaporation

5.1 Abstract

Efficient water management of a soil and plant system requires adequate knowledge of the separate components of soil evaporation and canopy transpiration. Sap flow techniques, together with knowledge of leaf area index or plant population density, allow for the measurement of canopy transpiration rate. However, transpiration is one component of total evaporation. In a partially covered row system, there is a need for the separate determination of canopy transpiration and soil water evaporation. In this integrative study, sap flow was measured using 25-mm diameter stem gauges using the stem steady state heat energy balance technique and total evaporation was measured using Bowen ratio (BR) and eddy correlation (EC) techniques. Soil water evaporation was calculated by subtracting canopy transpiration from total evaporation. For a period of five days, the total evaporation was 14.45 mm, the soil evaporation was 7.81 mm and the canopy transpiration 6.64 mm. Soil evaporation was therefore 54.4 % of the total evaporation for the five days. The integrity of the data was checked by comparing the calculated soil latent heat density as the difference between latent heat density (averaged from BR and EC data) and the actual soil water evaporation obtained from 19 microlysimeters (sunrise to sunset measurements). For one day, the spatial variation in the soil microlysimeter daily total evaporation was between 0.77 to 1.75 mm. For this period, the soil evaporation calculated from the difference between total evaporation (average of BR and EC evaporation) and stem gauge canopy transpiration was 1.70 mm. The study further confirmed the use of the 25-mm diameter gauges for the measurement of sap flow in plant stems. This is the first attempt at separating total evaporation into its two components for the row system studied.

5.2 Introduction

In row crops, compared to fully closed canopies, soil water evaporation may be an important water loss component that requires effective management if water use efficiency is to be improved. For such systems, there is insufficient knowledge of the relative values of soil evaporation and canopy transpiration. Usually, because of the measurement difficulties involved in partitioning the two components, soil evaporation is usually considered negligible. The stem steady state technique allows for the measurement of canopy transpiration directly with the Bowen ratio and eddy correlation techniques (Savage *et al.*, 1997) used for measuring total evaporation. It is therefore possible, in theory, to calculate soil evaporation from the difference between the total evaporation and measured canopy transpiration. Very few workers have attempted to separately measure the soil evaporation and canopy transpiration. The stem steady state technique therefore represents a powerful technique for determining this separation. This measurement, integrated over a day, is compared with the daily total soil evaporation using soil microlysimeters.

It is common practice in South Africa, especially in the case of maize, to increase the row width under water limiting conditions compared to the USA for example. Under conditions of increased row spacing, soil water evaporation may however be increased with the result that there are little water

savings. It is therefore important to investigate the importance of soil water evaporation relative to total evaporation. Methodology for the partitioning between soil water evaporation and canopy transpiration is difficult but the techniques investigated in this report and in a previously published Water Research Commission report allow for this to be done. The measurement of canopy latent heat (canopy transpiration) is possible with the use of stem gauges and with the simultaneous measurement of total evaporation from Bowen ratio (BR) and eddy correlation (EC) measurements, the soil latent heat (soil water evaporation) may be calculated by difference.

The aim of this work is to demonstrate the use of these measurement techniques for the calculation of soil water evaporation. For one day only, the soil water evaporation so-calculated is compared with soil microlysimetric evaporation measurements. This work illustrates the usefulness of the stem steady state heat energy balance technique in conjunction with aerodynamic techniques that are described by Savage *et al.* (1997). The link between the two research programs has therefore clearly been established.

5.3 Materials and methods

5.3.1 Experimental site

The experiment was conducted in a 183 m by 274 m vineyard of six-year old Chardonnay plants on the Delaney vineyards located at Lamesa, TX (33.50 N, 1020 W). The vineyard configuration was a vertical bilateral cordon with the cordon wire at 1.0 m above the soil surface, and catch wires at 1.25 and 1.5 m above the soil surface at a north-south orientation. Average plant height during the experiment was 1.6 m, while average plant width was 0.4 m. Row and plant spacing were 3 m and 1.7 m respectively, and the soil between rows were bare. A cotton field bordered the north edge of the Chardonnay block with the cotton at the seedling stage. Pasture was east of the block, while bare soil was south. A similar size vineyard of Cabernet Sauvignon plants was immediately adjacent to the west. The bare interrow having been ploughed a few days before measurements were performed.

5.3.2 Energy balance measurements[1]

Bowen ratio (BR) and eddy correlation (EC) methods are used to measure one or more of the energy balance components (Savage *et al.*, 1997). These and other measurements allow for the determination of total evaporation. Today the BR method is regarded as a common method for the measurements of total evaporation. Sensible heat flux density was determined using two eddy correlation systems and four Bowen ratio systems. For each EC system, fluctuations in wind speed w' and air temperature T' were measured using a CA27 sonic anemometer and a 127 fine wire chromel-constantan thermocouple (available from Campbell Scientific, Logan, Utah, USA). The 127 thermocouple supplied with the eddy correlation equipment allows a temperature difference measurement but not an absolute temperature measurement. Due to the fact that the response time of the reference junction could vary between 5 and 20 minutes (Biltoft, 1991, personal communication), the reference junction of the 127 thermocouple inside the metal arm of the sonic anemometer was further insulated. Also, the vertical metal arm of the sonic anemometer, housing the reference junction, was heavily insulated. The

1 The BR and EC measurement procedures are described in the Water Research Commission report by Savage *et al.* (1997)

datalogger program enabled the determination of $\overline{w'T'}$ in real-time. A 12-minute averaging period was used for all final measurements. Input measurements were performed every 0.1 s (corresponding to a frequency of 10 Hz). We used an air density of 1.07 kg m^{-3} and a specific heat capacity of 1056 J kg^{-1} K^{-1} for the calculation of F_h. Both EC systems were nearly 75 m from the south edge of the vineyard and 60 m from the east edge. The predominant wind direction was from the south and the canopy rows ran from 10° east of south to 10° west of north. It was not possible to place the eddy correlation systems any further south from the edge of the vineyard. The two EC systems were situated between two Bowen ratio system pairs, about 30 m from each pair. All EC measurements were obtained by placement of the system 1 m directly above the canopy surface (measured with the fine-wire thermocouple) with the thermocouple arm of the EC systems pointing in the southerly direction.

A number of REBS Q*6 net radiometers were used to measure net irradiance I_{net} (W m^{-2}). Two Middleton soil heat flux plates were placed at a depth of 100 mm and the heat flux density component stored above the plate calculated from soil's specific heat capacity and temporal change in soil temperature with F_s being defined as the sum of the former two flux densities. Soil temperature was measured using two pairs of chromel-constantan thermocouples, one pair placed at different positions but at a depth of 20 mm and the other pair at a depth of 80 mm. The one sensor was placed in the interrow and the other in the row in order to obtain an average measurement.

Bowen ratio sensible heat flux density was measured using four independent systems designed by Gay and Greenberg (1985) and used by Heilman *et al.* (1989) in their determination of Bowen ratio fetch requirements. Each system consisted of two exchanging wet and dry bulb psychrometers, net radiometers and three soil heat flux plates and soil temperature thermocouples. Measurements of sensible heat were obtained for two 3-minute periods every 12 minutes. The remainder of the time was required for exchanging the psychrometers and for sensor equilibration.

5.3.3 Determining canopy and soil latent heat flux densities

Canopy latent heat flux density ($(L_v F_w)_{canopy}$) was obtained from heat balance, sap flow measurements of transpiration (Sakuratani, 1981; Baker and Van Bavel, 1987). Lascano et al. (1992) found that heat balance measurements of transpiration in grapevines was accurate to within 5 to 10 % of gravimetric measurements of transpiration. Sap flow gauges (Model SGA 25, Dynamax, Inc., Houston, TX) were attached to trunks of 10 plants located an average distance of 43 m south of the Bowen ratio systems. Insulation was placed above and below the gauges to reduce effects of the environment on trunk heat balance. Gauges were sampled ever 15 s using a model CR7X data logger (Campbell Scientific Inc., Logan, UT) and 12 min averages computed for data storage. Sap flow measurements were converted to latent heat flux per unit land area by normalizing the measurements on a plant population basis. Mean $(L_v F_w)_{canopy}$ (W m^{-2}) was calculated as

$$(L_v F_w)_{canopy} = L_v \Sigma (M_{sap\,i}\, \rho_{plant})/n \qquad 5.1$$

where L_v is specific latent heat of vaporization ($\approx$ 2.45 MJ kg^{-1}), $M_{sap\,i}$ is sap flow (kg s^{-1}) of plant i, ρ_{plant} (plants m^{-2}) is the plant density and n is number of plants. Soil latent heat flux density $(L_v (F_w)_{soil})$ was calculated as

$$L_v (F_w)_{soil} = L_v F_w - (L_v F_w)_{canopy} \qquad 5.2$$

where $L_v F_w$ is the total latent heat flux density of the vineyard as measured by the eddy correlation and

Bowen ratio methods. Ham *et al.* (1990) used the above procedure to partition $L_v F_w$ from a cotton canopy at partial cover, and found that values of $L_v (F_w)_{soil}$ calculated with Eq. 5.2 were within 11 % of microlysimeter measurements.

5.3.4 Daily soil water evaporation measurements

In row crops, soil water evaporation may be larger than in the case of a fully closed canopy. The procedures for the measurement of soil water evaporation involved the placement of hollow cylindrical aluminium tubes pushed in soil at sunrise. The cylinders were removed and their masses determined and the tubes then returned to the same position from which they were removed. The cylinders were then removed at sunset. The difference in mass between two times divided by the product of the density of water and the area of the tube is the total soil water evaporation (in mm) for the given time period. In inserting and removing the tubes from soil, it was important that the soil surface disturbance was kept to a minimum. The surface of the tube was at the same level as the soil surface so as not to alter the wind regime above the soil surface.

Aluminium cylinders with a diameter of 73 mm and a height of 125 mm, sharpened at the one end were used. A small amount of teflon spray was used to ease the insertion of the microlysimeters in the soil. Care was required to ensure minimal alteration to the soil surface. Another aluminium microlysimeter placed on top of the microlysimeter in the soil was used to carefully push the microlysimeter into the soil so that the surface of the first microlysimeter was flush with the soil surface. Once the microlysimeter had been inserted into the soil, it was then carefully removed using a pair of pliers. On occasion a pancake knife was pushed down the outside of the microlysimeter. A force on either side of vertical was used to break away the soil at the base of the microlysimeter. Once the microlysimeter was removed from soil, the bottom end of the microlysimeter was covered with two layers of aluminium foil. The microlysimeter was numbered at the top and then placed in a sealed plastic bag. The assembly was then returned to the hole in soil. Excess plastic from the bag was folded to ensure that no plastic protruded above the soil surface. At sunrise, the microlysimeters were removed from soil, the bags sealed and then transported to the balance. Prior to mass determination, the bags were removed but the aluminium foil kept in place. After mass determination for all microlysimeters, the microlysimeters were sealed in their bags, and then returned to soil. As before, the plastic was folded to ensure no plastic protruded above the soil surface. At sunset, the microlysimeters were removed from the soil and weighed. The difference in mass (in grams) between sunrise and sunset divided by 4.1853 (for the microlysimeters we used) was the total soil water evaporation in mm for the day.

For the Lamesa vineyard row width of about 3 m, six microlysimeters at roughly equal distances were placed across the row for three rows. The evaporation measurements were averaged for all eighteen microlysimeters.

5.4 Results and discussion

5.4.1 Stem gauge measurements

The variation in canopy latent heat flux density $L_v (F_w)_{canopy}$ in a vineyard was observed by comparing the measured values from six different vines (**Fig. 5.1**). Relative to the calculated mean canopy latent heat flux density, the standard deviation in the measurements from the six vines was high in the early morning. This relatively high value in the early morning may have been due to the flow of overnight

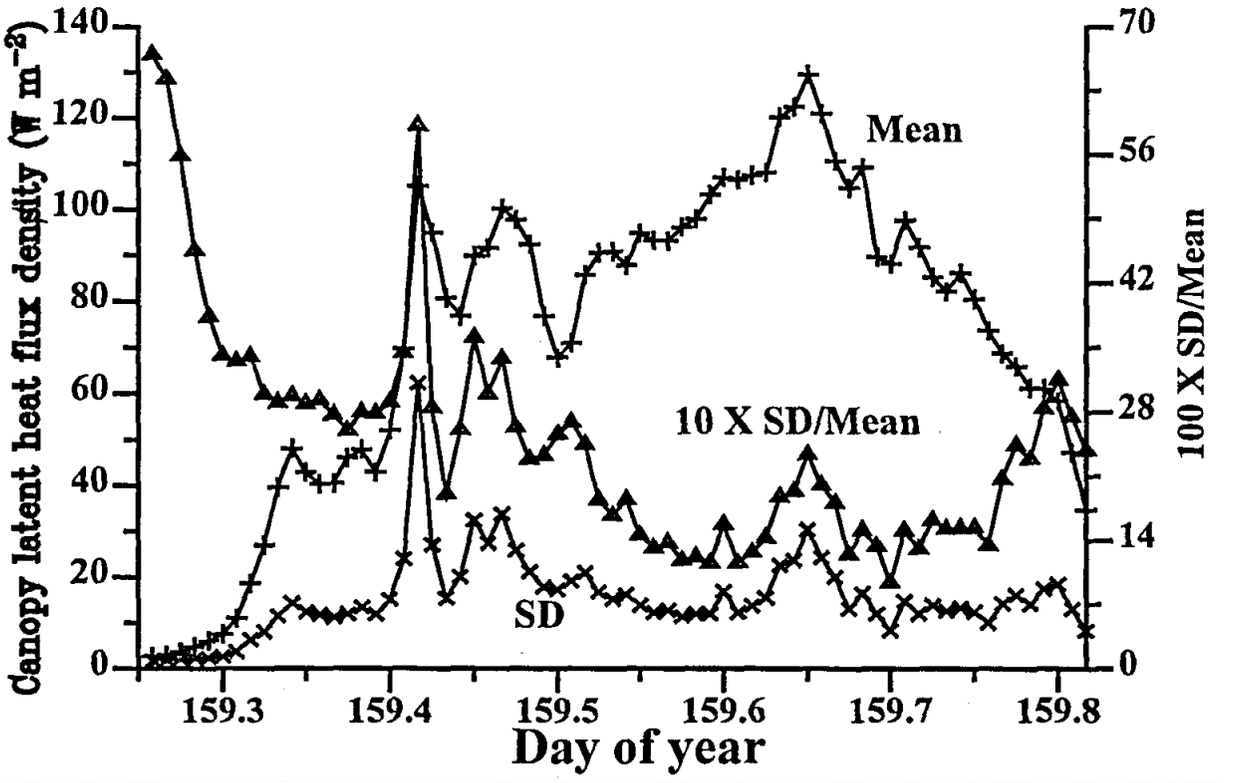

Fig. 5.1 The diurnal variation in the mean (+) and standard deviation (x) of the canopy latent heat flux density L_v $(F_w)_{canopy}$ (W m^{-2}) from six gauges for Day 159 (1992). Also shown (right-hand y-axis) is the variation in the standard deviation to mean ratio (expressed as a percentage)

heated sap moving past the thermocouples but it may have also been due to the non-steady state condition that may occur at sunrise. Also of particular note is the decrease in the standard deviation to mean canopy latent heat flux density with time after sunrise although this may be partly attributed to the increase in the mean value soon after sunrise. It would appear then that measurements from a single vine are insufficient to describe canopy latent heat flux density.

The hypothesis that a single K_{gauge} value can be used for a number of different gauges placed in a vineyard containing similar vines was tested. The diurnal variation in K_{gauge} for a couple of days for six gauges is shown. While some of the gauges had the same value K_{gauge} for extended periods, others had very different values (**Fig. 5.2**). It could be that the contact between stem and gauge was not the same for all gauges. The evidence presented therefore indicates that it is necessary to obtain K_{gauge} values for each gauge. Without lysimetric measurements, the K_{gauge} value was defined as that obtained by setting $E_{sap} = 0$ during the early morning hours.

Crucial to the calculation of M_{sap} (g s^{-1}) is the dT_{stem} value. This term appears in the denominator of the M_{sap} equation and it is therefore imperative that its value be examined in real-time to take decisions about increasing or decreasing the power supplied to the heater. The diurnal variation in dT_{stem} is shown for Days 153 and 154 (**Fig. 5.3**). In this experiment, the power to the heater was not switched off at night. This omission resulted in quite large dT_{stem} values (exceeding 5 °C during the night). During the day however, on occasion, there was insufficient power supplied to the heater (particularly on Day 154). On this day, for some of the gauges, the dT_{stem} value approached 0 which resulted in unstable canopy latent heat flux density L_v $(F_w)_{canopy}$ values. The stem gauge data for Days 154 and

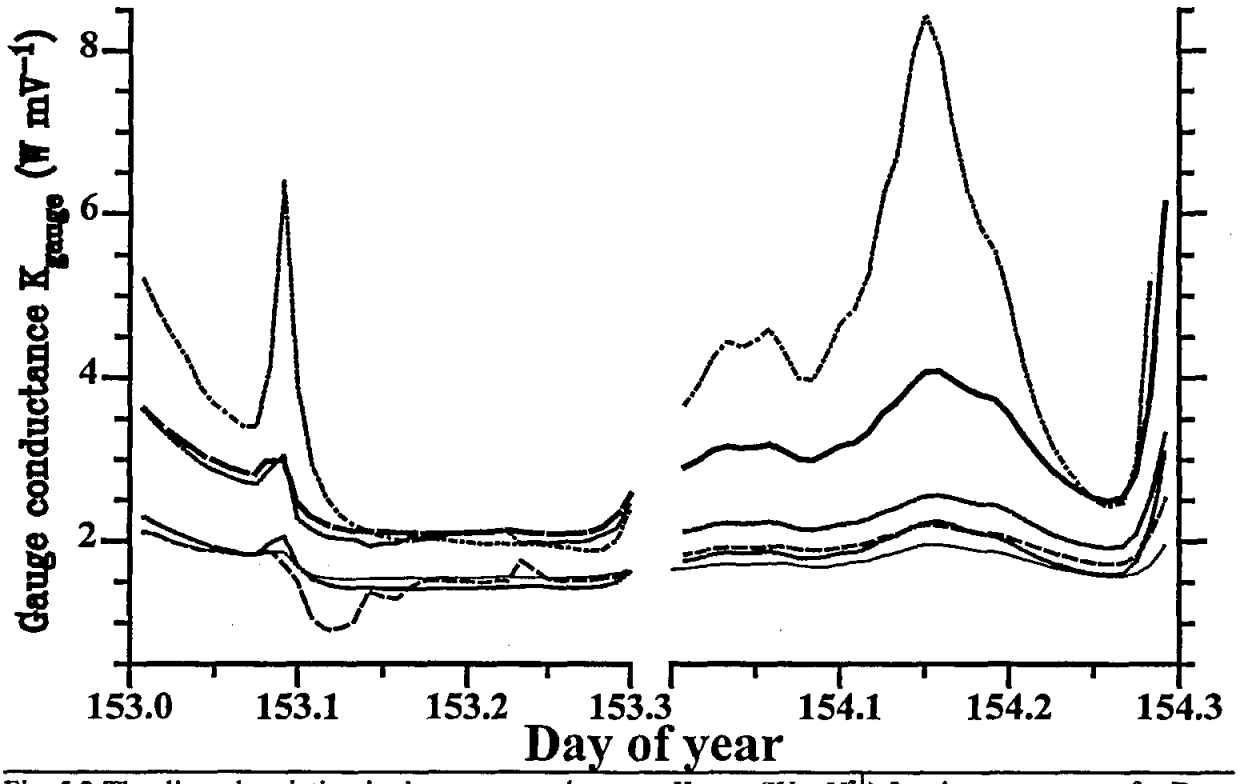

Fig. 5.2 The diurnal variation in the gauge conductance K_{gauge} (W mV^{-1}) for six stem gauges for Days 153 and 154, 1992

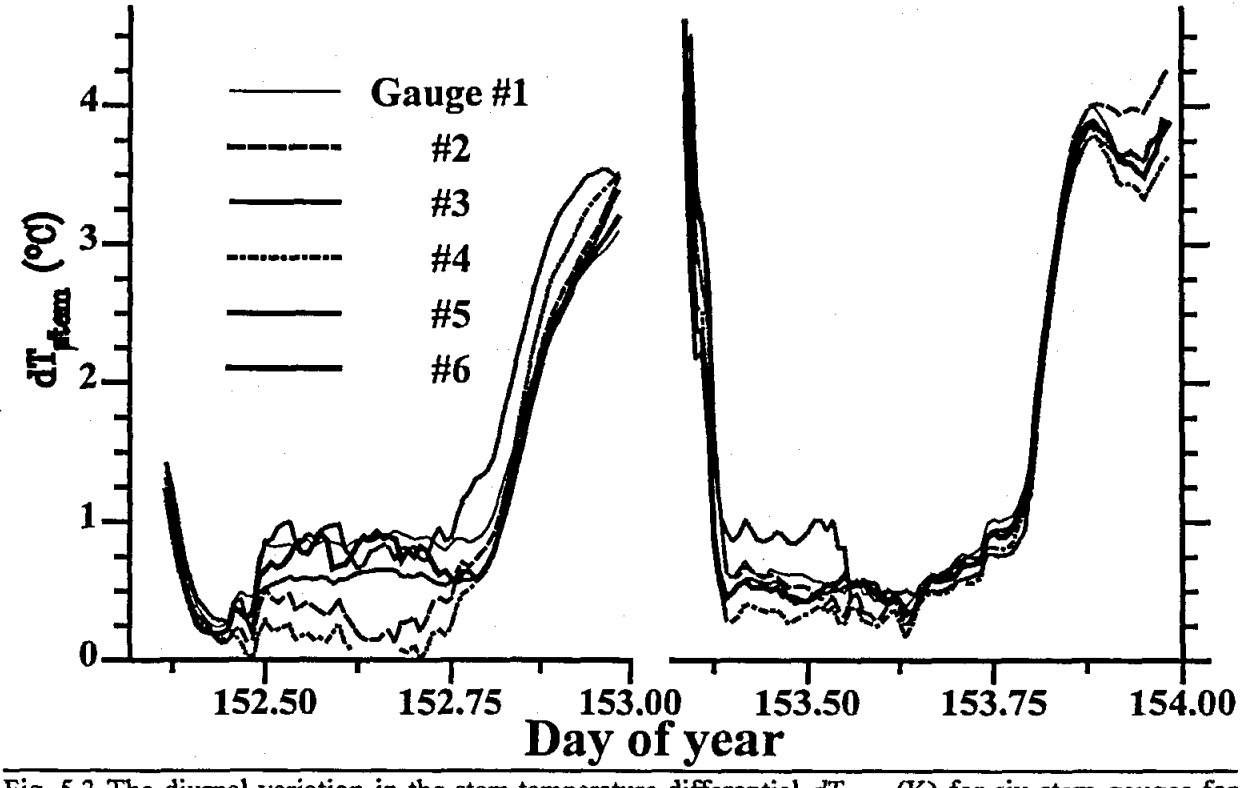

Fig. 5.3 The diurnal variation in the stem temperature differential dT_{stem} (K) for six stem gauges for Days 152 and 153, 1992

155 were excluded due to problems with the power supply. The main limitation of the technique is that under conditions of high canopy transpiration, the values of dT_{stem} decreased too close to zero, causing unreliable M_{sap} measurements, unless power to the heater is increased. However, there is a limit to the amount of power that may be supplied to the heater without sensor damage. The K_{gauge} and dT_{stem} measurements were useful in identifying reliable data.

5.4.2 Canopy and soil latent fluxes

For two typical days (152 and 159), the diurnal variation in the net irradiance, the canopy latent heat flux density $L_v(F_w)_{canopy}$ is shown (**Figs 5.4 and 5.5** respectively). The variation in the total evaporation $L_v F_w$ from the vineyard, calculated as the average of eddy correlation and Bowen ratio latent heat amounts, is shown. Of interest is the relatively close correspondence between the canopy latent heat flux density $L_v(F_w)_{canopy}$ values and the total evaporation flux density $L_v F_w$ measured using the Bowen ratio and eddy correlation techniques before 10h00 and after 18h00 CST. On both days however, the $L_v F_w$ values were greater than the $L_v(F_w)_{canopy}$ canopy measurements in the early morning times. In the late afternoon, the reverse was true: canopy $L_v(F_w)_{canopy}$ values were greater than the total evaporation values $L_v F_w$. Also shown in Fig. 5.4 and 5.5 is the diurnal variation in net irradiance and soil heat flux density. The data for Days 152 and 156 to 159 were integrated from about CST 06h00 to 18h00 (**Table 5.1**). The canopy latent heat, averaged from the six stem gauges, varied from about 2.2 (on Day 152) to 3.7 MJ m^{-2} (on Day 157), equivalent to a variation of 0.9 to 1.5 mm respectively. The soil latent heat density, calculated as the difference between the total latent heat density (the average of the BR and EC latent heat densities) and the canopy latent heat density

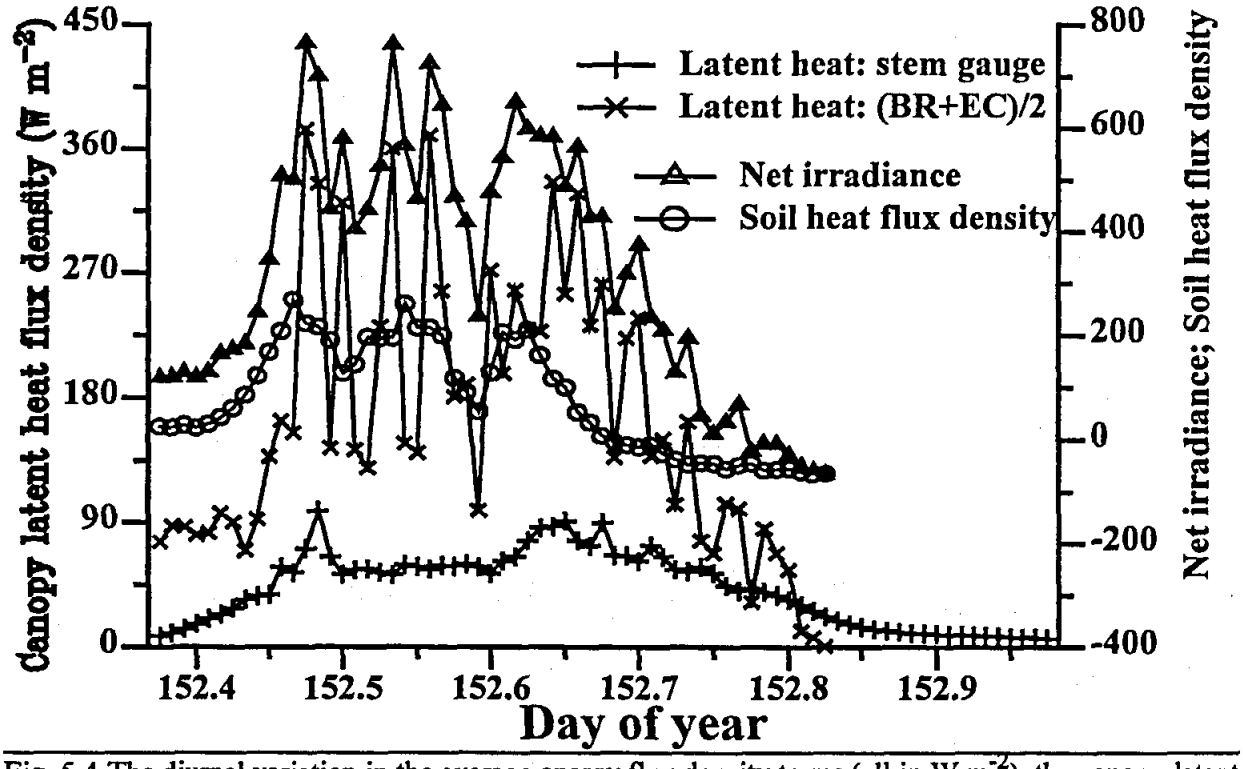

Fig. 5.4 The diurnal variation in the average energy flux density terms (all in W m^{-2}): the canopy latent heat flux density $Lv\,(Fw)_{canopy}$ from six stem gauges, the diurnal variation in the total latent heat flux density $Lv\,Fw$ (the average of the four Bowen ratio and two eddy correlation measurements) and the net irradiance (right-hand y-axis) for Day 152, 1992

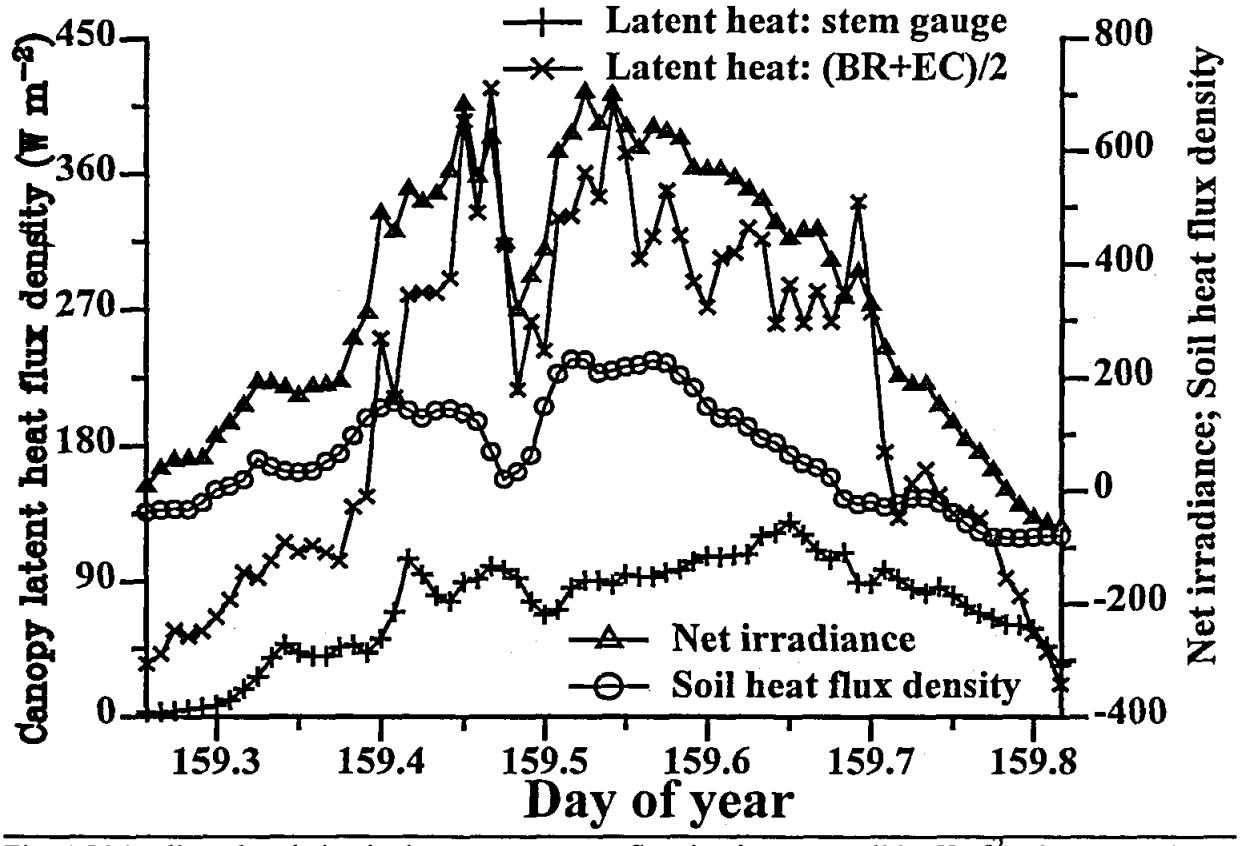

Fig. 5.5 The diurnal variation in the average energy flux density terms (all in W m^{-2}): the canopy latent heat flux density $L_v (F_w)_{canopy}$ from six stem gauges, the diurnal variation in the total latent heat flux density $L_v F_w$ (the average of the four Bowen ratio and two eddy correlation measurements) and the net irradiance (right-hand y-axis) for Day 159, 1992

measured using the six stem gauges, varied between about 3.16 to 4.49 M m^{-2} (equivalent to a variation of 1.29 to 1.84 mm or 1.29 to 1.84 *l* m^{-2}). For Days 152 and 156 to 159, the partitioning of the net radiant density (measured using net radiometers placed above the canopy) was distributed almost equally to canopy latent, soil heat, soil heat and sensible heat densities (apart from Day 158 when soil heat was considerably lower due to a lower net radiant density).

The integrity of the measurements was checked by calculating the difference between net radiant density and the sum of canopy latent heat density, soil latent heat density, soil heat density and sensible heat density. The calculated error was always positive and averaged about 9 % for all days. Considering the errors that are introduced through each component, these errors are not large. However, the fact that the errors are always positive (although only slightly so on Day 157) may imply that there is a bias in the data, either introduced through the theoretical assumptions imposed or a consistent measurement underestimation.

The integrity of the data was further checked by comparing the calculated soil latent heat density, as the difference between latent heat density (averaged from BR and EC data) and the actual soil water evaporation obtained from the sunrise to sunset mass differences from the 19 microlysimeters for Day 157 (**Table 5.2**). The spatial variation in the soil microlysimeter evaporation was between 1.885 to 4.283 MJ m^{-2} (equivalent to a variation of between 0.77 to 1.75 mm). There is therefore quite good correspondence in soil evaporation calculated using the two different measurement methods.

Table 5.1 Total energy balance components for Days 152, 156 to 159, 1992[1]. The last column of the table indicates the sensor used for the particular measurement in that row

Energy term/error	Day of year (1992)					Instrument/comment
	152	156	157	158	159	
Canopy latent heat density (MJ m^{-2}) $\Sigma L_v (F_w)_{canopy} \cdot \Delta t$	2.223	3.567	3.682	3.212	3.582	Average of six stem gauge measurements
Soil latent heat density (MJ m^{-2}) $\Sigma[L_v F_w - \Sigma L_v (F_w)_{canopy}] \cdot \Delta t$	3.566	3.729	4.160	3.164	4.492	Difference between BR and EC latent heat measurementaverages and canopy latent heat measured using six gauges
Soil heat density (MJ m^{-2}) $\Sigma F_s \cdot \Delta t$	3.151	4.506	4.977	1.742	3.149	Soil heat flux plates
Sensible heat density (MJ m^{-2}) $\Sigma[(F_h(EC) + F_h(BR))/2] \cdot \Delta t$	3.156	2.903	4.186	3.547	2.486	Average of BR and EC sensible heat
Above canopy net radiant density (MJ m^{-2}) $\Sigma I_{net} \cdot \Delta t$	13.322	15.436	17.119	12.493	16.642	Net radiometer placed above the canopy
Error (MJ m^{-2})	+1.225	+0.731	+0.114	+0.828	+2.932	Row 5 - sum (rows 1 to 4)
Error relative to net radiant density (%)	+9.2	+4.7	+0.7	+6.6	+23.1	
Total evaporation (mm) $\Sigma [L_v F_w / \rho_w L_v] \cdot \Delta t$	2.37	2.98	3.20	2.60	3.30	From BR and EC measurement averages
Canopy transpiration (mm) $\Sigma [L_v (F_w)_{canopy} / \rho_w L_v] \cdot \Delta t$	0.91	1.46	1.50	1.31	1.46	From the average of six stem gauge measurements
Soil evaporation (mm)	1.46	1.52	1.70	1.29	1.84	Total evaporation - canopy transpiration
Soil evaporation/total evaporation × 100	62	51	53	50	56	Canopy transpiration percentage of total = 100 - value shown

[1]The measurements from six stem gauges were used to determine the daily total canopy evaporation (MJ m^{-2} and in mm). Daily total evaporation was calculated from the average of the BR and EC measurements (MJ m^{-2} and in mm) and the soil evaporation (MJ m^{-2} and in mm) as a difference between the total and canopy daily totals. The difference between net irradiance above the canopy and the sum of the latent heat, sensible heat and soil heat measurements was calculated for each day as an indication of the overall error in the measurements. Note that 1 mm is equivalent to 1 $l\,m^{-2}$

For the five day period, the total evaporation was 14.45 mm, the soil evaporation was 7.81 mm and the canopy transpiration 6.64 mm. Soil evaporation was therefore 54.4 % of the total evaporation for the period

Table 5.2 A comparison between soil microlysimetric measurements of soil water evaporation (sunrise to sunset) against that computed from the difference (for 06h30 to 18h00 CST) between total evaporation (calculated as the average of BR and EC latent heat measurements) and canopy latent heat measurements obtained using six stem gauges for Day 157, 1992

Soil microlysimeter evaporation (n = 19) in mm	1.26 ± 0.49
Soil water evaporation = total evaporation - canopy evaporation (mm)	1.70
Soil microlysimeter evaporation (n = 19) in MJ m^{-2}	3.084 ± 1.199
Soil water evaporation = total evaporation - canopy evaporation (MJ m^{-2})	4.16

5.5 Conclusions

The partitioning of soil water evaporation and canopy transpiration was possible using stem steady state heat energy balance and aerodynamic (such as Bowen ratio and/or eddy correlation) techniques. On virtually all of the days, soil water evaporation exceeded canopy transpiration. On average, for the five experimental days, soil water evaporation was 54 % of the total evaporation. Under water limiting conditions of a wider row spacing, the soil interrow needs to be managed so that, for example, advective influences resulting in hot air from the soil advected across a transpiring canopy, do not diminish the savings. The management of the soil may therefore be as important as managing the crop under water limiting conditions.

Chapter 6

In situ measurement of sap flow in lateral roots and stems of *Eucalyptus grandis*, under conditions of marginality, using a steady state heat balance technique

6.1 Abstract

The steady state heat energy balance technique on stems is a non-destructive technique that allows *in situ* measurement of sap flow rate in herbaceous or woody plants. The technique relies on the continuous application of constant heat energy by a gauge surrounding a portion of a plant limb. We evaluated the use of the technique for measurement of lateral root and stem sap flow rates in *Eucalyptus grandis*. Gauges were attached to three *E. grandis* stems, approximately 100 mm in diameter, and to a lateral root of each tree, approximately 28 mm in diameter. The roots exhibited a similar sap flow pattern to the stems, but with reduced magnitude during the day. Following the diurnal comparison, the lateral roots on one tree was severed, while the tap root of another was also severed. Following severing, the lateral and tap root flow rates increased to meet continued stem sap flow.

6.2 Introduction

Measurement of sap flow rate in stems of herbaceous plants and woody trees is of great interest to researchers working in plant-water relations, micrometeorology, and plant physiology. The recently developed stem steady state heat energy balance method (SSS) for measuring sap flow rate in the stems of plants (Sakuratani, 1981, 1984; Baker and Van Bavel, 1987) provides a useful tool for monitoring sap flow rate of individual plants.

Water extraction from water tables and different soil profiles by trees in the genus *Eucalyptus*, is one of particular interest. In certain locations, some species of *Eucalyptus* are known to have deep roots (Carbon *et al.*, 1982) that can exploit ground water reserves (Greenwood *et al.*, 1985). *Eucalyptus* trees extract water from deep depths, creating soil large soil water deficits (Dye and Olbricht, 1993), compared to a water deficit of less than 150 mm under annual pasture, under similar conditions (Sharma, 1984). By contrast, Baldwin and Stewart (1987) found root densities of irrigated *E. grandis* W. Hill ex Maiden, to be particularly high in the top 300 mm of a soil profile, declining sharply with depth. They also found that in most cases, the highest density of roots occurred immediately below the surface, unless a lack of water or other factors restricted root development in this zone.

Water transport studies have shown that resistance to flow through the root, the root-soil interface or the soil can significantly affect the flux of water through the soil-plant-atmosphere continuum (Tinklin and Weatherley, 1966; Meyer and Ritchie, 1980; Herkelrath *et al.*, 1977; Zur *et al.*, 1982). Running (1980) estimated that soil and root resistance accounted for 52 to 74 % of the total resistance to flow through *Pinus contorta* (Dougl.). Roberts (1977) reported that when 16 m tall *Pinus sylvestris* (L.) were severed from their roots and placed in water, transpiration rates were almost as twice as high as in a rooted control. If the ability to absorb water is a critical limit to water movement through the plant, then it would follow that a plant which has produced a large root system would be able to maintain higher leaf water potentials than the same plant could if it had a smaller root system. The underlying assumption that root resistance to water inflow is always great enough to limit water movement had not been adequately tested, particularly in woody species under field conditions.

Recent development of nonintrusive stem gauges, using the SSS technique, allows direct measurement of water flow rate in stems or branches (Savage *et al.*, 1993a). However, we are unaware of the use of this technique for the measurement of sap flow in roots. Our aim was to evaluate the technique in terms of its capability of providing information on lateral root and stem water flow rates. We used root severing to stop soil water utilization from different depths, as may be represented by soil water depletion in different rooting zones.

To date, published results have been limited to plants with diameters from 8 to 79 mm. Steinberg *et al.* (1989) concluded that there was no contemporary evidence that pointed to a range limit of the technique. We also present data testing the functionality of the SSS techniques SGB100-WS gauge (110 mm diameter) on large *E. grandis* seedling trees (height 10 to 15 m, diameter 1000 to 1100 mm).

6.3 Materials and methods

6.3.1 Bloemendal Site

The experiment was conducted between September and November 1992, at the Bloemendal Experimental Station of the Institute of Commercial Forestry Research (University of Natal), situated 15 km north of Pietermaritzburg (latitude 29°37'S, longitude 30°19'E) at an altitude of 850 m. The site consists of a North-facing slope with gradients of between 17° and 22° (20 to 40 %). The site is regarded as marginal for all commercial forestry crops except wattle (*Acacia mearnsii*) due to the steep slopes, shallow soils and high air temperatures. The mean annual air temperature for this area is 17.3 °C and the mean annual rainfall is 905 mm (Boden, 1991). The soil was of a Glenrosa form (Macvicar *et al.*, 1977) (with a shallow orthic layer of about 150 mm) which had been terraced. The trees were 1.5 m apart with a row spacing of 4 m, resulting in a population density of 1667 trees ha^{-1}.

6.3.2 Materials for the Bloemendaal experiments

Gauges (Steinberg *et al.*, 1990) installed on the stems and on the roots were the commercially available models SGB100-ws and SGB25-ws (Dynamax Inc., Houston, Texas, USA). The mention of trade names or proprietary products does not imply endorsement or otherwise by the authors or their sponsors. An automatic weather station, 10 m from the experiment, included a 207 air temperature and relative humidity sensor (Phys-Chem Scientific Corporation, New York, New York, USA), a LI200S silicon pyranometer (Li-Cor, Lincoln, Nebraska, USA), a TE525 tipping bucket raingauge (Texas Electronics, Dallas, TX, USA) and a ECO model WS/D86 wind speed and direction sensor (ECO, Pretoria, RSA) for the measurement of air temperature and relative humidity, solar irradiance, rainfall, wind speed and wind direction, respectively.

Three dataloggers for the gauges (models 21X and CR7X from Campbell Scientific, Logan, Utah, USA) were used. Voltages were logged every 15 s and averaged or totaled every 15 minutes. Two 12 V batteries with a capacity of 125 A h were used in parallel to power gauges and dataloggers. The batteries were recharged every 2 or 3 days. A voltage of about 8 V was used to power the heater of the large (model SGB100-ws) 100-mm diameter gauges. For measurement of this voltage, potential dividers halved the voltage to 4 V since the datalogger had a voltage measurement limit of about 5.5 V. The appropriate multiplier was used in the datalogger program to record heater voltage required for the calculation of heater power. A voltage of about 4.5 V was applied to the smaller (SGB25-ws) 25-mm diameter gauges.

6.3.3 Methods for the Bloemendal experiments

Data from the automatic weather station, including wind speed (m s^{-1}) at a height of 2 m, the daily average wind speed (km/day), the daily maximum and minimum air temperatures (°C) and daily solar radiant density (MJ m^{-2}) were used to calculate potential evaporation in mm/day (Monteith and Unsworth, 1990). A reflection coefficient of 19 % was assumed for the *Eucalyptus* canopy (Monteith and Unsworth, 1990).

A stem thermal conductivity (K_{stem}) value of either 0.54 or 0.42 W m^{-1} K^{-1} has been assumed for most herbaceous or woody plants respectively (Ham and Heilman, 1990; Steinberg *et al.*, 1990). Savage *et al.* (1993b) obtained an average of measured stem thermal conductivity values for *E. grandis* of 0.34 W m^{-1} K^{-1}. This value was used for our study. The lateral roots, despite being smaller and physiologically different, were also assumed to have a thermal conductivity of 0.34 W m^{-1} K^{-1}. Gauge conductance (K_{gauge}) of the small (model SGB25-ws) 25-mm diameter gauges was assumed to be 1.676 W mV^{-1} (Lightbody, 1993; Savage *et al.*, 1993b). However, the gauge conductance of the larger (model SGB100-ws) 100-mm diameter gauges was determined using apparent values measured at midnight for each day when sap flow rate was assumed to be zero. This latter procedure is similar to that of Steinberg *et al.* (1990).

The details of the experiment are summarized (**Table 6.1**)

6.3.4 Bloemendal experiment A: Stem flow rate measurement.

Branches were carefully removed with a sharp knife from the gauge attachment area (a region from the soil surface to 0.85 m above the soil surface), and the bark sandpapered until smooth using fine (600 grit) emery paper. Dow Corning silicone grease was then applied to the stem and covered with commercially available clingwrap (thin plastic). One SGB100-ws gauge was then attached to each of three tree stems at a height of 0.15 m. Extra insulation was applied to the gauges in an attempt to maintain a steady state condition. Reflective aluminium foil was then wrapped around the extra insulation. White plastic was wrapped around the upper part of each gauge, and sealed against the tree, in order to keep the heater gauge and thermocouples dry from any rain or dew.

6.3.5 Bloemendal experiment B: Root flow rate measurement.

A SGB25-ws gauge was attached to a single lateral root of each of two of the three trees fitted with stem gauges. The top 300 mm of soil at the base of the trees was removed and a procedure, similar to that for the stems but excluding the use of aluminium foil, was used to attach gauges to roots. The excavated soil was then replaced around the lateral roots and attached gauges so that the sensors were entirely below the soil surface. Lateral roots were mostly found in the top 300 mm of the soil profile, despite the low soil water content. Shale restricted lateral root development. The gauges on the lateral roots were placed 900 mm from the stem along the root of tree I, and 300 mm from the stem along the root of tree II, where the root diameters were within the 24 to 32 mm diameter range of a SGB25-ws gauge.

6.3.6 Bloemendal experiment B1: Stem and lateral root flow rate measurements just prior to and after tap root severing.

Following the comparison of the diurnal sap flow rates between the stems and roots of trees I and II, the SGB25-ws gauge was left on the lateral root of tree I and sap flow measurements continued. In order to sever the tap root, soil was removed from the base of the tree again so as to expose the tap root. Without disturbance of the lateral roots, the tap root was severed below the lateral roots at 12h30

Table 6.1 Summary of the procedures and variables involved in Chapter 6

Experiment		
A (stems)	B (roots)	
Measurement of the sap flow rates through the stems of trees 1 and 2	Measurement of the sap flow rates through a single lateral root for trees 1 and 2	
Diameter of stem (tree 1) = 0.0985 m Diameter of stem (tree 2) = 0.1015 m	Diameter of lateral root (tree 1) = 0.0287 m Diameter of lateral root (tree 2) = 0.0271 m	
K_{stem} = 0.34 W m^{-1} K^{-1} K_{gauge} (SGA100-ws) determined using pre-dawn method (i.e. it varies daily)	K_{root} = 0.34 W m^{-1} K^{-1} K_{gauge} (SGB25-ws) determined from Chapter 2 (i.e. 1.656 W mV^{-1})	
Gauge placement: 150 mm above soil surface for both trees	Gauge placement: 900 mm along lateral root of tree 1 300 mm along lateral root of tree 2	
	B1 (tree 1)	B2 (tree 2)
	Excised the tap root on tree 1 Continued stem flow rate measurements on tree 1 as for experiment A Continued lateral root flow rate measurements on tree 1 as for experiment B	Excised the lateral roots on tree 2 Continued stem flow rate measurements on tree 2 as for experiment A

on day of year 292. All of the lateral roots for this tree were within 300 mm below the soil surface. A metal plate was used to completely separate the severed root parts. The SGB100-ws gauge was also left on the stem and sap flow measurement continued.

6.3.7 Bloemendal experiment B2: Stem flow rate measurements just prior to and after lateral root severing.

The soil at the base of tree II was also removed. Instead of severing the tap root as was the case for tree I (Experiment B1), all lateral roots were severed at 12h30 on Day 292 leaving only the tap root undisturbed. The SGB100-ws gauge was left on the stem while the SGB25-ws gauge was removed from the lateral root prior to severing.

6.4 Results of the Bloemendal experiments

Day of year 292 was typical of the days on which measurements were obtained. Data obtained for this day will be discussed in detail. The maximum air temperature was 25.2 °C (**Fig. 6.1**) and it was sunny for most of the day. The wind speed increased early in the morning, peaked in the afternoon, and was very calm after 21h00. The rainfall for the nine months preceding our experiments was well below the long-term average (**Table 6.2**). The total rainfall of 483 mm was the lowest recorded rainfall since 1952.

The various component energy fluxes are defined in Fig. 2.1. The heater flux E_{heater}, the vertically conducted energy flux $E_{upper} + E_{lower}$, the radial heat energy flux E_{radial} and the sap flux E_{sap}, measured for the lateral root and stem of tree I are illustrated for day of year 292 (**Figs 6.2 and 6.3**, Experiments A and B respectively). The power supplied to the gauge heater attached to the root was constant at 0.47

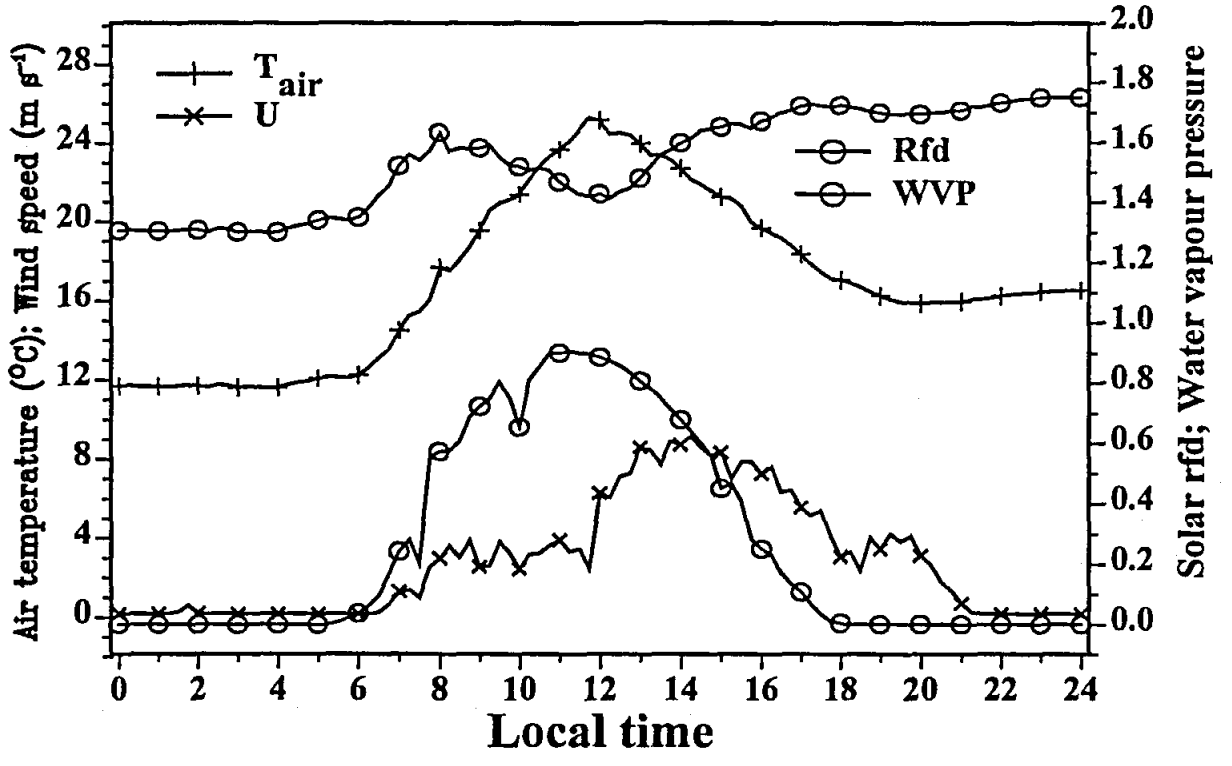

Fig. 6.1 Weather data for Day 292, 1992: air temperature T_{air} (°C) and wind speed U (m s^{-1}) on the left-hand y-axis and solar radiant flux density Rfd (kW m^{-2}) and water vapour pressure WVP (kPa) on the right-hand y-axis

Table 6.2 Five years of monthly and total rainfall illustrating how dry the year of experimentation (1992) was

Year	Rainfall in mm												
	Jan	Feb	Mar	Apr	May	Jun	Jul	Aug	Sep	Oct	Nov	Dec	Total
1987	144	156	216	53	10	45	14	115	412	69	97	118	1449
1988	79	147	212	26	61	64	24	16	22	57	100	182	990
1989	93	221	43	38	19	1	36	0	26	70	323	87	957
1990	130	129	214	64	20	6	0	100	29	123	80	153	1048
1991	257	191	108	19	46	7	6	3	60	170	123	67	1057
1992	116	88	48	31	0	0	1	9	27	40	68	55	483

W (Fig. 6.3). The radial energy flux component E_{radial} remained relatively constant during the day, and then increased in the evening when more heat energy was being conducted radially. The energy flux conducted vertically, $E_{upper} + E_{lower}$, followed a similar pattern to the radial heat flux E_{radial}. Most of the heat apportioned to sap flux E_{sap} during the day, was repartitioned to radial heat flux E_{radial} and vertically conducted energy flux $E_{upper} + E_{lower}$ at night.

Since the root temperature differential dT_{root} (Fig. 6.2) is in the denominator for the calculation of the sap mass flow rate M_{sap} (kg h^{-1}), if it approaches zero then M_{sap} (Fig. 6.2) will approach infinity (Savage *et al.*, 1993a). Root temperature differential dT_{root} for tree I was less than 7 °C (Fig. 6.4); excessive dT_{root} values may harm the tree physiologically. Stem temperature differential dT_{stem} (Fig. 6.3), reached about 18 °C at sunrise. Of note is that dT_{root} did not decrease much below 1 °C during the daylight hours implying that the M_{sap} would not be overestimated. Our lower limit of the temperature

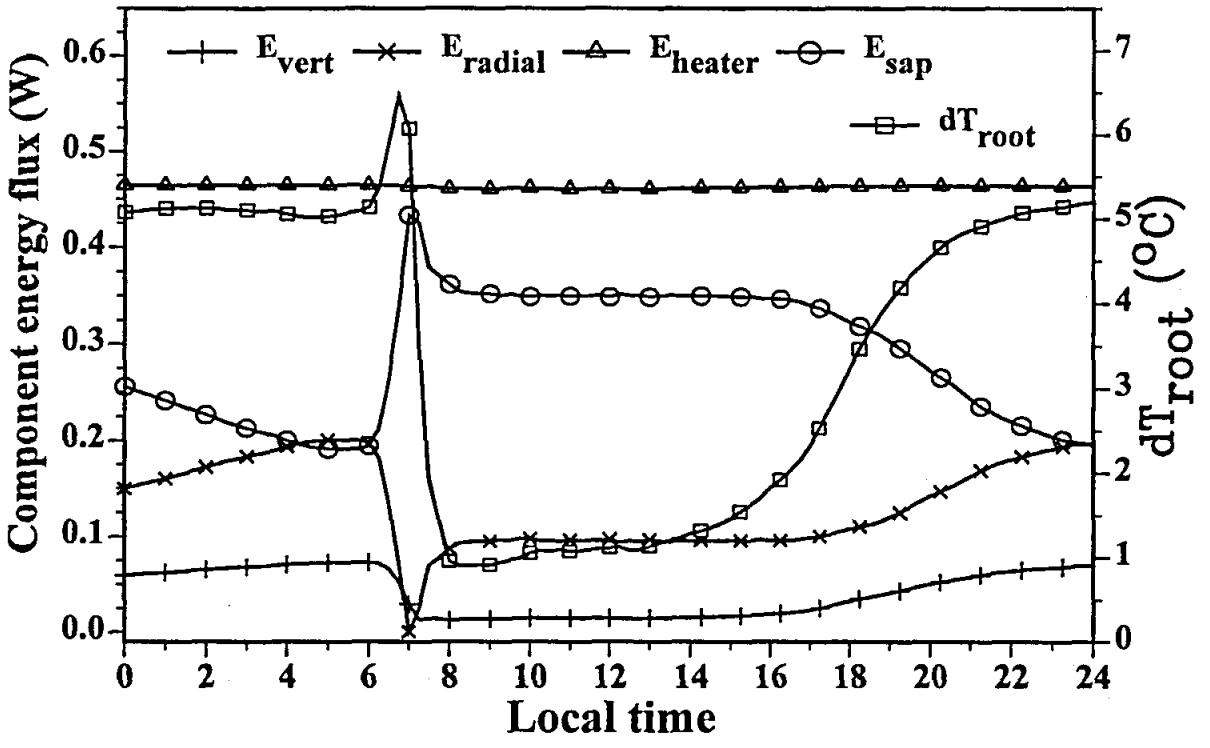

Fig. 6.2 Variation in the component energy fluxes (W) on the left-hand y-axis and the temperature differential, dT_{stem} (°C) on the right-hand y-axis for a 100-mm gauge attached to the stem of tree I for day of year 292, 1992 (Experiment A)

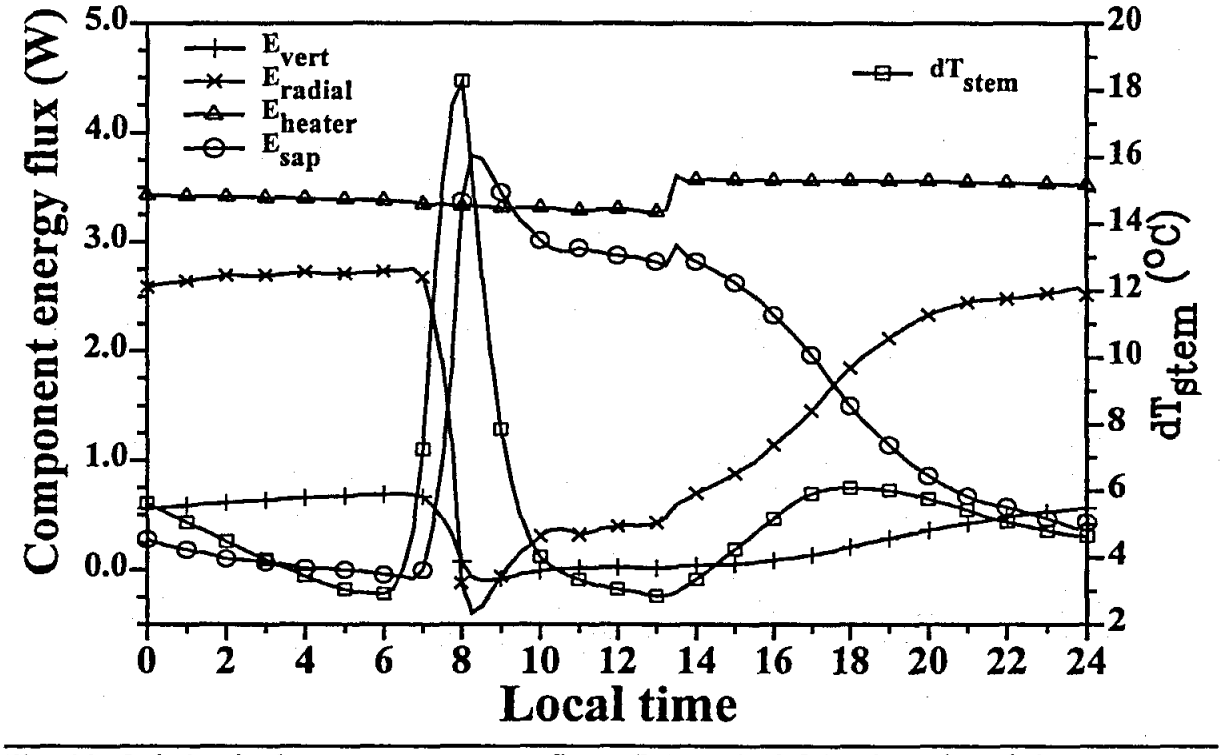

Fig. 6.3 Variation in the component energy fluxes (W) on the left-hand y-axis and the temperature differential, dT_{root} (°C) on the right-hand y-axis for a 25-mm gauge attached to a lateral root of tree I for Day 292, 1992 (Experiment B). Sunrise was at 05h49 and sunset was at 18h40

differential dT_{stem} for the stems only decreased to about 3 °C, whereas our unpublished data indicates that it may decrease to about 0.75 °C without M_{sap} being overestimated. These minimum dT_{root} and dT_{stem} values (1 and 3 °C respectively) indicate that the power supplied to the gauge heater was adequate. If we had applied less power to the gauges, so as to increase the times between battery replacement, lower dT_{stem} values could have occurred with corresponding erroneously large sap flow rates measured.

The E_{sap} component was high during the day and low at night for roots and stems as would be expected since it is the dominant term during conditions of high sap flux (Fig. 6.2, Experiment A and Fig. 6.3, Experiment B). Compared to the component energy fluxes for the root (Fig. 6.4), the steady state condition for the stem measurements was not always attained (Fig. 6.2, Experiment A) since for stems E_{sap} actually exceeded the heat flux E_{heater} for the first part of the morning. Concurrently, the radial (E_{radial}) and vertical ($E_{upper} + E_{lower}$) heat fluxes for stems were negative. The sudden increase in heater power shown in Fig. 6.3 is due to a battery replacement at 13h00.

The mass sap flux measurements in the stems (Experiment A) and roots (Experiment B) of trees I and II are illustrated in **Figs 6.4 and 6.5** respectively. The mass sap flux in the lateral root of the two trees (Experiment B) showed a very similar diurnal trend. The only major difference was in the amount of water transpired. The mass sap flux in the stems of the two trees also showed a similar diurnal trend with the main difference being that the flux through stem I (Fig. 6.4) was larger in magnitude. The low measured flow rates should be seen in the context of the lower than usual rainfall (Table 6.2).

Daily integrations of the mass sap fluxes for the stems (Experiment A) and lateral roots (Experiment B) for trees I and II were carried out for a five day period (day of year 289 to 293) (**Fig. 6.6**). The daily potential evaporation (mm/day) and total daily solar radiant density (MJ m^{-2}) are also

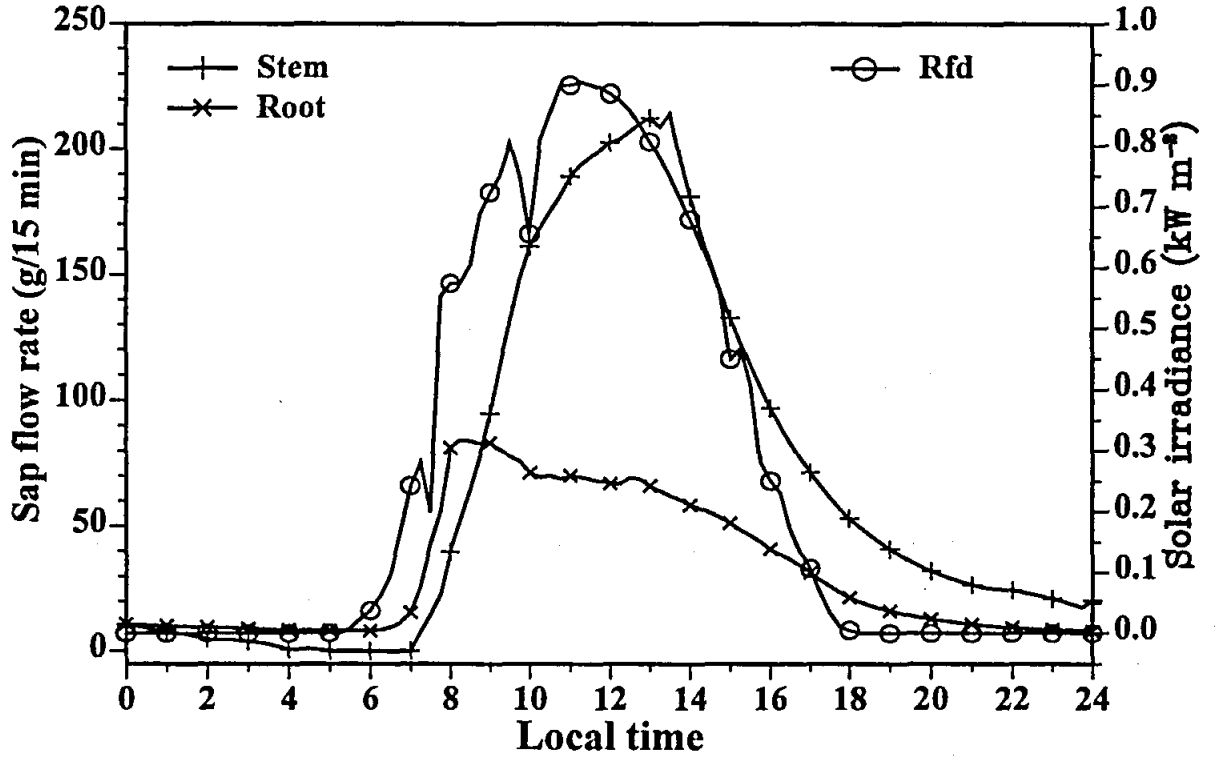

Fig. 6.4 Diurnal sap flow rates M_{sap} (g/15 min), between a lateral root (25-mm gauge) and the stem (100-mm gauge) of tree I for Day 292, 1992 (Experiment A and B). Also shown is the solar irradiance Rfd (kW m^{-2}, right-hand y-axis)

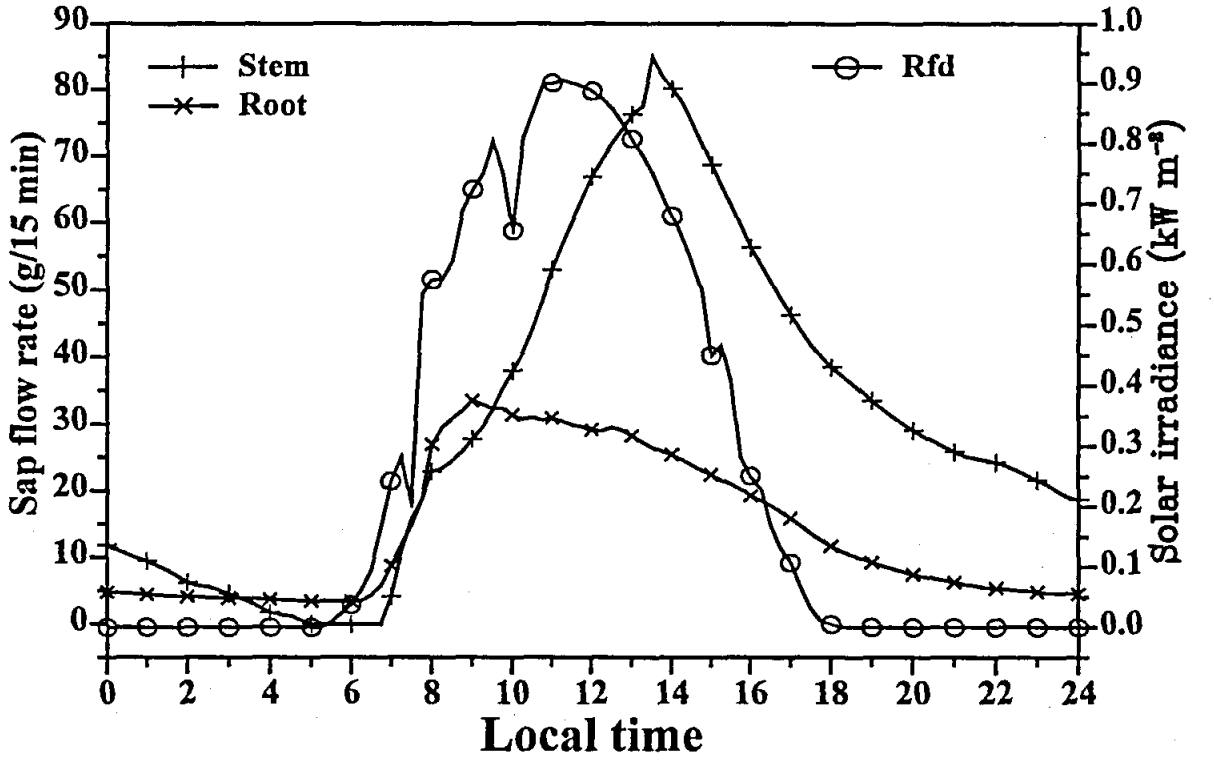

Fig. 6.5 Diurnal sap flow rates M_{sap} (g/15 min), for a lateral root (25-mm gauge) and the stem (100-mm gauge) of tree II for Day 292, 1992 (Experiment A and B). Also shown is the diurnal solar irradiance Rfd (kW m^{-2}, right-hand y-axis)

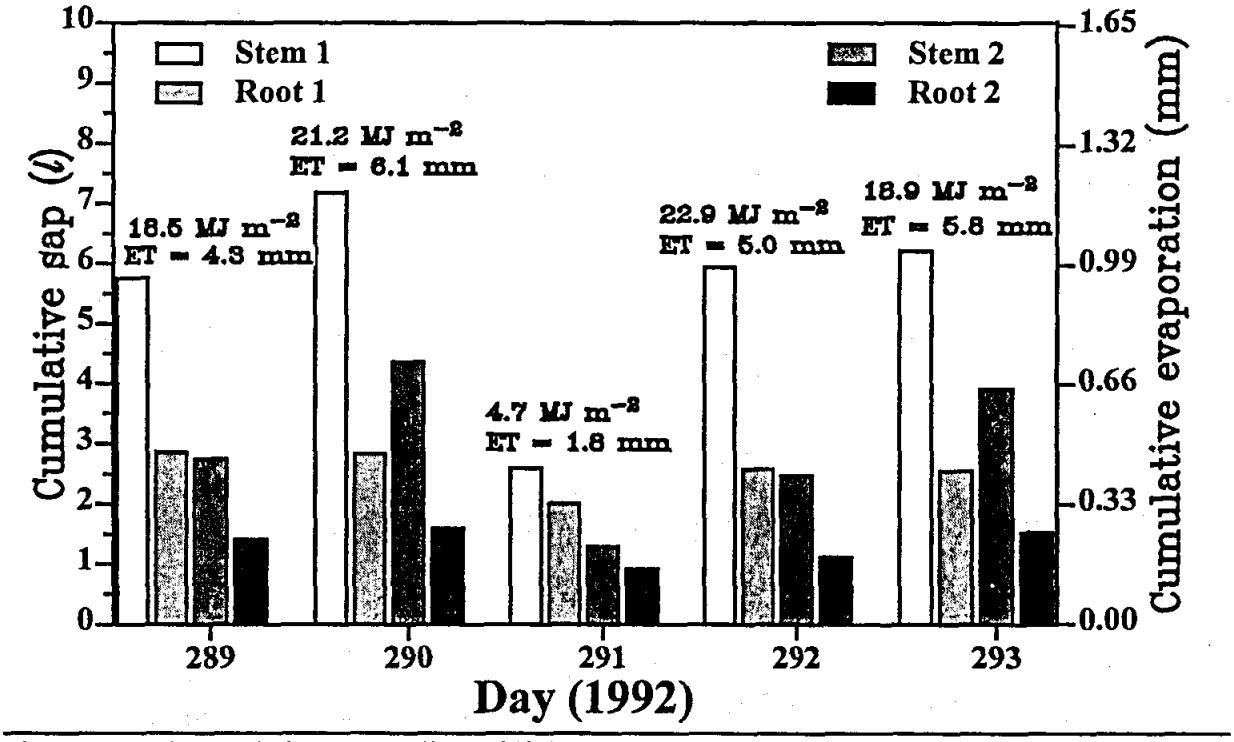

Fig. 6.6 Total cumulative water (litres, left-hand y-axis; mm, right-hand y-axis) through the stems (100-mm gauges) and lateral roots (25-mm gauges) of trees I and II for Day 289 to 293, 1992. During this time period no root severing occurred. The daily potential evaporation PE (mm/day) and total daily solar density (MJ m^{-2}) are shown above the histogram elements

presented (Fig. 6.6) to give perspective to magnitudes of the daily quantities of sap flowing through the stems and lateral roots.

For the lateral root and stem (**Fig. 6.7 and 6.8**), while the tap root was being severed from tree I (Experiment B1), the sap flow rate rapidly increased for a short period due to the severing. Similarly, when the lateral roots were severed from tree II (Experiment B2), the sap flow rate in the stem also increased markedly for a short period (**Fig. 6.9**).

6.5 Discussion

6.5.1 The Bloemendal experiments

In the case of stems and roots, during the daytime hours, it may be possible to ignore the vertically conducted heat $E_{upper} + E_{lower}$ but not the radial heat flux E_{radial} (Figs 6.2 and 6.3).

The peak stem flow rate of tree I (Experiment A) reached 220 g/15 min while the peak stem flow rate of tree II was 86 g/15 min (Figs 6.4 and 6.5, respectively). Similarly for the lateral roots, the flow rate (Experiment B) in tree I was much larger than the root flow rate in tree II (Figs 6.4 and 6.5 respectively). It should be noted that tree I and II appeared to have similar leaf areas. Immediately after the stem mass sap flux for tree I (Fig. 6.4) had peaked at about 13h00, it declined sharply. This is not illustrated as well for the measurements on the stem of tree II (Fig. 6.4) since the power supplied to the heater was increased at the time of the expected sharp decline. The peaks of the mass sap fluxes for the stems of trees I and II both lagged the peaks of the mass sap fluxes for their respective lateral roots.

The daily sap flow amount for tree I is much greater than that for tree II (Fig. 6.6). On Days 289 and

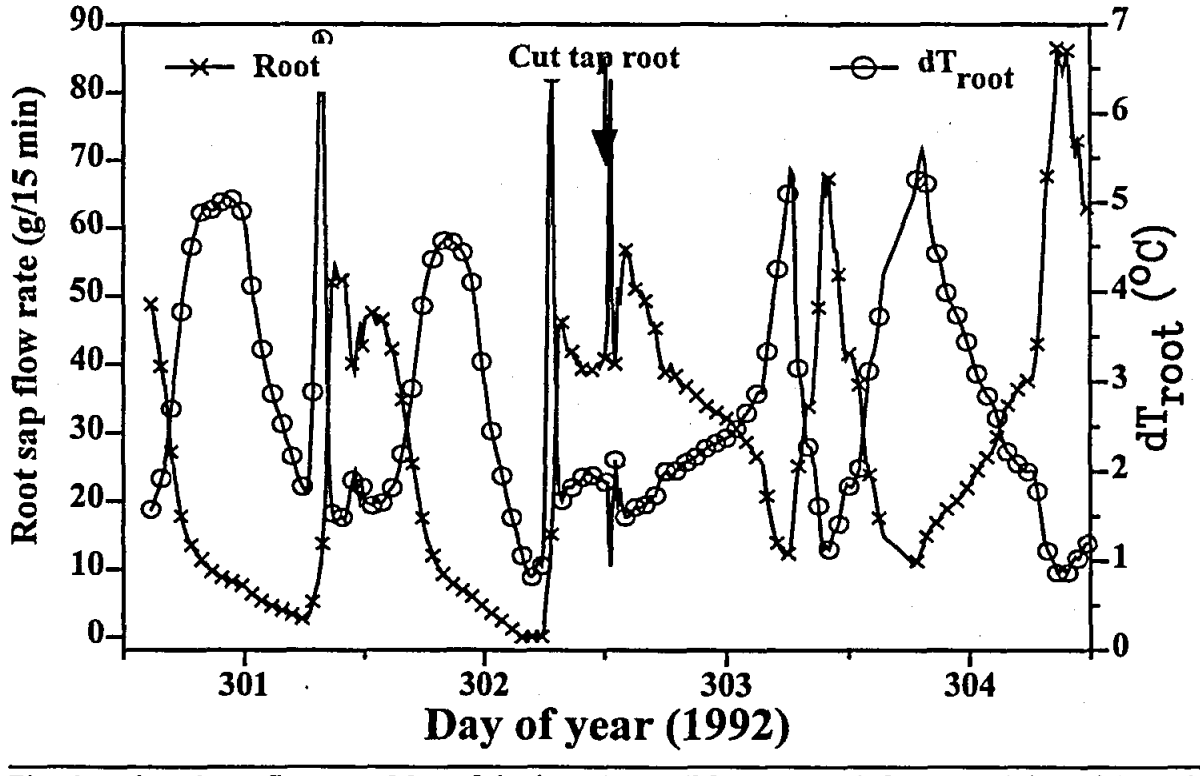

Fig. 6.7 Diurnal sap flow rate M_{sap} of the lateral root (25-mm gauge) for tree I (g/15 min) on the left-hand y-axis and the lateral root temperature differential dT_{root} (°C) on the right-hand y-axis for day of year 300 to 304, 1992 (Experiment B1). The time of cutting the tap root was 12h30 on Day 302

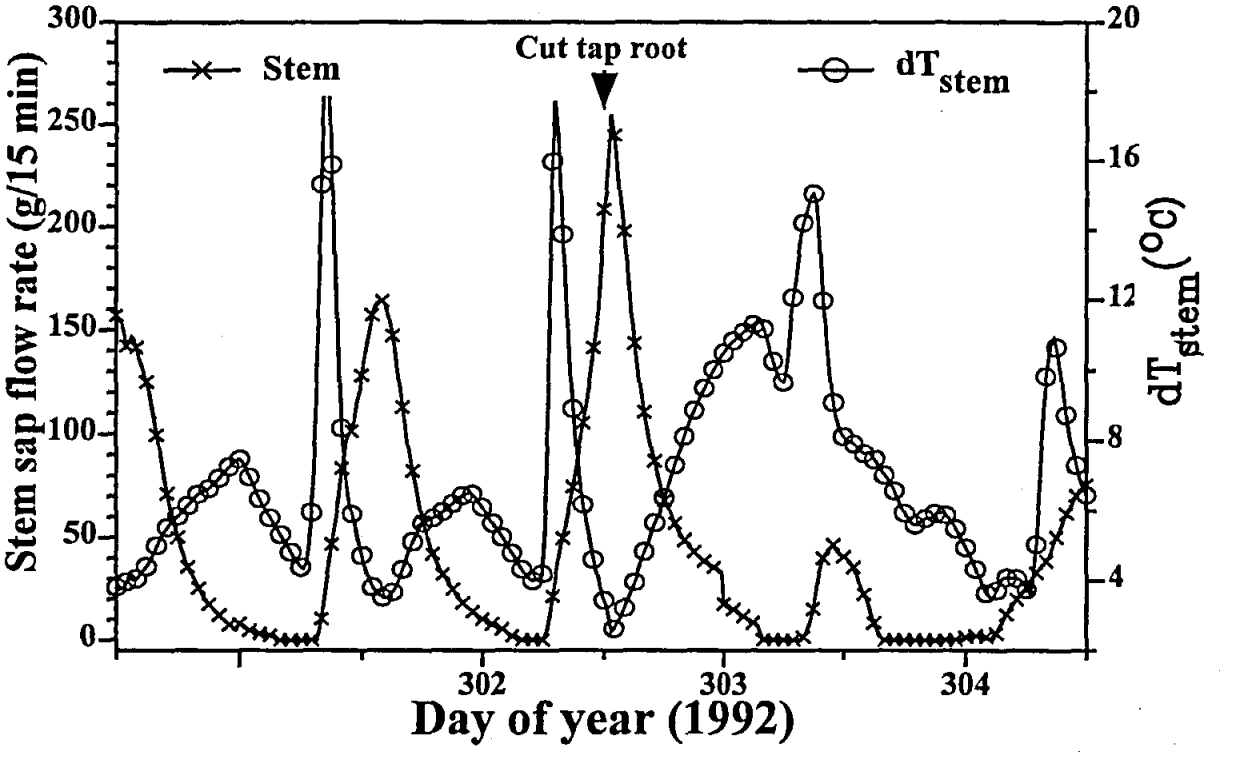

Fig. 6.8 Diurnal sap flow rate M_{sap} (g/15 min) on the left-hand y-axis through the stem (100-mm gauge) of tree I, and the stem temperature differential dT_{stem} (°C) on the right-hand y-axis for day of year 300 to 304, 1992 (Experiment B1). The tap root for tree I was cut at 12h30 on Day 302

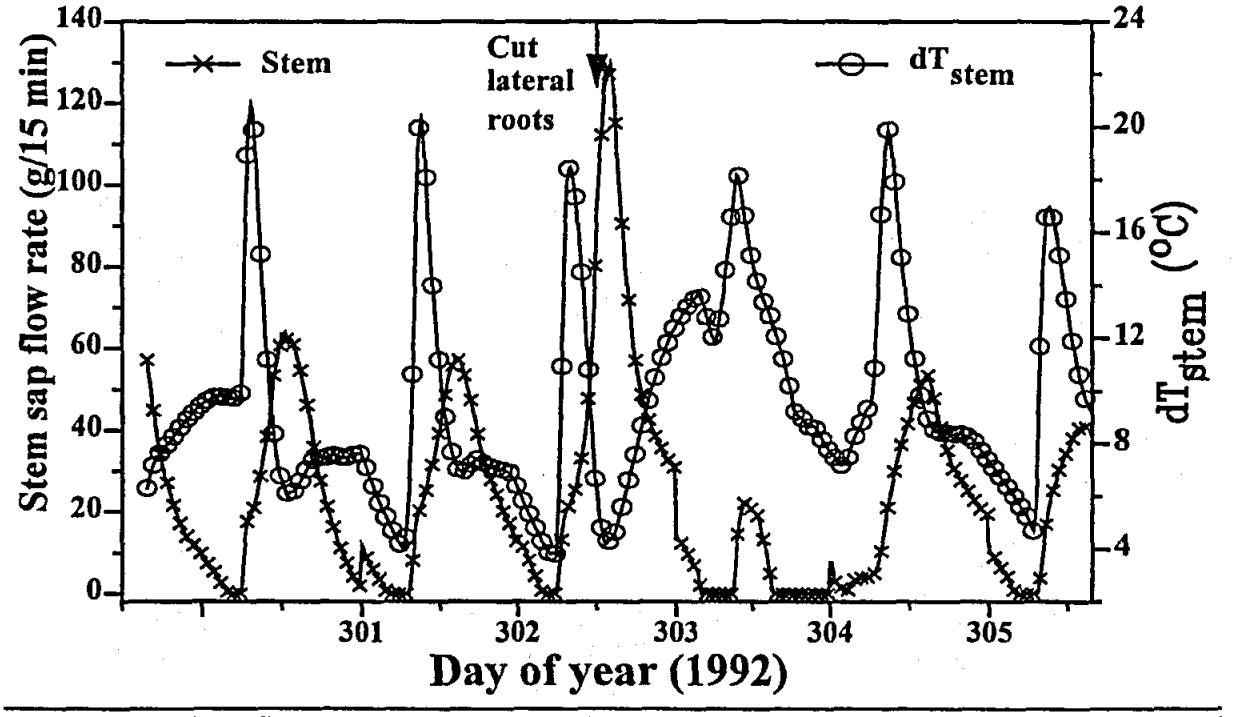

Fig. 6.9 Diurnal sap flow rate (g/15 min) on the left-hand y-axis through the stem (100-mm gauge) of tree II, and the stem temperature differential (°C) on the right-hand y-axis for day of year 300 to 305, 1992 (Experiment B2). The time of cutting the lateral roots was 12h30 on Day 302

292 the magnitudes of the accumulated sap flow for the lateral root of tree I is almost equal to that through the stem of tree II. The average daily accumulated sap flow for the stem of tree I is about 5.5 litres while that for the stem of tree II is about 3 litres. This demonstrates that two trees growing in close proximity may vary in water use. Such differences, for trees of similar size and leaf area, would not be expected, unless subjected to different levels of water availability.

The sap flow rate M_{sap} through the stem of both trees is shown to alter suddenly at midnight on certain days (Figs 6.8 and 6.9). This is as a result of changing the gauge conductance K_{gauge} at that time. By contrast, at midnight on Day 302, the apparent gauge conductance increased. We adjusted K_{gauge} to equal the apparent gauge conductance causing M_{sap} to decrease. On other days such as Day 301, M_{sap} did not change at midnight implying that the apparent K_{gauge} remained the same for the two days. For comparison however, K_{gauge} was not altered in Fig. 6.7. This implies that there may still have been nocturnal stem sap flow (Figs 6.8 and 6.9) and that altering K_{gauge} may have introduced artifact into the nighttime data and to a lesser extent the daytime data. This aspect is currently under further investigation.

Root severing experiments may yield valuable information on the response of trees to a reduced availability of soil water. In a root severing experiment on *Abies amabalis* (Douglas., Forbes) Teskey *et al.* (1985) found that in comparison to the responses of a control tree, severed-root treatments showed that removal of approximately 31 % of the xylem cross-sectional surface area of the root system had no apparent effect on xylem pressure potential or leaf conductance. Further, this severing had no effect on stem sap velocity or water relations of the foliage. When a larger portion was severed (56 %), xylem pressure potential was lower. After comparison of this response to that of a tree that had been completely cut from its roots, it was evident that water was being supplied to the trees through the remaining roots. Teskey *et al.* (1985) suggested that the ability of the trees with partially severed root systems to maintain leaf conductances and xylem pressure potentials comparable to that of a control was related to an adequate inflow of water from roots and not solely from stem capacitance. They noted that under the conditions of their experiment, stomata appeared to be the primary regulators of water movement in the system.

In our Experiment B1, when the tap root was severed, the sap flow rate in the lateral root and stem increased almost immediately (Figs 6.7 and 6.8 respectively). This is in accordance with the findings of Marshall (1958) that when vessels of a living tree are cut, the rate of sap flow displays a large and instantaneous change in magnitude. The sap flow rate through the stem decreased (Fig. 6.8) for the following two days while sap flow rate through the lateral root (Fig. 6.7) increased. In order to satisfy the transpiration demand the uptake through fewer roots resulted in an increased flow rate per root.

The effect of severing the lateral roots on tree II (Experiment B2) reduced the sap flux through the stem the next day. The following two days however showed a recovery in sap flux, though not to pre-severing levels (Fig. 6.9).

Lateral root flow rate increased following tap root severing (Fig. 6.7), while clearly the tap root flow rate must have increased following lateral root severing. We conclude that the lateral roots and tap roots are just as important for water uptake and that if water is available, roots continue to satisfy the transpiration if either lateral or tap roots are severed. We therefore hypothesize that *E. grandis*, under soil water limiting conditions, may be equally dependent on deep soil water supplies *via* the tap roots or on shallow soil water resources *via* the lateral roots depending on water availability to individual roots.

Working on *E. marginata* (Donn ex Smith) saplings, Stuart Crombie *et al.* (1987) showed that predawn leaf water potentials were unaffected by removal of up to 80 % of roots irrespective of whether surface soils were dry or wet. Leaf shedding and efficient stomatal closure prevented severe water stress developing in remaining leaves until nearly 90 % of the roots had been removed. The effects of root pruning on midday water potentials were variable especially when soils were dry, suggesting that not all trees had equal access to soil water. The effect a given level of root pruning would have on a tree's water relations would therefore depend on both the size of the root system and the location of the remaining roots with respect to available water reserves.

Tree root systems may have been optimised for other site specific conditions, possibly nutrient uptake or conditions of low soil water. The size of the root system may also reflect previous exposure to drought. During periods of low soil water potentials, resistance to water flow through the soil and the root-soil interface appears to increase (Tinker, 1976). Under conditions of fluctuating water supply, a large root system may be a very important drought-avoidance adaptation (Teskey *et al.*, 1985). Briggs and Wiebe (1982) found that removing 25 % of the roots of *Helianthus annus* (L.) caused a decrease in transpiration. These results suggest that the roots and shoots of annual plants may be more closely coupled than those of a perennial. It is still conceivable, however, that areas with sporadic rainfall and soil profiles restricting root development, be considered as marginal sites according to the conditions for marginality as described by Wessels (1984).

6.5.2 Potential evaporation for Zululand

As potential evaporation data for the KwaMbonambi district are not readily available, mean S-pan data from two sites at Richards Bay were averaged and compared to mean monthly rainfall data, collected over a period of approximately 60 years, averaged from three stations located in different parts of the Kwa-Mbonambi district (**Fig. 6.10**). A-pan data is also presented in Fig. 6.10. This was determined by multiplying the S-pan data by a set of date specific constants (Apan /Span) that is applicable to South African eastern seaboard maritime regions (Bosman, 1987; 1988). Both evaporation at Richards Bay and rainfall at KwaMbonambi increase steadily from July to December followed by a steady decline until June (Fig. 6.10). KwaMbonambi rainfall data are average means from the three stations: 0305128 S, 0305306 A, and 0305308 W (over a period of 60 years). Richards Bay S-pan data are average means from the two stations: 0305105 T and 0305137 T (recent). A-pan data were calculated by multiplying the S-pan data by a set of date specific constants (Apan /Span) that is applicable to South African eastern seaboard maritime regions. This set of monthly constants consists of the following: 1.24 (Jan); 1.26 (Feb); 1.28 (Mar); 1.29 (Apr); 1.32 (May); 1.34 (Jun); 1.40 (Jul), 1.41 (Aug); 1.37 (Sep); 1.33 (Oct); 1.28 (Nov) and 1.27 (Dec) (Bosman, 1987; 1988).

From August to December, evaporation is greater than rainfall. The significance of this is that the potential for transpiration is likely to follow a similar pattern. It is significant to note that healthy mature *Eucalyptus* trees tend to be more aerodynamically resistant and present a greater surface area for evaporation than the apparatus used to measure evaporation in most weather stations. Under such circumstances it is likely that, after a certain stage of growth, trees planted in this area possess the potential to transpire more water than is supplied by rainfall alone (Fig. 6.10) and consequently will depend on soil stored water for their sustained growth in the long term. There was some concern that available stored groundwater in parts of a large area incorporating Kwa-Mbonambi may be near depletion and that this may affect sustainable tree performance.

6.6 Conclusions

Root severing experiments may yield valuable information on the response of trees to a reduced availability of soil water. Trees growing in close proximity may vary in water use. Such differences, for trees of similar size and leaf area, would not be expected, unless subjected to different levels of water availability. When a tap root was severed, the sap flow rate in the lateral root and stem increased almost immediately. The effect of severing the lateral roots of tree II (Experiment B2) reduced the sap flux through the stem the next day. The following two days however showed a recovery in sap flux, though not to pre-severing levels. Lateral roots and tap roots are just as important for water uptake and if water is available, roots continue to satisfy the transpiration if either lateral or tap roots are severed. We therefore hypothesize that *E. grandis*, under soil water limiting conditions, may be equally dependent on deep soil water supplies *via* the tap roots or on shallow soil water resources *via* the lateral roots depending on water availability to individual roots.

References

1. Albrektson, A., 1984. Sapwood basal area and needle mass of Scots pine (P. sylvestris) trees in central Sweden 57, 35-43.
2. Alidi F.S., 1984. Afforestation of marginal lands for commercial timber production and to meet the needs of local communities in Botswana. South African Forestry Journal 130, 62-64.
3. Allaway, W.G., and Milthorpe, F.L., 1976. Structure and functioning of stomata. In: Water deficits and plant growth, ed. T.T. Kozlowski. New York, Academic press, pp. 57-102.
4. Aloni, R., 1987. Differentiation of vascular tissues. Annual Review of Plant Physiology 38, 179-204.
5. Aloni, R., 1991. Wood formation in deciduous hardwood trees. In: Physiology of trees, ed. A.S. Raghavendra. Wiley, New York, pp. 175-197.
6. Aloni, R., and Zimmermann, M.H., 1983. The control of vessel size and density along the plant axis - a new hypothesis. Differentiation 24, 203-208.
7. Anderson, M.C., 1981. The geometry of leaf distribution in some south-eastern Australian forests. Agricultural Meteorology 25, 195-205.
8. Aphalo, P.J., and Jarvis, P.G., 1991. Do stomata respond to relative humidity? Plant, Cell and Environment 14, 127-132.
9. Ashton, D.H., 1975. The root and shoot development of Eucalyptus regnans F. Muell. Australian Journal of Botany 23, 867-887.
10. Aston, A.R., 1979. Rainfall interception by eight small trees. Journal of Hydrology 42, 383-396.
11. Atkinson, D., 1978. The use of soil resources in high density planting systems. Acta Horticulturae 65, 79-89.
12. Atkinson, D., 1980. The distribution and effectiveness of the roots of tree crops. Horticultural Reviews 2, 424-490.
13. Attiwill, P.M., and Clayton-Greene, K.A., 1984. Studies of gas exchange and development in a sub-humid woodland. Journal of Ecology 72, 285-294.
14. Ayers, P.G., 1978. Water relations of diseased plants. In: Water deficits and plant growth (Vol V), ed. T.T. Kozlowski. New York, Academic Press, pp. 1-60.
15. Baker, J.M., and Nieber, J.L., 1989. An analysis of the steady-state heat balance method for measuring sap flow in plants. Agricultural and Forest Meteorology 48, 93-109.
16. Baker, J.M., and Van Bavel, C.H.M., 1987. Measurement of mass flow of water in the stems of herbaceous plants. Plant, Cell and Environment 10, 777-782.
17. Baldwin, P.J., and Stewart, H.T.L., 1987. Distribution, length and weight of roots in young plantations of Eucalyptus grandis W. Hill ex. Maiden irrigated with recycled water. Plant and Soil 97, 243-252.
18. Barber, H.N., 1955. Adaptive gene substitution in Tasmanian eucalypts. I. Genes controlling the development of glaucousness. Evolution 9, 1-14.
19. Barber, H.N., and Jackson, W.D., 1957. Natural selection in action in Eucalyptus. Nature UK 179, 1267-1269.
20. Bates, L.M., and Hall, A.E., 1981. Stomatal closure with soil water depletion not associated with changes in leaf water status. Oecologia 50, 62-65.
21. Barrett, D.J., Hatton, T.J., Ash, J.E., and Ball, M.C., 1995. Evaluation of the heat-pulse velocity technique for measurement of sap flow in rainforest and eucalypt forest species of south-eastern Australia. Plant Cell Environment 18, 463-469.
22. Baumgartner, A., 1934. Thermoelektrische untersuchungen über die geschwindigkeit des transpirationsstromes. [Zeitsch Botany Ges. 55, 514].
23. Benecke, U., and Nordmeyer, A., 1982. Carbon uptake and allocation by Nathofagus solandri var. cliffortoides (Hook. f.) Poole and Pinus contorta (Douglas ex Loudon) ssp. contorta at montane and subalpine altitudes. In: Carbon uptake and allocation in subalpine ecosystems as a key to management, ed. R.H., Waring. Proceedings of an IUFRO Workshop: P.1.07-00, Ecology of Subalpine Zones, Corvallis, OR, August 2-3, 1982. Forest Research Laboratory, Oregon State University, Corvallis, OR. pp 9-21.
24. Biddulph, O., 1959. Translocation of inorganic solutes. In: Plant physiology II. Plants in relation to water and solutes. Ed. F.C. Stewart. Academic Press, New York, pp. 553-604.
25. Binkley, D., 1984. Douglas-fir stem growth per unit leaf area increased by interplanted Sitka alder and red alder. Forest Science 30, 259-263.
26. Blackman, P.G., and Davies, W.J., 1985. Cytokinins, abscisic acid and the control of plant water balance. Acta Horticulturae 11, 255-261.
27. Blanche, E.A., Hodges, J.D., and Nebeker, T.E., 1985. A leaf-area sapwood-area ratio developed to rate Loblolly Pine vigour. Canadia Journal of Forest Research 15, 1181-1184.
28. Bloodworth, M.E., Page, J.B., and Cowley, W.R., 1955. A thermo-electric method for determining the rate of water movement in plants. Soil Science Society of America Proceedings 19, 411-414.
29. Bloodworth, M.E., Page, J.B., and Cowley, W.R., 1956. Some applications of the thermoelectric method for measuring water flow in plants. Agronomy Journal 48, 222-228.
30. Boden, D.I. 1991. Intensive site preparation on steep land: the effect on hydrological processes and growth of Eucalyptus grandis at 18 months. In Annual project report. Institute for Commercial Forestry Research, Pietermaritzburg, South Africa.
31. Bonsen, K.G.M., and Kucera, L.J., 1990. Vessel occulsions in plants: Morphological, functional and evolutionary aspects. International Association of Wood Anatomists Bulletin (new series) 11, 393-399.

32. Booker, R.E., and Kininmonth, J.A., 1978. Variation in longitudinal permeability of green radiata pine wood. New Zealand Journal of Forest Science. 8, 295-308.
33. Bosch, J.M., 1979. Treatment effects of annual and dry period streamflow at Cathedral Peak. South African Forestry Journal 108, 29-38.
34. Bosh, J.M., and Hewlett, J.D., 1982. A review of catchment experiments to determine the effects of vegetation changes on water yield and evapotranspiration. Journal of Hydrology 55, 3-23.
35. Bosman, H.H., 1987. The influence of installation practices on evaporation from Symons tank and American A-pan evaporimeters. Agricultural and Forest Meteorology.
36. Bosman, H.H., 1988. Measures to standardise American Class A-pan and Symons tank evaporation. South African Department of Water Affairs, Workshop on the standardisation of pan evaporation. Mineographed.
37. Bowen, G.D., 1985. Roots as a component of tree productivity. In: Attributes of trees as crop plants, ed. M.G.R. Cannell and J.E. Jackson. Institute of Terrestrial Ecology, Edinburgh, pp. 303-315.
38. Boyer, J.S., 1976. Water deficits and photosynthesis. In: Water deficits and plant growth, Vol 4, ed. T.T. Kozlowski. Academic Press, New York, 151-191.
39. Boyer, J.S., 1985. Water transport. Annual review f Plant Physiology 36, 473-516.
40. Boyer, J.S., 1989. Water potential and plant metabolism: comments on Dr P.J Kramer's article, Changing concepts regarding plant water relations, in: Plant, Cell and Environment 11, 565-568 and Dr J.B. Passioura's response, in: Plant, Cell and Environment 11, 569-571. Plant, Cell and Environment 12, 213-216.
41. Bradford, K.J., and Hsiao, T.C., 1982. Physiological responses to moderate water stress. In: Physiological Plant Ecology II. Water relations and carbon assimilation. Encyclopedia of plant physiology, Vol. 12B, ed. O.L. Lange, P.S. Nobel, C.B. Osmond and H. Ziegler. Springer-Verlag, Berlin, pp. 246-324.
42. Braekke, F.H., and Kozlowski, T.T., 1975. Effect of climatic and edaphic factors on radial stem growth of Pinus resinosa annd Betula papyrifera in northern Wisconsin. Advancing Frontiers of Science 30, 201-221.
43. Briggs, G.M. and Wiebe, H.H. 1982. The effects of root pruning on the water relations of Helianthus annus L. Journal of Experimental Botany 33, 966-976.
44. Britz, R.M., 1984. Afforestation of marginal lands for commercial timber production and to meet the needs of local communities of South-West Africa. South African Forestry Journal 130, 59-61.
45. Brix, , H., 7 Mitchell, A.K., 1983. Thinning and nitrogen fertilization effects on sapwood area and basal area in Douglas-fir. Canadian Journal of Forest Research 13, 384-389.
46. Brough, D.W., Jones, H.G., and Grace, J., 1986. Diurnal changes in water content of the stems of apple trees, as influenced by irrigation. Plant, Cell and Environment 9, 1-7.
47. Burschka, C., Tenhunen, J.D., and Hartung, W., 1983. Diurnal variation in abscisic acid in leaves of irrigated and non-irrigated Arbutus unedo plants under naturally fluctuating environmental conditions. Oecologia 58, 128-131.
48. Byrne, G.F., Begg, J.E., and Hansen, G.K., 1977. Cavitation and resistance to water flow in plant roots. Agriculture Meteorology 18, 15-21.
49. Calder, I.R., 1985. What are the limits on forest evaporation ? - a comment. Journal of Hydrology 82, 179-192.
50. Calder, I.R., 1986. Water use of Eucalypts - a review with special reference to South India. Agricultural Water Management 11, 333-342.
51. Calkin, H.W., Gibson, A.C., and Nobel, P.S., 1986. Biophysical model of xylem conductance in tracheids of the fern, Pteris vittata. Journal of Experimental Botany 37, 1054-1064.
52. Campbell, G.S., Calissendorff, C., and Williams, J.H., 1991. Probe for measuring soil specific heat using a heat-pulse method. Soil Science Society of America Journal 55, 291-293.
53. Cannell, M.G.R., 1985. Dry matter partitioning in tree crops. In: Attributes of trees as crop plants, ed. M.G.R. Cannell and J.E. Jackson. Institute of Terrestrial Ecology, Edinburgh, pp. 160-193.
54. Carbon, B.A., Bartle, G.A., and Murray, A.M., 1981. Patterns of water stress and transpiration in Jarrah (Eucalyptus marginata) forests. Australian Forestry Research 11, 191-200.
55. Carlquist, S., 1975. Ecological strategies of xylem evolution. Berkley, University of California Press.
56. Carlson, W.C., and Harrington, C.A., 1987. Cross-sectional area relationships in root systems of loblolly and shortleaf pine. Canadian Journal of Forest Research 17, 556-558.
57. Carslaw, H.S., and Jaeger, J.C., 1959a. Conduction of heat in solids. Oxford University Press, London, pp. 258.
58. Carslaw, H.S., and Jaeger, J.C., 1959b. Improved thermal method of continual recording of the transpiration flow rate dynamics. Biologia Plantarum 19, 413-420.
59. Cermák, J., Cienciala, E., Kuera, J., and Hällegren, J., 1992. Radial velocity profiles of water flow in trunks of Norway spruce and oak and the response of spruce to severing. Tree physiology 10, 367-380.
60. Cermák, J., Deml, M., and Penka, M., 1973. A new method of sap flow rate determination in trees. Biologia Plantarum (Praha) 15, 171-178.
61. Cermák, J., Jenik, J., Kuera, J., and Zidek, V., 1994. Xylem water flow in crack willow tree (Salix fragilis L.) In relation to diurnal changes of environment. Oecologia 64, 145-151.
62. Cermák, J., Kuera, J., and Penka, M., 1974. Improvement of the method of sap flowrate determination in adult trees based on heat balance with direct electric heating of xylem. Biologia Plantarum (Praha) 18, 105-110.
63. Chalk, L., and Bigg, J.M., 1956. The distribution of moisture in the living stem of Sitka spruce and Douglas fir. Forestry 29, 5-21.
64. Chaturvedi, A.N., Sharma, S.C., and Srivastava, R., 1984. Water consumption and biomass production of

some forest trees. Commonwealth Forestry Reviews 63, 217-223.
65. Chaturvedi, A.N., Sharma, S.C., and Srivastava, R., 1988. Water consumption and biomass production of some forest tree species. Commonwealth Forestry Reviews 63, 217-223.
66. Chaturvedi, A.N., Sharma, S.C., Srivastava, R., 1989. Water consumption and biomass production of some forest tree species. International Tree Crops Journal 5, 71-76.
67. Chaves, M.M., 1991. Effects of water deficits on carbon assimilation. Journal of Experimental Botany 42, 1-16.
68. Clark, J. and Gibbs, R.D., 1957. Studies on tree physiology. IV. Further investigations of seasonal changes in moisture content of certian canadian forest trees. Canadian Journal of Botany 35, 219-253.
69. Closs, R.L., 1958. The heat pulse method for measuring rate of sap flow in a plant stem. New Zealand Journal of Science 1, 281-288.
70. Cohen, Y., 1991. Determination of orchard water requirement by a combined trunk sap flow and meteorological approach. Irrigation Science 12, 93-98.
71. Cohen, Y., Fuchs, M., and Cohen, S., 1983. Resistance to water uptake in a mature citrus tree. Journal of Experimental Botany 34, 450-460.
72. Cohen, Y., Fuchs, M., and Green, G.S., 1981. Improvement of the heat pulse method for determining sap flow in trees. Plant, Cell and Environment 4, 391-397.
73. Cohen, Y., Fuchs, M., Valkenflug, V., and Moreshet, S., 1988. Calibrated heat pulse method for determining water uptake in cotton. Agronomy Journal 80, 398-402.
74. Cohen, Y., Takeuchi, S., Nozaka, J., and Yano, T., 1993. Accuracy of sap flow measurement using heat balance and heat pulse methods. Agronomy Journal 85, 1080-1086.
75. Colquhoun, I.J., Ridge, R.W., Bell, D.T., Loneragan, W.A., and Kuo, J., 1984. Comparative studies in selected species of Eucalyptus used in rehabilitation of the northern jarrah forest, Western Australia. I. Patterns of xylem pressure potential and diffusive resistance of leaves. Australian Journal of Botany 32, 367-373.
76. Cosgrove, D., 1986. Biophysical control of plant cell growth. Annual Reviews of Plant Physiology 37, 377-405.
77. Coutts, M.P., and Philipson, J.J., 1976. The influence of mineral nutrition on the root development of trees. I The growth of Sitka spruce with divided root systems. Journal of Experimental Botany 27, 1102-1111.
78. Cowan, I.R., 1977. Stomatal behaviour and environment. Advances in Botanical Research 4, 117-228.
79. Cowan, I.R., 1982. Regulation of water use in relation to carbon gain in higher plants. In: Physiological plant ecology, Vol. 2, encyclopedia of plant physiology, Vol. 12B, ed. O.L. Lange. Springer, Berlin. pp. 589-613.
80. Cowan, I.R., and Farquhar, G.D., 1977. Stomatal function in relation to leaf metabolism and environment. In: Integration of activity in the higher plant, ed. D.H. Jennings. University Press, Cambridge, pp. 471-505.
81. Creber, G.T., 1977. Tree rings: a natural data-storage system. Biological reviews 52, 349-383.
82. Dabral, B.G., and Raturi, A.S., 1985. Water consumption by a Eucalyptus hybrid. Indian Forester 111, 1053-1070.
83. Daubenmire, R., 1978. Plant Geography. New York, Academic Press.
84. Daum, C.R., 1967. A method for determining water transport in trees. Ecology 48, 425-431.
85. Davies, W.J., Metcalfe, J.C., Schurr, U., Taylor, G., and Zhang, J., 1987. Hormones as chemical signals involved in root to shoot communication of effects of changes in the soil environment. In: Hormone action in plant development: a critical appraisal, ed. G.V. Toad. Butterworth, London, pp. 201-216.
86. Davies, W.J., Rhizopoulou, S., Sanderson, R., Taylor, G., Metcalfe. J.C., and Zhang, J., 1989. In: Biomass production by fast-growing trees, ed. J.S. Pereira and J.J. Landsberg. Kluwer Academic Publishers, Netherlands, pp. 13-36.
87. Davis, S.D., Van Bavel, C.H.M., and McCree, K.J., 1977. Effect of leaf ageing upon stomatal resistance in bean plants. Crop Science 17, 640-645.
88. Dean, T.J., and Long, J.N., 1986. Variation in sapwood area-leaf area relations within two stands of lodgepole pine. Forest Science 32, 749-758.
89. Denmead, O.T., 1984. Plant physiological methods for studying evapotranspiration: problems of telling the forest from the trees. Agricultural Management 8, 167-189.
90. Diawara, A., Loustau, D., and Berbigier, P., 1991. Comparison of two methods for estimating the evaporation of a Pinus pinaster (Ait.) stand: sap flow and energy balance with sensible heat flux. Agricultural and Forest Meteorology 54, 49-66.
91. Dirichlet, G.L., 1850. Uber die preduction der positiven quadritschen formen mit drei unbestimmten ganzen zahlen. [Journal für die Reine und Angewandte Mathematik 40, 208-234].
92. Dixon, H.A., Grace, J., and Tyree, M.T., 1984. Concurrent measurements of stem density, leaf and stem water potential, stomatal conductance and cavitation on a sapling of Thuja occidentalis L. Plant, Cell and Environment 7, 615.
93. Dixon, H.H., 1914. Transpiration and the ascent of sap in plants. MacMillan and Co. Ltd., London.
94. Dixon, H.H., and Jolly, J., 1986. On the ascent of sap. Royal Society (London) Philosophical Transactions B86, 563-576.
95. Doley, D., 1967. Water relations of Eucalyptus marginata under natural conditions. Journal of Ecology 55, 597-614.
96. Doley, D., and Grieve, B.J., 1966. Measurement of sapflow in Eucalyptus by thermoelectric methods. Australian Forest Research 2, 3-27.
97. Downton, W.J.S., Loveys, B.R., and Grant, W.J.R., 1988. Non-uniform stomatal closure induced by water

stress causes putative non-stomatal inhibition of photosynthesis. New Phytologist 110, 503-509.
98. Dugas, W.A., Heuer, M.L., and Mayeux, H.S., 1992. Diurnal measurements of honey mesquite transpiration using stem flow gauges. Journal of Range Management 45, 99-102.
99. Dunin, F.X., and Mackay, S.M., 1982. Evaporation of eucalypt and coniferous communities. In: The first national symposium on forest hydrology. Institute of Engineers, Australia, pp. 18-25.
100. Dunn, G.M., and Connor, D.J., 1993. An analysis of sap flow in mountain ash (Eucalyptus regnans) forest of different age. Tree physiology 13, 321-336.
101. Dye, P.J., and Olbricht, B.W., 1993. Estimating transpiration from six-year-old Eucalyptus grandis trees: development of a canopy conductance model and comparison with independent sap flux measurements. Plant, Cell and Environment 16,45-53.
102. Dye, P.J., Christie, S.I., Olbricht, B.W., Ferreira, E., and Tallon, N., 1990. Determining transpiration from Pinus patula shoots - a comparative evaluation of the cut-shoot method and two null balance diffusion porometers. S.A. Forestry Journal 155, 10-15.
103. Dye, P.J., Olbrich, B.W., and Poulter, A.G., 1992. The influence of growth rings in Pinus patula on heat pulse velocity measurement. Journal of Experimental Botany 42, 867- 870.
104. Edwards, W.R.N., and Booker, R.E., 1984. Radial variation in the axial conductivity of Populus and its significance in heat pulse velocity measurement. Journal of Experimental Botany 35, 551-561.
105. Edwards, W.R.N., and Jarvis, P.G., 1983. A method for measuring radial differences in water content of intact tree stems by attenuation of gamma radiation. Plant, Cell and Environment 6, 255.
106. Edwards, W.R.N., and Jarvis, P.N., 1982. Relations between water content, potential and permeability in stems of conifers. Plant, Cell and Environment 5, 271-277.
107. Edwards, W.R.N., and Warwick, N.M.W., 1984. Transpiration from kiwifruit vine as estimated by the heat pulse technique and the Penman-Monteith equation. New Zealand Journal of Agricultural Research 27, 3-27.
108. Edwards, W.R.N., Jarvis, P.G., Landsberg, J.J., and Talbot, H., 1986. A dynamic model for studying flow of water in single trees. Tree Physiology 1, 309-324.
109. Epstein, E., 1972. Mineral nutrition of plants - principles and perspectives. J. Wiley. New York, 99, 39-117.
110. Esau, K., 1960. The stem: Secondary state of growth and structure types. In: Anatomy of seed plants. John Wiley and Sons, New York, pp. 238-257.
111. Esau,K., 1965. Plant anatomy, 2nd ed., John Wiley, New York, 1965.
112. Espinosa Banclari, M.A., Perry, D.A., and Marshall, J.D., 1987. Leaf area - sapwood area relationships in adjacent young Douglas-fir stands with different growth rates. Canadian Journal of Forest Research 17, 174-180.
113. Ewers, F.W., Fisher, J.B., and Chiu, S.-T., 1990. A survey of vessel dimensions in stems of tropical lianas and other growth forms. Oecologia 84, 544-552.
114. Ewers, F.W., 1985. Xylem structure and water conduction in conifer trees, dicot trees, and lianas. I.A.W.A. Bull. N.S. 6, 309-317.
115. Ewers, F.W., and Cruiziat, P., 1991. Measuring water tranaport and storage. In: Techniques and approaches in forest tree ecophysiology, eds J.P. Lassoie and T.M. Hinckley. CRC Press, Boca Raton, Florida, pp. 91-113.
116. Ewers, F.W., and Zimmermann, 1984a. The hydraulic architecture of eastern hemlock (Tsuga canadensis). Canadian Journal of Botany 62, 940-946.
117. Ewers, F.W., and Zimmermann, 1984b. The hydraulic architecture of balsam fir (Albies balsamea). Physiologia Plantana 60, 453-458.
118. Fabião A., Persson, H.Å., and Steen, E., 1985. Growth dynamics of superficial roots in Portuguese plantations of Eucalyptus globulus Labill. studied with a mesh bag technique. Plant and Soil 83, 233-242.
119. Fahn, A., 1964. Some anatomical adaptions of desert plants. Phytomorphology 14, 93-102.
120. Fayle, D.F.C., 1983. Differences between stem and root thickening at their junction in red pine. Plant and Soil 71, 161-166.
121. Fayle, D.F.C., and Axelsson, B., 1985. Effect of irrigation and fertilization on stem and root thickening at their junction in Scots pine. Plant and Soil 88, 285-287.
122. Feddes, R.A., 1981. Water use models for assessing root zone modification. In: Modifying the root environment to reduce crop stress, ed. G.F. Arkin, and H.M. Taylor. American Society of Agricultural Engineers, Michigan, pp. 347-390.
123. Feller, M.C., 1980. Biomass and nutrient distribution in two Eucalyptus forest ecosystems. Australian Journal of Ecology 5, 309-333.
124. Fichtner, K., and Schulze, E.D., 1990. Xylem water flow in tropical vine as measured by the steady state heating method. Oecologia 82, 355-361.
125. Fischer, R. A., and Turner, N.C., 1978. Plant productivity in the arid and semi-arid zones. Annual Review of Plant Physiology 29, 277-317.
126. Fiscus, E.L., 1983. Water transport and balance within the plant: resistance to water flow in roots. In: Limitations to efficient water use in crop production, eds. H.M. Taylor, W.R. Jordaan and T.R. Sinclair. ASA-CSSA-SSSA, Madison, p.183.
127. Fiscus, E.L., Klute, A., and Kaufmann, M.R., 1983. An interpretation of some whole plant water transport phenomena. Plant Physiology 71, 810-817.
128. Foster, R.D., and Gifford, E.M., 1974. Comparative morphology of vascular plants. W.H. Freeman, San Francisco.
129. Fritts, H.C., 1976. Tree rings and climate. London, Academic Press.

130. Gash, J.H.C., Wright, I.R., and Lloyd, C.R., 1980. Comparative estimates of interception loss from three coniferous forests in Great Britain. Journal of Hydrology 48, 89-105.
131. Gavloski, J.E., Whitfield, G.H., and Ellis, C.R., 1992a. Effect of restricted watering on sap flow and growth in corn (Zea mays L.). Canadian Journal of Plant Science 72, 361-368.
132. Gavloski, J.E., Whitfield, G.H., and Ellis, C.R., 1992b. Effect of larvae of Western Corn Rootworm (Coleoptera: Chrysomelidae) and of mechanical root pruining on sap flow and growth of corn. Journal of Economic Entomology 85, 1434-1441.
133. Gay, L.W. and Greenberg, R.J., 1985. The AZET battery-powered Bowen ratio system. Proc. 17th Conf. Agric. For. Meteorol., 7:329-334.
134. Gerdes, G., Allison, B.E., and Pereira, L.S, 1994. Overestimation of soybean crop transpiration by sap flow measurements under field conditions in Central Portugal. Irrigation Science 14, 135-139.
135. Gibbs, R.D., 1958. Patterns in the seasonal water content of trees. In: The physiology of forest trees, ed. K.V. Thimann. Ronald Press, New York, pp. 43-49.
136. Gibson, A.C., Calkin, H.W., and Nobel, P.S.,, 1985. Hydraulic conductance and xylem structure in tracheid-bearing plants. International Association of Wood Anatomy Bulletin 6, 293.
137. Gollan, T., Passioura, J.B., and Munns, R., 1986. Soil water status affects the stomatal conductance of fully turgid wheat and sunflower leaves. Australian Journal of Plant Physiology 13, 459-464.
138. Gollan, T., Turner, N.C., and Schulze, E.D., 1985. The responses of stomata and leaf gas exchange to vapour pressure deficits and soil water content. III. In the sclerophyllous woody species Nerium oleander. Oecologia 65, 356-362.
139. Green, S.R., and Clothier, B.E., 1988. Water use of kiwifruit vines and apple trees by the heat-pulse technique. Journal of Experimental. Botany 39, 115-123.
140. Greenwood, E.A.N., and Beresford, J.D., 1979. Evaporation from vegetation in landscapes developing secondary salinity using the ventilated-chamber technique. I. Comparative transpiration from juvenile Eucalyptus above saline groundwater seeps. Journal of Hydrology 42, 369-382.
141. Greenwood, E.A.N., Klein, L., Beresford, J.D., and Watson, G.D., 1985. Differences in annual evaporation between grazed pasture and Eucalyptus species in plantations on a saline farm catchment. Journal of Hydrology 78, 261-278.
142. Grier, C.C., and Waring, R.H., 1974. Conifer foliage mass related to sapwood area. Forestry Science 20, 205-206.
143. Grieve, B.J., and Hellmuth, E.O., 1970. Ecophysiology of western Australian plants. Oecologia Plantarum 5, 33-68.
144. Groot, A, and King, K.M., 1992. Measurement of sap flow by the heat balance method: numerical analysis and application to coniferous seedlings. Agricultural and Forest Meteorology, 59, 289-308.
145. Gutiérrez, M.V., Harrrington, R.A., Meinzer, F.C., and Fownes, J.H., 1994. The effect of environmentally induced stem temperature gradients on transpiration estimates from the heat balance method in two tropical woody species. Tree Physiology 14, 179-190.
146. Gwaitta-Magumba, D.A., 1984. Afforestation of marginal lands for commercial timber production and to meet the needs of the rural community. South African Forestry Journal 130, 71-78.
147. Hall, S.M., and Baker, D.A., 1972. The chemical composition of Ricinus phloem exudate. Planta 106, 131-140.
148. Ham, J.M., and Heilman, J.L., 1990. Dynamics of a heat balance stem flow gauge during high flow. Agronomy Journal 82, 147-152.
149. Ham, J.M., Owensby, C.E., Coyne, P.I., and Bremer, D.J., 1995. Fluxes of CO_2 and water vapour from a prairie ecosystem exposed to ambient and elevated atmospheric CO_2. Agricultural and Forest Meteorology 77, 73-93.
150. Ham. J.M., Heilman, J.L., and Lascano, R.J., 1990. Determination of soil water evaporation and transpiration from energy balance and stem flow measurements. Agricultural and Forest Meteorology 52, 287-301.
151. Ham. J.M., Heilman, J.L., and Lascano, R.J., 1991. Soil and canopy energy balances of a row crop at partial cover. Agronomy Journal 83, 744-753.
152. Hancock, N.H., Sellers, P.J., and Crowther, J.M., 1983. Evaporation from a partially wet canopy. Geophysicae 1, 139-146.
153. Harris, G.C., Cheeseborough, J.K., and Walker, D.A., 1983. Measurement of CO_2 and H_2O vapour exchange in spinach leaf disks. Effects of orthophosphate. Plant Physiology 71, 102-107.
154. Hartung, W., Slovik, S., and Baier, M., 1990. pH changes and redistribution of ABA+ within the leaf under stress. In: The importance of root to shoot communication in the responses to environmental stress. Monograph 21, ed. W.J. Davies and B. Jeffcoat. British Society for Plant Growth Regulation, Bristol, pp. 215-236.
155. Hatton, T.J., and Vertessy, R., 1990. Transpiration of plantation Pinus radiata estimated by the heat pulse method and the Bowen ratio. Hydrological Processes 4, 289-298.
156. Hatton, T.J., and Vertessy, R.A., 1989. Variability of sapflow in a Pinus radiata plantation and the robust estimation of transpiration. In: Hydrology and Water Resources Symposium, Christchurch, New Zealand, 23-30 Nov, 1989, pp. 6-10.
157. Hatton, T.J., Catchpole, E.A., and Vertessy, R.A., 1990. Integration of sapflow velocity to estimate plant water use. Tree Physiology 6, 201-209.
158. Heatwole, H., and Lowman, M., 1986. Dieback. Death of an Australian landscape. Reed Books, Singapore.
159. Heilman, J.L., and Brittin, C.L., and Zajicek, J.M., 1989. Water use by shrubs as affected by energy

exchange with building walls. Agricultural and Forest Meteorology 48, 345-357.
160. Heilman, J.L., and Ham, J.M., 1990. Measurement of mass flow rate of sap in Lingustrum japonicum. HortScience 25, 465-467.
161. Heine, R.W., 1970. Annals of Botany 34, 1019-1024.
162. Heine, R.W., and Farr, D.J., 1973. Comparison of heat-pulse and radioisotope tracer methods for determining sap-flow velocity in stem segments of poplar. Journal of Experimental Botany 24, 649-654.
163. Henrici, M., 1946. Transpiration of South African plant associations. II. Indigenous and exotic trees under semi-arid conditions. Scientific Bulletin of the Department of Agriculture and Forestry, South Africa No. 247.
164. Herkelwrath, W.N., Miller, E.E. and Gardner, W.R. 1977. Water uptake by plants. I. Divided root experiemnt. Soil Science Society of America Journal 41, 1033-1038.
165. Herwitz, S.R., 1985. Interception storage capacities of tropical rainforest canopy trees. Journal of Hydrology 77, 273-252.
166. Hibbert, A.R., 1967. Forest treatment effects on water yield. In: Forest Hydrology International Symposium, ed. W.E. Sopper and H.W. Lull. Pergamon, Oxford, 813 pp.
167. Hinckley, T.M., 1971. Estimate of water flow in Douglas-Fir seedlings. Ecology 52, 520-525.
168. Hinckley, T.M., and Bruckerhoff, D.N., 1975. The effects of drought on water relations and stem shrinkage of Quercus alba. Canadian Journal of Botany 53, 62.
169. Hinckley, T.M., and Ritchie, G.A., 1970. Within crown patterns of transpiration, water stress, and stomatal activity in Abies amabilis. Forest Science 16, 490-492.
170. Hinckley, T.M., Lassoie, J.P., and Running, S.W., 1978. Temporal and spacial variations in the water status of forest trees. Forest Science Monograph 20, 72p.
171. Hoffmann, H.P., Barrett, D.R., and Fox, J.E.D., 1987. A preliminary investigation into the plant-water relationships of plant species occurring in the Hamersley Ranges [Western Australia]. Mulga Research Centre Journal 9, 23-30.
172. Hsiao, T.C., 1973. Plant responses to water stress. Annual Review of Plant Physiology 24, 519-570.
173. Hsiao, T.C., Acevedo, E., Fereres, E., and Henderson, D.W., 1976. Water stress, growth, and osmotic adjustment. Philosophical transactions of the Royal Society of London B273, 538-545.
174. Huber, B., 1928. Weitere quantitative untersuchungen über das wasserleitungssystem der Pflanzen. Jahrb. Wiss. Botany 67, 877-959.
175. Huber, B., 1932. Beobachtung und messung pflanzlicher saftströme. [Berichte Deutsche Botanische Gessellenschaft 50, 89-109].
176. Huber, B., 1956. Die gefassleitung. In: Encyclopedia of plant physiology, Vol. 3, ed, E. Ruhland. Springer, Berlin, 541-582.
177. Huber, B., and Schmidt, E., 1937. Eine Kompensations-methode zur thermoelektrischen Messung langsmer Saftsröme. [Berichte Deutsche Botanische Gessellenschaft 55, 514-529].
178. Humble, G.D., and Raschke, K., 1971. Stomatal opening quantitatively related to potassium transport. Evidence from electron probe analysis. Plant Physiology 48, 447-453.
179. Hungerford, R.D., 1987. Estimation of foliage area in dense Montana lodgepole pine stands. Canadian Journal of Forest Research 17, 320-324.
180. Hutchings, M.J., and Discombe, R.J., 1986. The detection of spatial pattern in plant populations. Journal of Biogeography 13, 225-236.
181. Incoll, W.D., 1979. Root system investigations in stands of Eucalyptus regnans. Victoria Forestry Commission Technical Paper 27, 23-32. (Cited by Baldwin and Stewart, 1987).
182. Ishida, T., Campbell, G.S., and Calissendorff, C., 1991. Improved heat balance method for determining sap flow rate. Agricultural and Forest Meteorology 56, 35-48.
183. Jacobs, M.R., 1955. Growth habits of eucalypts. Canberra, Commonwealth Forestry and Timber Bureau, 262 pp.
184. Jakob, M., 1949. Heat transfer (Vol. 1, section 3-7). John Wiley and Sons, New York.
185. Jarvis, P.B., James, G.B., and Landsberg, J.J., 1976. Coniferous forests. In: Vegetation and the atmosphere. Vol. II., ed. J.L. Monteith. Academic Press, New York, pp. 171-236.
186. Jarvis, P.G., 1975. Water transfer in plants. In: Heat and mass transfer in the environment of vegetation. eds D.A. de Vries and N.H. Afgan. Seminar (1974) of the International Centre for Heat and Mass Transfer, Dubrovnik. Scripta Book Company, Washington D.C., pp. 369-394.
187. Jarvis, P.G., 1985a. Transpiration and assimilation of tree and agricultural crops: The 'omega-factor.' In: Attributes of trees as crop plants, eds. M.G.R. Cannell and J.E. Jackson. Institute of Terrestrial Ecology, Natural Environement Research Council, Huntingdon, pp. 460-480.
188. Jarvis, P.G., 1985b. Increasing forest productivity and the value of temperate coniferous forests by manipulating site water balance. In: Forest potentials: productivity and value, ed. P. Farnham. Weyerhauser, Washington, pp. 39-74.
189. Jarvis, P.G., and Leverenz, J.W., 1983. Productivity of temperate deciduous and evergreen forest. In: Physiological plant ecology, Vol 12D, ed. O.L. Lange. Springer, Berlin, pp. 233-280.
190. Jarvis, P.G., and McNaughton, K.G., 1986. Stomatal control of transpiration: scaling up from leaf to region. Advances in Ecological Research 15, 1-49.
191. Jarvis, P.G., and Stewart, J.B., 1979. Evaporation of water from plantation forest. In: The ecology of even-aged forest plantations, ed. E.D. Ford, D.C. Malcolm and J. Atterson. Institute of Terrestrial Ecology, Cambridge, pp. 327-350.
192. Jarvis, P.G., Edwards, W.R.N., and Talbot, H., 1981. Models of plant and crop water us. In: Mathematics

and plant physiology, eds. D.A. Rose and D.A. Charles Edwards. Academic Press, London, pp. 151-194.
193. Jones, H.G., 1976. Crop characteristics and the ratio between assimilation and transpiration. Journal of Applied Ecology 13, 605-622.
194. Jones, H.G., 1981. The use of stochastic modelling to study the influence of stomatal behaviour on yield-climate relationships. In: Mathematics and plant physiology, ed. D.A. Rose and D.A. Charles-Edwards. Academic Press, London, pp. 231-244.
195. Jordan, W.R., Brown, K.W., and Thomas, J.C., 1975. Leaf age as a determinant in stomatal control of water loss from cotton during water stress. Plant Physiology 56, 595-599.
196. Kaiser, W.M., 1987. Effects of water deficit on photosynthetic capacity. Physiologia Plantarum 71, 142-149.
197. Kaufmann, M.R., and Troendle, C.A., 1981. The relationship of leaf area and foliage biomass to sapwood conducting area in four subalpine forest tree species. Forest Science 27, 477-482.
198. Keane, M.G., and Weetman, G.F., 1987. Leaf area - sapwood cross-sectional area relationships in repressed stands of lodgepole pine. Canadian Journal of Forest Research 17, 205-209.
199. Kelliher, F.M., Black, T.A., and Price, D.T., 1986. Estimating the effects of understorey removal from a douglas fir forest using a two-layer evapotranspiration model. Water Resources Research 22, 1891-1899.
200. Kitano, M., and Egushi, H., 1989. Quantative analysis of transpiration stream dynamics in an intact cucumber stem by a heat flux control method. Plant Physiology 89, 643-647.
201. Kline, J.R., Reed, K.L., Waring, R.H., and Stewart, M.L., 1976. Field measurement of transpiration in Douglas-fir. Journal of Applied Ecology 13, 273-283.
202. Körner, C.H., and Cochrane, P., 1985. Stomatal responses and water relations of Eucalyptus pauciflora in summer along an elevational gradient. Oecologia 66, 443-455.
203. Kozlowski, T.T., 1968. Intoduction. In: Water deficits and plant growth, ed. T.T. Kozlowski. Vol I, pp. 1-21.
204. Kozlowski, T.T., 1972. Shrinking and swelling of plant tissues. In: Water deficits and plant growth, Vol. 3, ed. T.T. Kozlowski. New York, Academic Press.
205. Kozlowski, T.T., 1976. Water relations and tree improvement. In: Tree physiology and yield improvment, ed. M. Cannell and F.T. Last. London, Academic Press, pp. 307-327.
206. Kozlowski, T.T., 1979. Tree growth and environmental stresses. Seattle, University of Washington Press.
207. Kozlowski, T.T., Kunz, J.E., and Winget, C.H., 1962. Effect of oak wilt on cambial activity. Journal of Forestry 60, 558-561.
208. Kozlowski, T.T. and Peterson, T.A., 1962. Seasonal growth of dominant, intermediate, and suppressed red pine trees. Botanical Gazette 124, 146-154.
209. Kramer, P.J., 1969. Plant and soil water relationships: a modern synthesis. New York, McGraw-Hill.
210. Kramer, P.J., 1988. Changing concepts regarding plant water relations. Plant, Cell and Environment 11, 565-568.
211. Kramer, P.J., and Kozlowski, T.T., 1979. Physiology of woody plants. New York, Academic Press.
212. Kramer. P., and Kozlowski, T., 1979. Physiology of woody plants. Academic Press, Orlando, Florida, U.S.A.
213. Kuera, J., Cermák, J., and Penka, M., 1977. Improved thermal method of continual recording the transpiration flow rate dynamics. Biologia Plantarum 19, 413-420.
214. Landsberg, J.J., 1986. Physiological ecology of forest production. Academic Press.
215. Landsberg, J.J., and Fowkes, N.D., 1978. Water movement through plant roots. Annals of Botany 42, 493-508.
216. Landsberg, J.J., and Jones, H.G., 1981. Apple orchards. In: Water deficits and plant growth, Vol 6, ed. T.T. Kozlowski. Academic Press, New York, pp 419-469.
217. Landsberg, J.J., Blanchard, T.W., and Warrit, B., 1976. Studies on the water movement through apple trees. Journal of Experimental Botany 27, 579-596.
218. Langford, K.J., 1976. Change in yield of water following a bushfire in Eucalyptus regnans. Journal of Hydrology 29, 87-114.
219. Larcher, W., 1980. Physiological plant ecology, 2nd ed. Springer-Verlag, New York.
220. Larson, P.R., 1963. Stem form development of trees. Forest Science Monographs No. 5.
221. Lascano, R.J., Baumhardt, R.L., and Lipe, W.N., 1992a. Measurement of water flow in young grapevines using the Stem Heat Balance Method. American Journal of Enology and Viticulture 43, 159-165.
222. Lascano, R.J., Baumhardt, R.L., and Lipe, W.N., 1992b. Stem gauge measurements of sap flow in grape vines. In: Symposium on sap flow measurements. Collected summaries of papers presented at the 83rd annual meeting of the Amercian Society of Agronomy, ed. C.H.M. Van Bavel. Dynamax, Houston TX 7703, pp.13-14.
223. Lasoie, J.P., Scott, D.R.M., and Frischen, L.J., 1977. Transpiration studies in Douglas-fir using the heat pulse technique. Forest Science 23, 377-390.
224. Layzell, D.B., Pate, J.S., Atkins, C.A., and Canvin. D.T., 1981. Partitioning of carbon and nitrogen and the nutrition of root and shoot apex in a nodulated legume. Plant Physiology 67, 30-36.
225. Leopold, A.C., and Kawase, M., 1964. Benzyladenine effects on bean leaf growth and senescence. American Journal of Botany 51, 294-298.
226. Levitt, D.G., Simpson, J.R., and Tipton, J.L., 1992. Effects of thermal noise on stem flow gauge performance. In: Symposium on sap flow measurements. Collected summaries of papers presented at the 83rd annual meeting of the Amercian Society of Agronomy, ed. C.H.M. Van Bavel. Dynamax, Houston TX 7703, pp. 15-16.

227. Levitt, J., 1974. Introduction to plant physiology. University of Missouri, Columbia, pp. 104-113.
228. Levitt, J., 1980. Responses of plants to environmental stresses, Vol. 2. Academic Press, New York.
229. Leyton, L. 1969. Problems and techniques in measuring transpiration from trees. In: Physiology of the crops, eds L.C. Lucwill and C.V. Cutting. Academic Press, New York.
230. Lightbody, K.E., Savage, M.J., and Graham, A.D.N., 1994. In situ measurement of sap flow in lateral roots and stems of Eucalyptus grandis, under conditions of marginality, using a steady state heat energy balance technique. Jounal of the Southern African Society of Horticultutal Science 4, 1-7.
231. Lima, W.P., 1984. The hydrology of Eucalypt forests in Australia - A review. IPEF, Piracicaba.
232. Linder, S., 1985. Potential and actual production in Australian forest stands. In: Research for forest management, ed. J.J. Landsberg and W. Persons. CSIRO, Melbourne, pp. 11-45.
233. Long, J.N., and Smith, F.W., 1988. Leaf area - sapwood area relations of lodgepole pine as influenced by stand density and site index. Canadian Journal of Forest Research 18, 247-250.
234. Long, J.N., and Smith, F.W., 1989. Estimating leaf area of Abies lasiocarpa across ranges of stand density and site quality. Canadian Journal of Forest Research 19, 930-932.
235. Long. J.N., Smith, F.W., and Scot, D.R.M., 1981. The role of Douglas-fir stem sapwood and heartwood in the mechanical and physiological support of crowns and development of stem form. Canadian Journal of Forest Research 11, 459-464.
236. Lopushinsky, W., 1986. Seasonal and diurnal trends of heat pulse velocity in Douglas-fir and ponderosa pine. Canadian Journal of. Forest Research. 18, 841-821.
237. Lösch, R., Pereira, J.S., and Lange, O.L., 1982. Diurnal courses on stomatal resistance and transpiration of wild and cultivated Mediterranean perennials at the end of the summer dry season in Portugal. Flora 172, 138-160.
238. MacVicar, C.N., de Villiers, J.M., Loxton, R.F., Verster, E., Lambrechts, J.J.N., Merryweather, F.R., Le Roux, J., Van Rooyen, T.H. and Von M Harmse, H.J., 1977. Soil Classification, a Binomial System for South Africa. Soil and Irrigation Research Institute, Department of Agricultural Technical Services, Pretoria, Science Bulletin 390, pp. 150.
239. Marchand, P.J., 1984. Sapwood area as an estimator of foliage biomass and projected leaf area for Abies balsamea and Picea rubens. Canadian Journal of Forestry Research 14, 85-87.
240. Mark, W.R., and Crews, D.L., 1973. Heat pulse velocity and bordered pit condition in living Engelmann spruce and lodgepole pine trees. Forest Science 19, 291-296.
241. Marshall, D.C., 1958. Measurement of sap flow in conifers by heat transport. Plant Physiology 33, 385-396.
242. Marshall, J.D., and Waring, R.H., 1984. Conifers and broadleaf species: Stomatal sensitivity differs in western Oregon. Canadian Journal of Forest Research 14, 905-908.
243. Martin, C., and Thimann, K.V., 1972. The role of protein synthesis in the senescence of leaves 1. The formation of protease. Plant Physiology 49, 64-71.
244. Mathur, H.N., Raj, F.H., and Rajagopal, K., 1986. Root studies on Eucalyptus globulus. In: Eucalypts in India: past present and future, ed. J.K. Sharma, C.T.S. Nair, S. Kedharnath and S. Kondas. Kerala Forest Research Institute, India, pp. 225-228.
245. Mathur, H.N., Ram Babu, J.P., and Singh, B., 1976. Effects of clearfelling and reforestation on runoff and peak rates in small watersheds. Indian Forester 102, 219-226.
246. McNaughton, K.G., and Jarvis, P.G., 1983. Predicting effects of vegetation changes on transpiration and evaporation. In: Water deficits and plant growth. Vol. 7, Ed. T.T. Kozlowski. Academic Press, New York. pp. 1-47.
247. Meyer, W.S. and Ritchie, J.T. 1980. Resistance to water flow in the sorghum plant. Plant Physiology 65, 33-39.
248. Miller, D.R., Vavrina, C.A., and Christensen, T.W., 1980. Measurment of sap flow and transpiration in ring-porous oaks using the heat pulse velocity technique. Forest Science 26, 485-494.
249. Mitchell, B.W., 1983. Instrumentation and measurement for environmental sciences. American Society of Agricultural Engineering Special Publiation, pp. 13-82.
250. Mithen, R., Harper, J.L., and Weiner, J., 1984. Growth and mortality of individual plants as a function of "available area". Oecologia 62, 57-60.
251. Moehring, D.M., Grano, C.X., and Bassett, J.R., 1975. Xylem development of loblolly pine during irrigation and simulated drought. U.S.D.A. Forest Service Research Paper No. SO-110.
252. Monteith, J.L., 1965. Evaporation and environment. In: Environmental control of plant growth, ed. L.T. Evans. Academic Press, New York, pp. 95-112.
253. Monteith, J.L. and Unsworth, M.J., 1990. Principles of Environmental Physics, 2 nd Edition. Edward Arnold, London, pp. 289.
254. Morikawa, Y., 1974. Sap flow in Chamaecyparis obtusa in relation to water economy of woody plants. Tokyo Daigaku Nogakubu Enshurin Hokoku, Forests 66, 251-297. (Cited by Waring, Schroeder and Oren, 1982).
255. Myers, B.A., Küppers, M., and Neales, T.F., 1987. Effect of stem excision under water on bulk leaf water potential, leaf conductance, CO_2 assimilation and stemwood water storage in Eucalyptus behriana F. Muell. Australian Journal Plant Physiology 14, 135-145.
256. Nänni, U.W., 1971. The Mokobulaan research catchments. South African Forestry Journal 78, 5-13.
257. Neumann, P.M., and Noodén, D.L., 1983. Interaction of mineral and cytokinin supply in control of leaf senescence and seed growth in soybean explants. Journal of Plant Nutrition 6, 735-742.
258. Neumann, P.M., and Noodén, D.L., 1984. Pathway and regulation of phosphate translocation to the pods of soybean explants. Physiologia Plantarum 60, 166-170.

259. Neumann, P.M., and Stein, Z., 1983. Xylem transport and the regulation of leaf metabolism. Whats New in Plant Physiology. 14, 33-36.
260. Neumann, P.M., and Stein, Z., 1984. Relative rates of delivery of xylem solute to shoot tissues: possible relationship to sequential leaf senescence. Physiologia Plantarum 62, 390-397.
261. Newbanks, D., Bosch, A., and Zimmermann, M.H., 1983. Evidence for xylem dysfunction by embolisation in Dutch elm disease. Phytopathology 73, 1060.
262. Olbrich, B.W., 1991. The verification of the heat pulse velocity technique for estimating sap flux in Eucalyptus grandis. Canadian Journal of Forest Research. 21, 836-841.
263. Ong, C.K., and Kahn, A.A.H., 1993. The direct measurment of water uptake by individual tree roots. Agroforestry Today 4, 2-5.
264. Ong, C.K., Singh, R.P., Kahn, A.A.H., and Osman, M., 1990. Recent advances in measuring water loss through trees. Agroforestry Today 2, 7-9.
265. Pallardy, S.G., and Kozlowski, T.T., 1979. Relationship of leaf diffusion resistance of Populus clones to leaf water potential and environment. Oecologia 40, 371-380.
266. Panshin, A.J., and de Zeeuw, C., 1980. Textbook of wood technology, 4th ed., McGraw-Hill, New York.
267. Passioura, J.B., 1981. Water collection by roots. In: The physiology and biochemistry of drought resistance in plants, ed. L.G. Paleg and D. Aspinall. Academic Press, London; New York, pp. 39 -53.
268. Passioura, J.B., 1988. Response to Dr. P.J. Kramer's article, Changing concepts regarding plant water relations in Plant, Cell and Environment 11, pp. 565-568. Plant, Cell and Environment 11, 569-571.
269. Passioura, J.B., and Munns, R., 1984. Hydraulic resistance to plants. II. Effects of rooting medium and time of day in barley and lupin. Australian Journal of Plant Physiology 11, 341.
270. Pate, J.S, and Atkins, C.A., 1983. Xylem and phloem transport and the functional economy of carbon and nitrogen of a legume leaf. Plant Physiology 71, 835-840.
271. Pate, J.S., and Gunning, B.E.S., 1972. Transfer cells. Annual Review of Plant Physiology 23, 173-196.
272. Pearce, A.J., and Rowe, L.K., 1981. Rainfall interception in a multi-storied, evergreen mixed forest: Estimates using Gash's analytical model. Journal of Hydrology 49, 341-353.
273. Penka, M., ermák, J., and Deml, M., 1973. Water transport estimates in adult trees based on measurement of heat transfer by mass flow. Acta Univ. Agr., Series C (Facultas silviculturae) 42, 2-23.
274. Pereira, J.S., Chaves, M.M., Rodrigues, M.L., and Davies, W.J., 1989. The afternoon decline in leaf CO_2 fixation in the absence of water deficits involves stomatal closure and changes in photosynthetic capacity a the chloroplast level in grapevines in the field. Physiologia Plantarum 76, pp. A169.
275. Pereira, J.S., Tenhunen, D.L., Lange. O.L., Beyschlag, W., Meyer, A., and David M.M., 1986. Seasonal and diurnal patterns in leaf gas exchange of Eucalyptus globulus trees growing in Portugal. Canadian Journal of Forest Research 16, 177-184.
276. Pereira, J.S., Tenhunen, J.D., and Lange, O.L., 1987. Stomatal control of photosynthesis of Eucalyptus globulus Labill. trees under field conditions in Portugal. Journal of Experimental Botany 38, 1678-1688.
277. Peressotti, A., and Ham, J.M., 1996. A dual-heater gauge for measuring sap flow with an improved heat-balance method. Agronomy Journal 88, 149-155.
278. Perreira, J.S., and Kozlowski, T.T., 1976. Leaf anatomy and water relations of Eucalyptus camaldulensis and E. globulus seedlings. Canadian Journal of Botany 54, 2868-2880.
279. Petersen, K.L., Fuchs, M., Moreshet, Y., and Sinoquet, H., 1992. Computing transpiration of sunlit and shaded cotton foliage under variable water stress. Agronomy Journal 84, 91-97.
280. Philipson, J.J., and Coutts, M.P., 1977. The influence of mineral nutrition on the root development of trees. II. The effect of specific nutrient elements on the growth of individual roots of Sitka spruce. Journal of Experimental Botany 28, 864-871.
281. Pickard, W.F., and Puccia, C.J., 1972. A theory of the steady-state heat step method of measuring water flux in woody plant stems. [Math. Biosci. 14, 1-15].
282. Pielou, E.C., 1977. Mathematical Ecology. Wiley, New York, 385pp.
283. Pook, E.W., and Moore, P.H.R., 1991a. Rainfall interception by trees of Pinus radiata and Eucalyptus viminalis in a 1300 mm rainfall area of Southern New South Wales. I. Gross losses and their variability. Hydrological Processes 5, 127-141.
284. Pook, E.W., and Moore, P.H.R., 1991b. Rainfall interception by trees of Pinus radiata and Eucalyptus viminalis in a 1300 mm rainfall area of Southern New South Wales. II. Influence of wind-born precipitation. Hydrological Processes 5, 143-155.
285. Pospisilova, J., and Solarova, J., 1980. Environmental and biological controll of diffusive conductances of adaxial and abaxial leaf epidermis. Photosynthetica 14, 90-127.
286. Pothier, D., Margolis, H.A., and Waring, R.H., 1989. Patterns of change of saturated sapwood permeability and sapwood conductance with stand development. Canadian Journal of Forest Research 19, 432-439.
287. Pothier, D., Margolis, H.A., Poliquin, J., and Waring, R.H., 1989. Relation between permeability and the anatomy of jack pine sapwood with development. Canadian Journal of Forest Research 19, 1564-1570.
288. Poynton, R.J., 1971. A silivicultural map of southern Africa. South African Journal of Science 67, 58-60.
289. Puritch, G.S., 1971. Water permeability of the wood of Grand fir (Abies grandis (Doug.) Lindl.) in relation to infestation by balsam woolly aphid, Adeleges piceae (Ratz.). Journal of Experimental Botany 22, 936-945.
290. Quarrie, S.A., 1990. Water stress proteins. In: Importance of root to shoot communication in the responses to environmental stress. Monograph 21, ed. W.J. Davies and B. Jeffcoat. British Society for Plant Growth Regulation, Bristol, pp. 13-28.
291. Quraishi, M.A., and Kramer, P.J., 1970. Water stress in three species of Eucalyptus. Forest Science 16,

74-78.
292. Raupach, M.R., and Finnigan, J.J., 1988. "Single-layer models of evaporation from plant canopies are incorrect but useful, whereas multilayer models are correct but useless?" Discuss. Australian Journal of Plant Physiology 15, 705-716.
293. Raven, J., and Handely, L.L., 1987. Transport processes and water relations. New Phytologist 106 (suppl.), 217-233.
294. Rawat, P.S., Negi, D.S., Rawat, J.S., and Gurumurti, K., 1985. Transpiration, stomatal behaviour and growth of Eucalyptus hybrid seedlings under different soil moisture levels. Indian Forester 12, 1097-1112.
295. Rein, H., 1929. Die thermo-stromuhr. II. Mitteilung der srbeitsbedingungen and arbeitsmöglichkeiten im tierversuch. [Zeitschr. F Biol. 89, 195].
296. Reynolds, J.F., Acock, B, Dougherty, R.L., and Tenhunen, J.D., 1989. A modular struture for plant growth simulation models. In: Biomass production by fast-growing trees, eds J.S. Pereira and J.J. Landsberg. Kluwer Academic Publishers, London, 288 pp.
297. Richter, H., 1973. Frictional potential losses and total water potential in plants: a re-evaluation. Journal Experimental Botany 24, 983-994.
298. Richter, J.P., 1970. The notebooks of Leonardo da Vinci. Vol. I. Dover, New York. pp. 205.
299. Roberts, J., 1976. An examination of the quantity of water stored in mature Pinus sylvestris L. trees. Journal Experimental Botany 27, 473-479.
300. Roberts, J., 1977. The use of tree-cutting techniques in the study of the water relations of mature Pinus sylvestris L. I. The technique and survey of the results. Journal Experimental Botany 28, 751-767.
301. Roberts, J., 1978. The use of the 'tree cutting' technique in the study of the water relations of Norway spruce, Picea abies (L.) Karst. Journal Experimental Botany 29, 465-471.
302. Roberts, J., Cabral, O.M.R., and de Aguiar, L.F., 1990. Stomatal and boundary-layer conductances in an Amazonian terra firme rain forest. Journal of Applied Ecology 27, 336-353.
303. Rogers, R. and Hinckley, T.M., 1979. Foliar weight and area related to current sapwood area in oak. Forest Sciece 25, 298-303.
304. Rothwell, R.L., 1974. Sapwood water content of lodgepole pine. Ph.D. Thesis, University of British Columbia.
305. Running, S.W., 1980. Field estimates of root and xylem resistances in Pinus contorta using root excision. Journal Experimental Botany 31, 555-569.
306. Rusk, G.D., Pennefather, M., Dobson, D.A.G., and Ferguson, J.B., 1991. The economics of growing Eucalypts in the Republic of South Africa. In: Intensive forestry: The role of Eucalypts. IUFRO symposium, ed. A.P.G. Schönau. Southern African Institute of Forestry, Pretoria, pp. 870-879.
307. Rutter, A.J., 1966. Studies on the water relations of Pinus sylvestris in plantation conditions, IV. Direct observations on the rates of transpiration, evaporation of intercepted water, and evaporation from the soil surface. Journal Applied Ecology 3, 393-405.
308. Rutter, A.J., and Morton, A.J., 1977. A predictive model of rainfall interception of forests. III. Sensitivity of the model to stand parameters and meteorological variables. Journal of Applied Ecology 14, 567-588.
309. Rutter, A.J., Kershaw, K.A., Robins, P.C., and Morton, A.J., 1971. A predictive model of rainfall interception in forests. I Derivation of the model from observations in a plantation of Corsican pine. Agricultural Meteorology 9, 367-383.
310. Rutter, A.J., Morton, A.J., and Robins, P.C., 1975. A predictive model of rainfall interception in forests. II. Generalisations of the model and comparisons with observations in some coniferous and hardwood stands. Journal of Applied Ecology 12, 367-380.
311. Saddler, H.D.W., and Pitman, M.G., 1970. An apparatus for measurement of sap flow in unexcised leafy shoots. Journal of Experimental Botany 21, 1048-1059.
312. Sakuratani, T., 1979.Apparent thermal conductivity of rice stems in relation to transpiration stream Journal of Agricultural Meteorology (Japan) 34, 177-187.
313. Sakuratani, T., 1981. A heat balance method for measuring water flux in the stem of intact plants. Journal of Agricultural Meteorology (Japan) 37, 9-17.
314. Sakuratani, T., 1984. Improvement of the probe for measuring water flow rate in intact plants with the stem heat balance method. Journal of Agricultural Meteorology (Japan) 40, 273-277.
315. Sakuratani, T., 1987. Studies on evapotranspiration from crops. II. Separate estimation of transpiration and evaporation from a soybean field without water shortage. Journal of Agricultural Meteorology (Japan) 42, 309-317.
316. Sakuratani, T., 1990. Measurement of the sap flow rate in stem of rice plant. Journal of Agricultural Meteorology (Japan) 45, 277-280.
317. Sakuratani, T., and Abe, J., 1985. A heat balance method for measuring water flow rate in stems of intact plants and its application to sugarcane plants. JARQ 19, 92-97.
318. Salama, R.B., Bartle, G.A., and Farrington, P., 1994. Water use of Eucalyptus camaldulensis estimated by groundwater hydrograph separation techniques and heat pulse method. Journal of Hydrology 156, 163-180.
319. Saliendra, N.Z., Meinzer, F.C., Grantz, D.A., Neufeld, H., and Goldstein, G., 1992. Transpiration of diverse sugarcane genotypes during soil drying in the field. In: Symposium on sap flow measurements. Collected summaries of papers presented at the 83rd annual meeting of the Amercian Society o Agronomy. ed. C.H.M. Van Bavel. Dynamax, Houston TX 7703, pp. 19-20
320. Sato, K., and Sakuratani, T., 1982. Water consumption at different levels of soybean canopies of different plant spacings in the field estimated from water fluxes in the stem. Japanese Journal of Crop Science 51, 75-81.

321. Sauter, J.J., 1984. Detection of embolisation of vessels by a double staining technique. Journal Plant Physiology 116, 331.
322. Savage, M.J. and A. Cass, 1984. Measurement of water potential using *in situ* thermocouple hygrometers. Advances in Agronomy 37, 73-126.
323. Savage, M.J., 1978. Water potential terms and units. Agrochemophysica 10, 5-6.
324. Savage, M.J., 1996. Basic thermodynamic quantities. *In* F.B. Salisbury (ed) Units, Symbols and Terminology for Plant Physiology: A Reference for Presentation of Research Results in the Plant Sciences, Chapter 4, 45-54. Oxford University Press, Oxford.
325. Savage, M.J., C.S. Everson and B.R. Metelerkamp, 1997. Evaporation measurement above vegetated surfaces using micrometeorological techniques. Water Research Commission Report No. 349/1/97, p248, ISBN No: 1 86845 363 4.
326. Savage, M.J., Graham, A.D.N., and Lightbody, K.E., 1993. Use of a stem steady state heat energy balance technique for the in situ measurement of transpiration in Eucalyptus grandis: Theory and errors. Journal of the Southern African Society for Horticultural Sciences 3, 46-51.
327. Savage, M.J., H.H. Wiebe and A. Cass, 1983. *In situ* field measurement of leaf water potential using thermocouple psychrometers. Plant Physiology 73, 609-613.
328. Schanderl, H., 1956. Untersuchungen uber die geschwindigkeit des transpirations stromes in den jungsten gefassen der reben. Mitt Loh Bundeslehr u. VersAnst. Wein-Obst. u. Gartenb. (Mitteilungen Klosterneubug serie Arebe und wein) 6A, 269-286.
329. Scholander, P.F., 1972. Tensile water. American Scientist 60, 584-590.
330. Scholander, P.F., Hammel, H.T., Bradstreet, E.D., and Hemmingsen, E.A., 1965. Sap pressure in vascular plants. Science 143, 339-346.
331. Schulze, B.R., 1958. The climate of South Africa according to Thornthwait's rational classification. South African Geographical Journal 40, 31-54.
332. Schulze, E.D., 1986. Carbon dioxide and water vapour exchange in response to drought in the atmosphere and in the soil. Annual Review of Plant Physiology 37, 247-274.
333. Schulze, E.D., and Küppers, M., 1979. Short-term and long-term effects of plant water deficits on stomatal response to humidity in Corylus avellana L. Planta 146, 319-326.
334. Schulze, E.D., ermák, J., Matyssek, R., Penka, M., Zimmerman, R., Vasicek, F., Gries, W., and Kuera, J., 1985. Canopy transpiration and water fluxes in the xylem of the trunk of Larix and Picea trees - a comparison of xylem flow, porometer and cuvette measurements. Oecologia 66, 475-483.
335. Schulze, E.D., ermák, Mattysek, R. Penka, M., Zimmermann, R., Vasícek, R., Gries, W., and Kuera, J., 1985. Canopy transpiration and water fluxes in the xylem of the trunk of Larix and Picea trees - a comparison of xylem flow, porometer and cuvette measurements. Oecologia 66, 475-483.
336. Schulze, E.D., Lange, O.L., Kappen, L., Evenari, M., and Buschbom, U., 1975. The role of air humidity and temperature in controlling stomatal resistance in Prunus armeniaca L. under desert conditions II. The significance of leaf water status and internal carbon dioxide concentration. Oecologia 18, 218-233.
337. Schulze, E.D., Schilling, K., and Nagarajah, S., 1983. Carbohydrate partitioning in relation to whole plant production and water use of Vigna unguiculata (L.) Walp. Oecologia 58, 169-177.
338. Schulze, E.D., Steudle, E., Gollan, T., and Schurr, U., 1988. Response to Dr. P.J. Kramer's article, Changing concepts regarding plant water relations in Plant, Cell and Environment 11, 565-568. Plant, Cell and Environment 11, 573-576.
339. Scott, D.M., 1993. In S.A. Lorentz, S.W. Kienzle and M.C. Dent (eds). Proceedings of the Sixth South African National Hydrological Symposium, Volume 1.
340. Senock, R.S., and Ham, J.M., 1995. Measurements of water use by prairie grasses with heat balance flow gauges. Journal of Range Management 48, 150-158.
341. Shackel, K.A., Johnson, R.S., Medawar, K., and Phene, C.J., 1992. Substantial errors in estimates of sap flow using the heat balance technique on woody stems under field conditions. Journal of the American Society of Horticultural Science 117, 351-356.
342. Shaner, D.L., and Boyer, J.S., 1976. Nitrate reductase activity in maize (Zea mays L.) leaves. I. Regulation by nitrate flux. Plant Physiology 58, 499-504.
343. Sharma, M.L., 1984. Evapotranspiration from a Eucalyptus community. Agricultural Water Management 8, 41-56.
344. Shigo, A.L., and Hillis, W.E., 1973. Heartwood, discoloured wood and micro-organisms in living trees. Annual Review of Phytopathology 11, 197-222.
345. Shinozaki, K., Yoda, K., Hozumi, K., and Kira, T., 1964a. A quantitative analysis of plant form - the pipe model theory. I. Basic analyses. Japanese Journal of Ecology 14, 97-105.
346. Shinozaki, K., Yoda, K., Hozumi, K., and Kira, T., 1964b. A quantitative analysis of plant form - the pipe model theory. II. further evidence of the theory and its application in forest ecology. Japanese Journal of Ecology 14, 133-139.
347. Shiozawa, S., and Campbell, G.S., 1990. Soil thermal conductivity. Remote sensing Reviews 51, 301-310.
348. Shuttleworth, W.J., 1976. A one-dimensional theoretical description of the vegetation-atmosphere interaction. Boundary Layer Meteorology 10, 273-302.
349. Sinclair, R., 1980. Water potential and stomatal conductance of three Eucalyptus species in the Mount Lofty Ranges, south Australia: responses to summer drought. Australian Journal of Botany 28, 499-510.
350. Skaar, C., 1972. Water in wood. Syracuse University Press, New York
351. Slatyer, R.O., 1967. Plant-Water Relationships. Academic Press, New York.
352. Slatyer, R.O., and Morrow, P.A., 1977. Altitudinal variation in the photosynthetic characteristics of snow

gum, Eucalyptus pauciflora Sieb. ex Spreng. I. Seasonal changes under field conditions in the Snow mountains of south-eastern Australia. Australian Journal of Plant Physiology 25, 1-20.
353. Smith, M.K., Watson, K.K., and Pilgrim, D.H., 1974. A comparative study of the hydrology of Pinus radiata and Eucalyptus forests of Lidsdale, New South Wales. Hydrology Symposium. Sydney Institute of Engineers, Australia, pp.91-98. (Cited by Calder, 1986).
354. Smith, R.E., 1992. The heat pulse technique for determining water uptake of Populus deltoides. South African Journal of Botany 58, 100-104.
355. Snell, J.K.A, and Brown, J.K., 1978. Comparison of tree biomass estimators - dbh and sapwood area. Forest Science 24, 455-457.
356. Sperry, J., Donnelly, J.R., and Tyree, M.T.,1988. A method for measuring hydraulic conductivity and embolism in xylem. Plant, Cell and Environment 11, 35.
357. Sperry, J.S., and Tyree, 1988. Mechanism of water stress induced xylem embolism. Plant Physiology 88, 581-587.
358. Sperry, J.S., and Tyree, M.T., 1990. Water-stress-induced xylem embolism in three species of conifers. Plant, Cell and Environment 13, 427-436.
359. Sperry, J.S., Tyree, M.T., and Donnelly, J.R., 1988. Vulnerability of xylem to embolism in a mangrove vs. inland species of Rhizophoraceae. Physiologia Plantarum 74, 276-283.
360. Steinberg, S.L., 1988. Dynamax trunk-flow gauge test. In: Technical Application Report. Insulation and time of attachment test. Texas AandM University College Station, TX 77843, pp.1-33.
361. Steinberg, S.L., McFarland, M.J., and Worthington, J.W., 1990. Comparison of trunk and branch sap flow with canopy transpiration in pecan. Journal of Experimental Botany 41, 653-659.
362. Steinberg, S.L., Van Bavel, C.H.M., and McFarland, M.J., 1989. A gauge to measure mass flow rate of sap in stems and trunks of woody plants. Journal of the American Society of Horticultural Science 114, 446-472.
363. Steinberg, S.L., Van Bavel, C.H.M., and McFarland, M.J., 1990. Improved sap flow gauge for woody and herbaceous plants. Agronomy Journal 82, 851-854.
364. Steinberg, S.L., Zajicek, J.M., and McFarland, M.J., 1991a. Short-term effect of Uniconazole on the water relations and growth of Ligustrum. Journal of the American Society of Horticultural Science 116, 460-464.
365. Steinberg, S.L., Zajicek, J.M., and McFarland, M.J., 1991b. Water relations of Hibiscus following pruning or chemical growth regulation. Journal of the Amererican Society of Horticultural Science 116, 465-470.
366. Stewart, C.M., Tham, S.H., and Rolfe, D.L., 1973. Diurnal variations of water in developing secondary stem tissues of eucalypt trees. Nature U.K. 242, 479-480.
367. Stockle, C.O., Kjelgaard, and Campbell, G.S., 1992. Measuring sap flow with the heat balance approach using constant and variable heat input. In: Symposium on sap flow measurements. Collected summaries of papers presented at the 83rd annual meeting of the Amercian Society of Agronomy, ed. C.H.M. Van Bavel. Dynamax, Houston TX 7703, pp. 25-26.
368. Stone, J.F., and Shirazi, G.A., 1975. On the heat pulse method for measurement of apparent sap velocity in stems. Planta 122, 169-177.
369. Stuart-Crombie, D., and Tippett, J.T., and Gorddard, D.J., 1987. Water relations of root-pruned Jarrah (Eucalyptus marginata Donn ex Smith) saplings. Australian Journal of Botany 35, 653-663.
370. Swanson, R.H., 1962. Rocky Mountain Forest Range Experimental Station Paper 68:
371. Swanson, R.H., 1967. Seasonal course of transpiration of Lodgepole and Engelmann spruce. In: Proceedings of the International Symposium of Forest Hydrology, Penn. State Univ., U.S.A., eds W.E. Sopper and H.W Lull, Pergamon Press, Oxford, pp. 417-432.
372. Swanson, R.H., 1972. Water transpired by trees is indicated by heat pulse velocity. Agricultural Meteorology 10, 277-281.
373. Swanson, R.H., 1974. A thermal flowmeter for estimating the rate of xylem sap ascent in trees. In: Flow, its measurement and control in science and industry, Vol. I., ed. R.B. Dowell, Instrument Society of America, Pittsburgh, 647-652.
374. Swanson, R.H., 1983. Numerical and experimental analysis of implanted-probe heat-pulse theory. PhD Thesis, University of Alberta, Canada, pp. 1-235.
375. Swanson, R.H., and Whitfield, 1981. A numerical analysis of heat pulse theory and practice. Journal of Experimental Botany 32, 221-239.
376. Swanson, R.H., Beneke, U., and Havranek, W.M., 1979. Transpiration in mountain beech estimated simultaneously by heat-pulse velocity and climatizd ??? curvette???. New Zealand Journal of Forest Science 9, 170-176.
377. Taylor, H.M., and Klepper, B., 1978. The role of rooting characteristics in the supply of water to plants. Advances in Agronomy 30, 99-128.
378. Teixeira, P., and Sarmento, P., 1991. Assessing the environmental impact of Eucalyptus plantations in Portugal. In: Intensive forestry: the role of Eucalypts, ed. A.P.G. Schönau. Southern African Institute of Forestry, Pretoria, pp. 1069- 1080.
379. Teskey, R.O., Grier, C.C. and Hinckley, T.M.1985. Relation between root system size and water inflow capacity of Abies amabilis growing in subalpine forest. Canadian Journal of Forest Research 15, 669-672.
380. Thompson, D.C., 1989. The effect of stand structure and stand density on the leaf area - sapwood area relationship of lodgepole pine. Canadian Journal of Forest Research 19, 392-396.
381. Thompson, R.G., Tyree, M.T., LoGullo, M.A., and Salleo, S., 1983. The water relations of young olive trees in a Mediterranean winter: Measurements of evaporation from leaves and water conduction in wood. Annals of Botany 52, 399-406.

382. Thorpe, M.R., and Lang, A., 1983. Control of import and export of photosynthate in leaves. Journal Experimental Botany 34, 231-239.
383. Thorpe, M.R., Saugier, B., Auger, S., Berger, A., and Methy, M., 1978. Photosynthesis and transpiration of an isolated tree: model and validation. Plant, Cell and Environment 1, 279-284.
384. Tinker, P.B., 1976. Transport of water to the plant roots in soil. Philosophical transactions of the Royal Society of London B. 273, 445-461.
385. Tinklin, R. and Weatherley, P.E. 1966. On the relationship between transpiration rate and leaf water potential. New Phytologist 65, 509-517.
386. Tomos, A.D., 1985. Physical limitations of leaf cell expansion. In: Control of leaf growth, ed. N.R. Baker. University Press, Cambridge, pp. 1-33.
387. Torrey, J.G., 1976. Root hormones and plant growth. Annual Review of Plant Physiology 27, 435-459.
388. Turner, N.C., and Jones, M.M., 1980. Turgor maintenance by osmotic ajustments: a review and evaluation. In: Adaption of plants to water and high temperature stress, eds N.C. Turner and P.J. Kramer. New York, Wiley-Interscience.
389. Turner, N.C., Schulze, E.D., and Gollan, T., 1985. The response of stomata and leaf gas exchange to vapour pressure deficits and soil water content. II. In the mesophytic herbaceous species Helianthus annus. Plant Physiology 65, 348-355.
390. Tyree, M.T., and Ewers, F.W., 1991. Tansley Review No. 34. The hydraulic architecture of trees and other woody plants. New Phytologist 119, 345-360
391. Tyree, M.T., and Jarvis, P.G., 1982. Water in tissue and cells. In: Physiological plant ecology. Encyclopedia of Plant Physiology Vol. 12 B II. Water relations and carbon assimilation, eds O.L. Lange, P.S., Nobel and C.B. Osmond. Springer-Verlag, Berlin, p.35.
392. Tyree, M.T., and Sperry, J.S., 1988. Do woody plants operate near the point of catastrophic xylem disfunction caused by dynamic water stress? Plant Physiology 88, 574-580.
393. Tyree, M.T., and Yang, S., 1990. Water storage capacity of Thuja, Tsuga and Acer stems measured by dehydration isotherms. The contribution of capillary water and cavitation. Planta 182, 420-426.
394. Tyree, M.T., and Zimmermann, M.H., 1971. The theory and practice of measuring transport coefficients and sap flow in the xylem of red maple stems (Acer rubum). Journal of Experimetal Botany 22, 1.
395. Tyree, M.T., Caldwell, C., and Dainty, J., 1975. Water storage capacity of Thuja, Tsuga and Acer stems by dehydration isotherms: the contribution of capillary water and cavitation. Planta 182, 420-426.
396. Tyree, M.T., Graham, M.E.D., Cooper, K.E., and Bazos, L.J., 1983. The hydraulic architecture of Thuja occidentalis. Canadian Journal of Botany 61, 2105-2111.
397. Tyree, M.Y., 1988. A dynamic model for water flow in a single tree: evidence that models must account for hydraulic architecture. Tree Physiology 4, 195-217.
398. Valancogne, C., and Nasr, Z., 1989. Measuring sap flow in the stem of small trees by a heat balance method. HortScience 24, 383-385.
399. Van Bavel, M.G., and Van Bavel, C.H.M., 1990. Dynagauge installation and operation manual. Dynamax Inc., Texas U.S.A., pp. 1-80.
400. Van den Honert, T.H., 1948. Water transport in plants as a catenary process. Discussions of the Faraday Society 3, 146-153.
401. Van Lill, W.S., Kruger, F.J., and Van Wyk, D.B., 1980. The effect of afforestation with Eucalyptus grandis Hill. ex Maiden and Pinus patula (Schlecht. et Cham.) on streamflow from experimental catchments at Mokobulaan, Transvaal. Journal of Hydrology 48, 107-118.
402. Van Staden, J., and Davey, 1979. The synthesis, transport and metabolism of endogenous cytokinins. Plant, Cell and Environment 2, 93-106.
403. Van Volkenburgh, E., and Davies, W.J., 1983. Inhibition of light-stimulated leaf expansion by abscisic acid. Journal, of Experimental Botany 34, 835-845.
404. Van Wyk, G., 1987. Progress with Eucalyptus hybrids in South Africa. South African FRI Report No. P1/87.
405. Veselkov, B.M., and Tikhov, P.V., 1984. Relationship between water transport in xylem and transpiration rate in the pine Pinus sylvestris tree. [Fiziologia Rastenii (Moscow) 31, 1099-1106].
406. Vieweg, G.H., and Ziegler, H., 1960. Thermoelektrische Registrierung der Geschwindigkeit des Transpirationsstromes. [Berichte Deutsche Botanische Gessellenschaft 73, 221-226].
407. Von Dem Bussche, G.H., 1984. Afforestation of marginal land to meet the needs of local communities in South Africa. South African Forestry Journal 130, 65-70.
408. Waring, R.H., and Roberts, J.M., 1979. Estimating water flux through stems of Scots pine with tritiated water and phosphorous-32. Journal of Experimental Botany 116, 459-471.
409. Waring, R.H., and Running, S.W., 1976. Water uptake, storage and transpiration by conifers: a physiological model. In: Water and plant life: problems and modern approach, eds O.L. Kappen, and E.D. Schulze. Springer-Verlag, New York, p. 19.
410. Waring, R.H., and Running, S.W., 1978. Sapwood water storage: its contribution to transpiration and effect upon water conductance through the stems of old-grown Douglas-fir. Plant, Cell and Environment 1, 131-140.
411. Waring, R.H., Gholz, H.L., Grier, C.C., and Plummer, M.L., 1977. Evaluating stem conducting tissue as an estimator of leaf area in four woody angiosperms. Canadian Journal of Botany 55, 1474-1477.
412. Waring, R.H., Newman, K., and Bell, J., 1981. Efficiency of tree crowns and stemwood production at different canopy leaf densities. Forestry 54, 15-23.
413. Waring, R.H., Schroeder, P.E., and Oren, R., 1982. Application of the pipe model theory to predict canopy

leaf area. Canadian Journal of Forest Research 12, 446-560.
414. Waring, R.H., Whitehead, D., and Jarvis, P.G., 1979. The contribution of stored water to transpiration in Scots pine. Plant, Cell and Environment 2, 309-317.
415. Weast, R.C., 1979. CRC Handbook of chemistry and physics, 59th edition. Boca Raton, Florida. pp. E5-E17.
416. Wessels, N.O., 1984. Afforestation of marginal land for commercial timer production in South Africa. South African Forestry Journal 130, 54-58.
417. West, P.W., and Wells, K.F., 1990. Estimation of leaf weight of standing trees of Eucalyptus regnans. Canadian Journal of Forest Research 20, 1732-1738.
418. Westman, W.E., and Roger, R.W., 1977. Biomass and structure of a subtropical Eucalyptus forest, North Stradbroke Island. Australian Journal of Botany 25, 171-191.
419. Wheeler, E.A., 1983. Intervascular pit membranes in Ulmus and Celtis native to the United States. International Association of Wood Anatomy Bulletin 4, 79.
420. Whitehead, D., 1978. The estimation of foliage area from sapwood basal area in Scots pine. Forestry 51, 137-149.
421. Whitehead, D., and Jarvis, P.G., 1981. Coniferous forests and plantations. In: Water deficits and plant growth. Vol 6, ed. T.T. Kozlowski. Academic Press, New York, pp 49-152.
422. Whitehead, D., and Kelliher, F.M., 1991. Modeling the water balance of a small Pinus radiata catchment. Tree Physiology 9, 17-33.
423. Whitehead, D., Edwards, W.R.N., and Jarvis, P.G., 1984. Conducting sapwood area, foliage area, and permeability in mature trees of Picea sitchensis and Pinus contorta. Canadian Journal of Forest Research 14, 940-947.
424. Whitfield, G.H., Gavloski, J.E., and Ellis, C.R., 1992. Use of stem flow gauges in measuring the effect of plant stress in corn. In: Symposium on sap flow measurements. Collected summaries of papers presented at the 83rd annual meeting of the Amercian Society of Agronomy, ed. C.H.M. Van Bavel. Dynamax, Houston TX 7703, pp. 31-32.
425. Whitmore, F.W., and Zahner, R., 1976. Evidence for a direct effect of water stress in the metabolism of cell wall in Pinus. Forest Science 13, 397-400.
426. Wilson, B.F., 1975. The distribution of secondary thickening in tree root systems. In: The development and function of roots, eds J.G. Torrey and D.T. Clarkson. Academic Press, London. pp. 197-219.
427. Zahner, R, and Whitmore, F.W., 1960. Early growth of radically thinned loblolly pine. Journal of Forestry 58, 628-634.
428. Zahner, R., 1968. Water deficits and growth of trees. In: Water deficits and plant growth, ed. T.T. Kozlowski. Vol 2, pp 191-254. New York, Academic Press.
429. Zahner, R., Lotan, J.E., and Baughman, W.D., 1964. Early-wood-latewood features of red pine grown under simulated drought and irrigation. Forest Science 10, 361-370.
430. Zajicek, J.M., and Heilman, J.L., 1991. Transportation by Crape Myrtle cultivars surrounded by mulch, soil and turfgrass surfaces. HortScience 26, 1207-1210.
431. Zhang, J., and Davies, W.J., 1989. Abscisic acid produced in dehydrating roots may enable the plant to measure the water status of the soil. Plant, Cell and Environment 12, 73-81.
432. Zhang, J., Schurr, U., and Davies, W.J., 1987. Control of stomatal behaviour by abscisic acid which apparently originates in the roots. Journal of Experimental Botany 38, 1174-1181.
433. Zimmermann, M. H., and Jeje, A.A., 1981. Vessel length distribution in stems of some American woody plants. Canadian Journal of Botany 59, 1882.
434. Zimmermann, M.H., 1978a. Hydraulic architecture of some diffuse-porous trees. Canadian Journal of. Botany 56, 2286-2295.
435. Zimmermann, M.H., 1978b. Structural requirements for optimal water conduction in tree stems. In: Tropical trees as living systems. eds. B.P. Tomlinson and M.H. Zimmermann. Cambridge University Press, Cambridge.
436. Zimmermann, M.H., 1983. Xylem structure and the ascent of sap. Springer-Verlag, Berlin, 143 pp.
437. Zimmermann, M.H., and Brown, C.L., 1971. Trees. Structure and function, Springer-Verlag, New York.
438. Zur, B., Jones, J.W., Boote, K.J. and Hammond, L.C. 1982. Total resistance to water flow in field soybeans. II. Limiting soil moisture. Agronomy Journal 74, 99-105.